APRIL 2015
ENERGINET.DK

VESTERHAV NORD OFFSHORE WINDFARM

SEDIMENTS, WATER QUALITY AND HYDROGRAPHY
BACKGROUND REPORT FOR EIA-STUDY

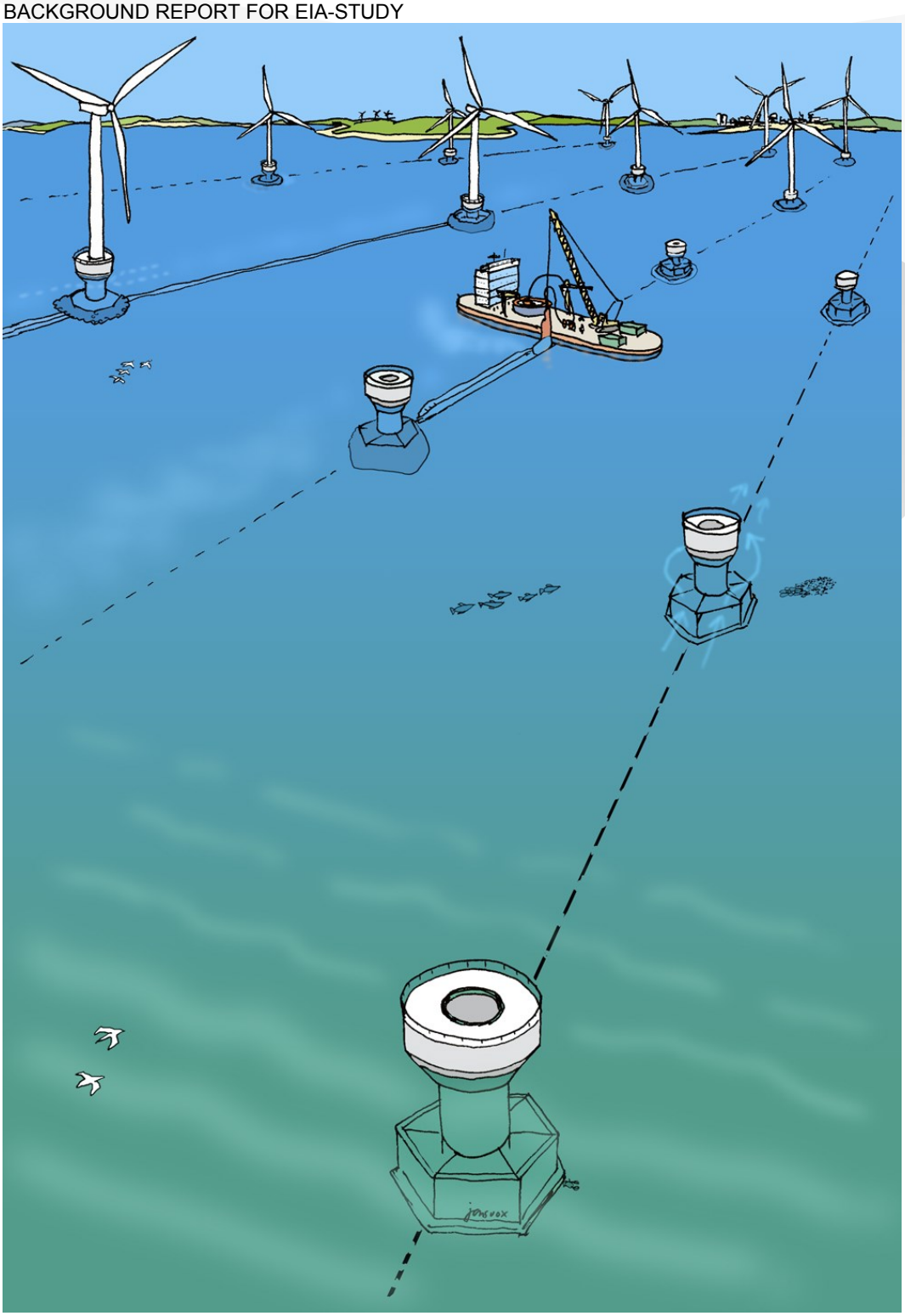

COWI

ADDRESS COWI A/S
Jens Chr. Skous Vej 9
8000 Aarhus C
Denmark

TEL +45 56 40 00 00
FAX +45 56 40 99 99
WWW cowi.com

APRIL 2015
ENERGINET.DK

VESTERHAV NORD OFFSHORE WIND FARM

SEDIMENTS, WATER QUALITY AND HYDROGRAPHY
BACKGROUND REPORT FOR EIA-STUDY

PROJECT NO. A048262
DOCUMENT NO. A048262-VN-SH-01
VERSION 3
DATE OF ISSUE 08.04.2015
PREPARED HGLN, CRJ, KAGB, CEL, HSV
CHECKED HGLN, HSV
APPROVED THGI

CONTENTS

APPENDICES

Summary

0.1 English summary

This report provides an assessment of the potential impacts of the proposed Vesterhav Nord offshore wind farm (OWF) on hydrography, sediment spill, water quality, seabed morphology and coastal morphology, both, offshore and along the nearest shoreline and south of Haboøre Tange. The planned OWF has an appointed capacity of up to 200 MW.

In order to assess the potential impacts of the wind farm (including all associated infrastructure) and the export cable corridor, relative to baseline (existing) conditions, a combination of detailed numerical modelling and expert assessment has been employed. These impacts have been assessed using the worst case characteristics of the proposed development as presented in the Technical Project Description [ref. /1/], as specific details about the OWF are not known at this stage of the project. Considerations have been made regarding the proposed impacts on the wave, hydrodynamics (currents and water levels), sediment transport and water quality for construction, operation and decommissioning phases of the development.

Pressures during construction

During construction there is the likelihood for short-term disturbances of the offshore seabed as the wind turbine foundations are installed and the export and inter-array cables are buried sequentially across the site. Seabed sediments may potentially be released into the water column resulting in the formation and distribution of sediment plumes.

In this assessment, the worst case scenario regarding sediment spill and transport was considered to be seabed preparation for concrete gravity based foundations (GBS) foundations and jetting for inter-array cable installation. These two operations (scenarios) were consequently modelled over a two month installation period. The worst case assumes a total of 66 foundations (3 MW turbines) to be installed, followed by the laying of inter-array cables in the offshore wind farm area continuing by six 36 kV cables via an export corridor onto shore, with no substation in between. Two export corridors exist at the present stage of the project, but only one of these will be used during construction. In the modelled worst case scenario it is assumed that inter-array cables are installed in both corridors simultaneously. This assumption is conservative and results in an overestimation of the sediment spill.

The results of the modelling show that seabed preparation related to installation of GBF-foundations (scenario 1) will result in minor increases in sediment concentrations (increased turbidity); less than 6 mg/l within most of the OWF area and very short periods with concentration of up to 20 mg/l in very limited areas. It is also found that maximum concentrations outside the OWF area are less than 3 mg/l at all times.

Installation of cables by jetting (scenario 2) is expected to cause larger sediment spill volumes and affects wider areas than dredging/excavation works for foundation installation (scenario 1). Model results predict maximum concentrations reaching the order of 100 mg/l in the export cable corridors and 200 mg/l at the landfall. Concentrations of up to 30-60 mg/l are expected along the coast 10-15 km north and south of the OWF. Maximum concentrations of more than 10 mg/l is predicted along the coast as far as 30 km north and south of the northern cable corridor because some of the spilled sediment is caught and transported by the strong littoral current and kept in suspension by wave breaking.

In the near vicinity along the coast where jetting is being performed, concentrations greater than 2 mg/l occur for up to 100-400 hours, whereas concentrations of 5 mg/l are experienced for up to 200 hours. Areas more than 5 km from the OWF are hardly affected by increased sediment concentrations in excess of 2 mg/l. But as mentioned above the shallow nearshore will experience concentrations of more than 10 mg/l as fare as 30 km north and south of the cable corridors.

Natural variations in sediment concentrations are caused by bed sediments brought into suspension by large waves and/or suspended particulate matter from the North-German rivers which gets carried up the West Coast by the coastal current at regular intervals. These natural variations in sediment concentrations are of the same order of magnitude as the concentrations of spilled sediments during dredging/excavation and jetting operations. Consequently, the transitory influence of the OWF on light attenuation at the seabed is considered within the range of the natural variations. The environmental pressures caused by increased turbidity - associated to construction – are considered to be *minor*.

The results show that spilled sediments will generally deposit in and near the OWF and associated cable corridors, and along the coast north and south of the OWF. In the OWF as well as along and between the cable corridors the model predicts depositions of up to 10 kg/m^2, whereas sedimentation values outside these areas are less than 200 g/m^2. Furthermore, the model predicts that some of the spilled material will enter Nissum Bredning through Thyborøn Kanal and deposit on the shallow shoals at amounts of up to 50 g/m^2. The predicted sedimentation values are very small and will be expected to result in local seabed accretion in the order of only a few millimetres. Consequently, the pressure on the environment due to deposition of spilled sediments is expected to be minor.

Pressures during operation

During the operational stage of the wind farm the greatest potential pressures in the context of this assessment are changes in currents and wave regimes. In this assessment, the effect of wind farm operation on these processes was modelled using a worst case layout of 66 3MW foundations across the site. No potential effects are considered for the inter-array and export cables because these will be buried during operation.

The results show that predicted changes to both currents and waves would be relatively small. The largest effect is observed locally near the individual foundations where average currents are reduced by up to 0.003 m/s (0.8%). Strong

currents (of around 0.8 m/s) are reduced by up to 0.015 m/s. The changes observed are of the same order of magnitude as the accuracy of the hydrodynamic model, and the pressure on hydrodynamics (currents and water levels) is thus considered *neutral*. Vesterhav Nord OWF is exposed to large waves from westerly directions ranging from 2 m to around 7-7.5 m during storms. The OWF causes a reduction of the average wave height by 2-4 cm inside the OWF. 10 km south to 12 km north of the OWF the influence is less than 0.5 cm. Storm wave heights of 7-7.5 m are reduced by up to 5-6 cm inside the OWF. In conclusion, the changes to the wave climate are in the order of 1-3.5% in the coastal area. This reduction of the wave heights is considered *minor* compared to the yearly variations of the wave climate.

The coastal zone off west Jutland displays a highly dynamic environment, where sediment transport is governed by strong tidal and wave-induced currents. The energetic wave climate with waves of up to 7.5 m from westerly directions governs the sediment transport along the west coast of Jutland and the formation of coast parallel sand bars found in the littoral zone in water depths less than 6-7 m.

At the OWF in water depths of 15-28 m the sediment transport is governed by the north bound coastal current which result in the formation and migration of bed forms towards north. Furthermore, the area is affected by sand mining conducted at nearby sand mining sites; *562-AE Thyborøn* and *562-AD Ferring.* A comparison of the surveys conducted in 2008, 2010, 2012 and 2013 shows that a channel of more than 28 m depth in the north-western part of the OWF has eroded by 10-20 cm/year and that sandbanks of up to 5.6 m in height are migrating towards north at rates of 20 m/year. The seabed is thus very dynamic and in this context a local reduction of the strongest currents by 0.015 m/s due to the OWF will not have any effect on the morphology. The OWF is therefore expected to have a *neutral* impact on seabed morphology and sediment transport patterns.

The Vesterhav Nord OWF causes a reduction of the near shore wave heights of 1-2% along the coast at and south of Haboøre Tange. The coast is generally eroding at rates of around 3 m/year. The sediment transport rates along the coast are modelled and show potential variations of more than 500,000 m^3/year from one year to the next due to natural variations in the wave climate alone. The modelled influence of the OWF is in the order of 20,000 m^3/year which is considered a *minor* impact well within the yearly variability.

Along the coast and in adjacent waters, the OWF is not expected to influence the exchange of water as a consequence of flow blocking. Furthermore, it is found that the OWF has a neutral effect on the mixing of stratified water bodies. Consequently, effects on the water quality are not anticipated during the operation of Vesterhav Nord OWF.

Pressures during Decommissioning

The decommissioning phase is generally considered to incur similar or less changes to currents, waves, sediment spill and transport than the construction phase.

Cumulative Effects

Cumulative effects have not been identified to interact with the operational effects of Vesterhav Nord OWF.

Impact Assessment

Table 0.1 below summarises the impact significance for the environmental factors related to hydrography and water quality during construction, operation and decommissioning of the offshore wind farm at Vesterhav Nord.

Table 0.1 Summary of effects.

	Overall impact	Remarks
Wave climate	Minor impact	Impact is regionally confined to Vesterhav Nord OWF and with average reduction in wave height ranging between 2 and 4 cm (1-3.5%).
Currents	No impact	The largest effect is observed locally near the individual foundations where average currents are reduced by up to 0.003m/s (0.8%). Strong currents of around 0.8 m/s are reduced by up to 0.015 m/s.
Water quality	No impact	Water quality is not affected since flow blocking is close to zero. Stratification and mixing conditions are also not affected, since additional turbulence is < 1% than natural background.
Sediment spill: Sediment concentration	Minor impact	Sediment concentrations are relatively low during the construction phase and environmental thresholds are only exceeded for very short periods of time during construction. Furthermore, the spilled sediment enters into a highly dynamic environment with significant natural suspended sediment transport.
Sediment spill: Sedimentation	Minor impact	Sedimentation occurs locally within the Vesterhav Nord OWF area and along the coast. Environmental threshold sedimentation rates are not exceeded.
Sediment spill: Light Attenuation	No impact	Light attenuation at the seabed is frequently affected by wave action and particulate material from the North-German rivers, which is carried up along the Danish West Coast by the coastal current. These natural variations are considered to contribute more to light attenuation at the seabed than the temporary effects of increased sediments during construction.
Seabed and coastal morphology	No to Minor impact	The effects on the wave and current climate by the Vesterhav Nord OWF are minor and the subsequent effects on both coastal and seabed morphology are thus found to be equally minor to negligible (within model accuracy or yearly variations).

0.2 Danish summary

Nærværende rapport indeholder en vurdering af Vesterhav Nord havmølleparks forventede potentielle påvirkning af bølgeforhold, hydrodynamik (strøm og vandstande), sedimentspild, vandkvalitet, havbundsmorfologi og kystmorfologi. Der ses på påvirkninger både offshore (i og omkring parken) og langs den tilstødende kyst langs og syd for Haboøre Tange. Havmølleparken har en forventet max kapacitet på 200 MW.

Vurderingerne er baseret på en kombination af numeriske modelstudier og ekspertvurderinger og omfatter både den potentielle påvirkning forårsaget af den

planlagte havmøllepark såvel som ilandføringskabler. Alle potentielle påvirkninger vurderes i forhold til baseline som beskriver eksisterende forhold.

Effektstudierne tager udgangspunkt i en “worst case”-betragtning, idet specifikke detaljer om havmølleparkens udformning ikke er fastlagt i denne tidlige fase af projektet. “Worst case”-tilgangen antager den for miljøet værst tænkelige projektudformning, indenfor projektets overordnede rammer, som defineret af Energinet.dk (ENDK) i *Technical Project Description* [ref. /1/]. Undersøgelserne omfatter alle faser af projektet fra anlægsfase til drift og dekommissionering.

Påvirkninger i anlægsfasen

I anlægsfasen vil der være en mulig påvirkning af havbunden som følge af etableringen af havmøllefundamenter såvel som nedspuling af inter-array- og ilandføringskabler. Anlægsarbejderne kan give anledning til, at der frigives havbundssedimenter i vandsøjlen, som danner sedimentfaner der kan føres med strømmen ud i de tilstødende områder.

Det er antaget, at det værst tænkelige sedimentspild (”worst case”) vil ske som følge af uddybningsarbejder i forbindelse med etablering af gravitationsfundamenter, samt installation af kabler ved hydraulisk nedspuling i havbunden (jetting). Disse to operationer (scenarier) er derfor blevet modelleret som kontinuerlige arbejder, der udføres hen over en to måneders anlægsperiode. I ”worst case” tilgangen er det antaget, at der opføres 66 fundamenter (3 MW møller) og at der efterfølgende nedspules inter-array kabler mellem møllerne og videre mod land i form af seks 36 kV kabler nedspulet i en ilandføringskorridor. Der vil ikke være nogen substation.

På nuværende tidspunkt i projektforløbet er der to mulige ilandføringskorridorer mellem parken og kysten. I spildmodelleringen er det antaget at der etableres seks kabler i begge korridorer samtidigt, hvorfor den modellerede sedimentspredning er overestimeret.

Modelresultaterne viser, at forøgelsen af sedimentkoncentrationer (forøget turbiditet) i forbindelse med etablering af gravitationsfundamenter (scenarie 1) er begrænset; dvs. mindre end 6 mg/l i det meste af havmølleparken og der er kun meget korte perioder og mindre områder med koncentrationer på op til 20 mg/l. Uden for havmølleparken forekommer der ikke koncentrationer over 3 mg/l på noget tidspunkt i løbet af de modellerede uddybningsarbejder.

Modelresultaterne viser at nedspuling af kabler (scenarie 2) giver anledning til større spildmængder og påvirker et større område end for uddybningsarbejderne i forbindelse med etablering af gravitationsfundamenterne (scenarie 1). Modelresultaterne viser, at der vil kunne forekomme sedimentkoncentrationer på op til 100 mg/l i kabelkorridorerne, dog 200 mg/l på lavt vand inderst i korridoren. Langs kysten, 10-15 km nord og syd for havmølleparken, forekommer koncentrations på op til 30-60 mg/l i løbet af perioden hvor nedspuling af kabler finder sted. I samme perioder forekommer der iht. modelberegningerne tidspunkter 30 km nord og syd for havmølleparken hvor sedimentkoncentrationen overstiger 10 mg/l. Dette skyldes, at noget af sedimentfanen kommer til at indgå i den

kystparallelle littoralstrøm, hvor kombinationen af stærk strøm og brydende bølger medfører, at materialet holdes i suspension og transporteres langt op ad kysten.

Ifølge modelresultaterne forekommer koncentrationer større end 2 mg/l i op til 100-400 timer i umiddelbar nærhed af hvor kablerne spules ned, mens koncentrationer større end 5 mg/l forekommer i op til 200 timer i samme område. Modellen viser, at koncentration større end 2 mg/l fortrinsvist forekommer indenfor ca. 5 km radius omkring havmølle parken, hvis man ser bort fra det sediment, som fanges i littoralstrømmen langs kysten. Langs kysten forekommer der som nævnt koncentrationer på op til 10 mg/l 30 km nord og syd for havmølleparken.

Der forekommer betydelige naturlige variationer i sedimentkoncentrationerne langs Vestkysten, som følge af bundsedimenter, som bringes i suspension i forbindelse med store bølger, samt forårsaget af fint partikulært materiale, som stammer fra de nordtyske floder, og som fra tid til anden føres op langs Vestkysten med kyststrømmen. Det findes derfor at påvirkningen af eksempelvist lysforholdene ved havbunden, som følge af forhøjede sedimentkoncentrationer i anlægsfasen, er af samme størrelsesorden som de naturlige variationer.

Spildt sediment aflejres ifølge modellen i eller tæt på havmølleparken, samt i de tilhørende kabelkorridorer. I projektområdet, langs kabelkorridorerne og mellem kabelkorridorerne viser modelresultaterne at der vil aflejres op til 10 kg/m^2 mens der udenfor disse områder vil aflejres op til 200 g/m^2. Resultaterne viser endvidere at noget af det spildte materiale bliver ført ind i Nissum Bredning via Thyborøn Kanal, og at materialet aflejres på de lavvandede sandbanker i Natura 2000 området, hvor der lokalt aflejres op imod 50 g/m^2. Den forventede sedimentation er sekundær i forhold til den naturlige dynamik som finder sted i området og kystfodringen langs den tilstødende kyst. Mængderne er meget små og forventes at give anledning til få millimeters aflejring af spildt sediment på havbunden. Således forventes kun *mindre* miljømæssig påvirkning på grund af aflejret spildt sediment.

Påvirkninger i driftsfasen

Den største påvirkning der forekommer i driftsfasen, og som falder ind under rammerne af denne undersøgelse, skyldes ændrede bølge- og strømforhold. Vurderingen af påvirkningen på strøm- og bølgeforhold er baseret på modellering af en ”worst case” udformning af havmølleparken med 66 3MW havmøllefundamenter fordelt over hele parkområdet. Der ses ikke på påvirkninger forårsaget af ilandføringskabler, som vil være nedgravede i driftsfasen.

Modelberegningerne viser, at påvirkningen af både bølge- og strømforhold er meget begrænsede. Beregningerne viser, at den dybdemidlede strømhastighed i gennemsnit vil blive reduceret med ca. 0,003 m/s (0,8%) i nærheden af fundamenterne i betydeligt mindre i resten af havmølleområdet. Stærke strømme på i størrelsesordenen 0,8 m/s reduceres lokalt med op til 0,015 m/s. Påvirkningen er således i samme størrelsesorden, som den numeriske models usikkerhed, og påvirkningen af strøm- og vandstandsforhold vurderes derfor at være *neutral*.

Vesterhav Nord havmøllepark opføres i et område hvor der forekommer store bølger fra vestlige retninger på i størrelsesordenen 2 m til 7-7,5 m i forbindelse med storm. Ifølge modelberegninger giver havmølleparken anledning til en reduktion af middelbølgehøjderne på 2-4 cm i havmølleområdet, mens påvirkningen 10 km syd og 12 km nord for mølleområdet vil være mindre end 0,5 cm. Modellerede stormbølger på 7-7,5 m reduceres med 5-6 cm indenfor havmølleparken. Påvirkningen er således i størrelsesordenen 1-3,5% indenfor mølleområdet og lang den tilstødende kyst hvilket er betydeligt mindre end de årlige variationer

Morfologien ved den jyske vestkyst er meget dynamisk og under konstant påvirkning fra store bølger såvel som stærke tidevands-, vind-/tryk- og bølgegenererede strømme. Bølger på op imod 7,5 m fra vestlige retninger driver sedimenttransporten i den kystnære zone på vanddybder mindre end 6-7 m, og er med til at skabe et meget dynamisk revlesystem, mens sedimenttransporten og havbundsmorfologien på 15-28 m vanddybde - i havmølleparken - i højere grad er drevet af den primært nordgående kyststrøm. Den stærke nordgående kyststrøm i projektområdet er bl.a. med til at skabe sandbølger udfor kysten, som over tid vandrer imod nord. Morfologien i projektområdet er endvidere påvirket af, at der i en årrække er blevet indvundet sand i råstofområdet *Thyborøn* og *Ferring*.

Ved sammenligning af pejlinger foretaget i år 2008, 2010, 2012 og 2013 findes, at en mere end 28 m dyb kanal i den nordvestlige del af havmølleområdet eroderer med en hastighed på 10-20 cm/år. Endvidere bemærkes at sandbanker på op til 5.6 m i højde fundet i det meste af mølleområdet vandrer imod nord med en gennemsnitlig hastighed på 20 m/år. Havbundsmorfologien i projektområdet vurderes således at være meget dynamisk og i den sammenhæng vurderes det samlet set ikke, at en reduktion af de stærkeste strømhastighederne i området - på mindre end 0,015 m/s - vil påvirke havbundsmorfologien i området.

Havmølleparken medfører en reduktion af de kystnære bølgeforhold på i størrelsesordenen 1-2% langs kysten syd for Thyborøn. Den berørte kyststrækninger har generelt oplevet en erosion i størrelsesordenen 3 m/år. Bølgeforholdene varierer betydeligt langs kysten og giver anledning til en potentiel variation i netto sedimenttransporten på op til 500.000 m^3/år fra et år til det næste (>1000%). Til sammenligning viser modellering af sedimenttransporten, at havmølleparken har en potentiel påvirkning af netto sedimenttransporten på i størrelsesordenen 20.000 m^3/år i det område hvor påvirkningen er størst. Det vurderes derfor, at påvirkningen af kystens morfologi er *lille* sammenholdt med de naturlige variationer.

Vesterhav Nord havmøllepark forventes ikke at give anledning til strømblokering eller forøget opblanding i vandsøjlens lagdeling. Det forventes derfor ikke, at havmølleparken vil påvirke vandkvaliteten i driftsfasen.

Påvirkninger under dekommissionering

Dekommissioneringsfasen forventes at give anledning til sammenlignelige eller mindre påvirkninger af bølgeforhold, hydrodynamiske forhold, sediment spild og

morfologiske forhold end anlægsfasen. Der er derfor ikke foretaget yderligere analyser af påvirkningerne i denne fase af projektet.

Kumulative påvirkninger

Der er ikke blevet identificeret projekter som forventes at give anledning til kumulative påvirkninger af Vesterhav Nord Havmøllepark.

Vurdering af påvirkninger

Tabel 0.2 nedenfor beskriver graden af påvirkning indenfor områderne hydrografi, sedimentforhold og vandkvalitet i forbindelse med anlægsfase, driftsfase og dekommissionering af havmølleparken.

Tabel 0.2 Resumé af effekter.

	Overall impact	Remarks
Bølgeklima	Mindre påvirkning	Påvirkningen af bølgeforholdene er begrænset til Vesterhav Nord havmøllepark, hvor den gennemsnitlige reduktion af bølgeforholdene forventes at være i størrelsesordenen 2-4 cm (1-3,5%).
Hydrodynamik (strøm- og vandstandsforhold)	Ingen påvirkning	Beregningerne viser at normale strømhastigheder reduceres med op til 0,003m/s (0,8%) i nærheden af fundamenterne, mens stærke strømme på i størrelsesordenen 0,8 m/s reduceres lokalt med op til 0,015 m/s.
Vandkvalitet	Ingen påvirkning	Vandkvaliteten forventes ikke påvirket, af hverken strømningsblokering eller ændrede lagdelingsforhold. Havmølleparken forventes at medføre en forøgelse af turbulensen i projektområdet med mindre end 1 % i forhold til baggrundsturbulensen som dannes af vind- og bundfriktion.
Sedimentspild: Sediment-koncentrationer	Mindre påvirkning	Sedimentkoncentrationerne forventes at være relativt lave i anlægsfasen og grænseværdier for påvirkninger forventes kun kortvarigt overskredet i forbindelse med grave- og nedspulingsarbejderne. Endvidere foregår spildet af sedimenter i et meget dynamisk miljø hvor koncentrationerne af suspenderet sedimenttransport er betydelig.
Sedimentspild: Sedimentation	Mindre påvirkning	De spredte sedimenter aflejres fortrinsvist langs kysten og indenfor havmølleområdet. Sedimentationsrater forventes samtidigt at være mindre end de gældende grænseværdier
Sedimentspild: Lysdæmpning	Ingen påvirkning	Langs Vestkysten er sigtbarheden i vandet ofte påvirket af forøgede stofkoncentrationer, forårsaget af store bølger eller partikulært materiale fra de nordtyske floder, som føres mod nord med kyststrømmen. Disse naturlige variationer vurderes at have større betydning for lysforholdene ved havbunden end den kortvaringe påvirkning, som vil forekomme i anlægsfasen.
Kyst og havbundsmorfologi	Ingen eller Mindre påvirkning	Påvirkningen af bølge- og strømforholdene som forårsages af havmølleparken er lille, og den afledte effekt på både havbundsmorfologien og kystmorfologien vurderes derfor at være tilsvarende lille (indenfor modelusikkerhed og årlige variationer).

1 Introduction

On 22 March 2012, a broad majority of the Danish Parliament reached an energy agreement. This agreement means tendering of 450 MW offshore wind turbines at six nearshore locations. The Ministry of Climate, Energy and Building has appointed Energinet.dk (ENDK) to conduct pre-investigations at six offshore wind farm sites in Danish seas towards the tendering process of the operational licenses as well as to conduct environmental impact assessments for each of the six project sites.

The six project sites are (see Figure 1.1):

- Bornholm
- Sejerø Bugt
- Smålandsfarvandet
- Sæby
- Vesterhav Nord
- Vesterhav Syd

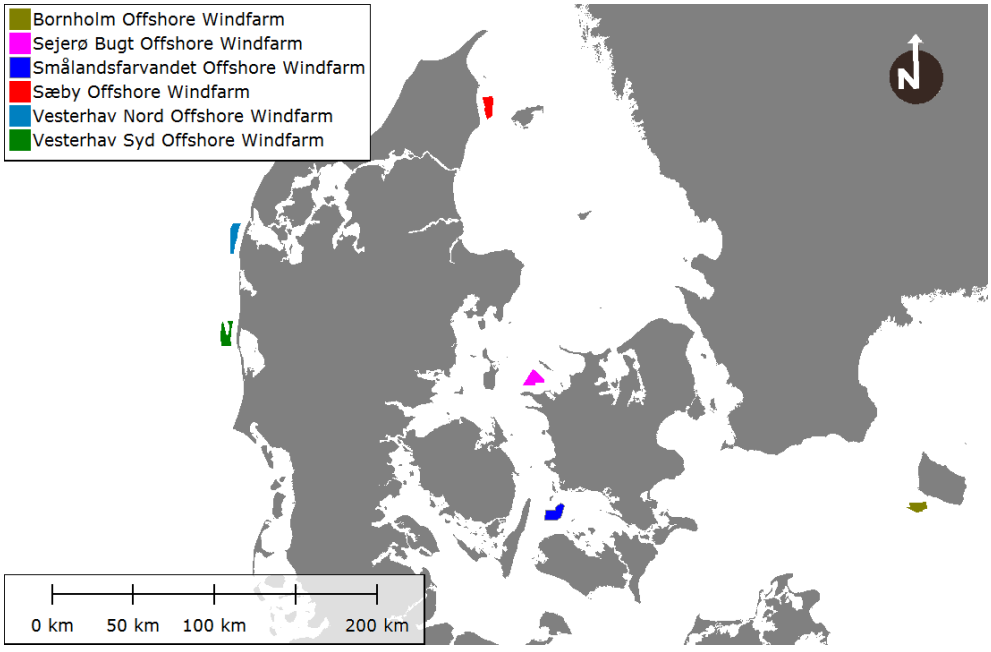

Figure 1.1 Project locations/sites.

Energinet.dk has contracted COWI A/S as Met-Ocean consultant to prepare background report to the EIA covering: hydrography, sediments and water quality including all meteorological and oceanographic information necessary as basis for the EIA.

The project stakeholders and their deliverables throughout the project are:

- Energinet.dk (Client):
  Energinet.dk provides geophysical data, as well as wave and current measurements from four of the sites. Furthermore, Energinet.dk provides park layouts, types of foundation and turbine, turbine height, methods for installation of cables.

- NIRAS:
  EIA consultant, who prepares EIA reports, scoping notes and Natura 2000 impact assessment with technical input from the Met-ocean consultant. NIRAS is responsible for the project locations/sites: North Sea (Vesterhav) North, North Sea (Vesterhav) South and Bornholm.

- RAMBØLL:
  EIA consultant, who prepares EIA reports, scoping notes and Natura 2000 impact assessment with technical input from the Met-ocean consultant. Rambøll is responsible for the project locations/sites: Sæby, Sejerø Bay and Smålandsfarvandet.

- COWI:
  COWI is the Met-ocean consultant and sets up local detailed numerical models and prepares background reports and notes to the EIA consultants. COWI furthermore prepares the met-ocean study with input from DMI and wind resource estimate based on mesoscale modelling by StormGeo.

1.1 Purpose

This report contains an assessment of the potential impacts to hydrographic conditions, seabed morphology, coastal morphology and water quality as a result of the construction, operation and decommissioning of Vesterhav Nord Offshore Wind Farm (OWF). The studies and effects feed into the assessments of possible impacts on a range of parameters (e.g. benthic ecology, fisheries) that will be studied as separate parts of the EIA process. The proposed OWF has an appointed max capacity of 200 MW.

The report presents a description of the existing coastal and marine physical processes across the Vesterhav Nord Offshore Wind farm and associated export cable corridors. This is followed by the definition of “worst case” scenarios for each element of the development in terms of their potential effects on hydrography, sediment spill, water quality, seabed morphology and coastal morphology which are then compared to the existing conditions through expert judgment and numerical modelling.

The EIA assessment will be compiled upon a comprehensive description of the technical project encompassing wind turbines specifications, foundation strategy and installation methods for inter-array and export cables, respectively. However, the description will not be constrained to one exact definition of the project, but instead describe the boundaries and span of a project that incorporate the “most-likely” with a “worst-case” in mind. The reason for this approach is that the Danish Energy Agency has not yet assigned concession of construction and operation of the offshore wind farms and therefore preserves degrees of freedom in the technical aspects of the project.

2 Project description

This section summarises the overall technical details which may be of relevance to the EIA studies on sediment transport and water quality. The technical description is based on *TECHNICAL PROJECT DESCRIPTION FOR THE NEARSHORE WIND FARMS (450 MW)* [ref. /1/].

An overview of the project area and nearby points of interest is shown in Figure 2.1.

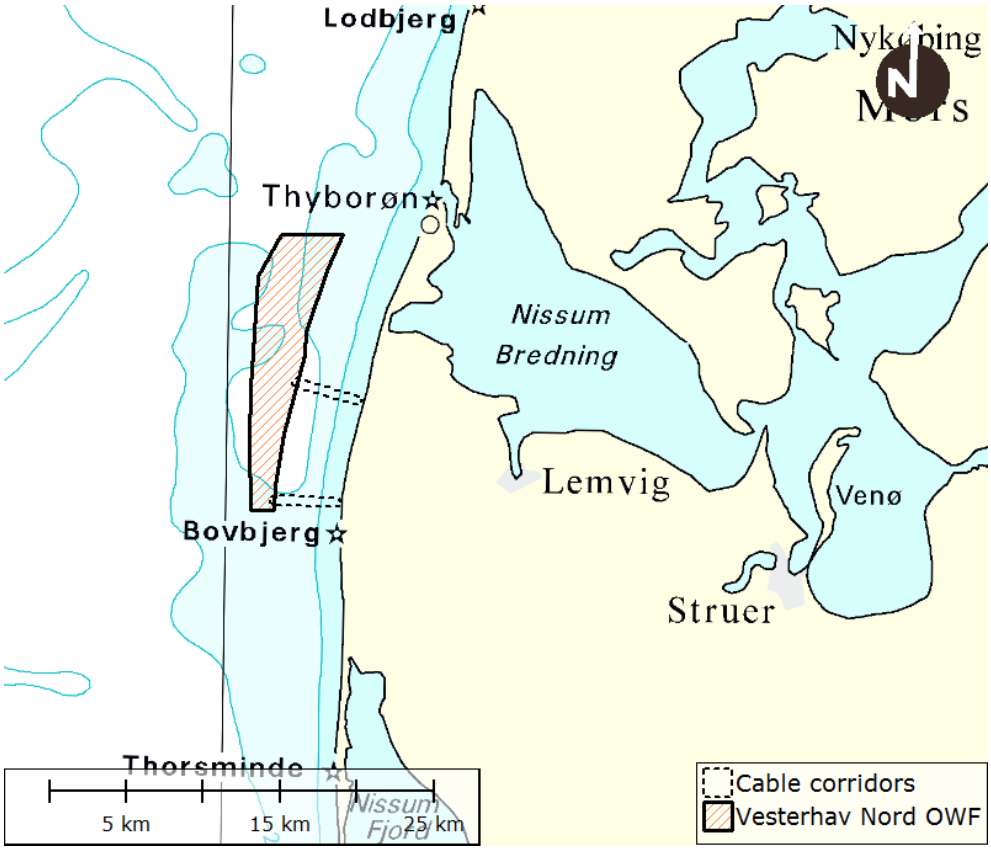

Figure 2.1 Location of Vesterhav Nord Offshore Wind Farm (OWF).

2.1 Park layout

The 3 MW and 10 MW wind turbines are the minimum and maximum sizes being considered so that any turbine between these two sizes will be covered by the assessment in this report. The planned maximum capacity of the wind farm is 200 MW and the wind farm will thus feature a maximum of 20 to 66 turbines depending on the rated energy of the selected turbines.

Suggested layouts by DTU Wind Energy for the 3 MW and 10 MW wind turbines at the Vesterhav Nord Offshore Wind farm are shown in Figure 2.1.

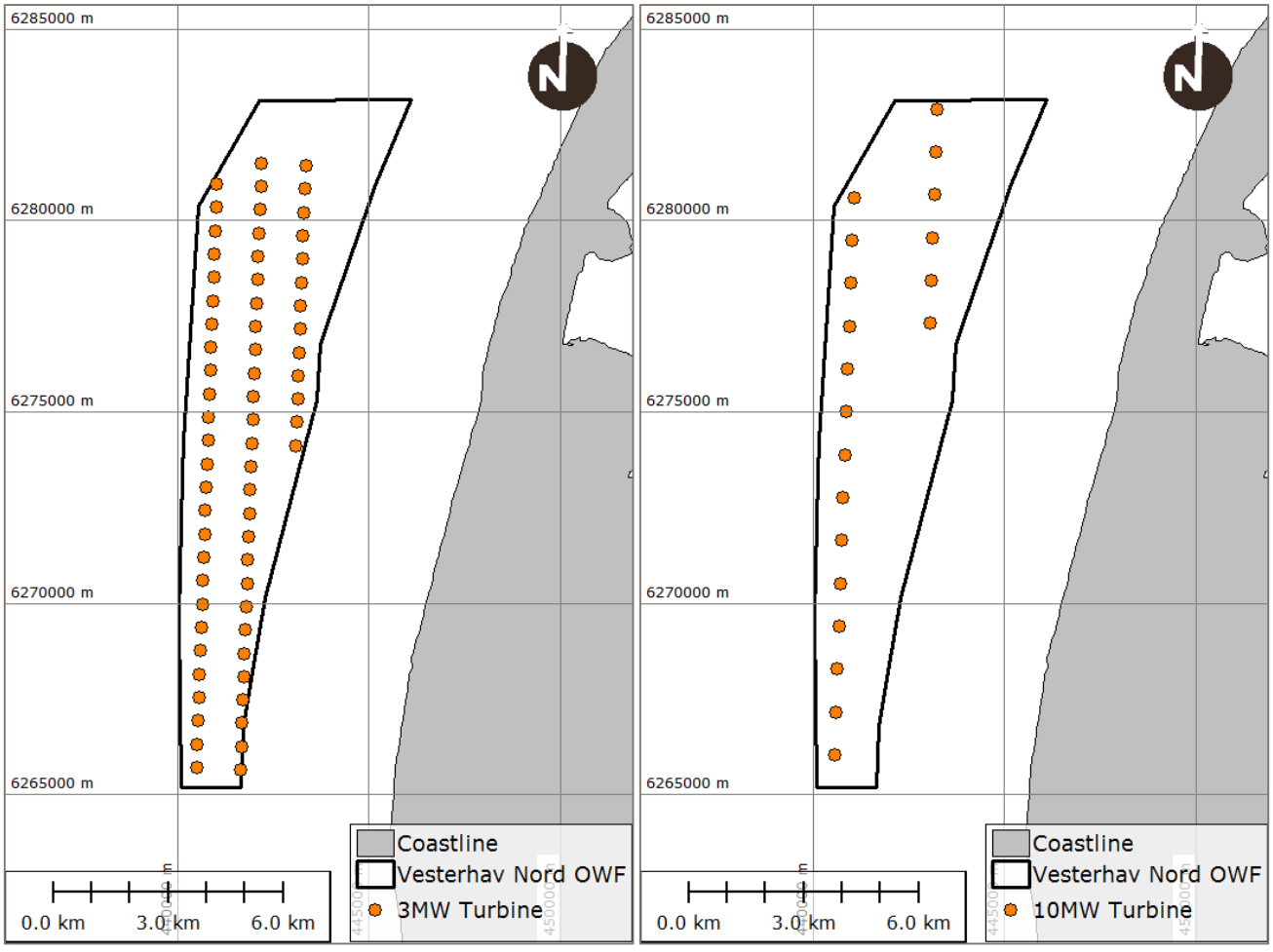

3 MW layout 10 MW layout

Figure 2.2 Suggested layouts by DTU Wind Energy for wind turbines at Vesterhav Nord.

2.2 Foundation type

It is expected that the wind turbine foundations for the six project sites will comprise one or more of the options shown in Figure 2.2.

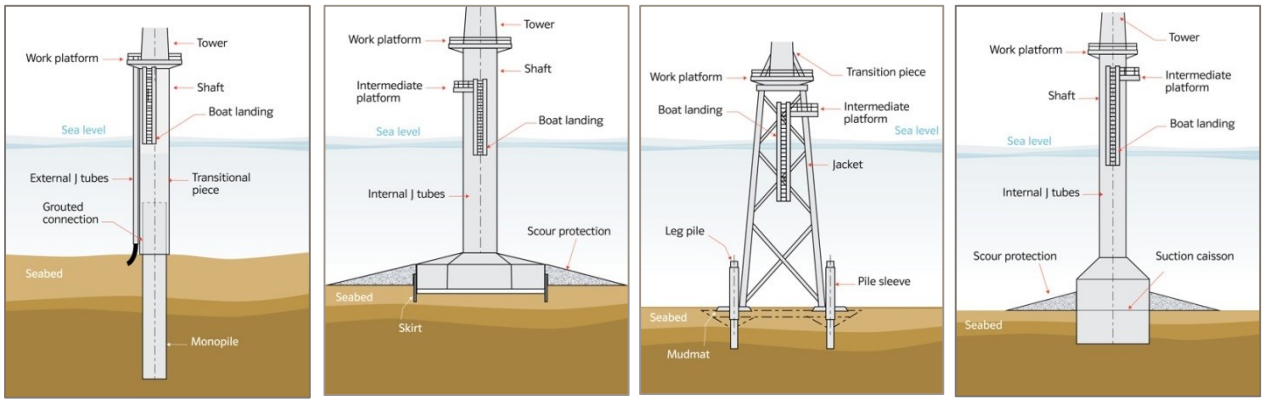

DRIVEN STEEL MONOPILE | CONCRETE GRAVITY BASE | JACKET FOUNDATION | SUCTION BUCKET

Figure 2.3 Illustration of possible foundation types [ref. /2/].

Driven steel monopiles

The solution comprises of driving a hollow steel pile into the seabed. Pile driving may be limited by deep layers of coarse gravel or boulders, and in these circumstances the obstruction may be drilled out.

Concrete gravity base

Gravity base structures rely on their mass including ballast to withstand the loads generated by the met-ocean environment and the wind turbine.

Jacket foundation

Jacket foundation is a three or four-legged steel lattice structure with the shape of a tower. The three or four legs are connected to each other by cross bonds. For support of the jacket structure, each leg is attached to a pile by grouting.

Suction bucket

The relatively new concept combines the main recognised aspects of a gravity base foundation, a monopile and a suction bucket and can be adopted for various site conditions including homogeneous deposits of sand and silts, clays, and layered soils.

2.3 Dimensions

The dimension of the foundations will be specific to the selected type of turbine and the particular site conditions (water depth, ground and met-ocean conditions) at the location at which the turbine is to be installed. A very general estimate of the dimensions of each foundation type for two different sizes of turbines considering the expected average water depth at Vesterhav Nord OWF is presented in Table 2.1.

Table 2.1 General estimate of dimensions for foundations at Vesterhav Nord OWF.

	Average water depth (and range) [m]	20 (15-25)	
	Wind turbine size	3 MW	10 MW
Mono-pile	Outer diameter at seabed level [m]	5.0-6.0	7.0-9.5
Gravity based	Shaft diameter [m]	4.0-5.5	6.0-7.0
	Area of base [m^2]	330-440	450-600
Jacket	Distance between legs at seabed [m]	18 x 18	40 x 40
	Diameter of pile at each leg [mm]	1,200-1,500	1,500-1,800
Suction bucket	Shaft diameter [m]	4.0-5.5	6.0-7.0
	Skirt height [m]	2.0-2.8	3.0-3.5
	Cross sectional area of bucket [m^2]	*	*

**/ The suction bucket is still (in 2014) a relatively unproven concept. Dimensions are expected to be equal to or below GBF foundations.*

2.4 Seabed preparation

Depending on the seabed conditions, pre-dredgind/excavation may be necessary due to very soft soil and/or sand banks. Dredging/excavation may be done by back-hoe excavator placed on a stable platform (jack-up) or floating vessel. Sediment spill may be expected during these operations.

To prevent bearing capacity failure, scour protection consisting of well graded stones/rock may be applied at the foundation piles depending on the soil conditions (required for e.g. sandy soils), see Table 2.2 and Figure 2.3.

Where the seabed consists of erodible sediments there will be a risk of scour development around the foundation structure(s) due to wave and current impact. Development of scour holes can impact the stability of the foundation structures.

Table 2.2 General estimate of quantities of seabed preparation.

	Average water depth (and range) [m]	20 (15-25)	
	Wind turbine size (number of turbines)	3 MW (66)	10 MW (20)
Monopile	Foot print area of scour protection (per foundation) [m²]	1,500	2,000
	Volume of scour protection (per foundation) [m³]	2,100	3,500
Gravity based	Size of excavation (diameter) [m]	25-28	40-50
	Volume of excavation (per foundation) [m³]	1,200-1,600	2,000-3,200
Jacket	Foot print area of scour protection (per foundation) [m²]	700 (+/-100)	1,600 (+/-100)
	Volume of scour protection (per foundation) [m³]	800 (+/-150)	2,500 (+/-150)
Suction bucket	Foot print area of scour protection (per foundation) [m²]	*	*
	Volume of scour protection (per foundation) [m³]	*	*

**/ The suction bucket is still (in 2014) a relatively unproven concept. Dimensions are expected to be equal to or below GBF foundations.*

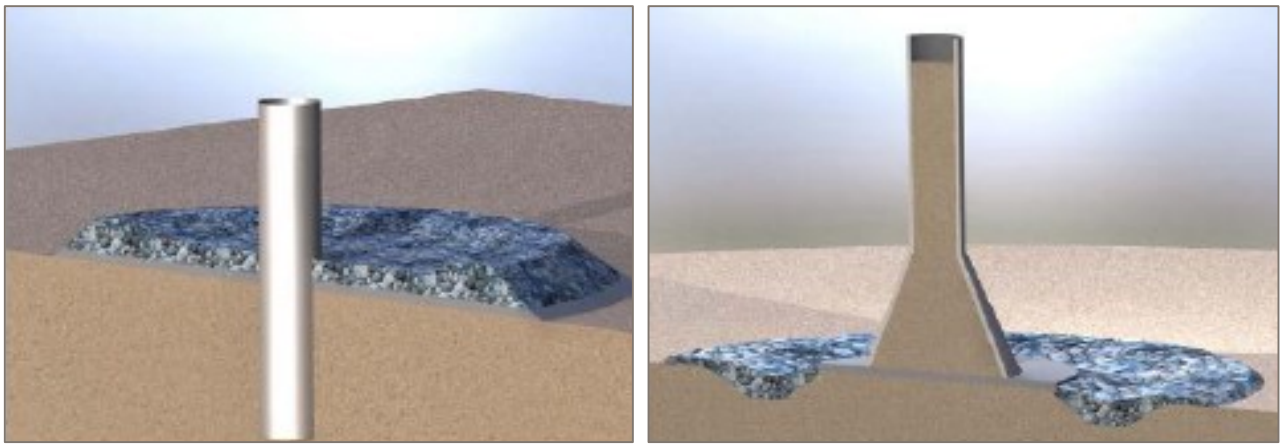

Figure 2.4 Example of scour protection for monopile (left) and gravity based foundation (right) [ref. /1/]

2.5 Submarine cables

Submarine cables will be connected to each of the wind turbines and will run to landing points at shore. The total length of the cables (inter-array cables between wind turbines and export cables to shore) depends on the layout configuration and thus the size of turbines.

The turbines are connected with 33 kV cables allowing 36 MW of wind turbines to be connected to each cable, thus requiring a total of six parallel cables in the export cable corridors.

Excavated material can be deposited near the trench. After the cables are installed, the trench will be covered by backfilling trenched material. Very fine grained seabed material may get washed away during trenching and may impact the volume of backfilling. Sediments will also naturally settle back into the trench assisted by waves and currents.

The duration of jetting depends on the length of cables, soil conditions and weather standby. Generally, a progress of 500-2000 m/day is expected and the jetted trench volume is approximately 2 x 1.6 m^3/m. Dredged/jetted volumes and duration for installation of submarine cables at Vesterhav Nord OWF is provided in Table 2.3.

Table 2.3 General estimate of excavation/dredging/jetting volumes for installation of submarine cables.

Wind turbine size (number of turbines)	3 mw (66)	10 mw (20)
Inter array cables [m^3]	65,000	25,000
Cable corridor CR01 – North [m^3]	51,000	51,000
Cable corridor CR02 – South [m^3]	39,000	39,000
Duration of dredging/excavation works [days]	35-150	10-45

Prior to installation of cables, a clearance of the seabed will take place in the cable corridors of approximately 50 m width. Clearance may be conducted as pre-lay grapnel runs and boulder clearance by trawling.

Scour protection for protection of the cables from fishing activity, dragging of anchors, etc. may be adopted.

2.6 Decommission

It is unknown at this stage how the wind farm may be decommissioned but the Technical Project Description [ref. /1/] gives a tentative description, which is summarized in the following.

The lifetime of the wind farm is expected to be around 25-30 years. It is expected that two years in advance of the expiry of the production time the developer shall submit a decommissioning plan. The method for decommissioning will follow best practice and the legislation at that time.

The decommission process will have to be agreed with the competent authorities before the work is being initiated. It is expected that an EIA will be required for the decommissioning of the wind farm.

The objectives of the decommissioning process are to minimize both the short and long term effects on the environment whilst making the sea safe for others to navigate. Based on current available technology, it is anticipated that the following level of decommissioning on the wind farm will be performed:

1 Wind turbines – to be removed completely.

2 Structures and substructures – to be removed to the natural seabed level or to be partly left in situ.

3 Infield cables – to be either removed (in the event they have become unburied) or to be left safely in situ, buried to below the natural seabed level or protected by rock-dump.

4 Export cables – to be left safely in situ, buried to below the natural seabed level or protected by rock-dump.

5 Cable shore landing – to be either safely removed or left in-situ, with particular respect to the natural sediment movement along the shore.

6 Scour protection – to be left in situ.

2.7 Environmental designations

Further to an overall impact from the OWF on wave and current climate, environmentally designated areas can be more sensitive to these impacts. It is therefore important to take special considerations regarding these areas.

Three Natura 2000 areas are present in the vicinity of the Vesterhav Nord OWF:

1 Nissum Bredning
2 Sandbanks off the coast of Thyborøn
3 Thyborøn rock reefs

Nissum Bredning consists of several smaller areas with natural resources with low water depth at the western entrance to Limfjorden.

An overview of the Natura 2000 areas is shown in Figure 2.4.

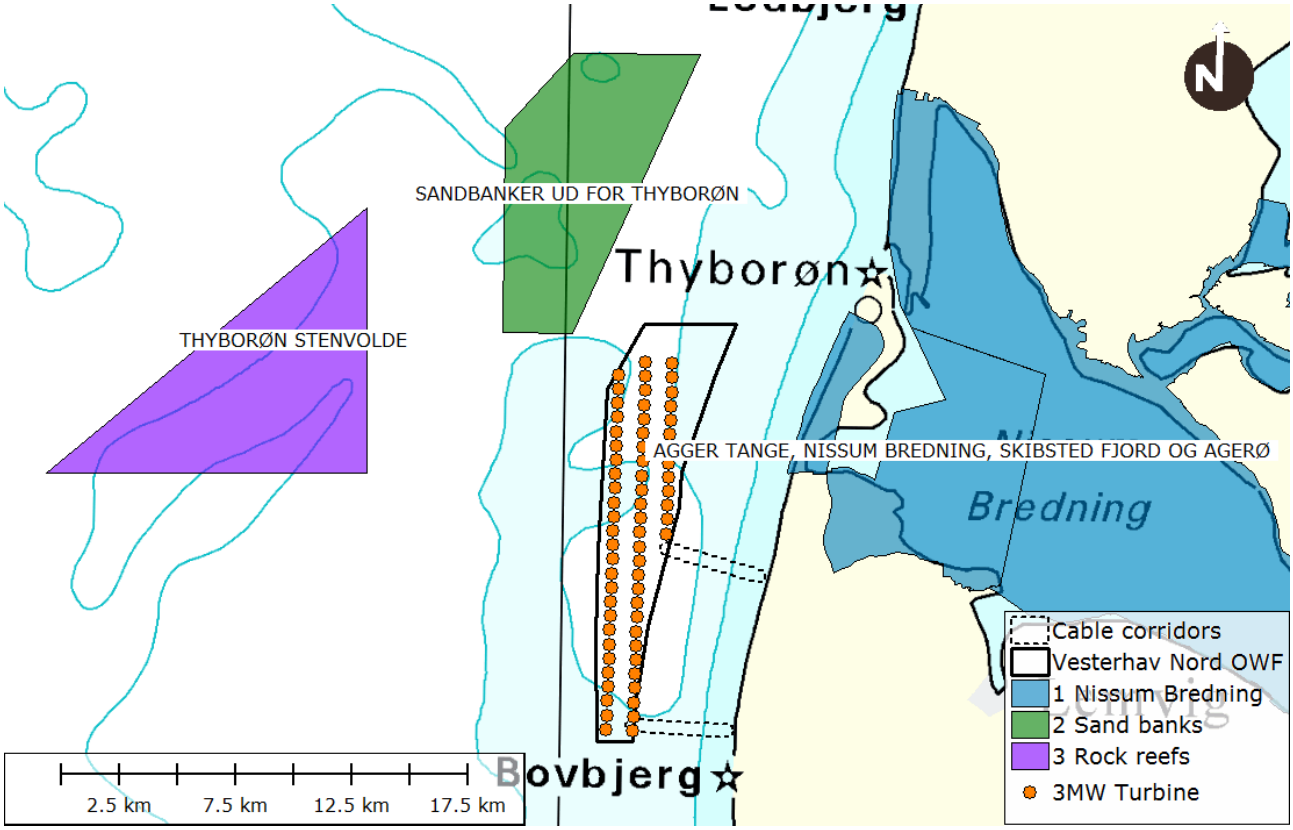

Figure 2.5 Natura 2000 areas adjacent to the OWF.

3 Assessment background

3.1 Potential environmental impacts

Previous EIA studies for offshore wind farms have shown that the impacts on hydrography, sediments and water quality ranges from *positive* to *neutral* and *minor*. Some of these conclusions are considered generally applicable to offshore wind farms in Danish Waters and independent of local conditions (waves, hydrodynamics, sediments, and water quality) while other effects will have to be studied in detail for each project site in order to take into account local conditions.

For instance, the possible impact to coastal development and morphology is influenced by the relative distance between the coastline and the wind farm, as well as the layout of the turbines, the wave climate, coastal geology, coastal structures etc. The coastal impact of a wind farm is thus governed by local conditions and must be studied specifically for each site.

Other effects to i.e. water quality caused by increased filtration from marine growth and rock scour protection (reef-creation), increased phytoplankton production, increased water temperatures due to emission of heat from marine cables etc. are considered universal to offshore wind farms in Danish Waters. These effects were rated *minor* or *neutral* subsequent to detailed numerical studies by DHI in the EIA for Anholt Offshore wind farm [ref. /3/].

Based on the experience gained from previous EIA studies of offshore wind farms at Anholt, Horns Rev 1, 2 & 3, Rødsand 1 and 2 and Sprogø, the potential environmental impacts on waves, hydrodynamics, sediments and water quality during construction, operations and decommissioning of Vesterhav Nord OWF have been identified as follows:

Coastal	Impacts to the littoral sediment transport and coastal development, caused by reduced wave explosion in lee of the offshore wind farm.
Morphology	Impact caused by flow amplification and formation of eddies near turbine foundations during operation, e.g. scour.

Sediment spill	Spill from dredging/excavation, trenching and jetting during installation of turbine foundations and inter-array and export cables.
Water quality ST[1]	Light reduction at the seabed due to sediment spill and release of toxic components, nutrients and organic contaminants.
Water quality LT[2]	Impacts to water quality due to reduced water exchange in water bodies close to the wind farm, e.g. in fjords, bays and estuaries.
Mixing	Impacts to water stratification caused by increased mixing near the turbine foundations.
Hydrodynamics	Changes to currents and fluxes caused by resistance to flow imposed by turbine foundations during operation.
Waves	Changes to the wave climate caused primarily by the wind wake of wind turbines in operation.

The environmental impacts during decommission are assessed to be similar or smaller compared with the effects listed above (see section 7).

3.2 Worst case scenarios

3.2.1 Site layout and turbine type

As described in section 2.1 the number of turbines to be installed in the project site is directly linked to the rated power production of the turbines. Hence, 66 no of 3 MW or 20 no of 10 MW turbines will be required to form a 200 MW site. This difference is also reflected in the tentative site layouts, as there is one 3 MW layout and one 10 MW layout (see Ref. /1/ and Figure 2.1).

Worst case evaluation:

Hydrodynamics	The total volume of the 3 MW foundations is larger than with 10 MW foundations, regardless of foundation type. 3 MW turbines are thus expected to introduce more hydrodynamic “friction” than 10 MW.
Waves	The total volume of the 3 MW foundations is larger than with 10 MW foundations, regardless of foundation type. 3 MW turbines are thus expected to introduce more wave reflection than 10 MW. Furthermore, the 3 MW turbines are placed in a larger

[1] ST : Short term impact during installation
[2] LT : Long term impact during operation

	geographical area and more densely than the 10 MW turbines, meaning that the wake zone downwind will be larger with 3 MW turbines than with 10 MW turbines.
Coastal	Due to the larger impact on waves and currents, 3 MW turbines will be expected to cause a larger impact on the adjacent coastline.
Morphology	Due to the larger impact on waves and currents, 3 MW turbines are expected to cause a larger impact on the sediment transport patterns and seabed morphology.
Sediment Spill	Dredging/excavation volumes during installation of foundations and inter-array cables will be larger with 3 MW turbines than with 10 MW turbines. 3 MW turbines are thus expected to cause higher spill volumes.
Water quality ST	Larger spill volumes with 3 MW turbines are expected to cause more light reduction at the seabed and larger release of toxic components, nutrients and organic contaminants than 10 MW turbines.
Water quality LT	Hydrodynamics and water renewal is interlinked, meaning that 3MW turbines are expected to have a larger impact on the water quality in the operational phase than 10 MW turbines.
Mixing	Only turbines installed in deep water may affect mixing of stratified water bodies, and since the 3 MW turbines are generally placed in deep water along the seaward edge of the project area than 10 MW turbines 3 MW turbines are expected to have a larger influence on mixing.

The evaluation above is summarised in Table 3.1.

Table 3.1 Summary of worst case evaluation for site layout / turbine type.

	Worst case site layout / turbine type	
	3 MW	10 MW
Hydrodynamics	X	
Wave Conditions	X	
Coastal	X	
Morphology	X	
Sediment spill	X	
Water Quality ST	X	
Water Quality LT	X	
Mixing	X	

3.2.2 Foundation type

As described in section 2.2 the following four foundation concepts are considered:

- Driven steel monopile
- Concrete gravity base
- Jacket foundation
- Suction buckets

Worst case evaluation:

Hydrodynamics — The total volume of concrete gravity base foundations is generally larger than other foundation types. Therefore, a gravity base foundation is expected to have a larger hydrodynamic impact than other foundation concepts.

Waves — The wave energy dissipation due to drag, reflection and diffraction around the structure, is expected to be higher with concrete gravity base foundations than with other foundation concepts.

Coastal — Concrete gravity base foundations are expected to have the largest impact on wave conditions and thus also on the adjacent coastline.

Morphology	Concrete gravity base foundations are expected to have the largest impact on wave conditions and thus also on seabed morphology.
Sediment Spill	Dredging/excavation volumes during installation of inter-array and export cables are only marginally affected by the foundation type, whereas dredging/excavation activities and volumes prior to installation of foundations will depend on foundation type. The removal of top soils and weaker soil layers will be more extensive for gravity base foundations, than for other types, and it is thus expected that concrete gravity base foundations will cause more sediment spill than other foundation concepts.
Water quality ST	Larger spill volumes with concrete gravity base foundations are expected to cause more light reduction at the seabed and larger release of toxic components, nutrients and organic contaminants than other foundation concepts.
Water quality LT	Hydrodynamics and water renewal is interlinked, meaning that concrete gravity base foundations are expected to have a larger impact on the water quality than other foundation concepts.
Mixing	Jacked foundations are expected to cause more turbulence at the seabed than other foundation types, and it is thus expected that jacket foundations will result in more mixing than other foundation types.

The evaluation above is summarised in Table 3.2.

Table 3.2 Summary of worst case evaluation for foundation type.

	Worst case foundation type			
	Driven steel monopile	Concrete gravity base	Jacket foundation	Suction buckets
Hydrodynamics		X		
Wave Conditions		X		
Coastal		X		
Morphology		X		
Sediment spill		X		
Water Quality ST		X		
Water Quality LT		X		
Mixing			X	

3.2.3 Foundation installation

The environmental impacts during installation of foundations are primarily related to sediment spill during dredging/excavation works. In this context the intensity of the dredging/excavation activities will influence the turbidity and concentration of suspended sediments in the water column, sedimentation rates and the duration of the environmental impact.

Removal of top soils and weaker (organic) soil layers will be performed with backhoe dredgers, and may involve up to two vessels operating simultaneously in different locations. Dredging/excavation works are expected to last two (2) days per foundation, meaning that dredging/excavation for 66 x 3 MW foundations will take 132 days for one dredger and 66 days for two dredgers.

Worst case evaluation:

Sediment Spill — The total spill volume and sedimentation will be unaffected by the number of dredgers working in parallel, but areas affected by more than one sediment plume will experience higher turbidity and sedimentation rates than other areas. Therefore, two (2) dredgers are expected to cause larger impacts than one (1).

Water quality ST — Sediment spill concentrations and water quality is interlinked, and it is thus expected that the water quality in the installation phase will be more affected by two (2) dredgers than one (1).

The evaluation above is summarized in Table 3.3.

Table 3.3 Summary of worst case evaluation for foundation installation operations.

	Number of dredgers in operation at the same time	
	1	2
Sediment spill		x
Water Quality ST		x

3.2.4 Cable installation

The environmental impacts during installation of inter-array and export cables are primarily related to sediment spill during dredging/excavation works. In this context the dredging/excavation procedure and intensity may influence the spill percentage as well as turbidity and sedimentation rates/thickness.

Inter-array and export cables are expected to be installed by jetting, in pre-dredged trenches or in a combination of the two, depending on ground conditions.

Trenching or jetting for export cables will last approximately 1-2 continuous months and involve one back hoe dredger or jetting ROV (Remotely Operated Vehicle).

Worst case evaluation:

Sediment Spill — During jetting very fine grained seabed material will tend to get suspended and washed away during dredging/excavation. Therefore, the spill during jetting is much higher than trenching performed with a backhoe dredger.

Water quality ST — Sediment spill volumes and water quality is interlinked, and it is thus expected that the water quality will be more affected by jetting than trenching.

The evaluation above is summarized in Table 3.4.

Table 3.4 Summary of worst case evaluation for cable installation operations.

	Cable installation operation		
	Jetting	Trenching	Combined Trenching and Jetting
Sediment spill	X		
Water Quality T	X		

3.2.5 Selection of worst case scenarios

The definition of “worst case” is given in the following, incorporating the outcome of the evaluation contained within this chapter.

Site Layout and Turbine Type

3 MW turbines are generally expected to cause larger environmental impacts than larger turbines.

3 MW turbines and layouts define the “worst case”

Foundation Type

Concrete gravity base foundations are expected to cause the largest environmental impact measured on all parameters aside from mixing.

Concrete Gravity Foundations define the “worst case”

Foundation Installation

High intensity dredging/excavation works with two backhoe dredgers working in parallel are expected to cause the largest environmental impact during installation of gravity base foundations. With up to two (2) vessels operating in parallel, seabed preparation for 66 x 3 MW turbine foundations will last 66 days.

Two dredgers working in parallel for 66 days define the “worst case” operations during installation of foundations

Cable Installation

Jetting of inter-array and export cables is expected to cause more spillage of fine sediments and possible release of toxic components, nutrients and organic contaminants than trenching.

Jetting for approximately 1-2 months with a jetting ROV’s is expected to cause the largest environmental impact during the installation operation

3.3 Alternatives

The EIA assessment is compiled on the “worst-case” scenario described in section 3.2 and will not be constrained to one exact definition of the project, but instead describe the boundaries and span of a project that incorporate the “most-likely” with a “worst-case” in mind. In this context the “worst-case approach” defines a “worst case alternative” (park layout, foundation type, turbine type and construction method) that would potentially cause the largest environmental impact. As such the “worst-case” approach envelopes a number of alternatives that may be considered mitigative to the potential environmental impacts of the “worst case alternative”.

The impacts of the “worst case alternative” will be assessed relative to a “0-alternative” which define a situation where the wind farm is not constructed.

3.3.1 “0-alternative”

The so-called “0-alternative” defines the situation where the wind farm is not constructed. In this case, the energy, that the wind park would have produced, will have to be produced by other and alternative sustainable energy sources, in order to reach the political goals set out by the Danish government. Such sustainable energy could be produced by wind parks at other locations or from other sources of sustainable energy. Several sources for sustainable energy have experienced a significant development through the recent years. However, compared to the development within wind farms, they have not achieved the same degree of efficiency, which would make them less effective alternatives. Therefore, it is assessed that the only realistic alternative to sustainable energy production at a wind farm at Vesterhav Nord would be an alternative location of the wind farm. The question of alternative location is dealt with in the set-up of this investigation, as six different wind park locations are investigated in parallel to the Vesterhav Nord OWF.

3.4 Method description

3.4.1 Wave modelling

Wave modelling is performed with a high resolution MIKE 21 SW FM model. The model is forced with high resolution wind fields from the atmospheric DMI-HIRLAM model and with wave boundary conditions from the regional hindcast wave model DMI-WAM (See descriptions in Appendix A).

The wave model is used to study the influence of the offshore wind farm on the wave climate, and provides the basis for assessing the potential impact to the adjacent coastline and seabed morphology. Furthermore, the wave climate is implemented in sediment plume modelling.

A schematic description of the inputs to the wave model is found in Figure 3.1 and a more detailed description of the wave modelling is provided in Appendix B.

Figure 3.1 Inputs to the MIKE 21 SW wave model.

Bathymetry

The bathymetry of the wave model is found in Figure 3.2. The bathymetry combines a detailed project survey with available surveys from the Danish Coastal Authority (KDI), Danish Geotechnical Institute (GEO) and the Danish model bathymetry of Farvandsvæsnet (FRV). The mesh is primarily detailed in high resolution at the project area.

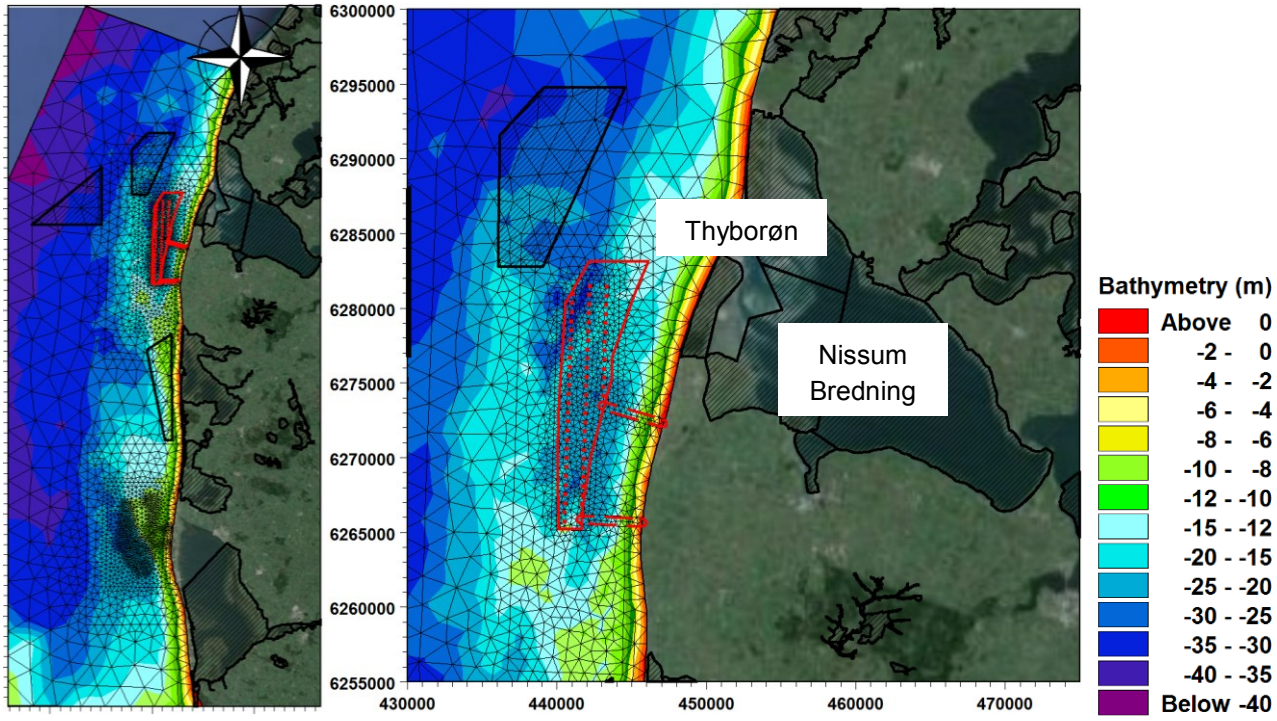

Figure 3.2 Model bathymetry at the OWF. Left: full domain and right: zoomed in the area. Wave modelling MIKE 21 SW FM model. Hatched areas with black frames show Natura 2000 areas.

Boundary Conditions

The input parameters for the wave model are the wind forcing and the wave conditions at the open boundaries of the model domain. Wave conditions are applied as integrated wave parameters (H_{m0}[3], T_p[4] and MWD[5]) from DMI-WAM along the four open boundaries of the model (see Figure 3.3). Wind conditions are applied as 2D wind fields in a 0.03° grid (1.9 km east/west and 3.3 km north/south resolution) and hourly time steps from the DMI-HILRAM model.

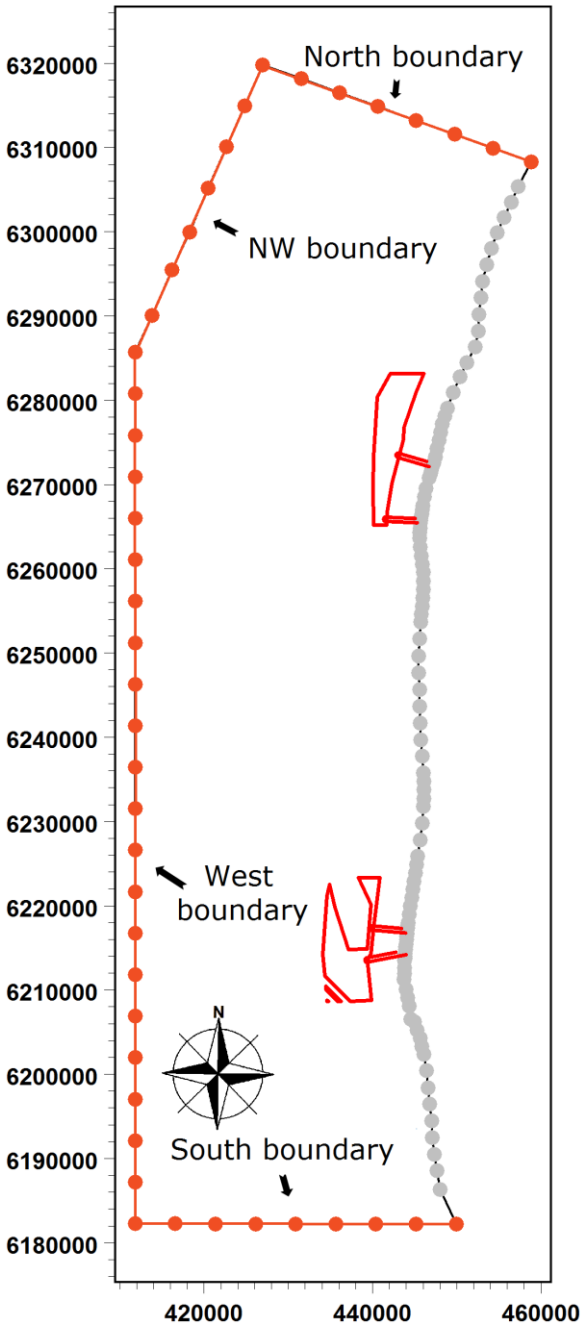

Figure 3.3 Definition of boundaries in the wave and hydrodynamic model domain.

[3] H_{m0} = spectral significant wave height
[4] T_p = Peak wave period
[5] MWD = Mean wave direction

Baseline

The wave conditions in Danish waters vary considerably from year to year, and it is thus important that the baseline define a period (calendar year) with relatively typical/average wave conditions at the project site and along the adjacent coastline.

The baseline year is selected based on the yearly average wave energy density during 8 full calendar years, compared to the average of all 8 years (2005-2012). The yearly average energy density is calculated based on the following formula:

$$E_{dir} = \sum_{t=0}^{1\,yr} H_{m0}(t)^2 \rho_w g \cdot \frac{1}{8} \qquad \text{for } dir - \frac{\Delta}{2} < MWD(t) \leq dir + \frac{\Delta}{2}$$

At Vesterhav Nord it is found that the year 2012 represents a typical year, as the wave energy corresponds well with the average yearly energy in an 8 year period from 2005 to 2012 (see Figure 3.4).

This typical year is used throughout the report, to assess the impact on the wave climate due to the presence of the OWF.

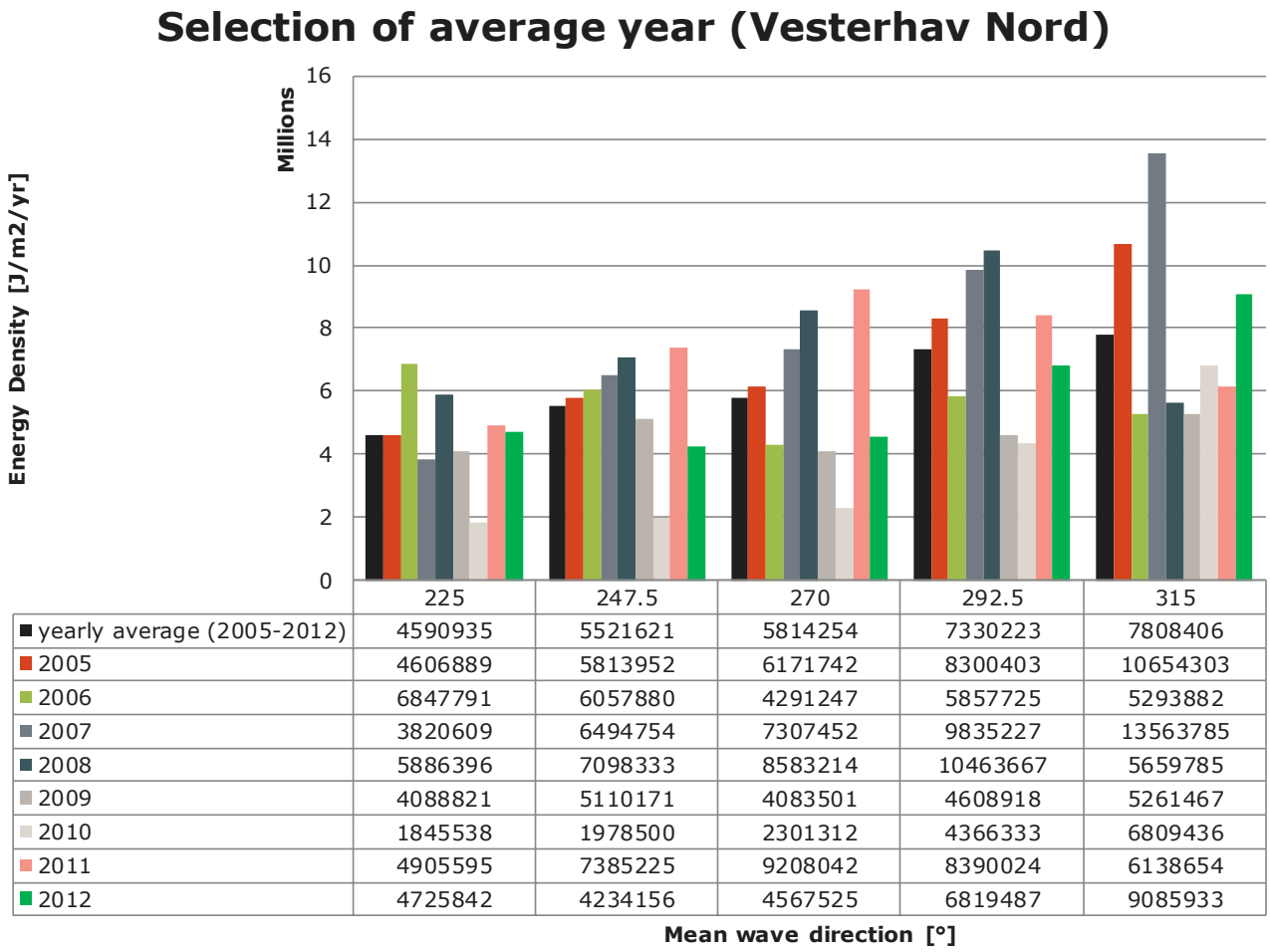

	225	247.5	270	292.5	315
yearly average (2005-2012)	4590935	5521621	5814254	7330223	7808406
2005	4606889	5813952	6171742	8300403	10654303
2006	6847791	6057880	4291247	5857725	5293882
2007	3820609	6494754	7307452	9835227	13563785
2008	5886396	7098333	8583214	10463667	5659785
2009	4088821	5110171	4083501	4608918	5261467
2010	1845538	1978500	2301312	4366333	6809436
2011	4905595	7385225	9208042	8390024	6138654
2012	4725842	4234156	4567525	6819487	9085933

Figure 3.4 *Selection of baseline conditions (typical "wave year") at Vesterhav Nord based on the yearly directional wave energy density, in a point at the centre of the Vesterhav Nord OWF. 8 years of wave data from DMI-WAM.*

Offshore wind farm

The influence of the wind turbines is included in the form of the *wind effect* and *diffraction/reflection*.

The *wind effect* is caused by the wind wake in lee of the wind turbines. Studies by RISØ of SAR[6] wind maps in and downstream of offshore wind farms have shown wind velocity deficits[7] of up to 10 % and wake persistency of at least 10 km [ref. /4/]. Figure 3.5 shows the wind velocity deficit in and downstream of the Horns Reef 1 offshore wind farm based on 19 satellite SAR wind maps. It is noted that the wind velocity deficit increases gradually inside the wind farm and peaks at around 10 % approximately 2-3 km downstream of the wind farm, after which the wake declines gradually with the distance from the wind farm.

The *wind effect* is conservatively included in the wave model by reducing the wind speed in the 2D wind field (from DMI-HIRLAM) by 10 % inside the wind farm and 10 km downstream, as shown in Figure 3.5.

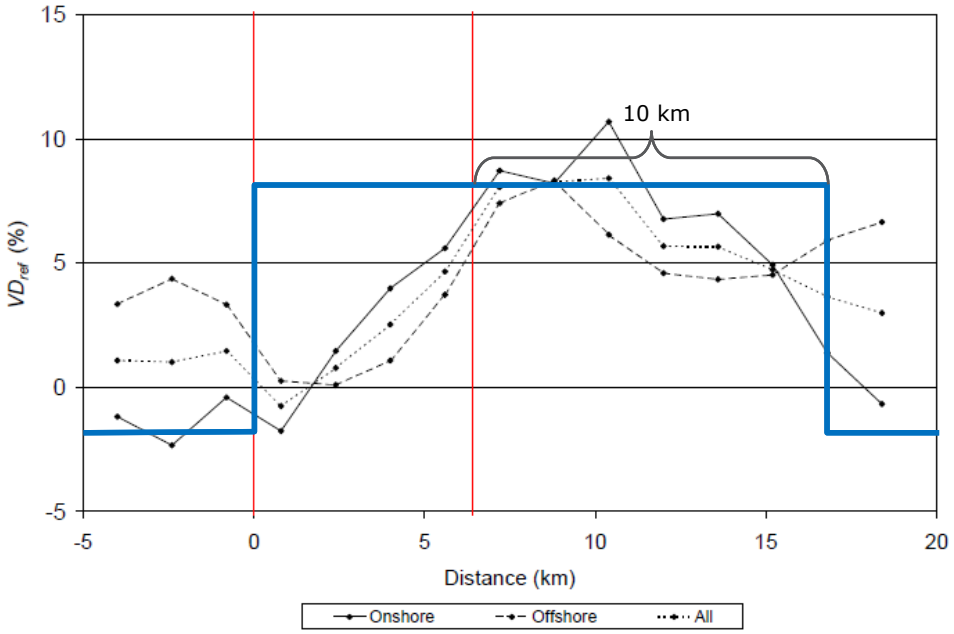

Figure 3.5 *Average wind velocity deficit (VD) at Horns Reef 1 wind farm obtained from 19 satellite SAR wind maps. Vertical red lines indicate maximum wind farm boundaries [ref. /4/]. The blue line indicates the wind velocity deficit applied in the wave model.*

The *diffraction/reflection effect* is caused by the physical presence of the wind turbine foundations in the wave field. The effects of the foundations are implemented in the MIKE 21 SW as energy dissipation at each wind turbine position [ref. /5/].

[6] SAR = Synthetic Aperture Radar

[7] Velocity Deficit (VD) = $(U_{freestream} - U_{wake})/U_{freestream}$ x 100%

The geometry of the gravity based foundations is simplified to a circular structure of 14 m diameter. This corresponds to the average diameter of the shaft and base of the gravity based foundation described in section 2.3.

Calibration

The wave model is calibrated against measured wave conditions at Fjaltring and Nymindegab (see Figure 3.6). Six months of measurements are used for calibration (May to October 2012).

The wave model calibration consists of fine tuning the model calibration parameters until the model produces a good fit between the simulated and measured wave conditions at the position of the measurements.

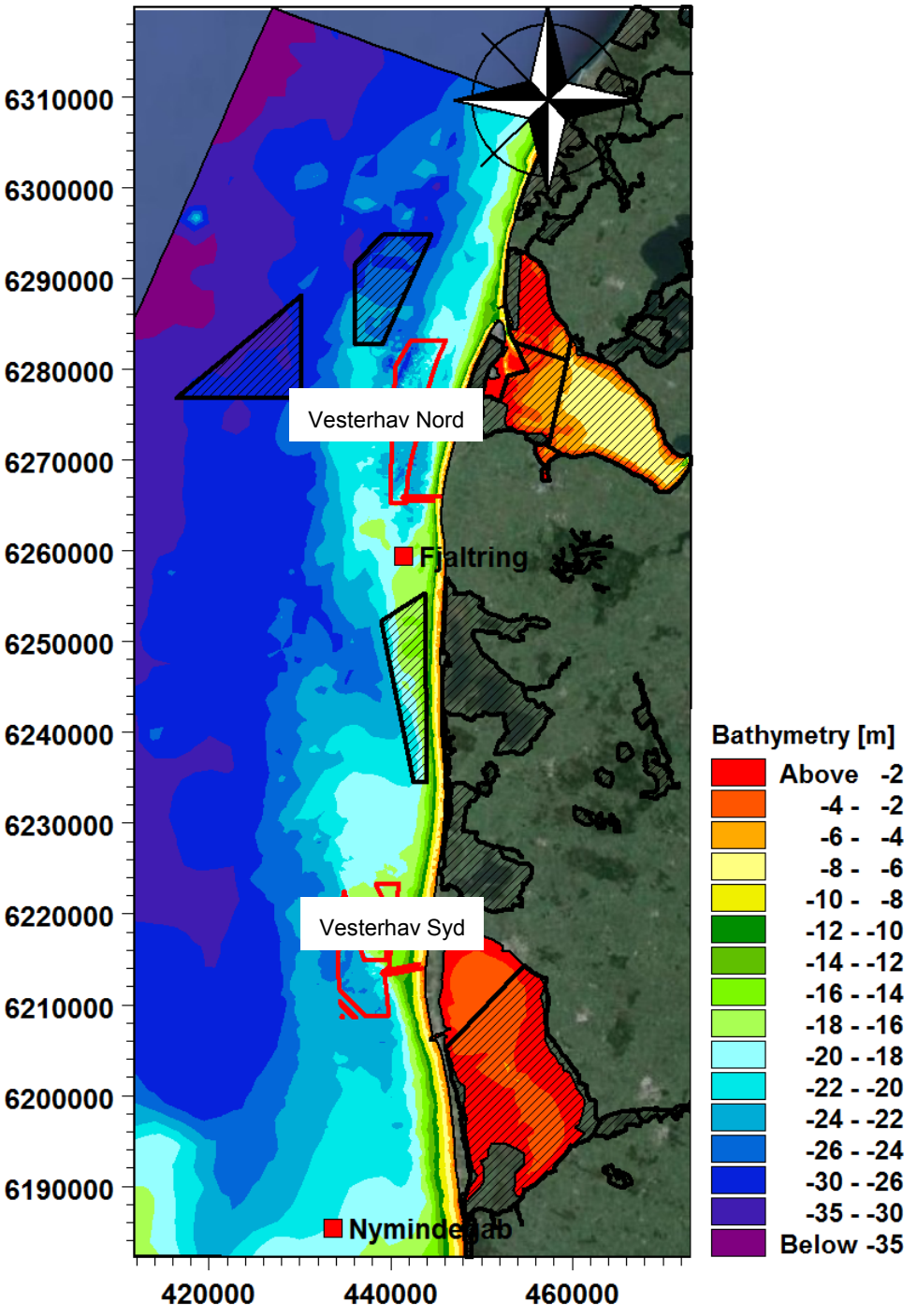

Figure 3.6 *Location of wave measurements. Hatched areas with black frames show Natura 2000 areas.*

Results

The typical year (2012) is modelled with and without the presence of the offshore wind farm and the two results are compared in order to quantify the influence of the wind farm on the wave conditions. Results are presented in section 4.3 and 6.1.

3.4.2 Hydrodynamic modelling

The hydrodynamic model MIKE 21 HD FM is driven by wind and pressure fields from DMI's atmospheric model DMI-HIRLAM and boundary conditions from DMI's regional current model DMI-HBM. Furthermore, because the waves at the west coast of Jutland will give rise to significant wave induced currents compared to tide and meteorological induced currents; waves (radiation stresses) from the MIKE SW model is included in the hydrodynamic model. It is noted that the effect of wave induced currents are only relevant in the nearshore coastal areas – the surf zone; i.e. at water depths of less than approximately 6-7 m and thus not inside the OWF.

The hydrodynamic model is used to study the influence of the OWF on currents and water levels, and form the basis of evaluating the seabed morphology and water quality. Furthermore the results are applied in the sediment plume modelling.

A schematic description of the inputs to the hydrodynamic model is shown in Figure 3.7 and a more detailed description of modelling is found in Appendix C.

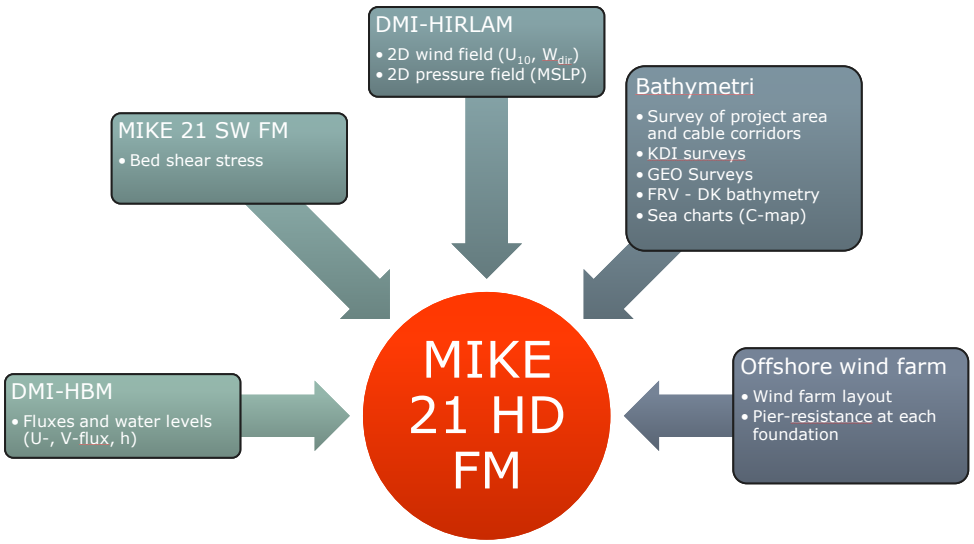

Figure 3.7 *Input for MIKE 21 HD FM current model, used to study the effects of the OWF on the currents and water levels.*

Bathymetry

The bathymetry of the hydrodynamic model is shown in Figure 3.8. The bathymetry combines a detailed project survey with available surveys from the Danish Coastal Authority (KDI), Danish Geotechnical Institute (GEO) and the Danish model bathymetry of Farvandsvæsnets (FRV). The mesh is primarily detailed in high resolution at the project area and at the coast in the surf zone.

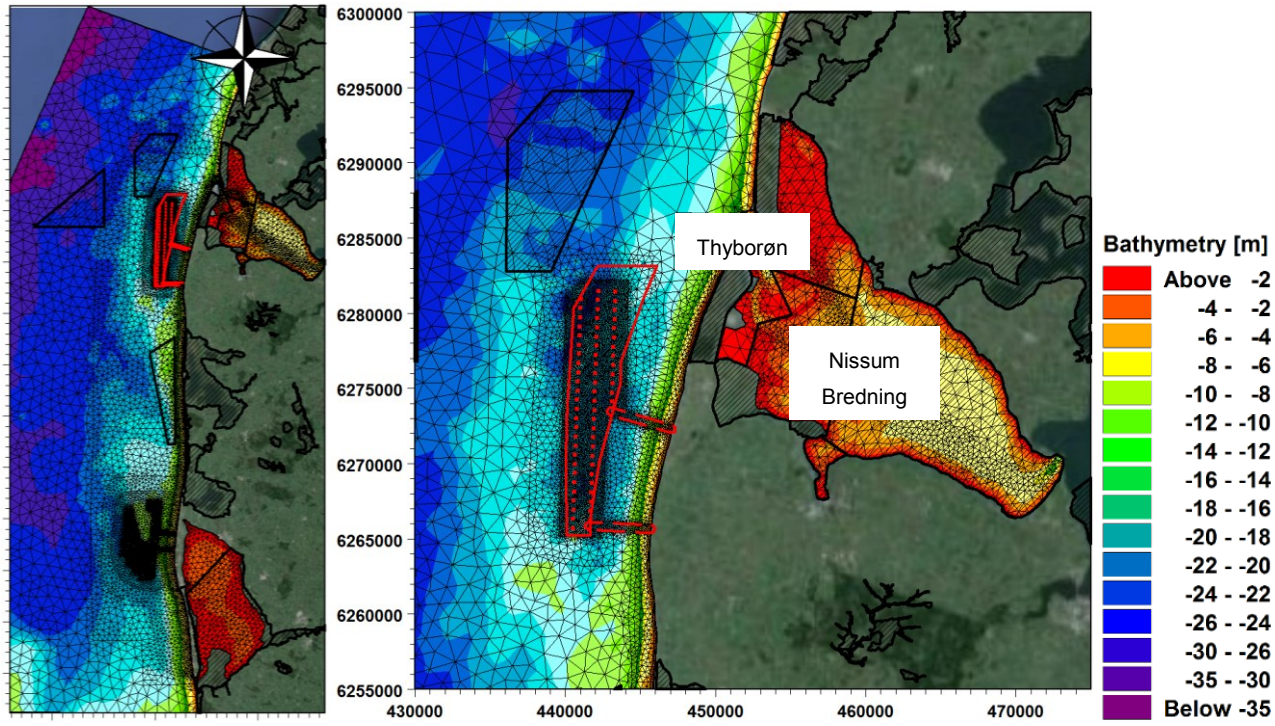

Figure 3.8 *Hydrodynamic model bathymetry at the OWF. Left: full domain and right: zoomed in the area. Hydrodynamic modelling (MIKE 21 HD FM model). Hatched areas with black frames show Natura 2000 areas.*

Boundary Conditions

The forcing of the hydrodynamic model comprises wind forcing, barometric pressure and water levels at the open boundaries of the model domain.

Water level variations along the four open boundaries (see Figure 3.3) are applied from DMI's regional hydrodynamic model (DMI-HBM) at 4.5-5 km intervals. Wind/pressure fields are applied in a 2D grid from DMI's atmospheric model DMI-HIRLAM in 0.03° grid spacing.

Baseline

The baseline conditions consist of a three month period with varying current directions and speeds, corresponding to the duration of the effects that are to be studied in the EIA.

The basis period is selected based on two years of data from DMI-HBM. The three month period shall represent average flow patterns in the project area in terms of current directions and magnitudes.

Based on the evaluation the reference period is selected as 01.06.2012 to 30.08.2012. The reference period is used throughout the report, to assess the sediment spill, flow blocking and the impact on the currents due to the presence of the OWF.

Current roses at the wind farm, covering the two year dataset and the reference period are presented in Figure 3.9 and Table 3.5.

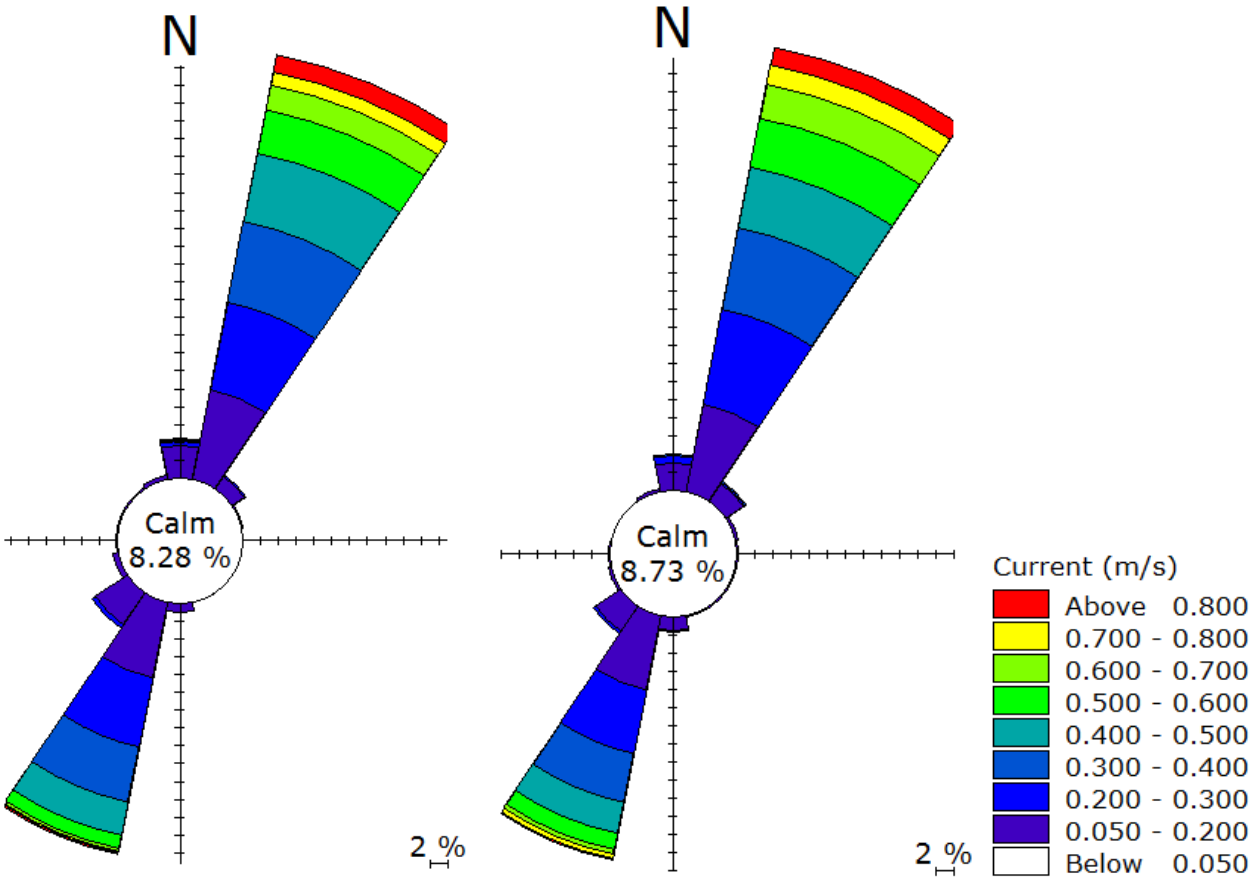

Figure 3.9 *Current rose during three month reference period and two year dataset at [56.58°N, 8.04°E], 22.5 m water depth. Dataset: DMI-HMB hindcast.*

Table 3.5 *Current statistics during reference period and two year dataset at [56.58°N, 8.04°E], 22.5 m water depth. Dataset: DMI-HMB hindcast.*

		Current vector component [m/s]		
	Current direction	Minimum	Maximum	Average
2011 - 2012	East/West, U	-0.51	0.64	0.03
	North/South, V	-1.25	2.19	0.10
Jun. 2012 - Aug. 2012	East/West, U	-0.39	0.45	0.03
	North/South, V	-0.90	1.33	0.09

Offshore wind farm

The influence of the offshore wind turbines on the hydrodynamic conditions (currents and water levels) is modelled in MIKE 21 HD FM as pier-resistance [ref. /6/].

The geometry of the gravity based foundations is implemented based on the dimensions provided in section 2.3 and the geometric scheme shown in Figure 3.10. Hence, the varying diameters and the influence of water depth at the location

of individual turbines are implemented in the geometric representation of the foundation in the model.

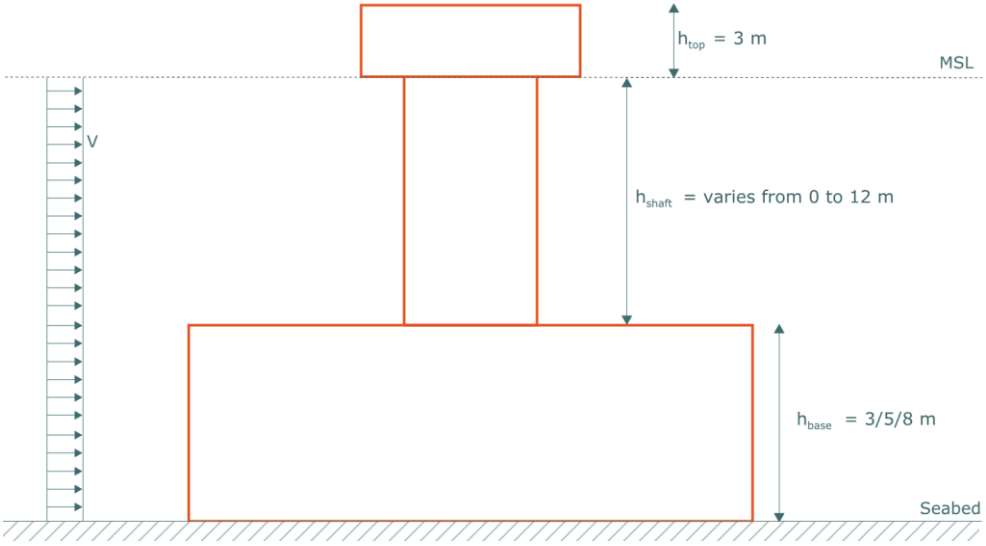

Figure 3.10 Geometric scheme of gravity based foundations.

The resistance to the flow due to the turbine foundations is included in terms of the drag force, *F*, which acts against the current direction:

$$F = \frac{1}{2}\rho_w \gamma C_D A_e U^2$$

Where,

- γ: Streaming factor, γ = 1.02
- C_D: Drag coefficient
- A_e: Cross area of pier exposed to current
- ρ_w: Water Density
- U: Current speed

Calibration

The hydrodynamic model is calibrated against water level measurements from four locations (Thyborøn, Ferring, Torsminde and Hvide Sande), see Figure 3.11. The model is simulated for a period of three months (June to August 2012) and model parameters are fine-tuned in order to minimize the deviation between the measured and modelled values within physically reasonable limits. The calibration is presented in Appendix C.

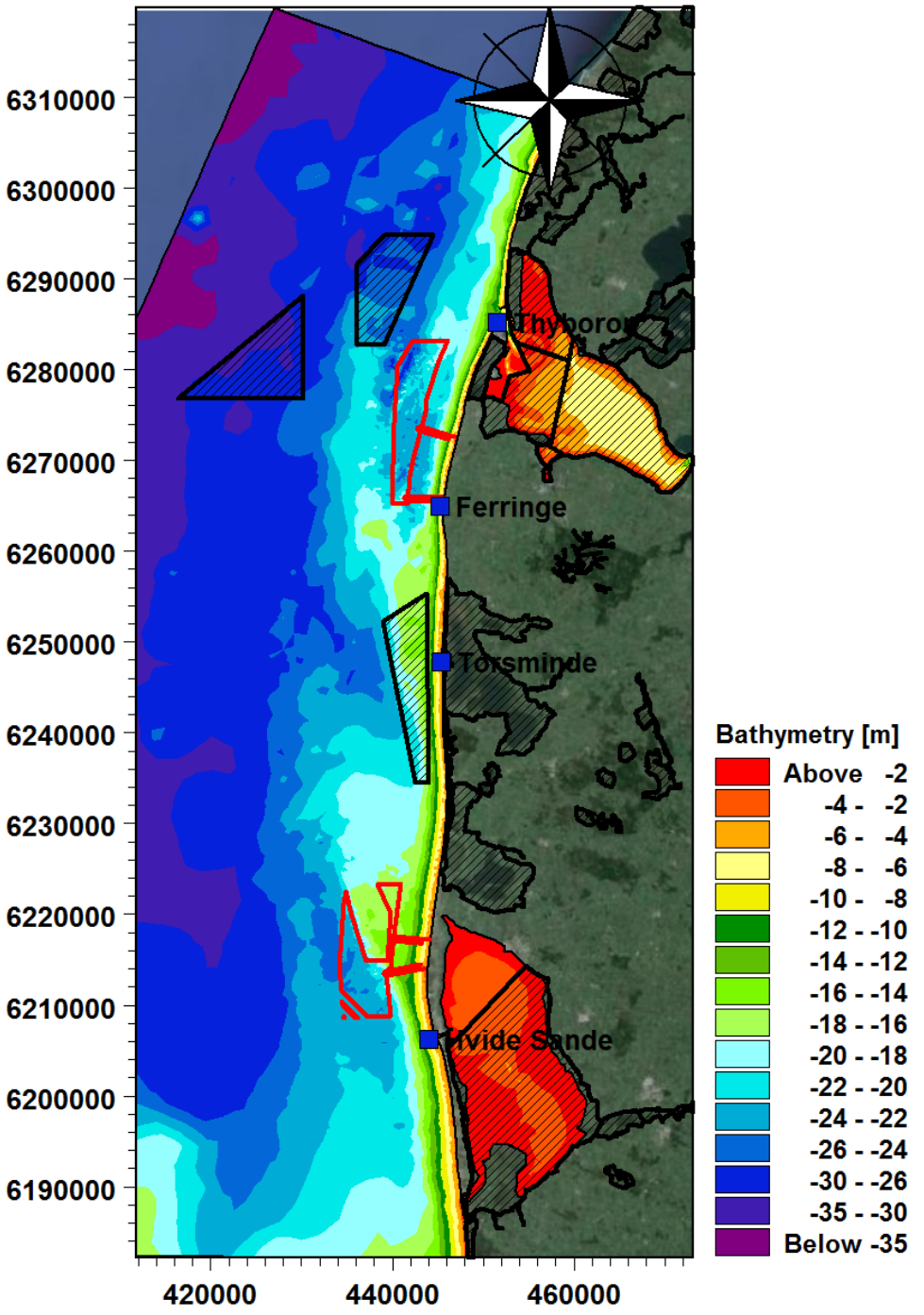

Figure 3.11 *Location of water level measurements near the OWF. Hatched areas with black frames show Natura 2000 areas.*

Results

The model period (June to August 2012) is modelled with and without the presence of the offshore wind farm and the two results are compared in order to quantify the hydrodynamic impact of the wind farm. Results are presented in section 4.2 and 6.2.

3.4.3 Coastal impact

The site of the Vesterhav Nord OWF is situated at the middle of the exposed Danish West Coast at Thyborøn. The beaches adjacent to the OWF are naturally eroding sandy beaches.

The purpose of the coastal impact assessment is to quantify the potential impact that the OWF may cause to the adjacent coast. Downwind of the windfarm, the coastline could erode or accrete due to changes in wave conditions induced by the installation of the OWF.

The coastal impact is assessed through the combined analysis of landscape maps, aerial photos, images from the coast and numerical modelling of waves with MIKE21 SW and longshore sediment transport with LITDRIFT. LITDIRFT is a part of the LITPACK software package developed by DHI (see http://www.mikebydhi.com/Products/CoastAndSea/LITPACK/SedimentTransport.aspx)

Method

Landscape map

The starting point for the coastal impact assessment is an assessment of the landscape in the area at and adjacent to the OWF. The landscape map of Per Smed is used, ref. /7/. The map shows the dominant landscape features and thus provided important information on how the landscape was formed and the type of sediment and geology found along the coast. The information indicates how sensitive the coast is to changes in wave climate etc.

Aerial photos

Aerial photos are ideal to assess the present nature of the coast in a large area such as at the Danish West Coast. The aerial photos show details such as type of sediment at the beach and in the nearshore environment, vegetation lines and coastal structures etc. Aerial photos are applied in the coastal impact assessment to describe the existing coast at south of Thyborøn.

When comparing historic and recent aerial photos or maps it is possible to assess the historic development of the coast. The historic shoreline development shows how dynamic the coast is and which area that are eroding and accreting.

The Danish Coastal Authorities have published an assessment of the historic shoreline development in Denmark based on maps from around year 1900 and aerial photos from around year 2000, ref. /8/. The results are presented in Google Earth.

The assessment indicates how the coast has developed in the past and thus how it will develop naturally in the near future without the OWF, which is an important reference for evaluating the potential impact of the OWF.

The Danish Coastal Authorities are undertaking beach nourishment along this coast, which has reduced the actual erosion.

Images from the coast

In order to get an impression of the scale and nature of the coastal features and beaches a series of in house images from the site and images from Google Earth have been included in the assessment.

Modelling

Wave modelling

The coastal impact of the OWF is mainly through a reduction in wave energy and wind speed at the down drift side of the installation.

The influence of the OWF on the wave climate are modelled applying the wave model MIKE 21 SW FM.

The impact assessment are focused near the OWF and towards the adjacent coast.

Sediment transport modelling

The influence of the OWF on the sediment transport capacity are studied in detail in the coastal model LITDRIFT.

Gradients in the sediment transport capacity defines the erosive power (energy) of the waves and currents at a given locations. The capacity defines the quantity of sediment that can potentially be mobilized and transported by the littoral current, in a given location if sufficient non-cohesive bed material is available. In many locations, the sediment transport capacity is higher than the actual sediment transport, because the sediment is not available, either due to the presence of coastal structures that block the sediment transport, or due rocky or cohesive sediments in the beach profile. Therefore, it is considered a "worst case" to evaluate the change in sediment transport rates based on the transport capacity.

The LITDRIFT modelling provides qualitative and quantitative information on the nearshore sediment transport patterns. LITDRIFT is used to identify where sediment transport is occurring in the beach profile and in what quantities and directions.

In particular the purpose of the sediment transport modelling is to assess the average annual gross and net longshore sediment transport capacity along the most affected coastline before and after the construction of the OWF and to compare with the natural sediment transport in the area.

Boundary conditions

The following parameters are the main inputs for LITDRIFT:

Wave climate

- Beach profile
- Sediment characteristics
- Bed roughness

This information is provided from wave modelling and the project specific geophysical survey, ref. /9/.

LITDRIFT is applied for the baseline calendar year (2012), which is considered typical at the project location. The sediment transport capacity is modelled with and without the OWF for a series of characteristic shoreline orientations along the coast. Additionally, an 11 year time series is modelled to assess the natural variability of the littoral drift from one year to the other in relation to the impact of the OWF.

The analysis is based on one beach profile, where the impact of the OWF is assessed to be larger than elsewhere along the coast (see Figure 3.12). Waves from WNW are predominant, and that the influence of the OWF on the near shore wave climate will be most significant in the selected location.

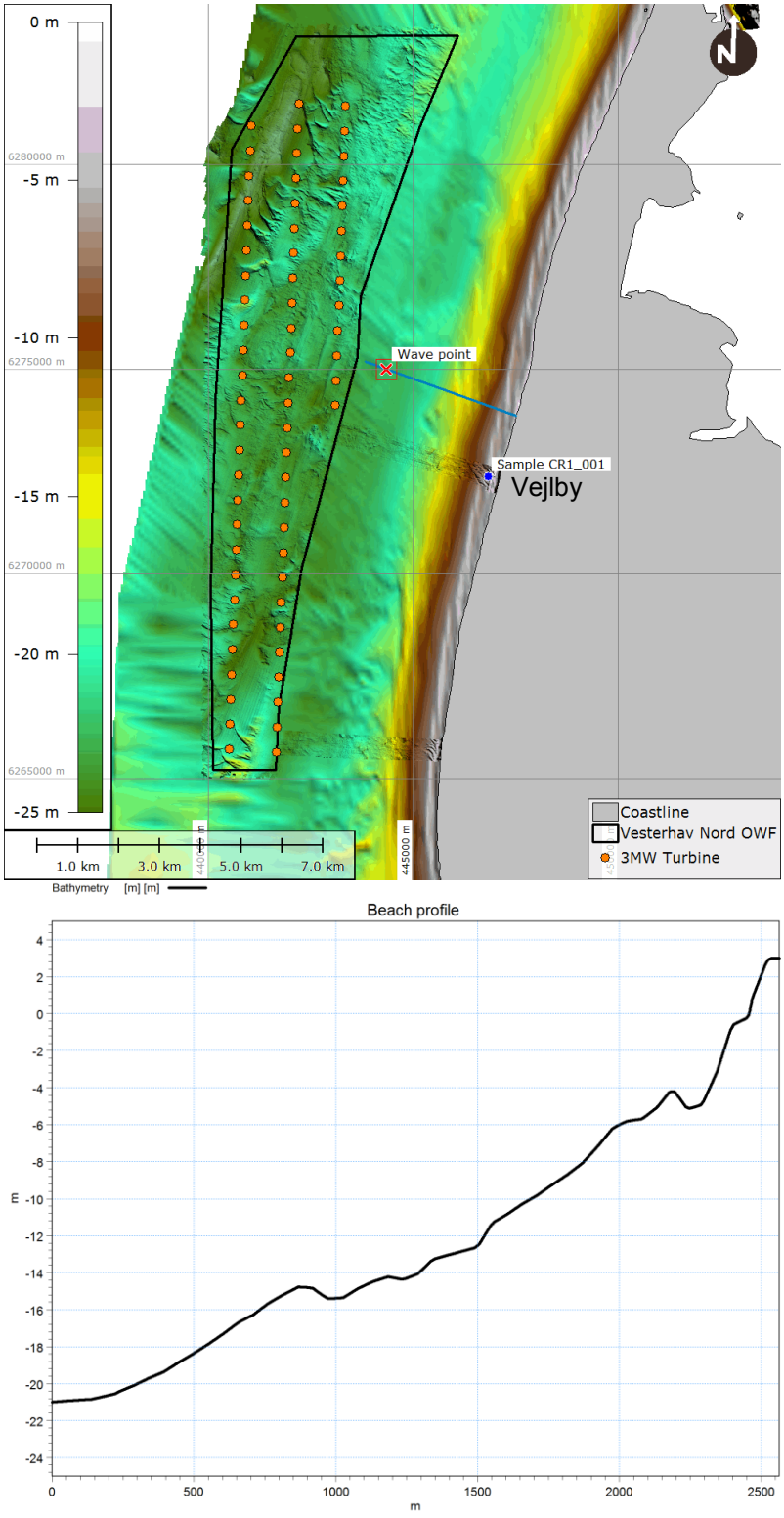

Figure 3.12 Location of Beach Profile 1 modelled in LITDRIFT.

Results

The results of the sediment transport modelling are compared in order to quantify the influence of the OWF. Results are presented and assessed section 6.5.

3.4.4 Morphological impact on seabed

The purpose of the activity is to quantify the effects of the OWF on the adjacent seabed. This includes whether the OWF can have an effect on the natural sediment transport patterns and possibly lead to erosion of or deposition on the seabed.

Method

Based on the seabed composition, surveys from 2008, 2012 and 2013 and available literature about the morphology of the nearshore area of the Danish west coast, the natural morphological development of the seabed inside the OWF area is established. The effect of OWF on the natural morphological development is evaluated based on change in hydrodynamic forcing caused by the wind turbine foundations. The change in hydrodynamic forcing is based on MIKE 21 HD FM modelling performed with and without the presence of the OWF.

3.4.5 Suspended sediment concentrations and sedimentation of spilled sediments

Sediment spill during dredging/excavation works and jetting of cables is modelled in the MIKE 21 MT (Mud Transport) model. Wave conditions and hydrodynamics originate from the calibrated MIKE 21 SW FM and HD FM models, respectively.

The model is used to study sediment concentrations, sedimentation quantities and rates of spilled sediments during installation works and provide the input for assessing the potential environmental pressures on flora and fauna.

A schematic description of the inputs to the spill model is found in Figure 3.13.

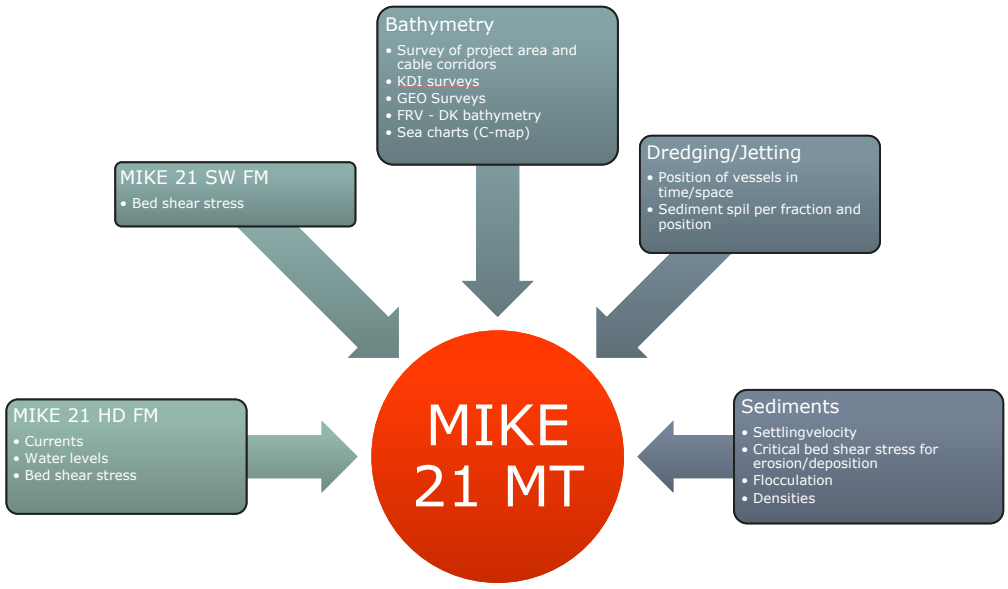

Figure 3.13 Input for the MIKE 21 MT sediment spill model.

Bathymetry

The model uses the same bathymetry as the hydrodynamic model. Hence, the spatial resolution of the computational mesh varies from an average element size of ~ 100 m inside the wind farm area to ~ 1800 m in offshore regions (see Figure 3.8).

Seabed characteristics

An overview of the bathymetry and sample locations is shown in Figure 3.14.

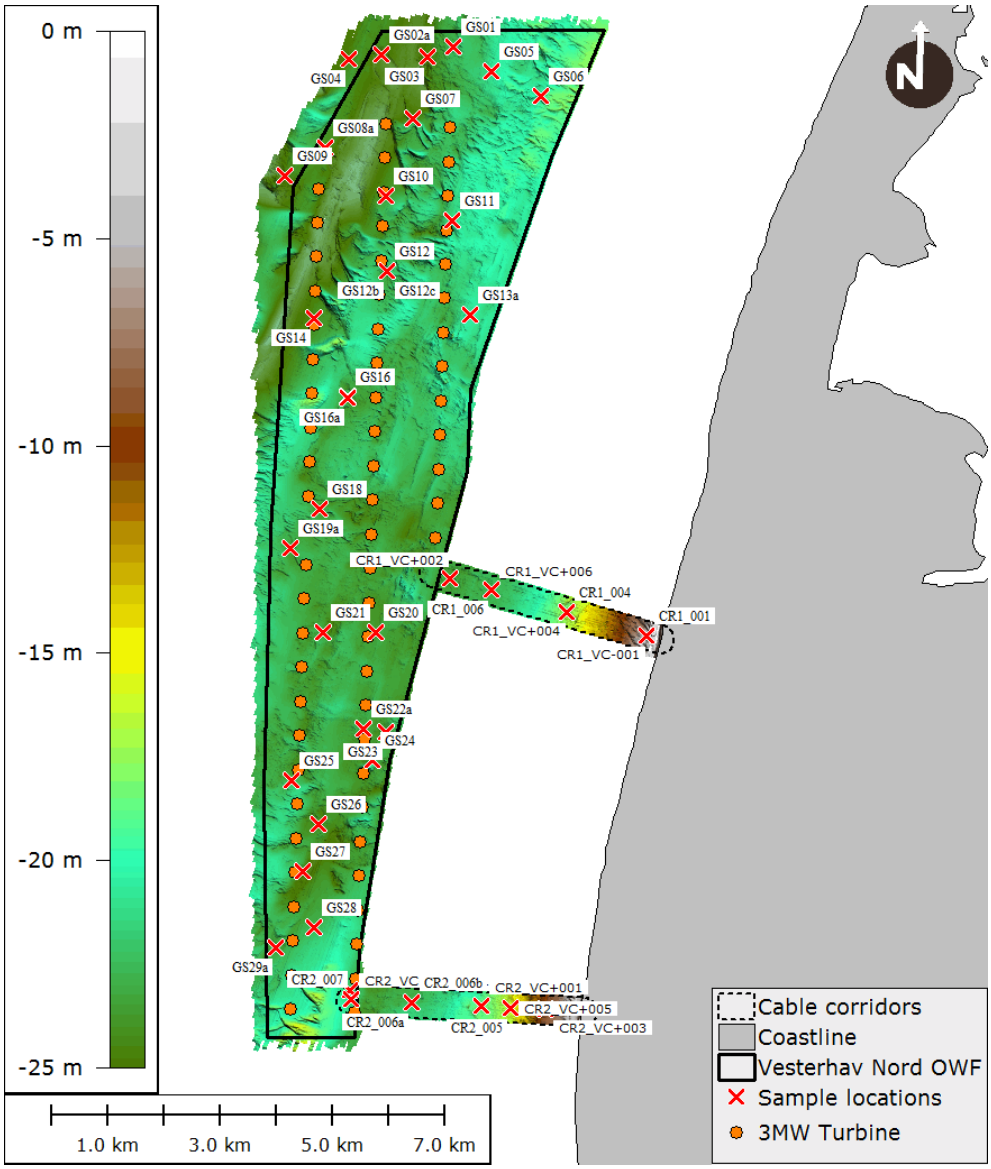

Figure 3.14 Vesterhav Nord OWF layout (3 MW) and location of geotechnical samples [ref. /10/ /9/. Depths are relative to DVR90.

The seabed and subsurface sediment in the OWF area consists mainly of sand and gravel. In the cable corridors, the grain size shifts to silt and clay, with some gravel content.

Grain size distributions analysed based on the geophysical survey [ref. /10/ /9/] are summarised in Table 3.6.

Sediment spill scenarios are based on the average sediment characteristics as described in Appendix E. The scenarios will thus not consider the spatial variation of the seabed substrate. This simplification is justifiable because sediment samples and wind turbines are evenly distributed in the project area. Moreover, the computed average sediment characteristics are considered representative for the site according to the associated computed standard deviation (see Table 3.6).

Table 3.6 Grain size distribution at Vesterhav Nord OWF [ref. /10/ /9/].

Classification	Sample	Coarse silt 31-63 µm	Medium silt 15.6-31 µm	Fine silt 7.8-15.6 µm	Very fine silt 3.9-7.8 µm	Clay i 2-3.9 µm	Clay ii <2 µm	Loss on ignition
SAND	GS01	1%	0%	0%	0%	0%	0%	0.5%
SAND	GS02a	2%	0%	0%	0%	0%	0%	0.7%
GRAVEL	GS03	9%	0%	0%	0%	0%	0%	1.5%
SAND	GS04	2%	0%	0%	0%	0%	0%	0.7%
SAND	GS05	1%	0%	0%	0%	0%	0%	0.3%
SAND	GS06	1%	0%	0%	0%	0%	0%	0.3%
SAND	GS07	5%	0%	0%	0%	0%	0%	0.3%
CLAY	GS08	5%	9%	9%	15%	10%	29%	4.6%
CLAY	GS08a	10%	4%	6%	12%	8%	28%	4.2%
SAND	GS10	2%	0%	0%	0%	0%	0%	0.7%
GRAVEL	GS11	1%	0%	0%	0%	0%	0%	0.9%
GRAVEL	GS12b	0%	0%	0%	0%	0%	0%	0.8%
GRAVEL	GS12c	0%	0%	0%	0%	0%	0%	0.5%
SAND	GS13a	0%	0%	0%	0%	0%	0%	0.3%
SAND	GS14	3%	0%	0%	0%	0%	0%	0.8%
SAND	GS16	4%	0%	0%	0%	0%	0%	0.6%
SAND	GS16a	1%	0%	0%	0%	0%	0%	0.3%
SAND	GS18	0%	0%	0%	0%	0%	0%	0.3%
SAND	GS19a	1%	0%	0%	0%	0%	0%	0.3%
SAND	GS20	3%	1%	0%	1%	0%	5%	1.7%
GRAVEL	GS21	1%	0%	0%	0%	0%	0%	1.0%
SAND	GS22a	3%	0%	0%	0%	0%	0%	0.9%
GRAVEL	GS23	1%	0%	0%	0%	0%	0%	0.9%
SAND	GS24	4%	0%	0%	0%	0%	0%	1.0%
SAND	GS25	2%	0%	0%	0%	0%	0%	0.9%
SAND	GS27	3%	0%	0%	0%	0%	0%	0.7%
SAND	GS28	3%	0%	0%	0%	0%	0%	1.0%
GRAVEL	GS29a	10%	0%	0%	0%	0%	0%	2.9%
SAND	GS30	1%	0%	0%	0%	0%	0%	0.3%
CLAY	CR1+002	5%	28%	17%	12%	6%	17%	6.5%
CLAY TILL	CR1+004	3%	9%	4%	7%	7%	21%	5.9%
SILT	CR1+006	9%	17%	10%	15%	13%	33%	9.3%
SAND	CR1-001	0%	0%	0%	0%	0%	0%	0.3%
CLAY TILL	CR2+001	3%	6%	5%	6%	6%	24%	3.4%
SAND	CR2+003	3%	0%	0%	0%	0%	0%	0.5%
CLAY TILL	CR2+005	3%	6%	6%	6%	7%	22%	2.1%
GRAVEL	CR2+006b_1.2D	1%	0%	0%	0%	0%	0%	0.8%
SAND	CR2+006b_1.3D	4%	0%	0%	0%	0%	0%	0.8%

Classification	Sample	Coarse silt 31-63 µm	Medium silt 15.6-31 µm	Fine silt 7.8-15.6 µm	Very fine silt 3.9-7.8 µm	Clay i 2-3.9 µm	Clay ii <2 µm	Loss on ignition
SAND	CR2+007	2%	0%	0%	0%	0%	0%	0.4%
Average		**2.9%**	**2.0%**	**1.4%**	**1.9%**	**1.4%**	**4.5%**	**1.6%**
Standard deviation		2.7%	5.5%	3.6%	4.3%	3.3%	9.8%	2.0%

Fractions	**Fraction 1 "Coarse Silt" 31-63 µm**	**Fraction 2 "Medium – fine silt" 3.9-31 µm**	**Fraction 3 "Clay" <3.9µm**	**"Fines" <63 µm**
Average	2.9%	5.3%	5.9%	14.0%

Seabed preparation for installation of concrete gravity base foundation

Preparation of the seabed by removal of the topsoil and replacement by a stone bed is normally required prior to installation of the worst case-defined GBS-foundations. Depending on the seabed/ground conditions, water depth and available equipment, the seabed preparation can be performed in the following sequence:

- Removal of the top surface of the seabed to a level where undisturbed soil is encountered
- Gravel is placed into the excavated hole to form a firm level base

The quantities for seabed preparation depend on the seabed/ground conditions including variations within the area of the wind farm. Quantities are presented in Table 3.7 for two different sizes of turbines considering the expected average water depth in the offshore wind farm.

Table 3.7 General estimate of dredging/excavation for gravity base foundation.

Gravity base	Vesterhav Nord	
Average water depth (and range) [m]	20 (15-25)	
Wind turbine size (number of turbines)	3.0 MW (66)	10.0 MW* (20)
Size of excavation (diameter) [m]	25-28	40-50
Volume of excavation [m³] (per foundation)	1,200-1,600	2,000-3,200

* rough estimate

The excavated material may be used as ballast within the gravity base structures or loaded onto split-hopper barges and transported to use elsewhere or to an approved disposal site at sea.

The excavation may be carried out by dredger or using a back-hoe excavator from a barge. The approximate duration of dredging/excavation (average 2 m depth) is expected to be 2 days for each gravity base.

The spill scenarios will be based the installation of 66 x 3 MW turbines, because this will result in a larger total volume of dredging/excavation and thus larger spill volumes than installation of 20 x 10 MW turbines. dredging/excavation works for 66 x 3 MW gravity based foundations of 1,600 m^3 per foundation is considered “worst-case”.

Furthermore, the scenarios will assume that dredging/excavation is performed at two foundations in parallel (by two dredgers). This assumption is considered “worst -case” because intense dredging/excavation activities result in larger turbidity.

The experience of “Sund og Bælt” from the Øresund bridge project was, that backhoe dredgers cause 2.7-3.9 % of spill when dredging in clay till (see Table 3.8). The “worst case” assumption is that 5 % of the material is spilled, and that all spill will be particles smaller than 63 µm. The gradation and volume of the spill is defined in Table 3.9. It is assumed that the spill will occur at the water surface.

Table 3.8 Measured sediment spill for all dredging activities during the Øresund bridge project [ref. /11/].

Dredging Area	Dredged amount	Spill						Equipment	Dominating material	Typical layer thickness	Dredging period
		Dredging	Reclama-tion	Total	Dredging	Reclama-tion	Total				
	(m3)	(ton)	(ton)	(ton)	(%)	(%)	(%)	(-)	(-)	(m)	(ww/yy)
Peninsula Harbour	86.000	7.288	71	7.359	4,5%	0,0%	4,5%	Dipper	Limestone	1 - 2	45/95-49/95
Island harbour no. 1	179.000	8.469	1.027	9.496	2,4%	0,3%	2,7%	Dipper	Clay till	1 - 3	02/96-18/96
Island harbour no. 3	41.000	1.258	138	1.396	1,6%	0,2%	1,7%	Dipper	Clay till	2 - 3	14/96-15/96
South west access channel	263.000	14.666	787	15.452	2,8%	0,2%	3,0%	Dipper	Clay till	1 - 2	49/95-19/96
CD#3-1	632.000	23.411	2.082	25.493	1,9%	0,2%	2,1%	Dipper	Clay till	1 - 2	19/96-35/96
East access channel	201.000	15.128	1.211	16.340	4,0%	0,3%	4,3%	Dipper	Clay till	0.5 - 2	10/96-15/96
Flinte Channel, central area	217.000	11.142	623	11.764	2,7%	0,2%	2,9%	Dipper	Clay till	0.5 - 1	42/95-18/96
Tunnel Trench (Castor)	2.189.000	167.789	2.506	170.295	4,0%	0,1%	4,1%	Cutter	Limestone	10 - 13	29/96-35/97
CD#1	207.000	33.292	162	33.454	8,6%	0,0%	8,6%	Cutter	Limestone	1 - 3	48/96-51/96
CD#3-2	680.000	59.578	2.613	62.191	4,5%	0,2%	4,7%	Cutter	Clay till	2 - 3	24/97-34/97
Flinte Channel, other areas	2.050.000	113.931	9.352	123.284	2,9%	0,2%	3,1%	Back-hoe	Clay till	0.1 - 1	16/97-52/98
Tunnel Trench (back-hoe)	68.000	2.323	92	2.416	1,8%	0,1%	1,9%	Back-hoe	Limestone	10 - 12	20/98-34/98
Drogden Construction channel	133.000	12.582	892	13.475	5,0%	0,4%	5,4%	Back-hoe	Limestone	0.1 - 1	14/97-20/97
East Construction channel	164.000	11.016	2.770	13.786	3,4%	0,9%	4,3%	Back-hoe	Clay till	0.5 - 2	30/96-34/96
Drogden Navigation channel	243.000	12.548	326	12.874	2,7%	0,1%	2,8%	Back-hoe	Clay till	0.1 - 1	33/97-48/98
Access channel Lernacken	309.000	23.578	1.046	24.624	3,9%	0,2%	4,0%	Back-hoe	Clay till	2 - 4	41/96-24/97
Foundation pits for Bridge piers	295.000	30.847	3.717	34.563	5,3%	0,6%	5,9%	Back-hoe	Limestone	10	46/96-10/99
Total	7.957.000	548.846	29.414	578.261	3,6%	0,2%	3,8%				

Table 3.9 Spill gradation and volume per foundation.

	Fraction 1 "coarse silt"	Fraction 2 "medium – fine silt"	Fraction 3 "clay"	Total
% of all	1.0%	1.9%	2.1%	5.0%
% of spill	20%	38%	42%	100%
Dry density [kg/m^3]	1,600	1,600	1,600	-
Spill [m^3]	16	30	34	80
Spill [kg]	26,000	48,000	54,000	128,000

Jetting of cables

The installation of the export cables is assumed to be carried out by a specialist cable laying vessel, with the cables stored on a turn-table, designed to carry the necessary lengths and maintain the minimum bend radius.

All the submarine cables, both array and export cables will be buried to provide protection from fishing activity, dragging of anchors etc.

Depending on the seabed condition the cable will be jetted, ploughed, installed in a pre-excavated trench or rock covered for protection. However, as a "worst case" assumption jetting will be assumed for the sediment spill study.

Water jetting is a cable laying protection method in which an underwater machine (usually a ROV) that is equipped with water jets fed by high power water pumps liquefy the sediment below the cable, allowing it to sink to a specified depth (dependent on the penetrating length of the swords), after which coarse sediments are deposited.

The width of the seabed affected by the jetting operation itself will be in approx. 0.7-1.2 meters depending on the size of cable and the jetting equipment used. A sketch of the jetted trench with indicative dimensions is provided in the *Technical Project Description* [ref. /1/] shown in Figure 3.15. The jetting trench has a dimension of approximately 1.6 m^3/m.

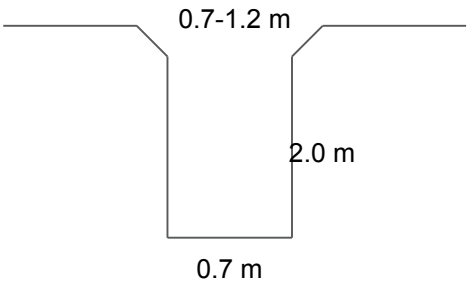

Figure 3.15 Sketch of the jetted trench with indicative dimensions [ref. /1/].

The rate of progress, of the jetting operation, is depending on the seabed encountered. Generally, a progress of 500-2000 m/day can be expected.

The spill scenarios will be based on the assumption that 2000 m is jetted per day, corresponding to a volume of 3200 m^3 per day. It is conservatively assumed that all fines (<0.063 mm) will be spilled, corresponding to 14.0 % of spill ~ 449 m^3/day or 720 tons/day (see Table 3.10).

When cables are jetted the particles are released very close to the seabed, but in the sediment spill model the sediment is released at the sea surface. This is considered conservative –especially when jetting is performed in water depths of more than say 5 m because sediment will remain in suspension for a longer time and give cause to higher turbidity in the model than in nature.

Table 3.10 Spill gradation and volume per 2,000 m (1 day) of jetting.

	Fraction 1 "coarse silt"	Fraction 2 "medium – fine silt"	Fraction 3 "clay"	Total
Average	2.9%	5.3%	5.9%	14.0%
% of spill (total)	20%	38%	42%	100%
Dry density [kg/m3]	1,600	1,600	1,600	-
Spill [m3]	91	169	189	449
Spill [kg]	145,000	270,000	300,000	720,000

Scenarios

The two spill scenarios are described below.

- Scenario 1 - Seabed preparation for foundations
- Scenario 2 – Jetting of cables

Scenario 1 – Seabed preparation

The tentative 3 MW layout of the Vesterhav Nord OWF is presented in Figure 3.16. It is noted that the turbines are placed in a rectangular mesh, containing the rows 1-27 and columns B-D.

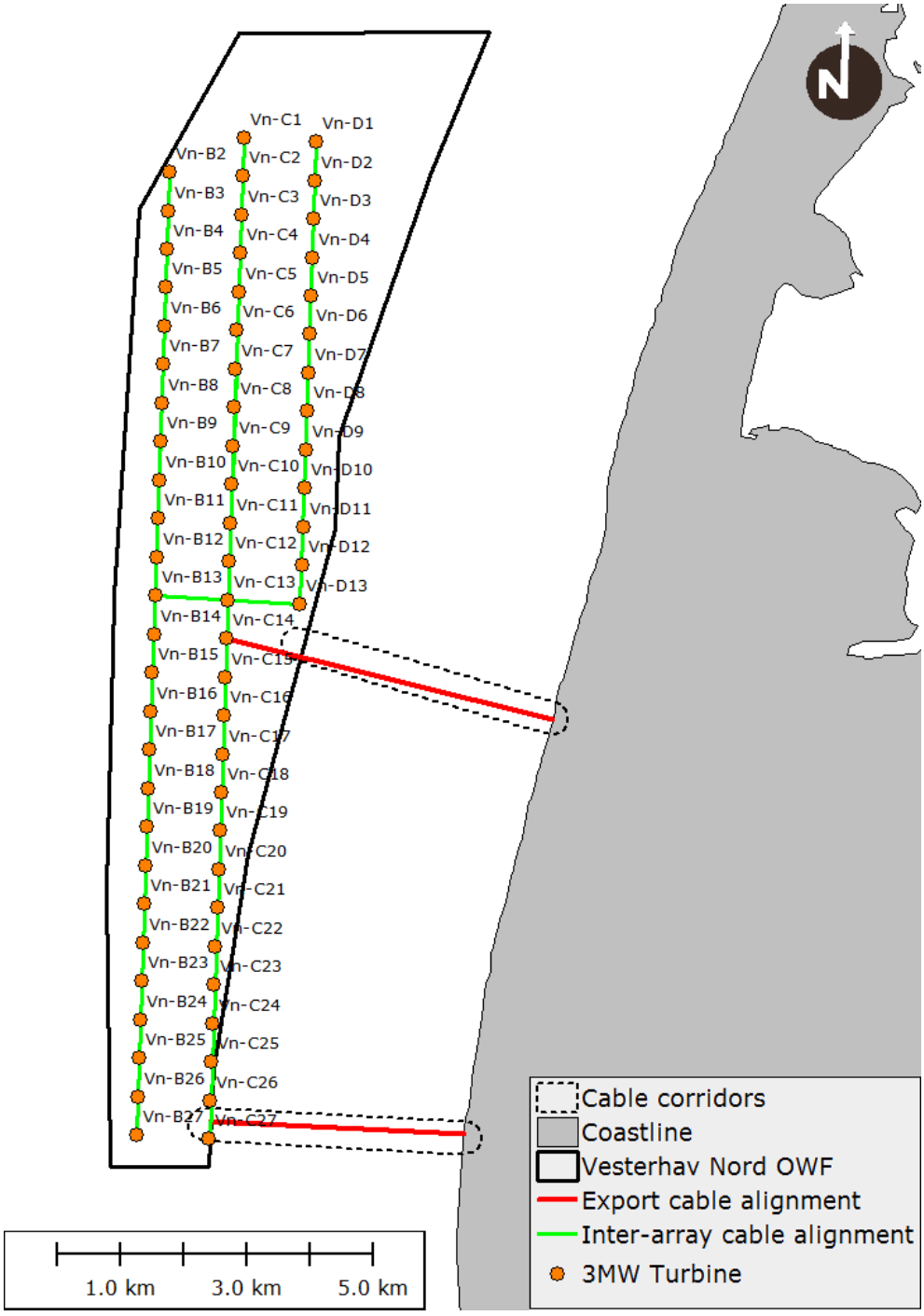

Figure 3.16 Tentative 3 MW layout of Vesterhav Nord OWF.

Dredging/excavation is assumed to last for 66 consecutive days and the simulation will be extended another 14 days in order to allow the spill material to settle. In total 105,600 m^3 is dredged as part of the seabed preparation and 8,450 tons of fines are spilled during installation of foundations.

Scenario 2 – Jetting of cables

The turbines are connected with 33 kV cables allowing 36 MW of wind turbines to be connected to each cable. The layout of the inter-array and export cables has not been defined at this stage, but in the spill scenario it is assumed that turbines are connected as shown in Figure 3.17.

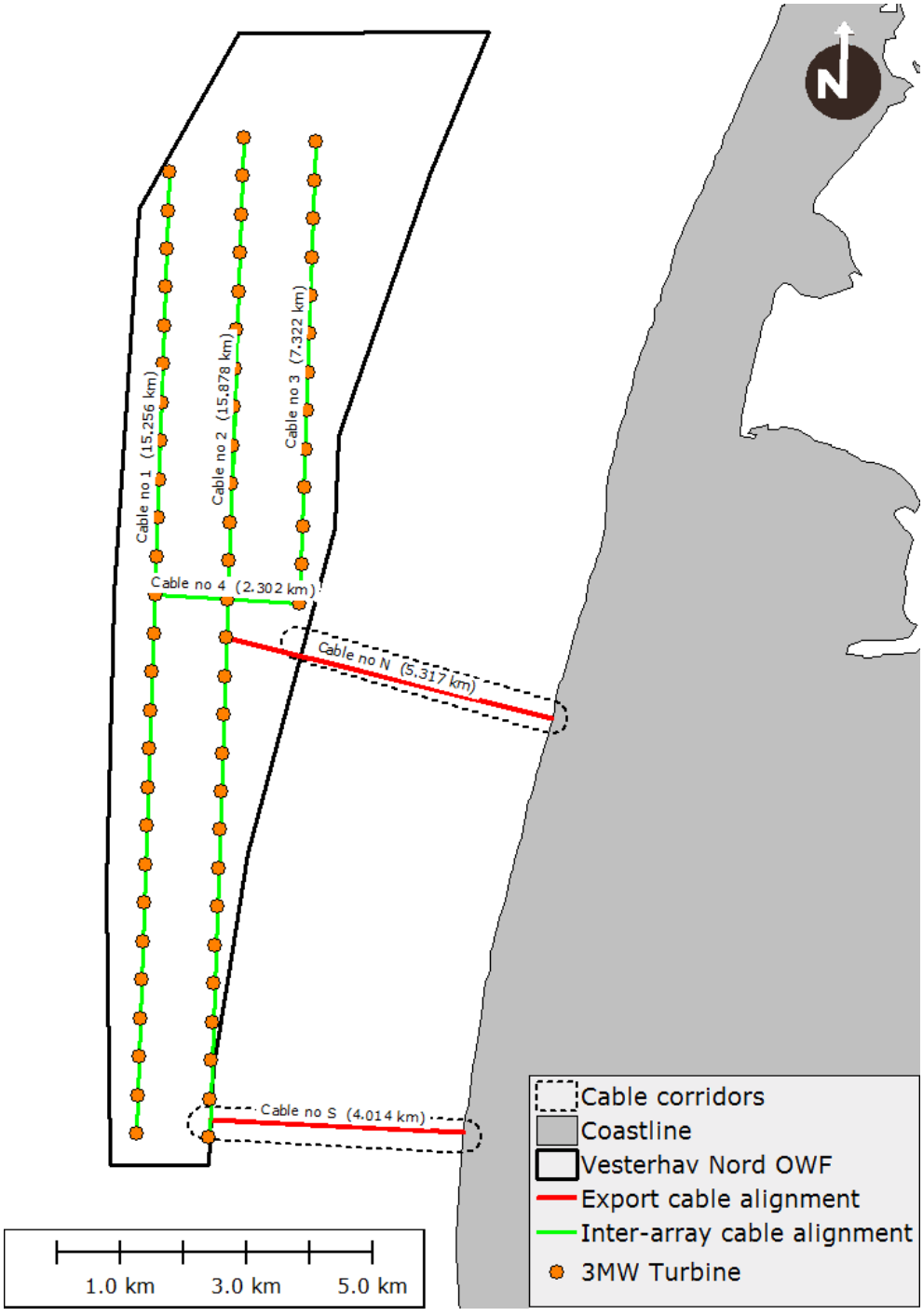

Figure 3.17 *Assumed layout of inter-array cables (green) and export cables (red) for the 3 MW layout of Vesterhav Nord OWF.*

In total 41 km will be jetted inside the park area and the operation is assumed to last for 21 days.

At the present stage, two export cable corridors are considered as shown in Figure 3.17, whereas eventually only one of them will be constructed. The northern and southern corridors are 5.3 km and 4.0 km long. The spill scenarios will assume that 200 MW are transmitted in both corridors, corresponding to 6 x 33 kV cables. The six cables are jetted individually in parallel trenches with 50-100 m spacing. It is assumed that export cables are jetted simultaneously in the two cable corridors

and after inter-array cables are jetted inside the OWF. Consequently, the total jetting operation will last for 37 days and simulations will be extended another 14 days in order to allow the spill material to settle.

In total 154,800 m^3 of material will be jetted and 34,700 tons of fines will be spilled.

A detailed description of the model inputs and scenarios is found in Appendix E.

Results

Results are presented in terms of sediment concentrations and sedimentation quantities/rates in section 5.

3.4.6 Pressures on water exchange and fluxes

Pressure on water exchange

The pressure on water exchange is defined as the degree to which the presence of the OWF will give rise to reduced water exchange in the areas where the water quality could be influenced negatively if the water exchange is changed.

The method applied to quantify such changes on the water exchange is based on the hydraulic modelling of current velocities. As described above the MIKE 21 HD FM model is run for the reference situation without any wind turbines and for a situation where the OWF is included in the model.

Pressure on fluxes of water

Fluxes of water are defined as the total and directional discharge across a chosen transect over a three month period.

The method is applied to quantify such changes on the water exchange and is based on the blocking calculation method applied at all major infra-structure projects in Denmark and many international projects since its introduction at the construction of the Great Belt Crossing. The change in flux, also called the blocking to flow, is expressed in the following term:

$$\Delta Q(T) = \int_T \frac{\left[\left|Q_{ref}(t)\right| - \left|Q_{scenario}(t)\right|\right]dt}{\int_A \left|Q_{ref}(t)\right|dt} \cdot 100\%$$

Where, Q_{ref} and $Q_{scenario}$ are the instantaneous discharges at time t, for the reference situation (existing) and the scenario situation (future), respectively.

A transect perpendicular to the coastline and cutting through the centre of the OWF is selected to illustrate the possible blocking effect of the OWF on the currents (see Figure 3.18).

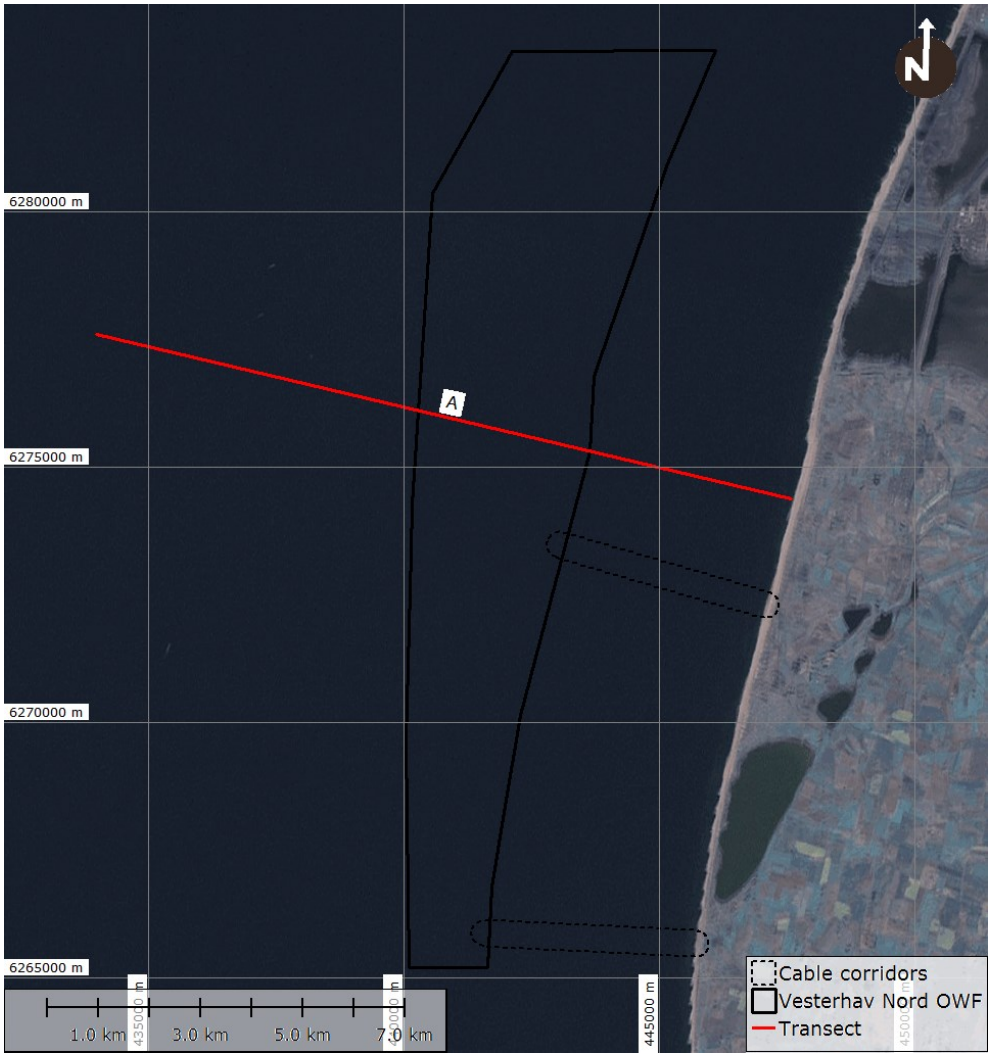

Figure 3.18 Transect for flux and blocking calculations.

3.4.7 Pressures on stratification and mixing

Stratification of flow, where water masses with different properties form layers separated from each other, occurs rarely at positions close to the wind farm Vesterhav Nord since the stratification is very weak.

The pressure on stratification and hence on mixing is therefore not of practical relevance for this site. Therefore, no calculations of mixing effects are conducted for Vesterhav Nord.

3.5 Assessment methodology

The assessment of environmental impact aims to identify and evaluate significant impact which is likely to take place. The assessment focuses on the environmental impact identified as significant as well as environmental impact considered not to be significant due to a minor impact or no impact at all. Impacts may be both positive and negative. COWI uses a method for the assessment of environmental impact based on the EIA legislation.

The following terminology is applied in the assessment method with regard to the relative size of the impact: neutral/no impact, insignificant impact, minor impact, moderate impact, major impact against probability (see Table 3.11). Major impact is only used for specific categories such as protected landscapes, protected cultural heritage and Natura 2000 areas which may be significantly affected by the project.

Table 3.11 Definition of impact terminology.

Magnitude of impact	The following effects are dominant
Neutral/no impact	No impacts compared to status quo.
Negligible negative impact	Small impacts on a local scale and with low complexity that persist for a short-term or are without long-term effects and without any irreversible effects.
Minor negative impact	Impacts with a certain extent or complexity, a certain degree of persistence aside from short-term effects, and a certain probability to occur, but which will very likely not cause irreversible effects
Moderate negative impact	Impacts with either a relatively large extent or long-term effects (e.g. throughout the lifespan of the wind farm), that occurs occasionally or with a relatively high probability and which may cause some irreversible but local effects for instance on elements worthy of preservation (culture, nature etc.).
Major negative impact	Impacts with a large extent and/or long-term effects, frequently occurring and with a high probability, and with the potential of causing significant irreversible impacts.
Positive impacts	Positive impacts on one or more of the above mentioned.

The main purpose of the assessment method is to ensure that the assessment of environmental impact is based on specific terms and to increase the transparency of the environmental assessments conducted. The purpose is also to propose possible mitigating measures and to calculate the remaining environmental impact as a basis for the authorities' approval or rejection of the project. It is important to emphasize that the method cannot be used on its own, and that it is unable to predict the exact scope of environmental impact or change in all situations. Thus, the method cannot replace technical knowledge and project-specific assessments, but it can create a common and transparent reference framework and terminology.

4 Baseline

This section describes the existing conditions (baseline) in terms of wave conditions, hydrodynamics, seabed morphology and coastal morphology at the proposed Vesterhav Nord OWF.

The baseline description is based on a combination of modelling results, survey data, satellite images and visual observations. Background data and baseline modelling is presented in Appendix D.

4.1 Water levels

In general terms, the main water level variability at the project site is caused by tidal currents in the North Sea, but the water level is also influenced by wind and barometric pressure.

According to the Danish Pilot Guide [ref. /12/] the difference between mean high water and mean low water is between 0.5 m at Thyborøn Harbour, whereas storms from south-westerly and north-westerly directions generate surge levels of up to approximately 1.5 m Danish Vertical Reference 1990 (DVR90) and storms from north-easterly and south-easterly directions generate negative surge levels of down to about -1.2 m DVR90.

Measured water levels relative to DVR90 (which is approximately mean sea level) are available for Thyborøn Harbour and Ferring Harbour from January 2003 to January 2014. Further to the south (at Vesterhav Syd OWF) measured water levels are available for Hvide Sande Harbour and Thorsminde Harbour. Water levels ranges from -1.50 m to 3.00 m DVR90 (Thyborøn). An example of water level measurements for Thyborøn Harbour is presented in Figure 4.1. Water levels separated by months are shown in Appendix D, Table D.2.

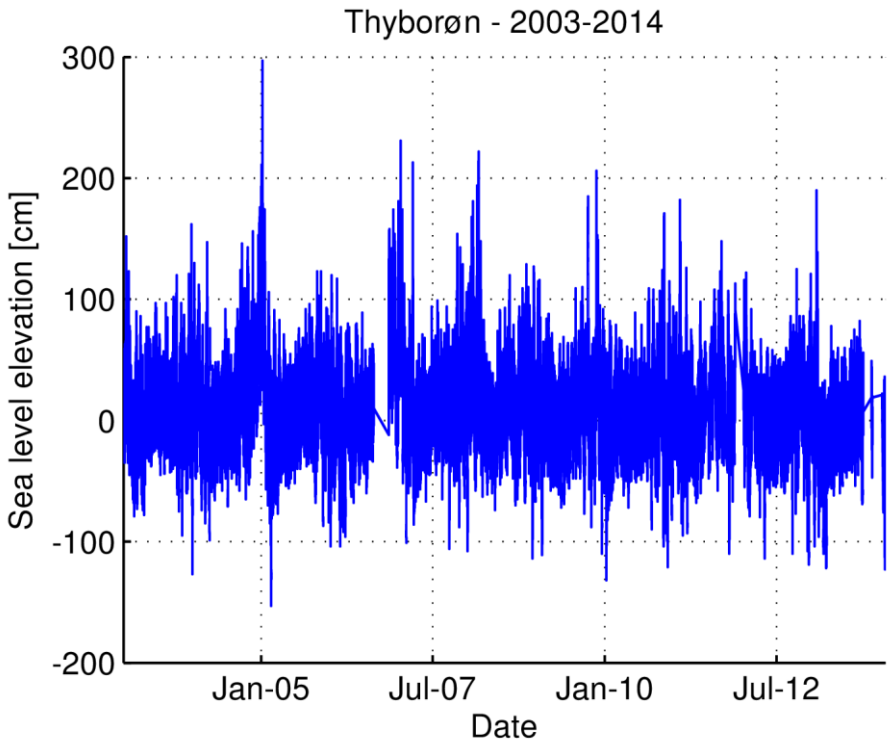

Figure 4.1 *Water levels relative to DVR90 measured at Thyborøn Harbour 2003-2014.*

4.2 Currents

Currents on the west coast of Jutland are governed by strong tidal and wave-induced currents running parallel with the coastline. Stronger currents mainly consist of south going wave-generated currents and north going coastal currents [ref. /13/]. The coastal currents originate from counter-clockwise currents in the North Sea.

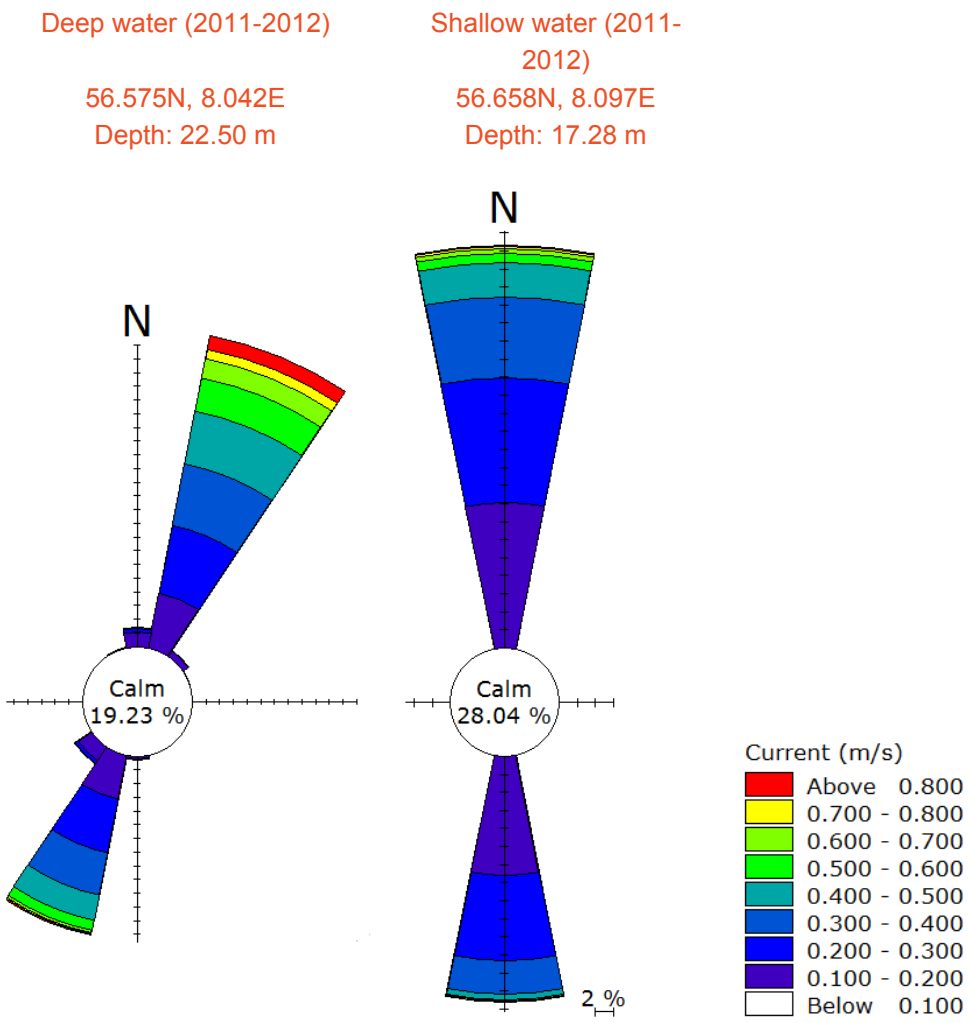

Figure 4.2 *Current rose based on two year dataset at deep and shallow water within the Vesterhav Nord OWF. Dataset: DMI-HBM hindcast.*

The currents extracted from the DMI-HBM hindcast model at the southern and northern-eastern boundary of the OWF (deep and shallow water location respectively) show predominant currents from 22.5 (NNE) and 200.5 (SSW) for the deep water location and strictly 0 (N) and 180 (S) for the shallow water location at the OWF. In both locations the current is parallel to the coastline, and the difference observed at the two locations is caused by the curvature of the coastline.

Two typical situations are captured in the MIKE 21 HD FM model as illustrated in Figure 4.3 and Figure 4.4. The illustrations show that typical north and south going currents reach 0.3-0.6 m/s inside the project area, whereas currents in shallow water (less than 3-4 m) are typically an order of magnitude larger due to the influence of waves and the wave generated current (the littoral current). The illustrations also show that the coastal current towards north is stronger than currents towards south.

Current statistics and monthly distributions of current magnitudes are presented in Table 4.1 and Table 4.2. Additional statistics are found in Appendix D.

Table 4.1 *Current direction vs. current speed in deep water near the southern boundary of the OWF. Frequency of occurrence [%].*

U_{dir} (°) / current speed (m/s)	0°	30°	60°	90°	120°	150°	180°	210°	240°	270°	300°	330°	Total
0 – 0.1	2.9	3.3	1.0	0.4	0.4	0.5	1.5	3.9	2.1	1.1	0.8	1.3	19.2
0.1-0.2	3.0	8.0	0.1	-	-	<0.1	0.8	8.3	0.5	<0.1	-	<0.1	20.7
0.2-0.3	1.4	9.2	-	-	-	-	0.1	8.4	<0.1	-	-	-	19.1
0.3-0.4	0.5	8.9	-	-	-	-	<0.1	6.2	-	-	-	-	15.7
0.4-0.5	0.2	7.6	-	-	-	-	<0.1	3.8	-	-	-	-	11.7
0.5-0.6	0.1	4.9	-	-	-	-	-	1.5	-	-	-	-	6.5
0.6-0.7	0.1	2.7	-	-	-	-	-	0.4	-	-	-	-	3.1
0.7-0.8	0.1	1.4	-	-	-	-	-	0.2	-	-	-	-	1.6
0.8-0.9	<0.1	0.8	-	-	-	-	-	0.1	-	-	-	-	0.9
0.9-1.0	<0.1	0.4	-	-	-	-	-	<0.1	-	-	-	-	0.4
1.0-1.1	<0.1	0.3	-	-	-	-	-	<0.1	-	-	-	-	0.3
>1.1	<0.1	0.5	-	-	-	-	-	<0.1	-	-	-	-	0.6
Total	8.4	48.1	1.1	0.4	0.4	0.5	2.5	32.8	2.7	1.1	0.8	1.3	100

Table 4.2 *Month vs. current speed in deep water near the southern boundary of the OWF (see Appendix D). Frequency of occurrence pr. month [%].*

Month / current speed (m/s)	Jan	Feb	Mar	Apr	May	Jun	Jul	Aug	Sep	Oct	Nov	Dec	Total
0 – 0.1	19.2	21.1	19.3	21.3	19.8	19.9	21.6	19.4	19.2	15.5	17.7	17.0	19.2
0.1-0.2	22.5	21.5	22.7	18.1	22.5	21.1	23.0	21.6	18.8	18.9	21.0	17.1	20.7
0.2-0.3	18.6	20.0	22.3	21.5	21.4	19.8	20.2	20.9	16.8	16.0	17.8	14.7	19.1
0.3-0.4	16.6	16.8	17.1	16.7	16.3	15.3	15.9	16.7	15.5	13.1	13.8	14.0	15.7
0.4-0.5	12.7	12.0	12.0	13.5	12.7	13.7	10.1	8.9	10.6	13.5	9.7	11.0	11.7
0.5-0.6	6.0	5.6	4.6	6.5	4.8	5.6	5.2	6.3	9.3	9.0	7.6	8.0	6.5
0.6-0.7	2.9	1.6	1.6	2.1	1.6	2.8	2.4	3.6	5.0	4.5	3.8	5.8	3.1
0.7-0.8	0.9	1.0	0.3	0.2	0.6	1.5	1.1	2.3	2.4	2.8	2.7	3.9	1.6
0.8-0.9	0.5	0.5	-	-	0.2	0.2	0.4	0.3	0.5	2.4	2.5	2.7	0.9
0.9-1.0	0.2	-	-	-	0.1	-	0.1	0.1	0.6	1.1	0.8	1.7	0.4
1.0-1.1	-	-	-	-	-	-	-	-	0.5	0.7	0.9	1.9	0.3
>1.1	-	-	-	-	-	-	-	-	0.8	2.6	1.7	2.0	0.6
Total	100	100	100	100	100	100	100	100	100	100	100	100	100

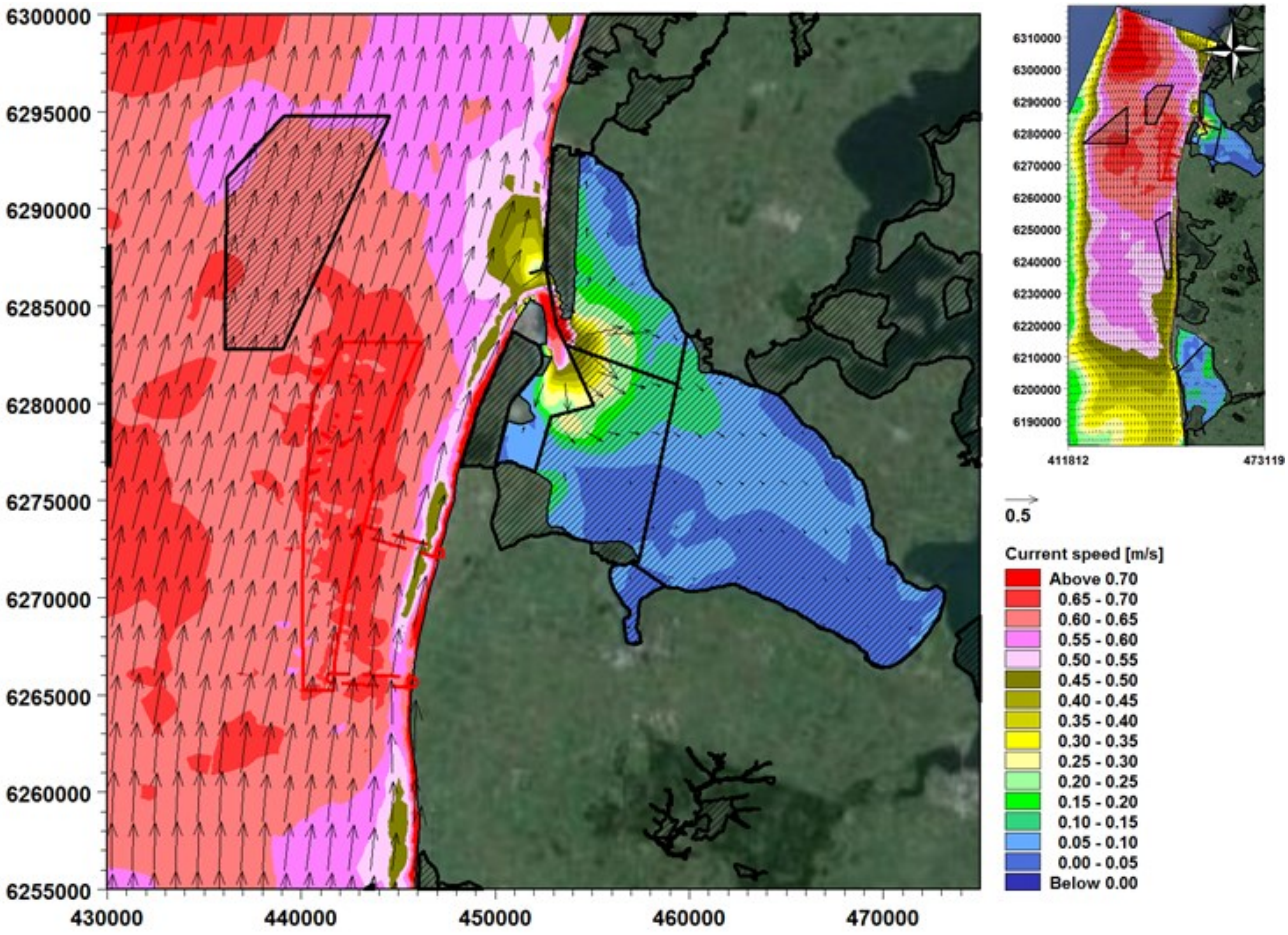

Figure 4.3 Typical northerly flow at the Vesterhav Nord OWF. Hatched areas with black frames show Natura 2000 areas.

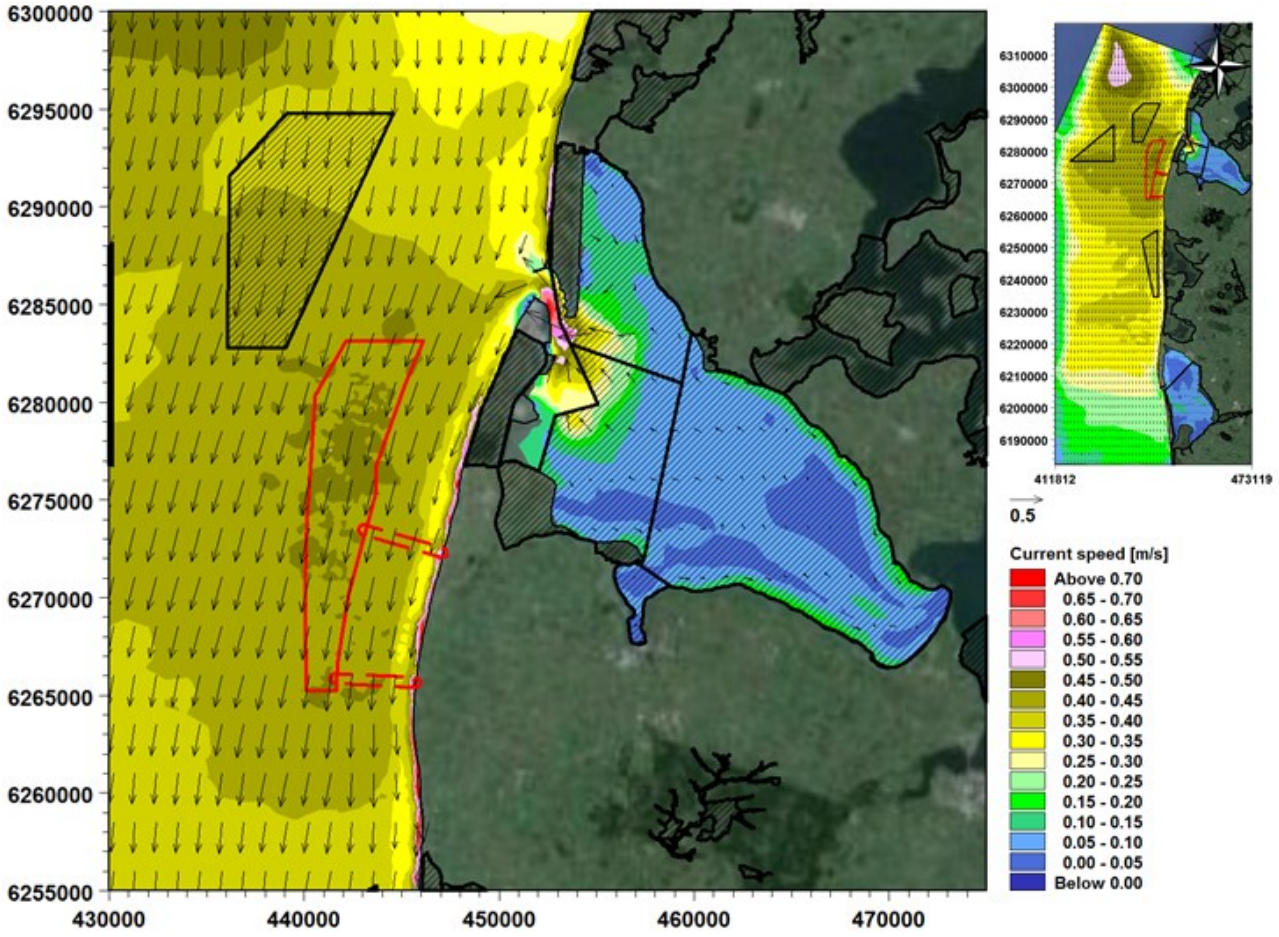

Figure 4.4 Typical southerly flow at the Vesterhav Nord OWF. Hatched areas with black frames show Natura 2000 areas.

4.3 Wave climate

Wave conditions at the OWF are governed by the geographical location of the project in the exposed West Coast of Jutland with long fetches towards north- and south-west. As illustrated in the wave measurements conducted at Fjaltring south of the site (see Figure 4.5), the predominant wave direction is north-westerly, with secondary waves from the English Channel approaching from south-west. Similar trends are present in synoptic wave data from the DMI-WAM model and shown in Figure 4.6.

MIKE 21 SW FM results are presented in Figure 4.7 and Figure 4.8. The results show statistical average and maximum wave conditions in the model area and near the Vesterhav Nord OWF. From the results it is evident that there is little shelter from exposure to large waves from westerly directions, and that there is little variation in the wave conditions across the OWF. The figure also shows that storm significant wave heights (H_{m0}) reach 7 m in year 2012. Wave statistics, scatterplots and monthly distributions of wave heights are provided in Appendix D.

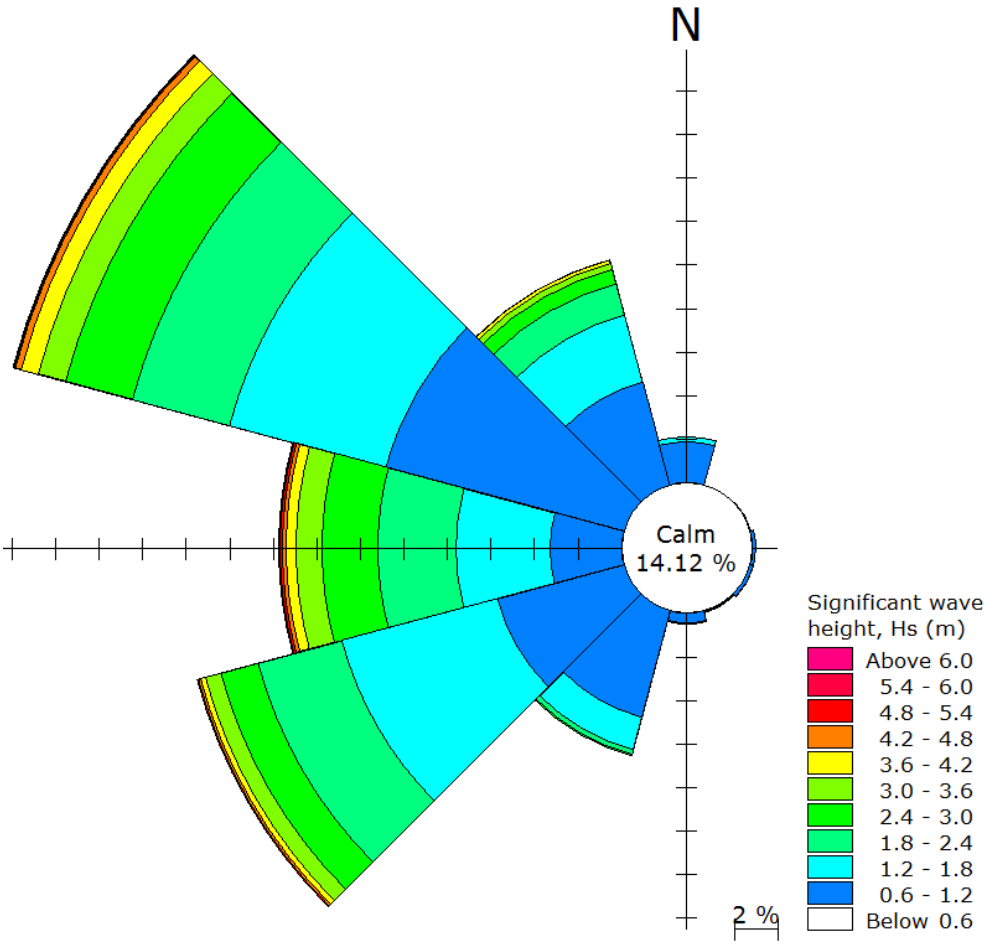

Figure 4.5 *Wave rose based on measurements at Fjaltring conducted January 2011 – December 2012 [56.475° N; 8.048° E].*

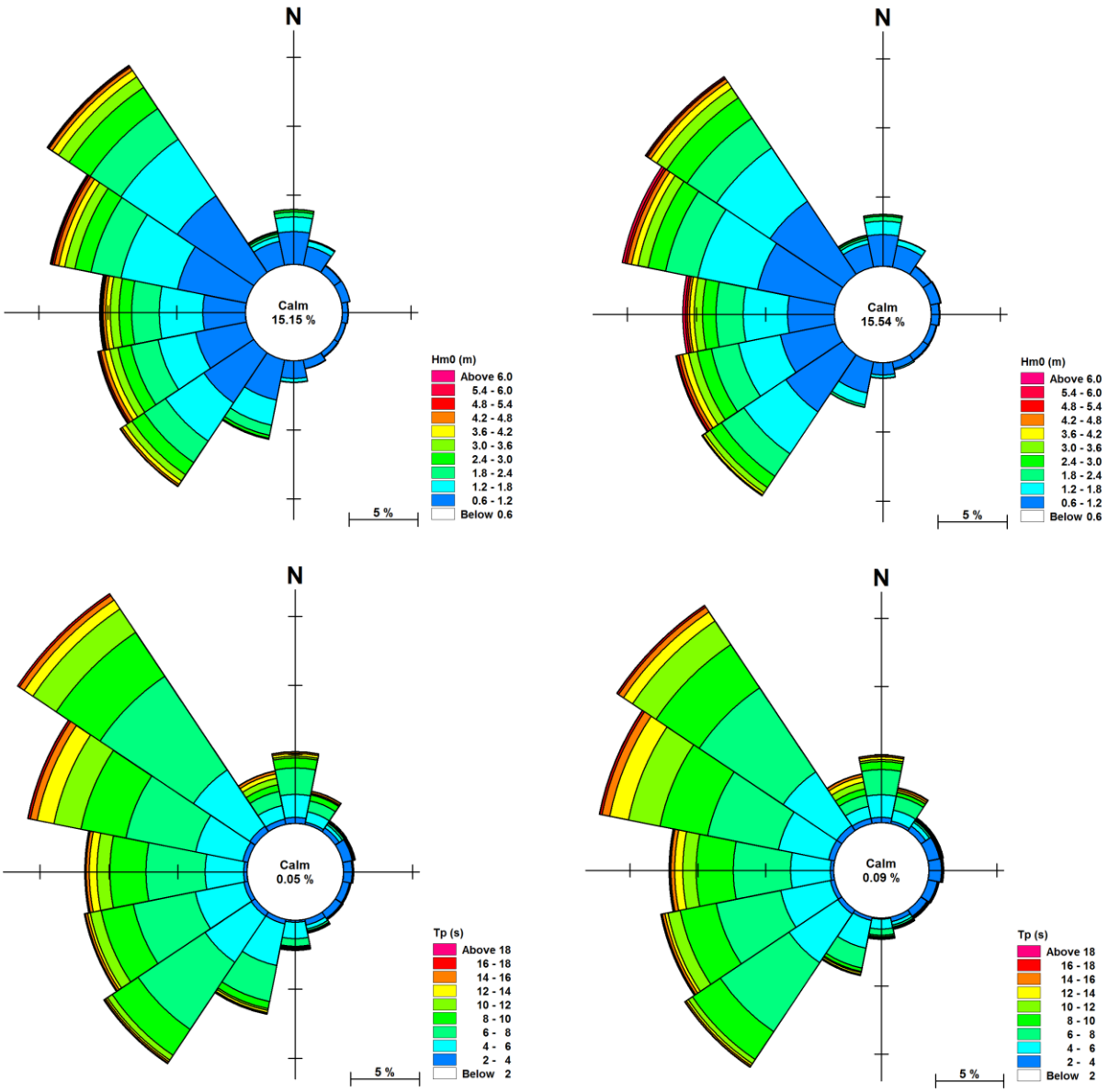

Deep water
[56.580°n, 8.033°e]

Shallow water
[56.680°n, 8.100°e]

Figure 4.6 *Significant wave height (H_{m0}) and peak period (T_p) roses based on DHI-WAM model data for the years 2005-2012 in a deep and shallow location towards west and east in the Vesterhav Nord OWF area. Locations are shown in Figure D.2.*

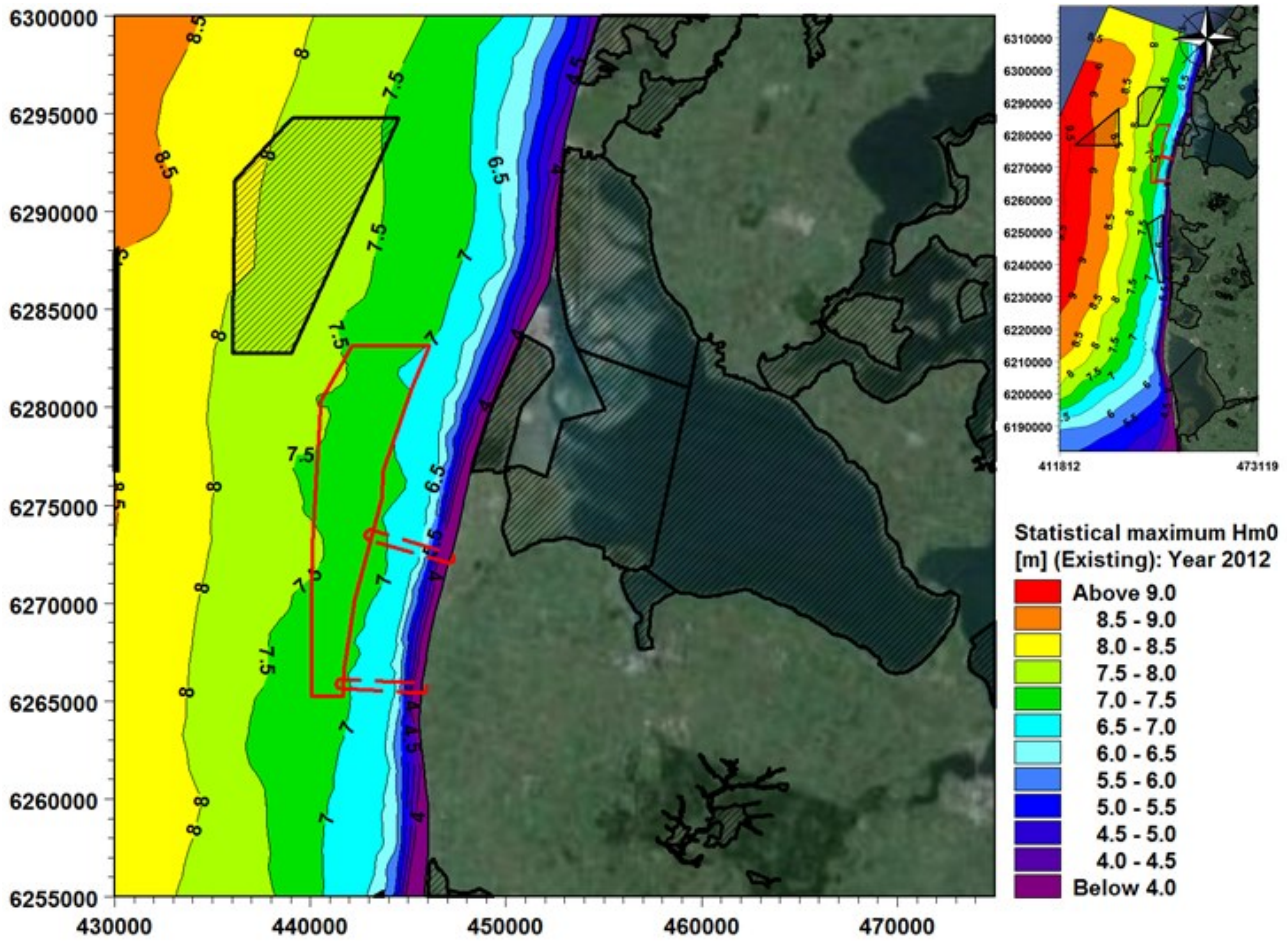

Figure 4.7 *Statistical maximum significant wave height H_{m0} [m] in year 2012. Hatched areas with black frames are NATURA 2000 areas.*

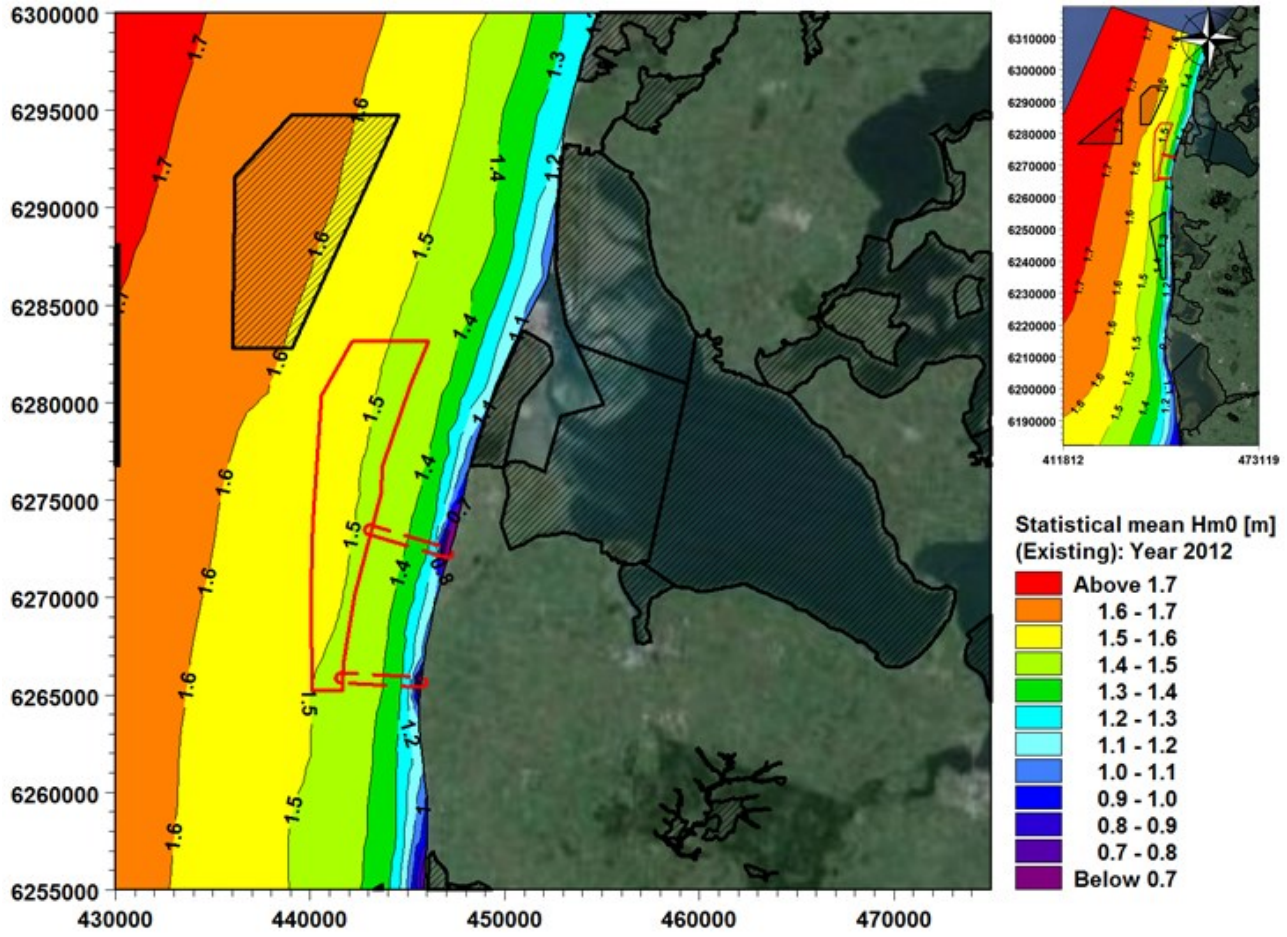

Figure 4.8 *Statistical mean significant wave height H_{m0} [m] in year 2012. Hatched areas with black frames are NATURA 2000 areas.*

4.4 Sediment transport patterns and seabed morphology

The coastal zone off west Jutland displays a highly dynamic environment, where sediment transport is governed by strong tidal and wave-induced currents. The net wave-generated current and the coastal current have a net direction towards the north [ref. /13/], see Figure 4.9.

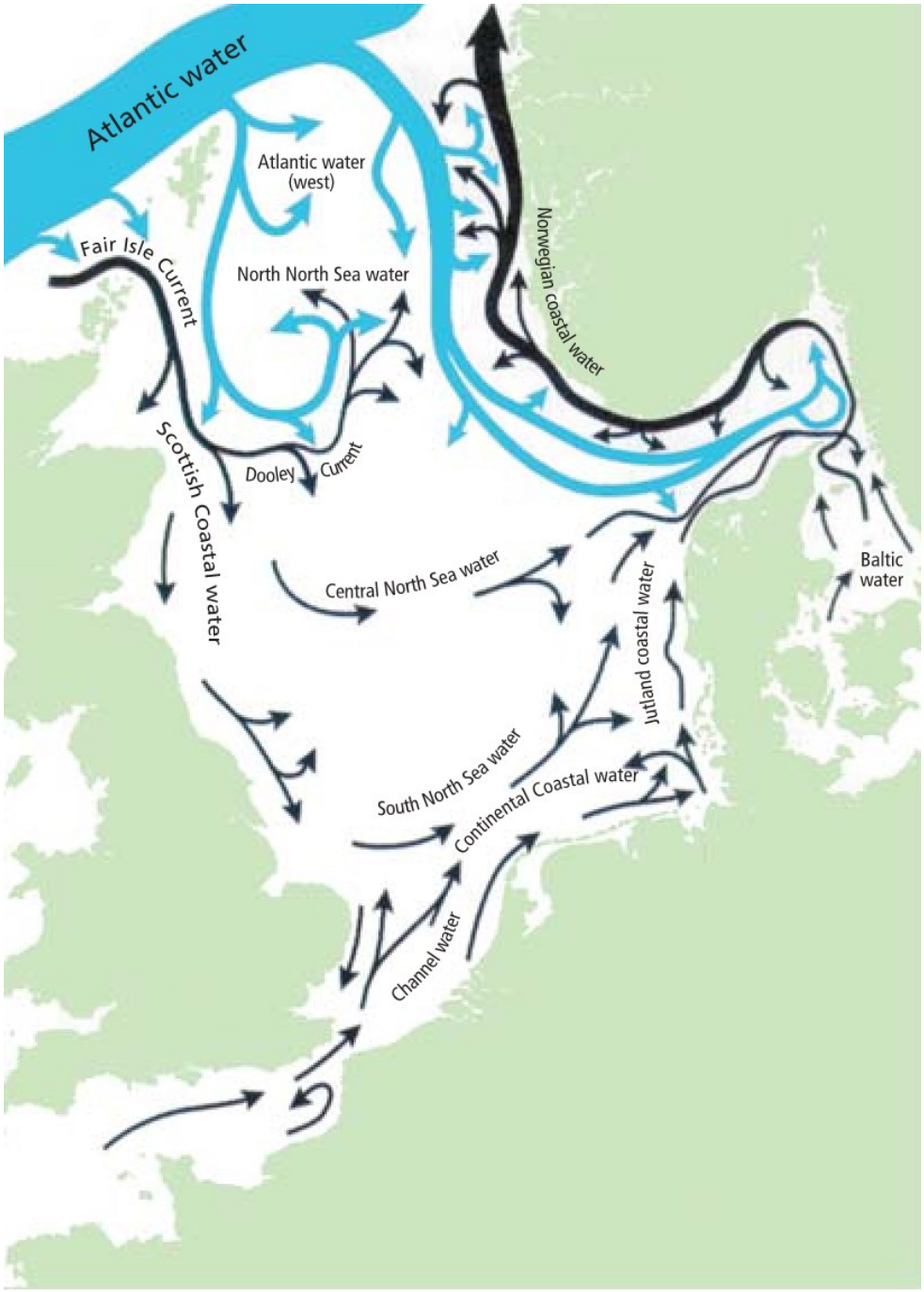

Figure 4.9 Net currents in the North Sea [ref. /14/].

The energetic wave climate with waves of up to 5 m from westerly directions governs the sediment transport along the west coast of Jutland and results in a general coastal retreat in the order of 1-5 m per year. Furthermore, the wave regime has resulted in the formation of coast parallel sand bars found in the littoral zone in water depths less than 6-7 m. The inner coastal profile and the sand bars are under constant influence by seasonal changes in wave climate, water levels and human intervention in the form of artificial nourishment conducted under the authority of the Danish Coastal Authorities at regular intervals.

In water depths of 15-28 m the sediment transport is governed by the north bound coastal current which result in the formation and migration of bed forms towards

north. In this context the project site displays numerous sandwaves scattered across the Vesterhav North OWF.

The bathymetry across Vesterhav Nord can be described as smoothly undulating throughout particularly in the northern half of the site, and at the very southern extent, where large sandwaves are observed. The crests of the sandwaves are oriented with a 10-15° clockwise rotation relative to the shore normal. Hence, the sandwaves are nearly perpendicular to the shore unlike ripples in shallow water which are parallel to the shore.

A very noticeable feature of the site is the channel located towards the northwest of the site. This erosional feature is approximately 1 km wide and 4-5m deeper than the surrounding seabed (see Figure 4.10 and Figure 4.12).

The seabed comprise mobile sediments ranging from silty sand to sandy gravel. It is noted that gravel and numerous boulders are found in the bottom of the channel towards northwest, which may be an indication that finer material is not able to deposit in this area due to strong occasional currents in the channel.

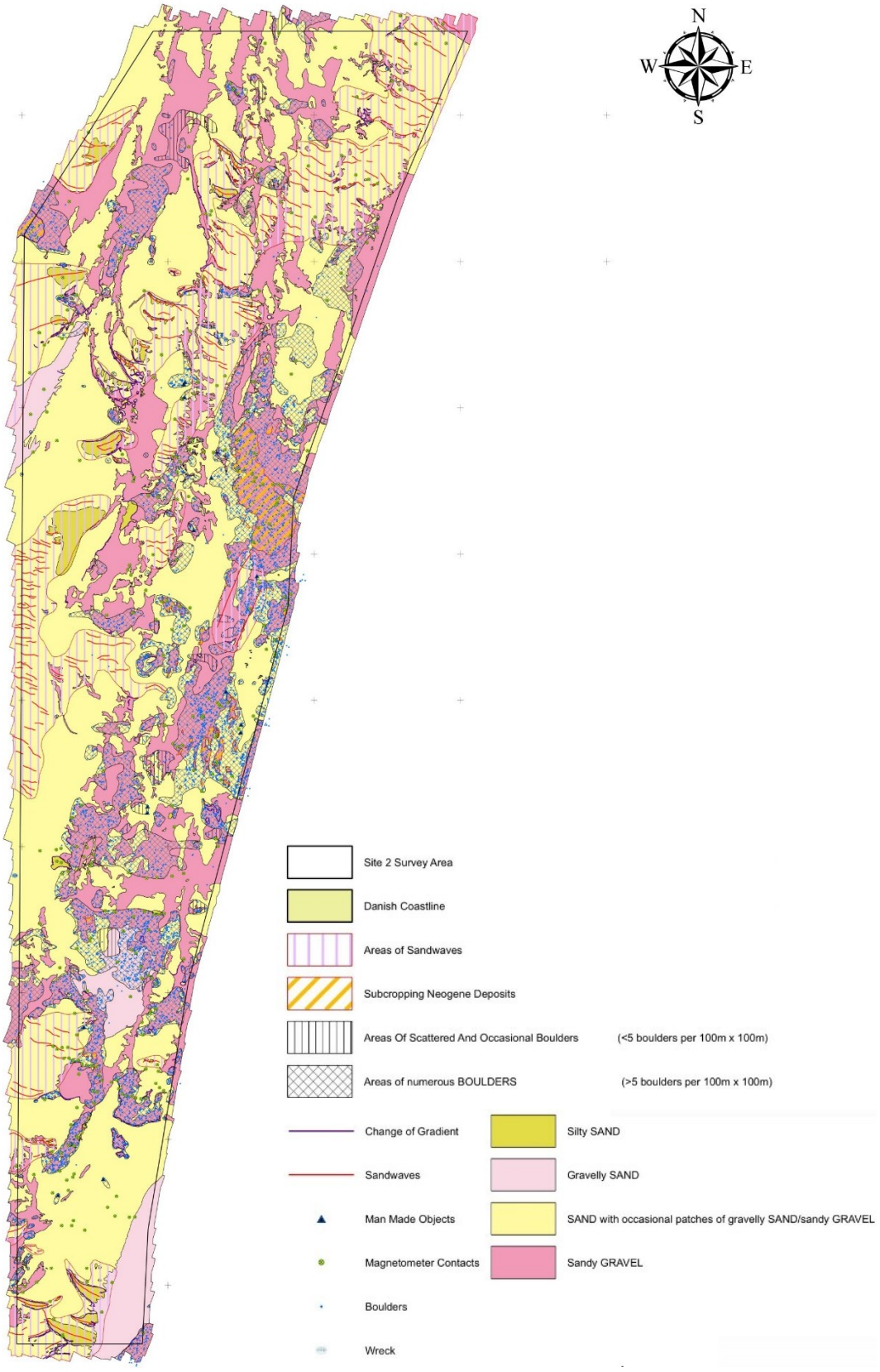

Figure 4.10 Composition of seabed surface and location of sand waves. [ref /9/].

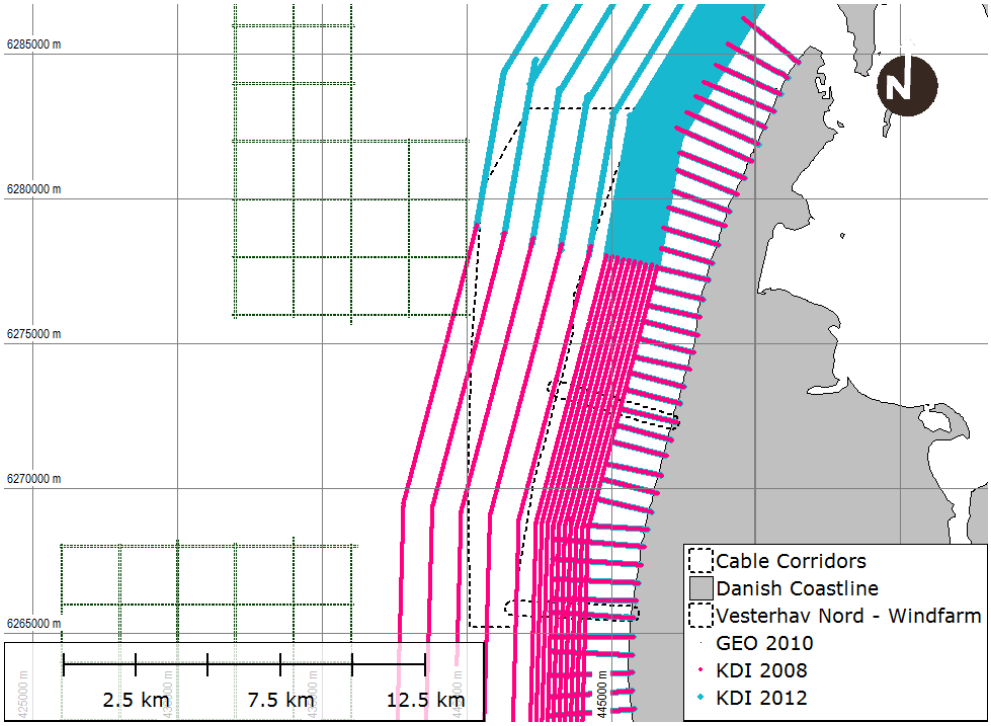

Figure 4.11 *Overview of survey lines and profiles conducted by GEO in 2010 (green) and the Danish Coastal Authorities – KDI in 2008 (purple) and 2012 (blue).*

The Danish Coastal Authorities conducted line and profile surveys in 2008 and 2012 in the area (see Figure 4.11). Furthermore, GEO conducted a line survey 10-20 km from shore in 2010. These, surveys are compared to the detailed multi-beam survey by EGS in 7 selected profiles inside the project area and in the cable corridors (see Figure 4.12 to Figure 4.15). Results are summarised in the following:

Profile 1 — The seabed in the central part of the OWF is relatively smooth with a few smaller sandwaves of 1-1.5 m height (~400 m wave length). In the 5 year period from 2008 to 2013 the sand waves have migrated 40-50 m towards north (10 m/yr). The seabed in the project area displays variations in the order of 25 cm within 5 years, but there is no general trend of erosion or accretion.

Profile 2 — The seabed along the edges of the deep channel in north-western corner of the OWF features large scale sandwaves of up to 5.7 m heights. The wavelength of the sand waves is 250-500 m and they have migrated 80-100 m towards north within 5 years from 2008 to 2013 (20 m/year).

Profile 3 — The bottom of the channel goes to -28 m DVR 90. From year 2012 to 2013 the channel has become 10-20 cm deeper due to erosion (10-20 cm/year).

Profile 4 & 5 — The seabed features numerous smaller sandwaves in the north-eastern corner of the project area. The sandwaves are 0.3-2.5 m high with wavelengths of 30-400 m. There is a tendency that the bedforms have migrated towards north within the 1 year period from 2012 to 2013.

Profile CR1 & 2

The beach profiles features a single ripple with a crest in levels of -2 m to -4 m. The shallow part of the profile until depths of -7 is very dynamic, with vertical variations of +/- 3 m within 5 years primarily due to migration of the nearshore ripple by more than 100 meters towards shore. Furthermore, the coastline at (0.0 m DVR90) has accreted by more than 20 m within the 5 years period at CR2.

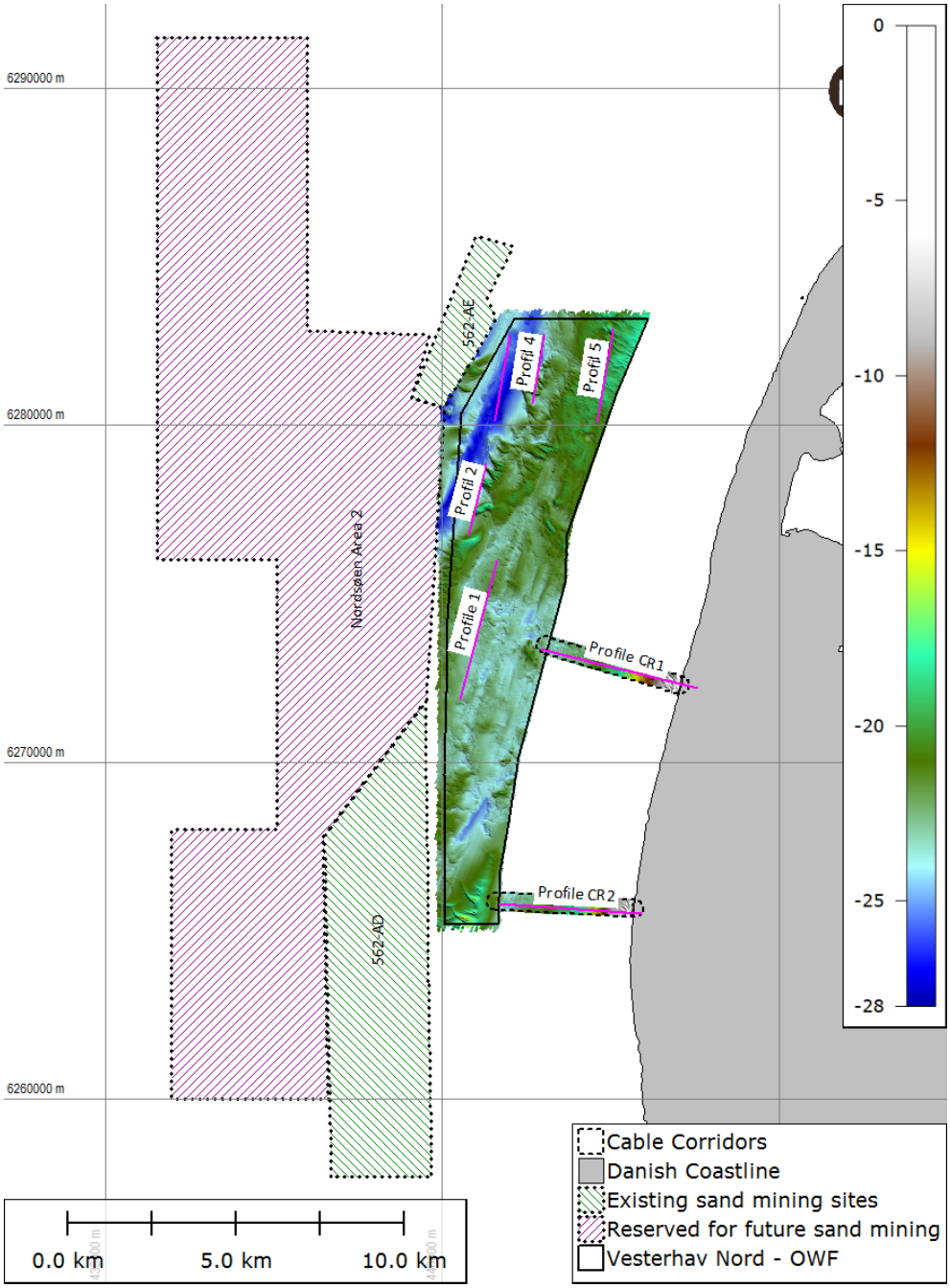

Figure 4.12 *Bathymetric survey by EGS [ref. /9/] overlayed with sand mining area 562-AD and 562-AE and areas reserved for future sand mining. Furthermore, the figure shows the location of profiles used to assess morphological development. Depths are relative to DVR90.*

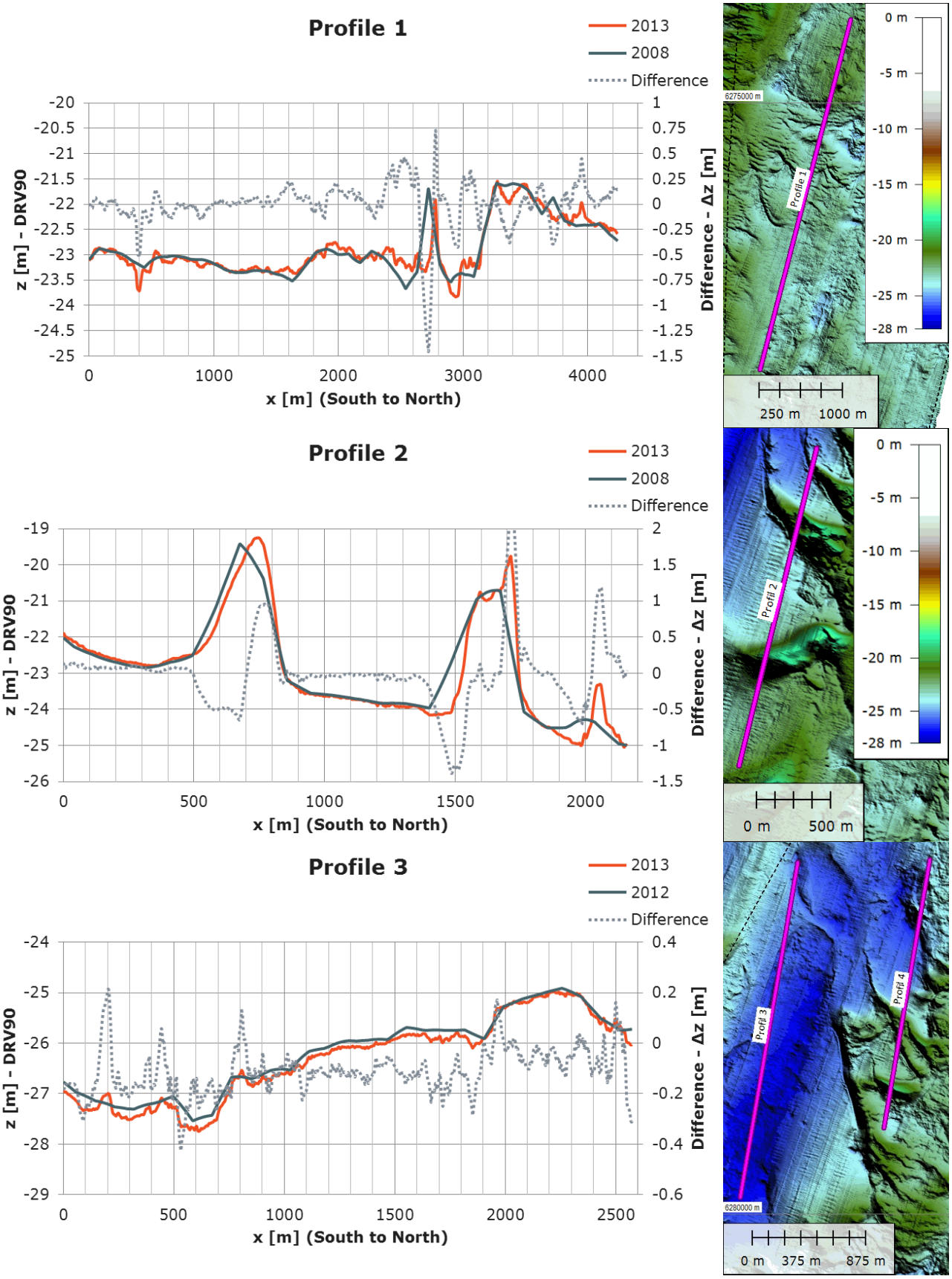

Figure 4.13 *Comparison of surveys from 2008, 2012 and 2013. Profile 1 – 3.* Depths are relative to DVR90.

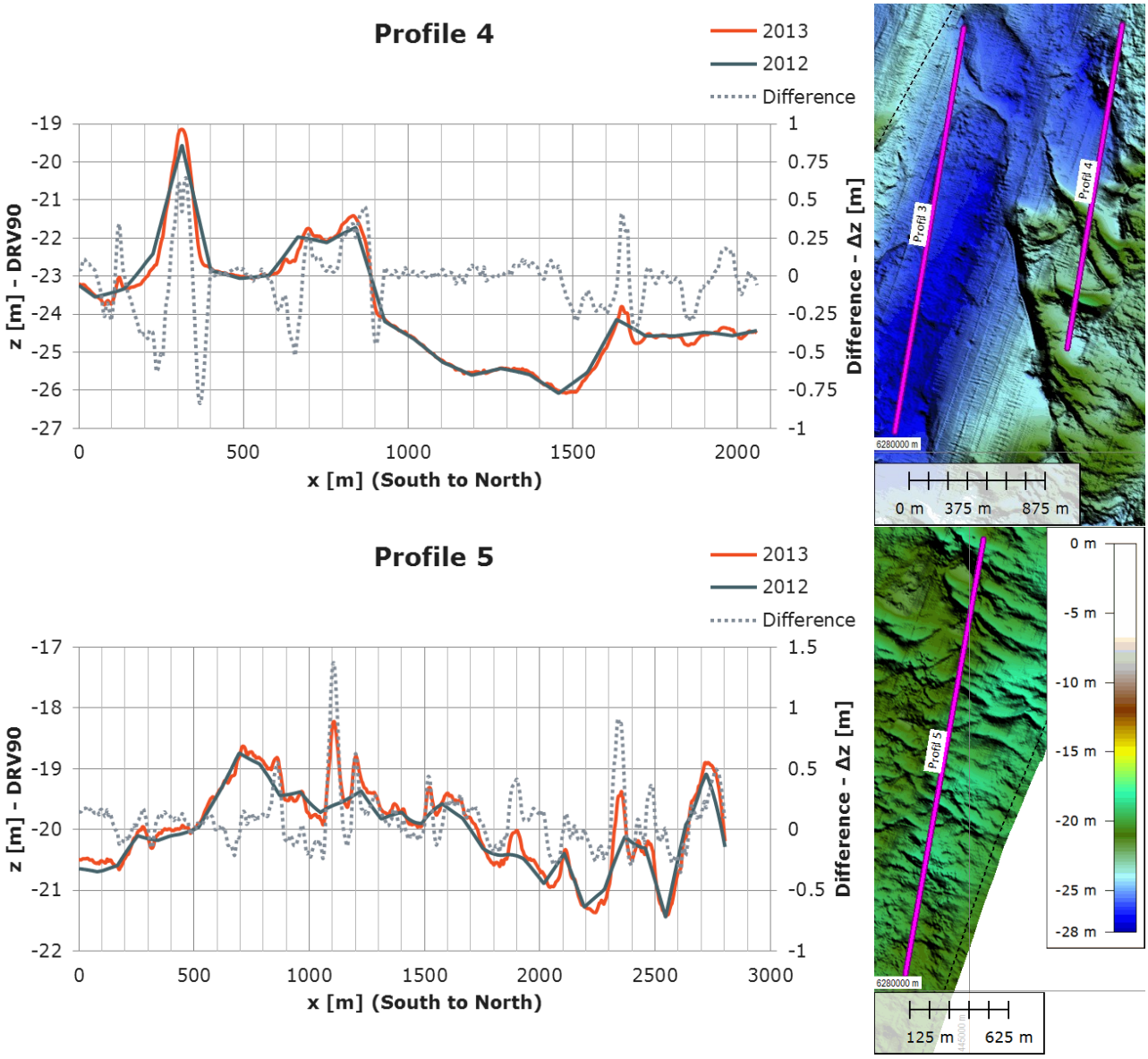

Figure 4.14 *Comparison of surveys from 2012 and 2013. Profile 4 and 5.* Depths are relative to DVR90.

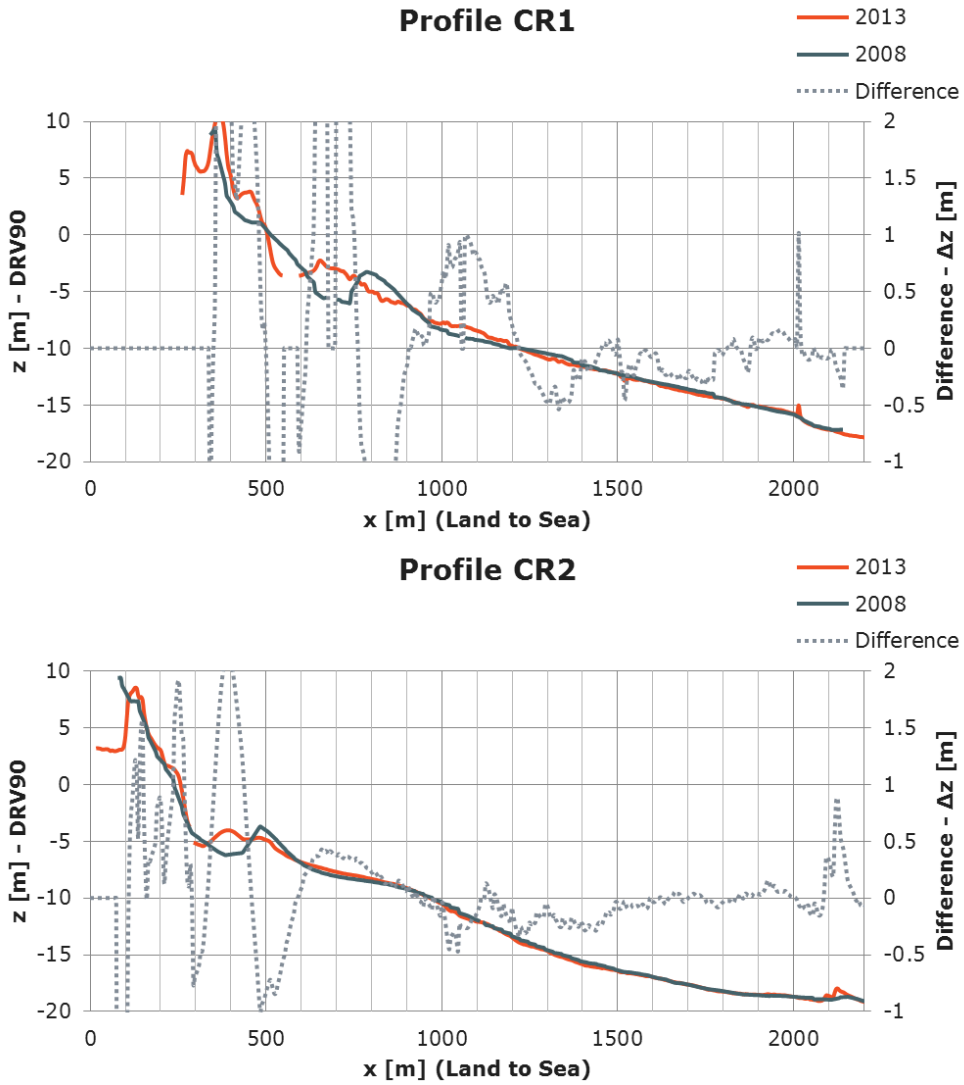

Figure 4.15 Comparison of surveys from 2008 and 2013. Profile CR1 and CR2.

It is underlined that the above conclusions may be corrupted by sand mining conducted in the adjacent sand mining areas (562-AE *Thyborøn* and 562-AD *Ferring*) see Figure 4.12. The Danish Coastal Authorities have been allowed to borrow up to 6.3 million m^3 sand per year (12.5 million m^3 in total) within a 10 year period at 562-AE until January 2025.

Sand borrowed in the area is used as beach and bar nourishment along the west coast and it is therefore cautiously assumed that the OWF area would have experienced some accumulation of sand if the adjacent area had not been exploited.

In addition to the above mentioned sand mining sites, the Danish Coastal Authorities have made reservations in *Nordsøen Område 1* and *Nordsøen Område 2* north and west of the proposed Vesterhav Nord OWF. Sand mining will thus continue in these areas for at least the next 10 years. It is noted that this may have an effect on the future morphology inside the OWF area.

4.5 Coastal morphology

The starting point for the coastal assessment is the recent aerial photo that shows the present situation along the coast adjacent to the proposed OWF, see Figure 4.16 and Figure 2.1. Additionally, Figure 4.17 shows the dominant landscape features along the coast adjacent to the proposed OWF.

The dominant moraine landforms between Bovbjerg, Lemvig and Struer were formed during the last ice age, Weichsel. After the Weichsel glaciation coastal and fluvial processes have shaped the moraine landscape forming coastal cliffs, beaches, marine forelands, barrier islands, dunes and deltas etc. At Bovbjerg a moraine cliff is found and the coastal erosion is thus slower here, which has resulted in a protrusion on the coastline. Barrier islands enclose Ferring Sø and Nissum Bredning, which were formed primary by the littoral drift after the last ice age.

The recent coastal processes in the area are dominated by the effect of Thyborøn Kanal that provides access from the North Sea to Limfjorden. The barrier island at Thyborøn was breached by a storm some 150 years ago forming Thyborøn Kanal. Since then, the canal has been kept open to provide navigation access to the Port of Thyborøn and Limfjorden as well as providing water exchange between Limfjorden and the North Sea.

The opening through the barrier island at Thyborøn Kanal has resulted in extensive erosion of the adjacent coasts as sediment is transported along the barrier islands Harboøre Tange and Agger Tange by the littoral drift and deposits at large shoals in Nissum Bredning east of the canal.

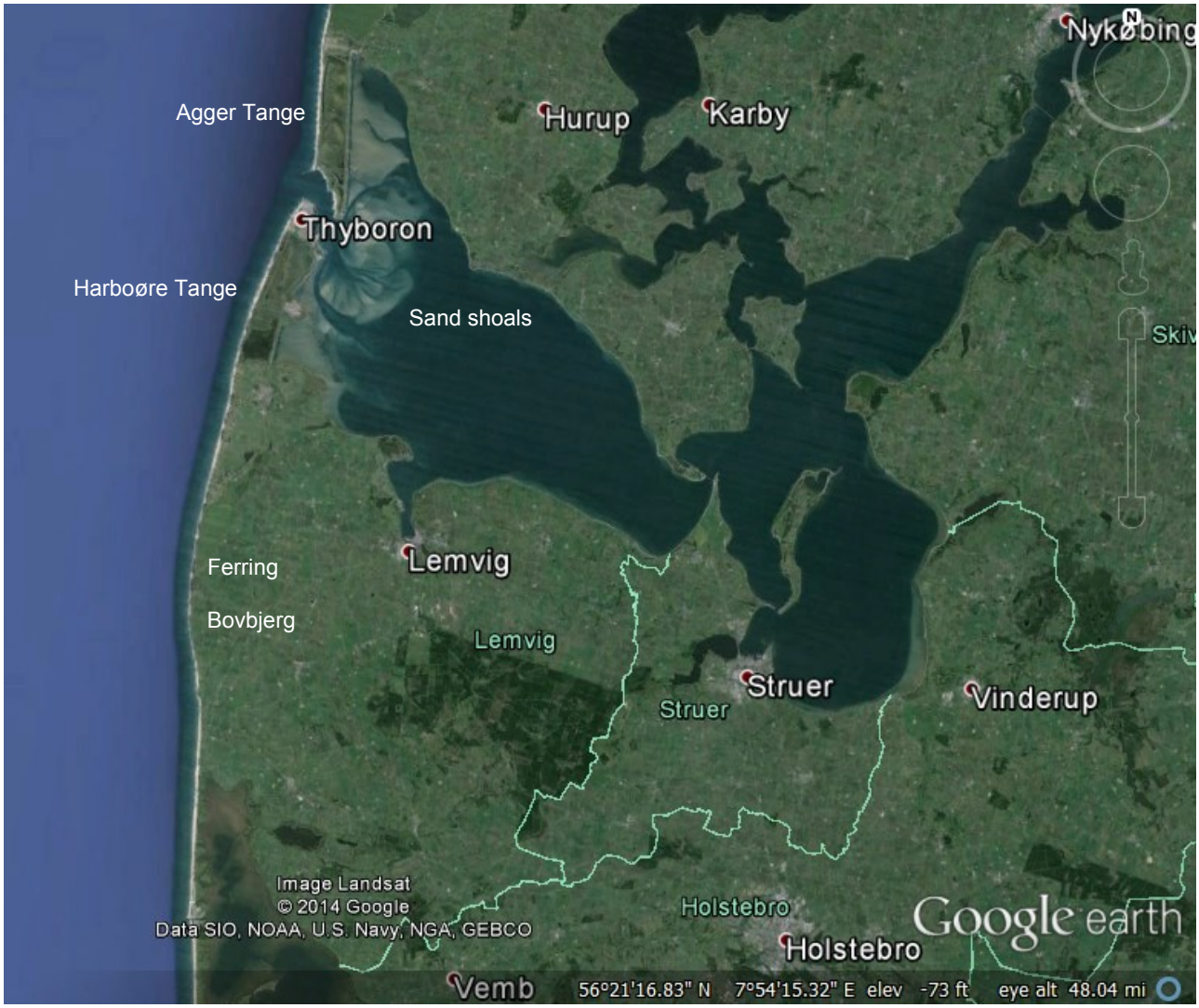

Figure 4.16 Aerial photo of the West Coast around the proposed OWF West Coast North, Google Earth, 2011.

Due to the extensive erosion a large groyne field was constructed along Harboøre Tange and Agger Tange to stabilise the barrier islands. Additionally, sea dikes and revetments have been constructed along the coast.

Over the recent decades the Danish Coastal Authorities has undertaken extensive beach nourishment along Harboøre and Agger Tange to strengthening the barrier islands and beaches.

The coast adjacent to the OWF is subject to large man-made interventions such as groyne field, revetments and beach nourishment. Additionally, the coast is subject to natural variability in wave climate and littoral sediment transport.

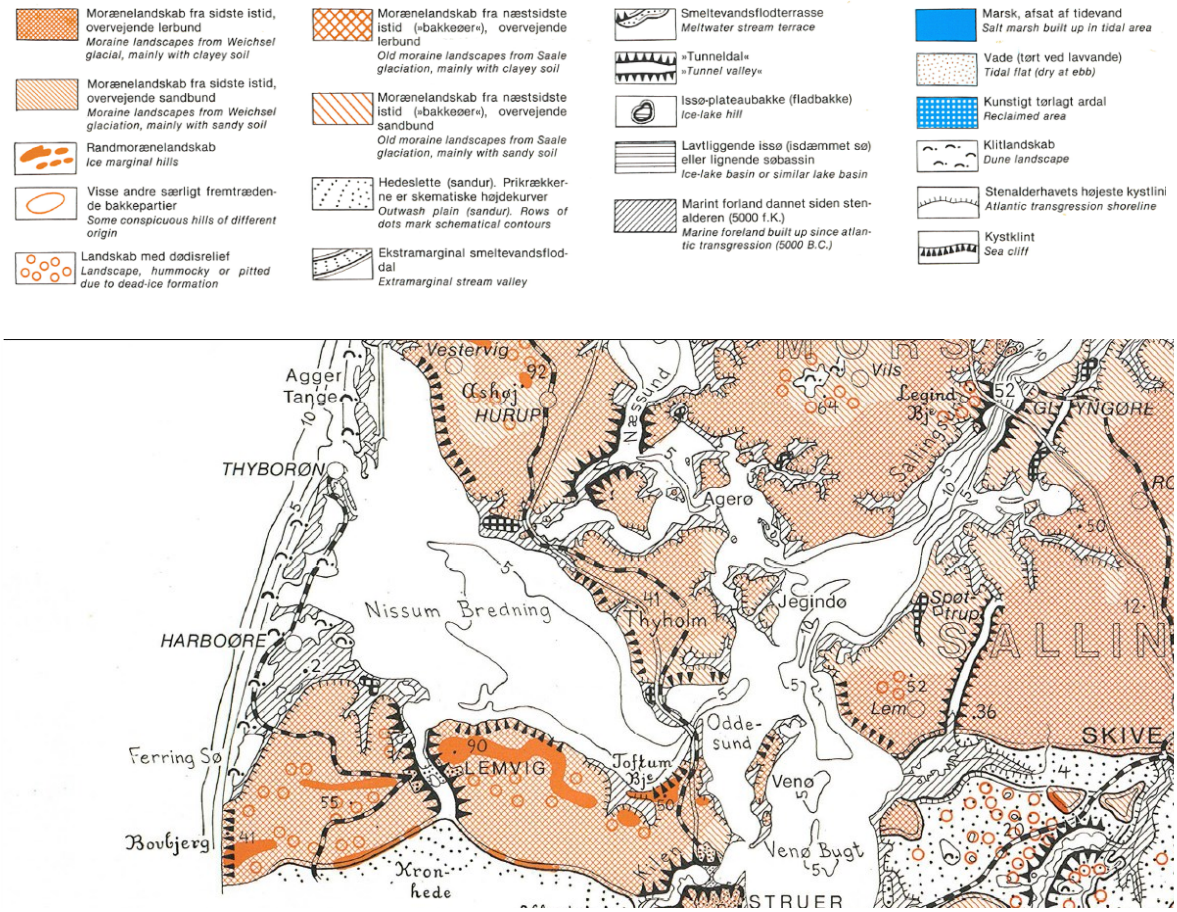

Figure 4.17 Landscape map of the area around Nissum Bredning [ref. /7/].

Figure 3.12 shows the bathymetry of the North Sea along Harboøre Tange south of Thyborøn and at the proposed OWF. The depth contours are generally parallel to the beach out to around the 15 m depth contour and water depths of 20 m are reached within 2.5 km from coast at Harboøre Tange.

When comparing historic and recent aerial photos and maps it is possible to assess the historic development of the coast and how dynamic it is. The Danish Coastal Authorities have published an assessment of the historic shoreline development in Denmark based on maps from around year 1900 and aerial photos from around year 2000, see Figure 4.18, [ref. /8/].

Generally, Figure 4.18 and Figure 4.19 shows that the coast at and south of Harboøre Tange is eroding significantly as described above due to littoral drift towards Thyborøn Kanal.

Figure 4.19 shows the magnitude of the natural erosion rate at and south of Harboøre Tange, Danish Coastal Authorities 2014. Generally, the beaches erode by up to 3 m/yr, which is characterised as very large by the Danish Coastal Authorities. The erosion rate at Bovbjerg is small due to the groyne field and the moraine cliffs.

Figure 4.18 *Assessment of historic shoreline recession at and south of Harboøre Tange (year 1882 and 2005). Danish Coastal Authorities [ref. /8/].*

Figure 4.19 Magnitude of natural erosion rate. Danish Coastal Authorities [ref. /8/], 2011.

Figure 4.20 shows the direction of the typical net littoral drift around Bovbjerg and Harboøre Tange, ref. /8/.

The net transport is generally towards north towards Thyborøn Kanal, but towards south south of Bovbjerg that forms a protrusion on the coast. The change in orientation of the coast around Bovbjerg result in diverges in net sediment transport direction.

Figure 4.20 *Direction of the net littoral drift. Danish Coastal Authorities [ref. /8/], 2011.*
Green: towards right when looking at the sea from land
White: near stable
Red: towards left when looking at the sea from land.

The littoral drift capacity along the coast at Profile 1 east of the Vesterhav Nord OWF at Vejlby (see Figure 3.12) is modelled in LITDRIFT for a typical profile orientation of 290°N between 2003 and 2013. Figure 4.33 shows that the modelled *gross littoral drift capacity* varies around 0.5 mio. m^3/year from around 0.6 mio. m^3/yr to 1.1 mio. m^3*/yr* and the *net littoral drift capacity* varies from 0 to -0.7 mio. m^3/year. Hence, there is large natural variability in the wave climate and thus littoral sediment drift from one year to the next adjacent to the proposed Vesterhav Nord OWF.

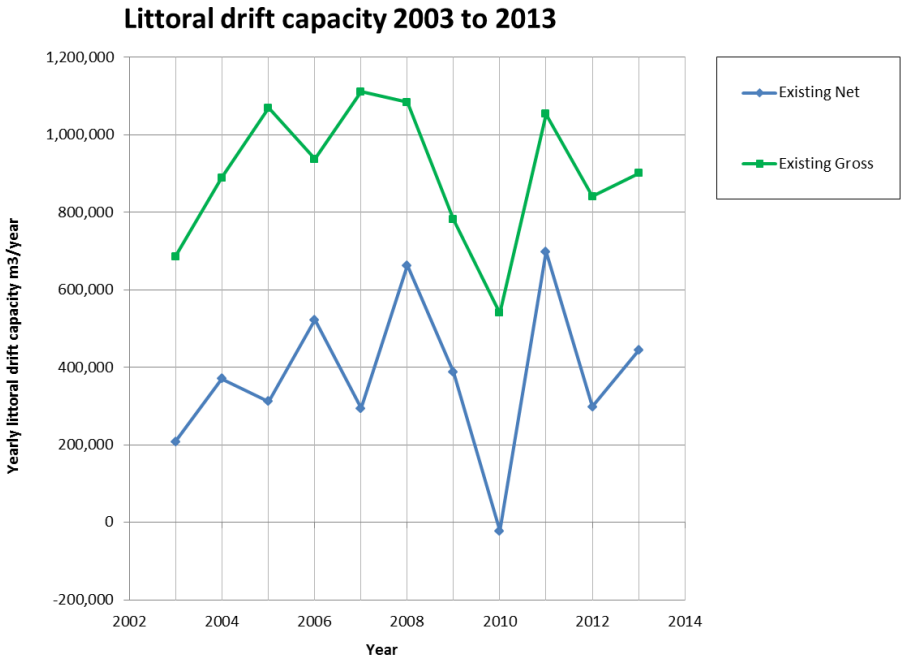

Figure 4.21 *Modelled natural variability of littoral drift for 2003 to 2013 at Profile 1, 290 deg. North, Vejlby. (see Figure 3.12).*

Figure 4.22 to Figure 4.32 shows the coast from Fjaltring south of Bovbjerg to Thyborøn. The sediment is generally sandy with a mean grain size of in the order of d_{50}=0.3mm, which provides wide and attractive beaches. However, there is a content of pebbles, which tends to concentrate in the swash zone and provides a steep foreshore. Therefore, the shore break can be intense. There is a groyne field along most of the coast because of the large erosion potential due to the sediment dynamics at Thyborøn Kanal.

Figure 4.22 *Beach with groynes at Fjaltring south of Bovbjerg.*

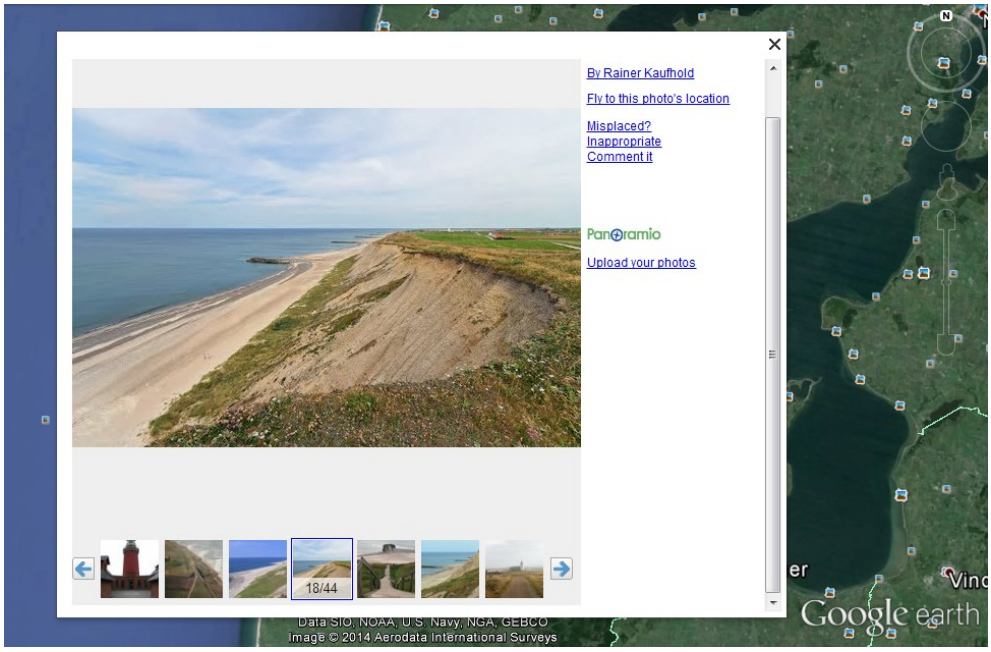

Figure 4.23 Moraine cliffs at Bovbjerg, Google Earth.

Figure 4.24 Moraine cliffs north of Bovbjerg towards Ferring.

Figure 4.25 Beach at Ferring towards south (top) and towards north (bottom).

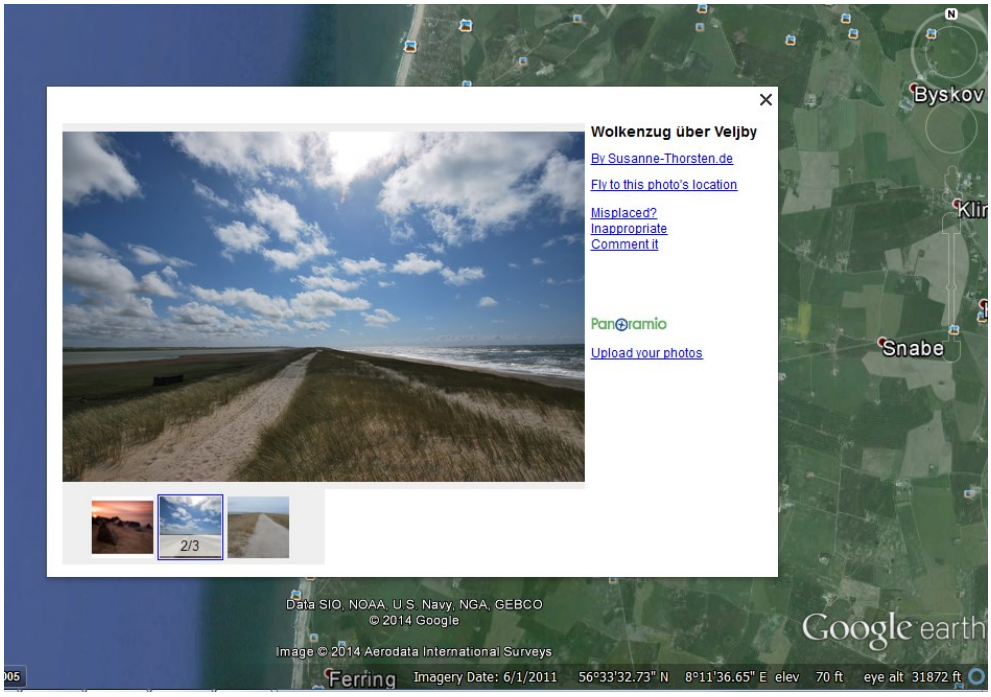

Figure 4.26 Beach, narrow barrier and lagoon at Ferring Sø, Google Earth.

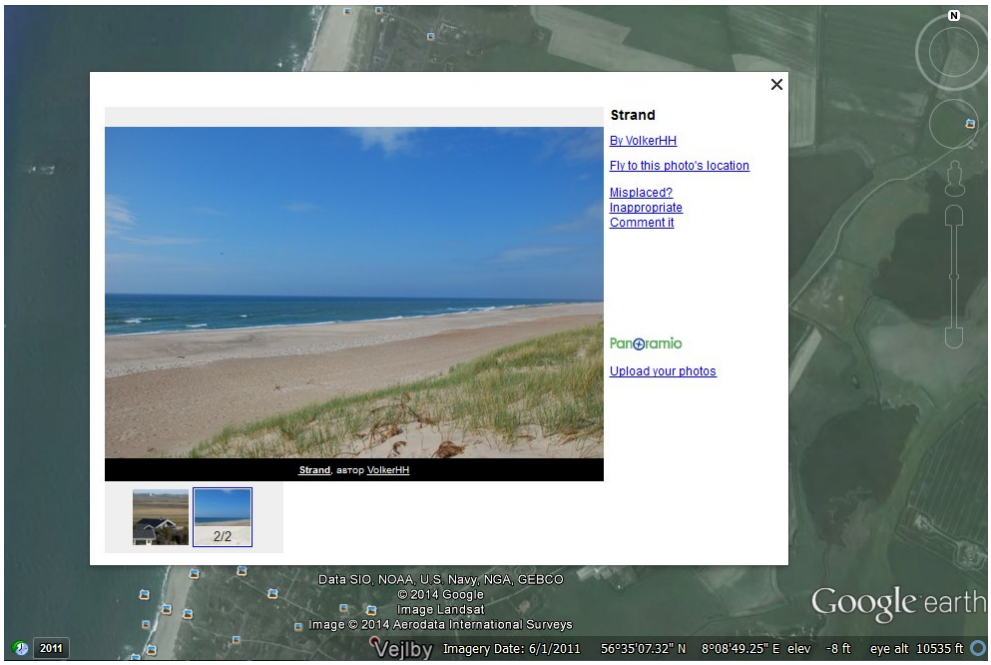

Figure 4.27 Open beach at Vejlby, Google Earth.

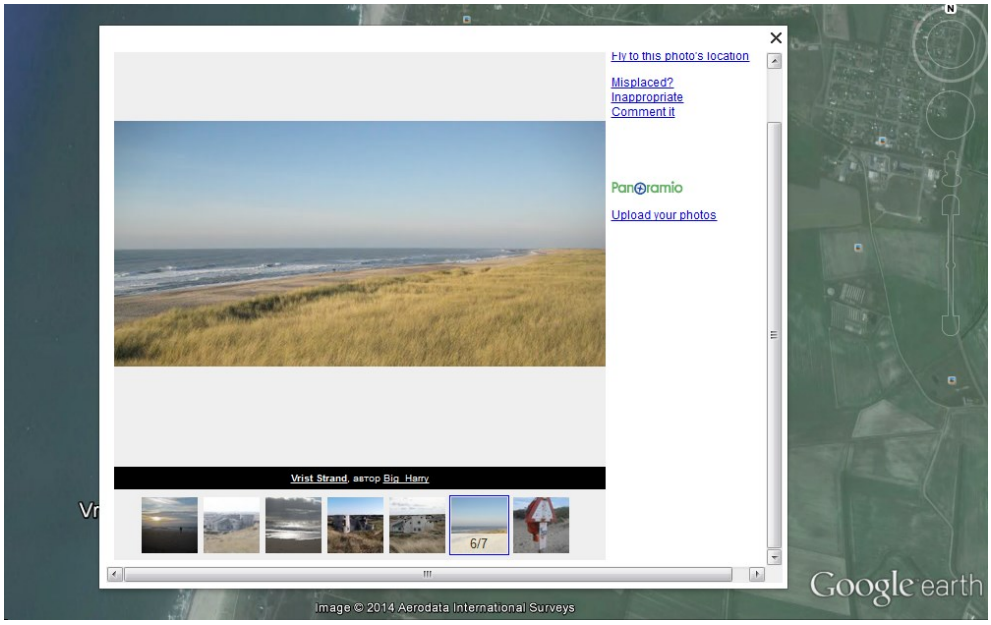

Figure 4.28 Beach and dunes at Vrist, Google Earth

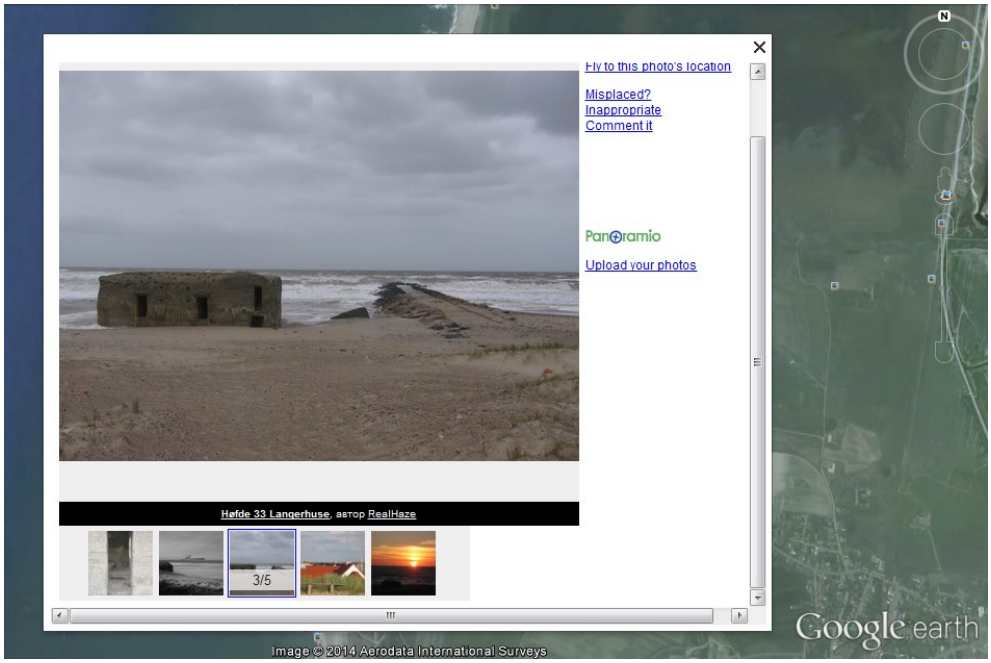

Figure 4.29 Beach with groynes at Langerhuse, Google Earth

Figure 4.30 Beach at Groyne 42 at Ceminova and toxic waste dump site

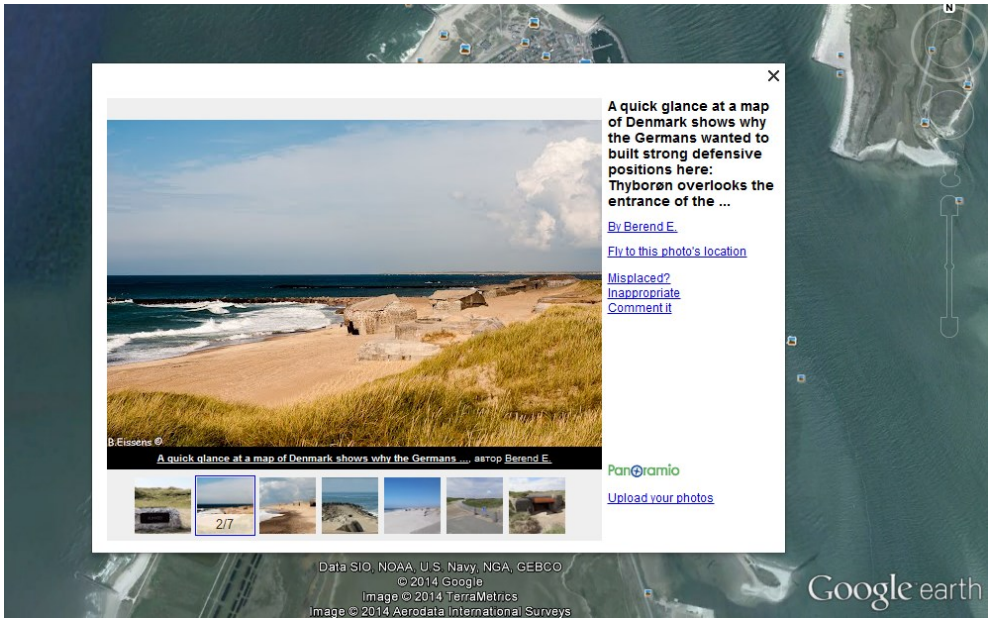

Figure 4.31 Beach with groynes at Thyborøn

Figure 4.32 Beach with groynes and beach nourishment at Thyborøn

4.6 Stratification of flow

The general picture of stratification in the North Sea is given in Figure 4.33. The stratification at the site of the wind farm is slightly affected by Jutland coastal current that carries the input from primarily the river Elbe but also the other large European rivers flowing into the North Sea. Hence a slight freshwater effect can be seen in the upper part of the water column, see Figure 4-36.

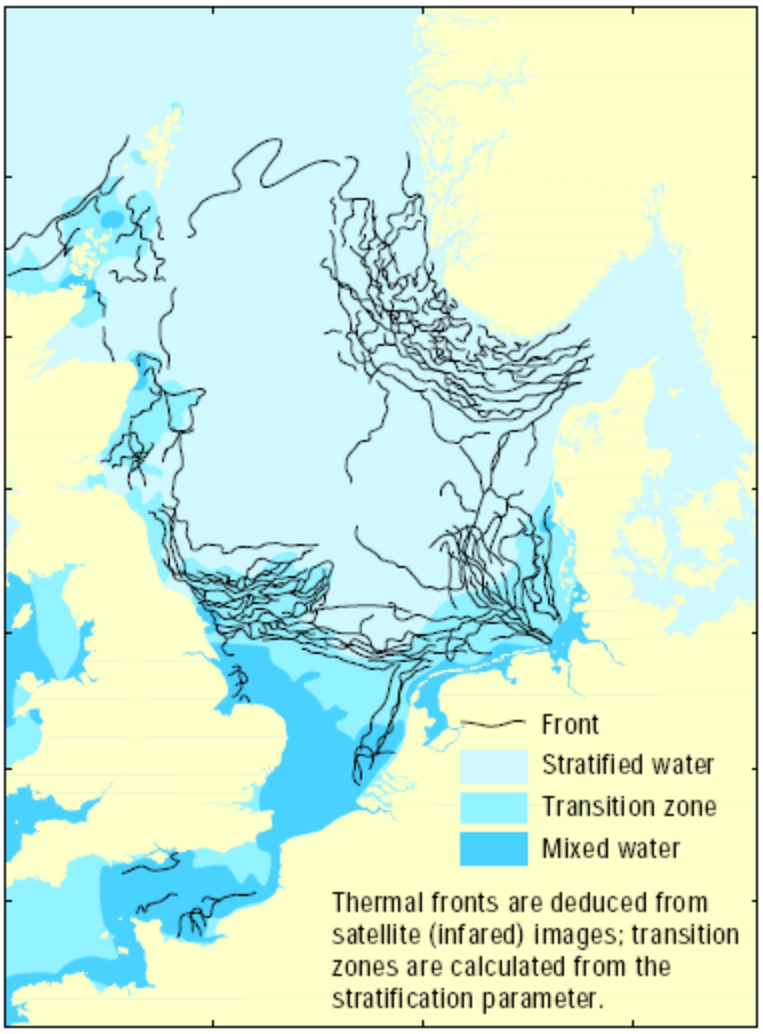

Figure 4.33 Schematic presentation of stratification in the North Sea /15/.

As described in section 3.4.2 the hydrodynamic modelling is based on MIKE 21 HD FM, which is a 2D model that does not include stratification. This simplification is justifiable because the stratification is only periodical and rare. Consequently, the influence of offshore wind farm can be described in a 2D model and on the basis of depth average currents.

4.7 Seabed sediments

Due to the seabed consisting mostly of sand and gravel, with little organic content, the potential for contaminated seabed sediments is low [ref. /16/]. Hence, environmental testing of sediments has not been performed.

4.8 Water quality

For the present project the relevant baseline for water quality comprises:

› Salinity and temperature at surface and sea floor

› Nutrient content at the surface

Influence on water exchange, stratification and nutrient release is described as pressures that may have an effect on water quality. These features are analysed in more details in the chapter and on pressures during construction and operation (see chapter 5 and 6).

The baseline description is based on national monitoring data obtained in the period 1993 to 2003 by the County of Ringkøbing. The national monitoring programme was reduced significantly 2003. Based on observations from other stations it is found that the background concentrations or nutrients are approximately of the same level.

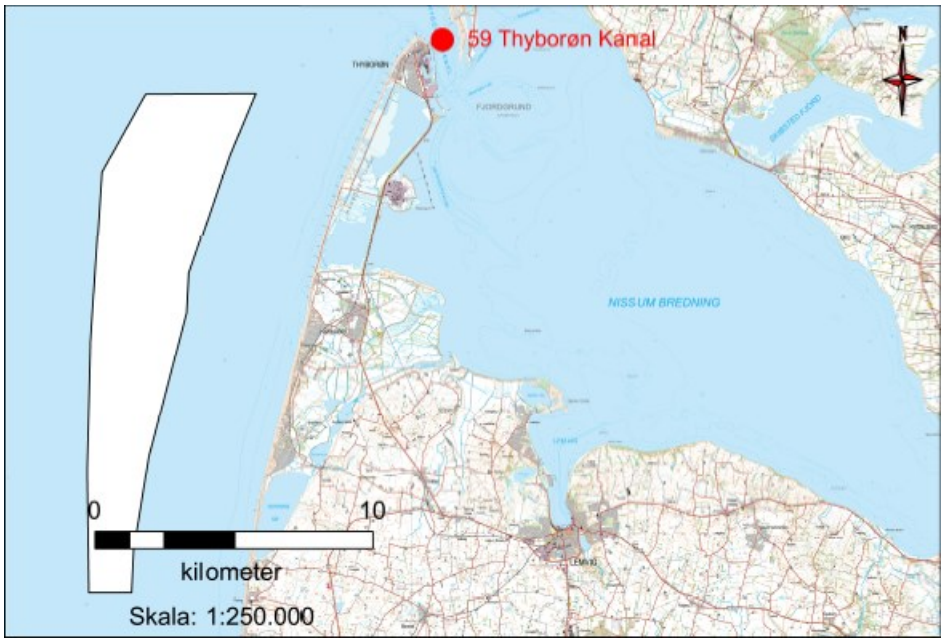

Figure 4.34 *The monitoring station 59 Thyborøn Kanal, and the wind farm area marked in white.*

4.8.1 Salinity and temperature at surface and sea floor

Measurements of salinity and temperature have not been conducted at the site of the wind farm. The nearest monitoring station is found at station 59 at Thyborøn Kanal. Since these measurements are influenced by relatively fresh water flowing out from the Limfjord, it is expected that the condition at the wind farm will be more saline and with less salinity variation than those reported for station 59.

The monthly variation of salinity at the surface and the seafloor at the monitoring station 59 Thyborøn Kanal is indicated in Figure 4.35. The values are given as monthly median values for the measurements in the period 1993 to 2003.

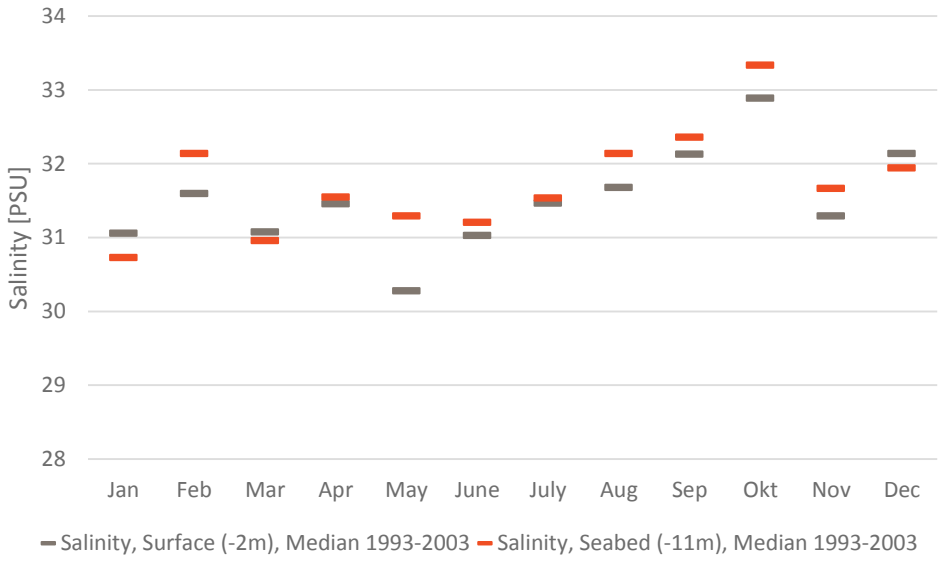

Figure 4.35 *Monthly median values for salinity at monitoring station 59 Thyborøn Kanal [ref. /17/].*

The different vertical structures of the salinity condition is illustrated in Figure 4-36, where it is seen that the water mass above approx. 12 m water depth is affected by slightly less saline water of the Jutland Coastal Current, which typical has a salinity of 31-34 PSU whereas the central North Sea has about 35 PSU. The stratification is, however, very weak and of little environmental importance.

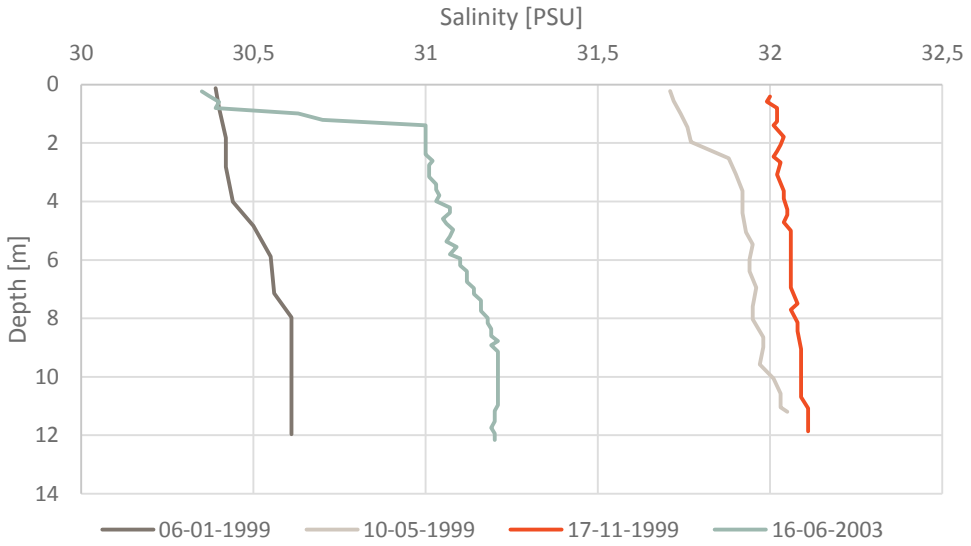

Figure 4.36 *Vertical salinity profiles from four different days, representing different stratification situations at the location of the monitoring station 59 Thyborøn Kanal [ref. /17/].*

The monthly temperature variation at the surface and the seafloor at the monitoring station are indicated in Figure 4-37. The values are given as monthly median values for the measurements in the period 1993 to 2003.

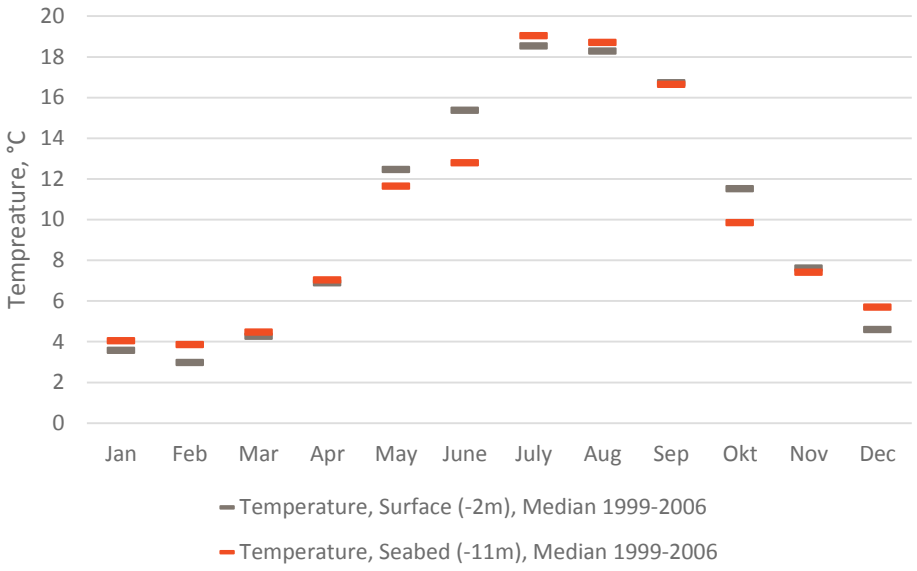

Figure 4.37 *Monthly median values for temperature at monitoring station 59 Thyborøn Kanal [ref. /17/].*

The figure illustrates the typical annual temperature variation where the lower layer temperature is slightly delayed compared to the upper layer temperature.

4.8.2 Oxygen concentration at the sea floor

The monthly variation of oxygen at the seafloor at the monitoring station is indicated in Figure 4-38. The values are given as monthly median values for the measurements in the period 1993 to 2003.

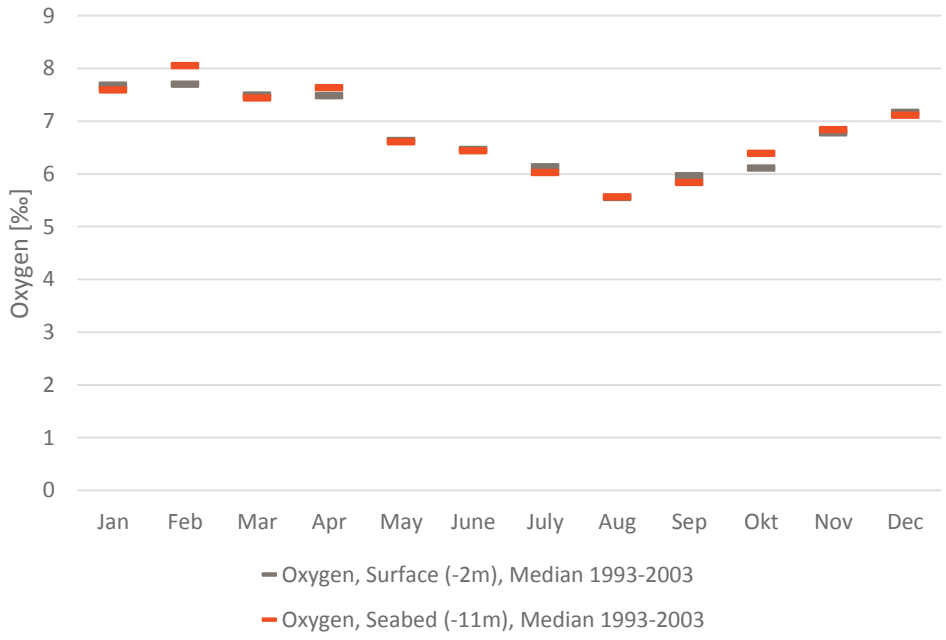

Figure 4.38 *Monthly median values for oxygen at monitoring station 59 Thyborøn Station [ref. /17/].*

The annual oxygen variation reflects the dependency of oxygen concentration by temperature. During the year the water column is well-mixed and shows no sign of stratification. Variation in oxygen levels is due to increased oxidation during summertime and vice versa in wintertime reduced oxidation is reflected in increased oxygen levels.

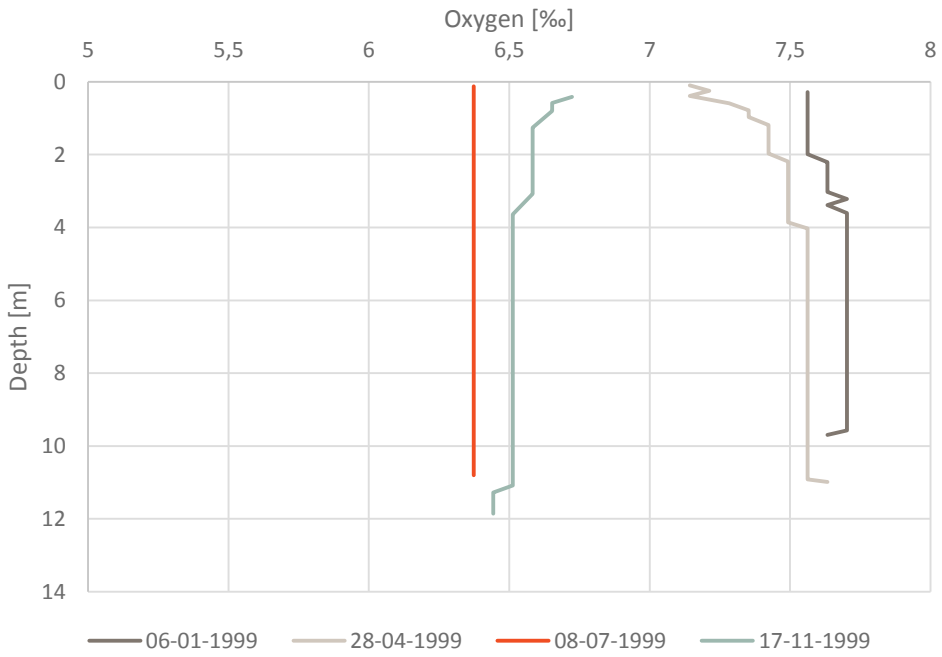

Figure 4.39 *Vertical oxygen profile from the monitoring station 44 illustrating the conditions during spring and autumn [ref. /17/].*

At 4 mg/l organisms seek to leave the area and at 2 mg/l organisms die. The above profile (see Figure 4-39) and median values, clearly indicates that the oxygen conditions throughout the year are good for organisms.

4.8.3 Nutrient concentrations

The monthly variation of nutrients, total nitrogen (N_{tot}) and total phosphorous (P_{tot}) at the surface at the monitoring station, is indicated in Figure 4-40 and Figure 4-41. The values are given as monthly median values for the measurements in the period 1998 to 2003. Unfortunately, no N_{tot} and P_{tot} data are available for the sea floor.

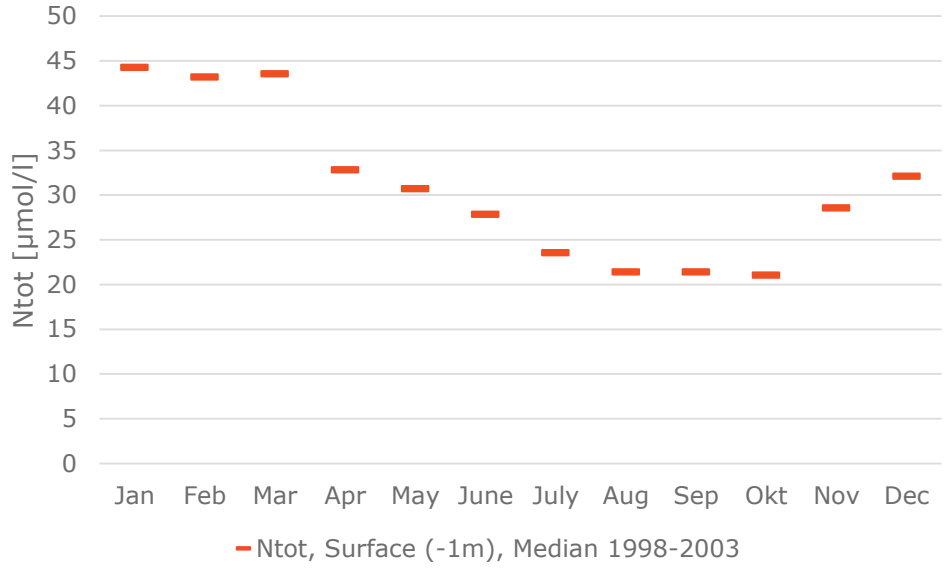

Figure 4.40 *Monthly median values for total nitrogen at monitoring station 59 Thyborøn Kanal.*

The concentrations increase in the surface during winter months due to riverine input of nitrogen and also of freshwater that (together with westerly winds) gives rise to the Jutland Coastal Current and hence a (weak) stratification.

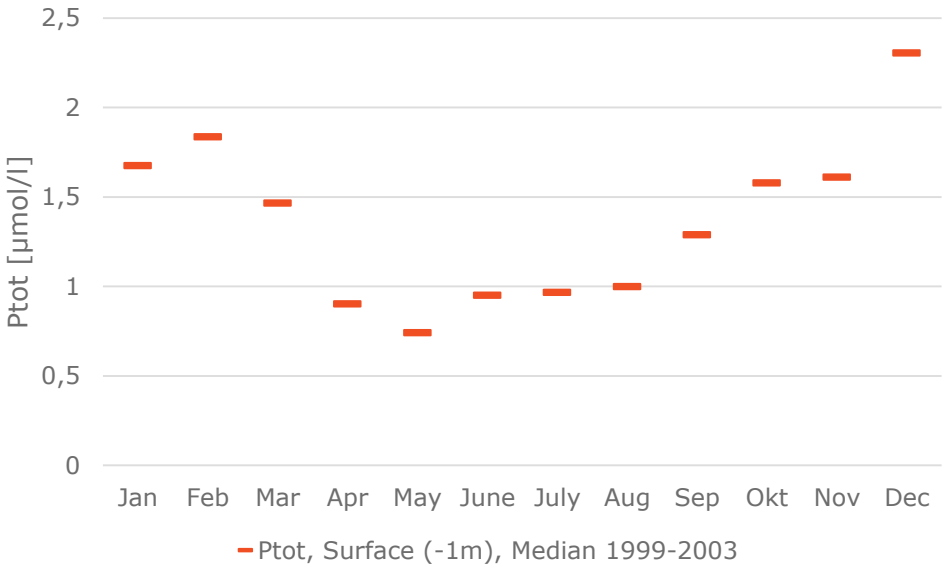

Figure 4.41 *Monthly median values for total phosphorous at monitoring station 59 Thyborøn Kanal.*

It is noted that total phosphorous concentration in the upper layer shows a sudden decrease (drop) after spring bloom due to sinking out of algae. During autumn and winter period concentrations increase due to load from land. The layer shows an increase in August and forward. This is due to the phosphorous release from the sediment during oxygen depletion and high temperature period in late summer at other locations in the North Sea and runoff from the mainland.

4.8.4 Suspended matter concentrations

The concentration of suspended matter in the water column gives rise to reduced light penetration (light attenuation). A high light attenuation will cause reduced growth of plants and hence reduce the environmental quality.

The light attenuation is traditionally measured in terms of “Secchi depth”. This is the depth at which a Secchi disc of Ø20 cm is no longer visible when lowered into the water. The secchi depth in Danish waters is investigated by Lund-Hansen, L. C. (2004) [ref. /18/] and shows that the average secchi depth near coast at the location of the OWF is 5.4 ± 2.0 m.

Secchi depths may be converted into concentrations of suspended particulate matter (SPM) as described by Devlin (2008) [ref. /19/]:

$$\left.\begin{array}{rcl} \ln(\widehat{K_D}) & = & -0.010 - 0.861\ln(S) \\ \widehat{K_D} & = & 0.039 + 0.067SPM \end{array}\right\} \rightarrow SPM = \frac{14.777}{\exp(0.861\ln(S)} - 0.582$$

Where,

SPM is the concentration of suspended particular matter (mg/l)
S is the secchi depth (m)
$\widehat{K_D}$ is the attenuation coefficient (m^{-1}), $\widehat{K_D} = \frac{\ln(I_0/I_z)}{z}$
I_0 is the light at the sea surface
I_z is the light at the depth, z
z is the depth below sea surface

Based on the above equation it is found that a secchi depth of 5.4 ± 2.0m corresponds to natural variations in sediment concentration of around 2.1-4.6 mg/l, and average concentrations of 2.9 mg/l.

In this context it is however noted that the secchi depth has probably only been measured under favourable weather conditions. Wave breaking and suspended sediment transport along with suspended particulate matter from the North-German rivers reduce the visibility underwater significantly in the winter months. Studies, that include the above effects show that seasonal average surface concentrations of SPM are in the order of 5 mg/l in and near the project site during the winter season [ref. /20/] (see Figure 4.42).

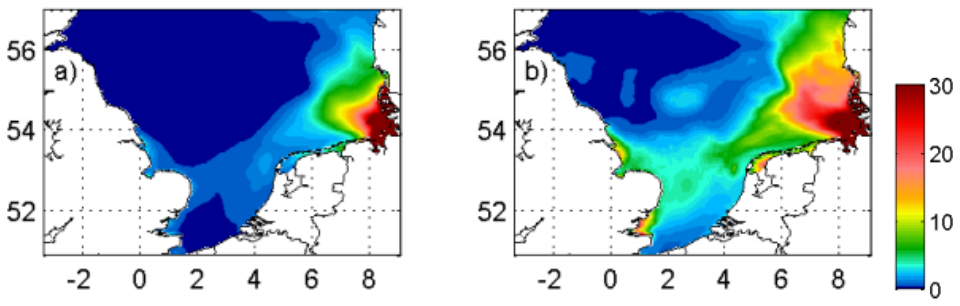

Figure 4.42 Seasonal mean concentration of suspended particulate matter (SPM) 14 April – 15 April (left) and 15 October – 15 April (right) [ref. /20/]

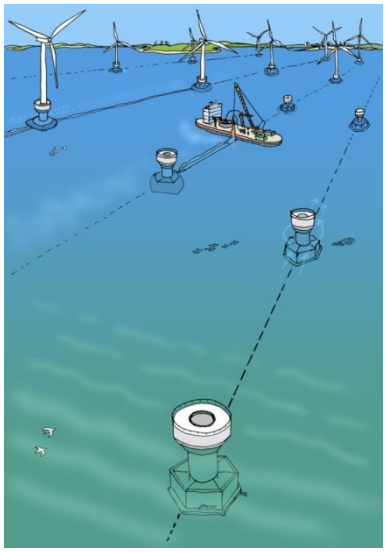

5 Potential pressures during construction

Potential pressures during construction arise from sediment spill due to seabed preparation prior to installation of gravity based foundations and from jetting of inter-array and export cables. Sediment spill is modelled in the MIKE 21 MT (Mud Transport) model as described in section 3.4.5. Using this model, the sediment concentrations, sedimentation quantities and rates of spilled sediments during installation works have been studied and the results are described in the following.

As described in section 4.7 present information on sediment types did not give indications on high contents of nutrients or toxic substances. Therefore, it is assumed that the establishment of wind farms will not give rise to nutrient enrichment or toxic impact.

Plots showing exceedance frequencies of environmentally related thresholds are given in the following for each scenario studied. Evaluated threshold values are based on experiences from construction of the Great Belt and Øresund Link.

Suspended sediment concentrations and related effects:

- 2 mg/l : Sediment is visible
- 5 mg/l : Sediment is more visible
- 10 mg/l : Secchi depth is approx. 2.5 m and sensitive fish will abandon
- 15 mg/l : Bathing water threshold, and limitation of birds foraging due to impaired visibility depth

Sedimentation rates and effects:

- 60 g/m^2/day or 2.5 g/m^2/hour: Mussel larvae growth is inhibited

5.1 Increase in suspended sediment concentrations

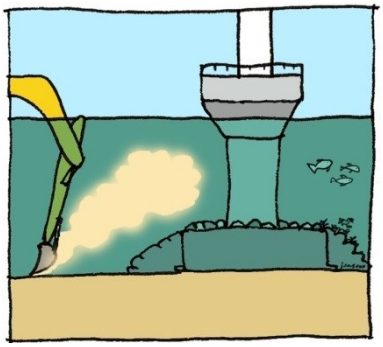

5.1.1 Installation of foundations

This section describes the predicted increase in sediment concentrations (increased turbidity) for installation of 66 gravity based foundations – defined as scenario 1 (see Appendix E). Figure 5.1 illustrates the exceedance frequency of depth averaged sediment concentrations in excess of 2, 5, 10 and 15 mg/l.

The following is concluded:

- 2 mg/l: Threshold exceeded for around 5 hours inside the OWF area. Locally (around foundations) for up to 10-20 hours
- 5 mg/l: Threshold exceeded only locally around some foundation for 3-6 hours
- >10-15 mg/l: Threshold exceeded for less than 2 hours

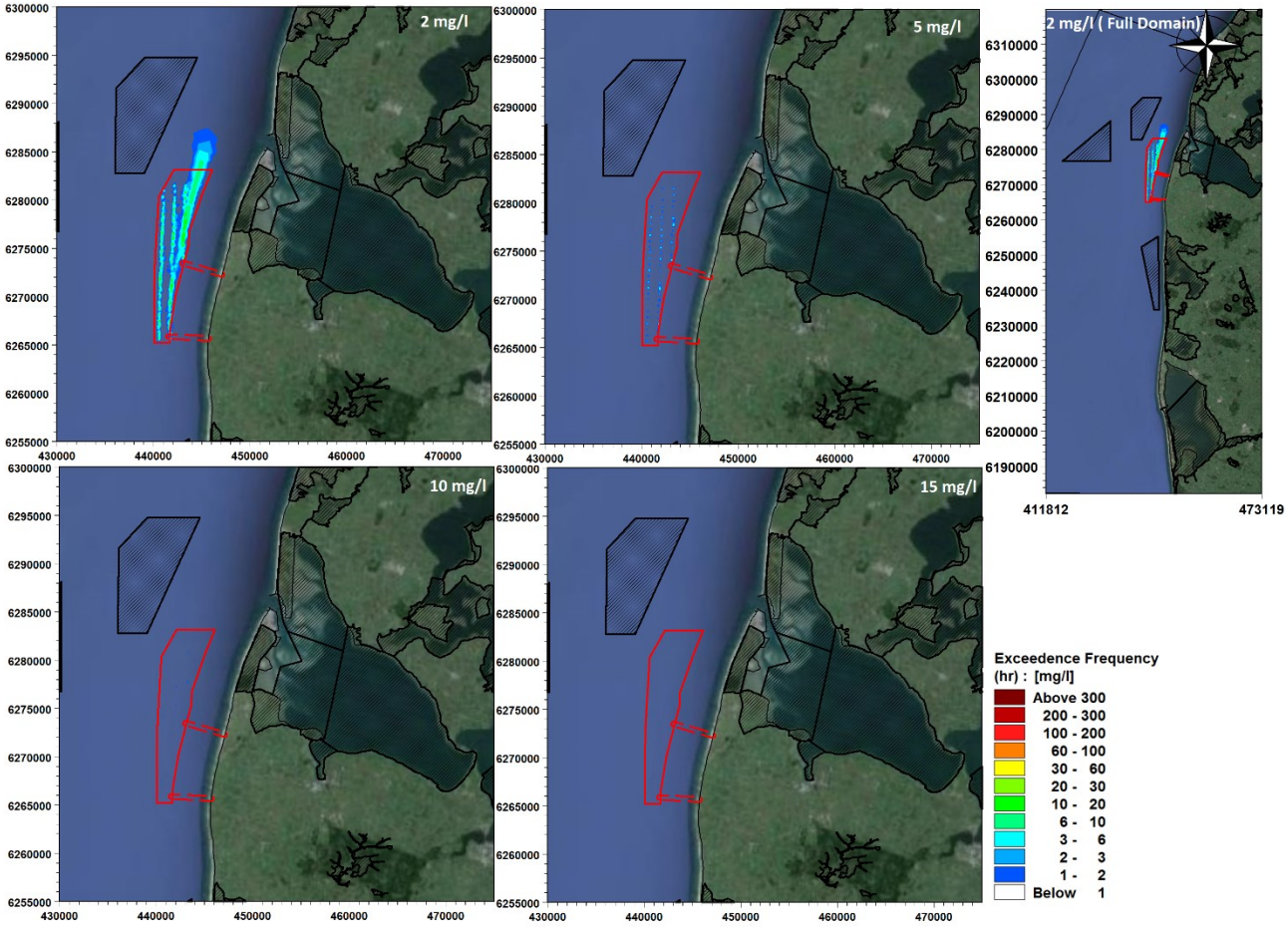

Figure 5.1 Exceedance frequency of depth averaged suspended sediment concentrations in excess of 2, 5, 10 and 15 mg/l, during the dredging/excavation works. Hatched areas with black frames are Nature 2000 areas.

Figure 5.2 shows the maximum depth average suspended sediment concentration at any time during the entire dredging/excavation works. The sediment concentration will generally not exceed 6 mg/l inside the OWF area, but at a few foundations the concentration reaches 10-20 mg/l for a short time (< 2 hours) during the installation period. Outside the OWF area concentrations are less than 3 mg/l.

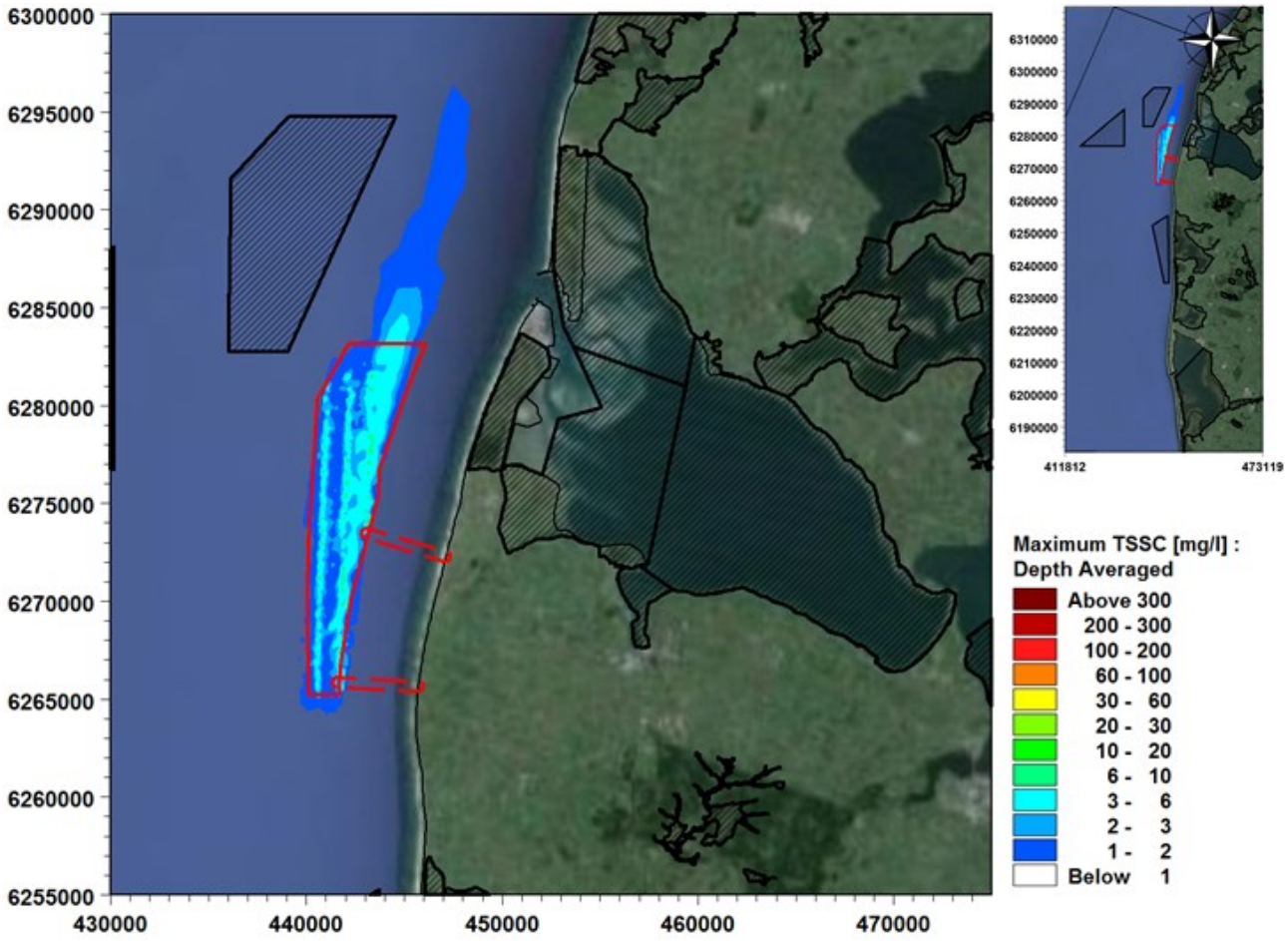

Figure 5.2 *Maximum depth averaged total suspended sediment concentrations (TSSC) at any given location during the dredging/excavation works. Hatched areas with black frames are Nature 2000 areas.*

The above modelling results indicate an average increase locally around foundations of 1 to 6 mg/l. In the 2-month installation period, an exceedance of 2 mg/l will occur for up to 5 to 20 hours (less than ½-1 day), whereas an exceedance of 5, 10 and 15 mg/l will only occur at very local areas in 2 to 6 hours. This clearly demonstrates that the suspended matter due to dredging/excavation for foundations will be of orders smaller than the natural variability in the region (see section 4.8.4).

5.1.2 Jetting of cables

Figure 5.3 illustrates the exceedance frequency of depth averaged total suspended sediment concentrations (TSSC) in excess of 2, 5, 10 and 15 mg/l.

It is noted that jetting of cables will influence the concentration of suspended sediments in the shallow nearshore waters (less than 4-5 m water depth) several kilometres (>50 km) towards north and south. The fine sediment is caught by the strong wave-induced (littoral) current and remains in suspension of a long time due to wave breaking and high turbulence. Consequently, the fines may remain in suspension for several weeks until they get caught by a rip current that forces the fines into deeper and calmer waters, or until they settle on the shoals inside Nissum Bredning or in some of the other fjords along the west coast of Denmark.

It is recognized that the fines enter into natural sediment patterns and processes along the highly dynamic West Coast and that not all fines have settled by the end of the simulation period. This does however not influence the overall conclusion highlighted in the following:

- 2 mg/l: Threshold exceeded for up to 30-60 hours and locally for up to 100-200 hours inside the OWF. In the area between the OWF and the coast the threshold is exceeded for up to 30-60 hours. In shallow water, at the coast 10-15 km north and south of the OWF, the threshold is exceeded for 100-400 hours. Further up the coast, around 30 km north of the OWF, the threshold is exceeded for up to 20-30 hours. Inside Nissum Bredning the sediment settles on the shallow shoals inside the Natura 2000 area. Here the threshold is exceeded for up to 20 hours. 20 km to the south of the OWF along the coast, the threshold is exceeded for up to 60 hours. The threshold is not exceeded in the Natura 2000 areas to the north, south and west of the OWF.

- 5 mg/l: Threshold exceeded for up to 30-60 hours locally inside the OWF. In the area between the OWF and the coast the threshold is exceeded for up to 20-30 hours. Along the coast the threshold is exceeded for up to 200 hours north and south of the landfall of the cable corridors. Further south at the coast, the threshold is exceeded for up to 20 hours. 20 km to the north of the OWF, the threshold is exceeded for up to 20-30 hours along the coast. Just inside Nissum Bredning entering the Natura 2000 area, the threshold is exceeded for up to 6-10 hours.

- >10-15 mg/l: Inside the OWF the thresholds are exceeded along the cables for 6-20 hours, and locally of up to 40 hours. Along the cable corridors between the OWF and landfall thresholds are exceeded for 10 to 20 hours, and close to the coast just north and south of the landfalls for up to 30-60 hours, locally up to 100 to 200 hours. Along the coast; 10 km south of the OWF and up Thyborøn Kanal towards north, thresholds are exceeded for up to 10 to 20 hours. At Nissum Bredning entering the Natura 2000 area, the threshold is exceeded for up to 3-6 hours.

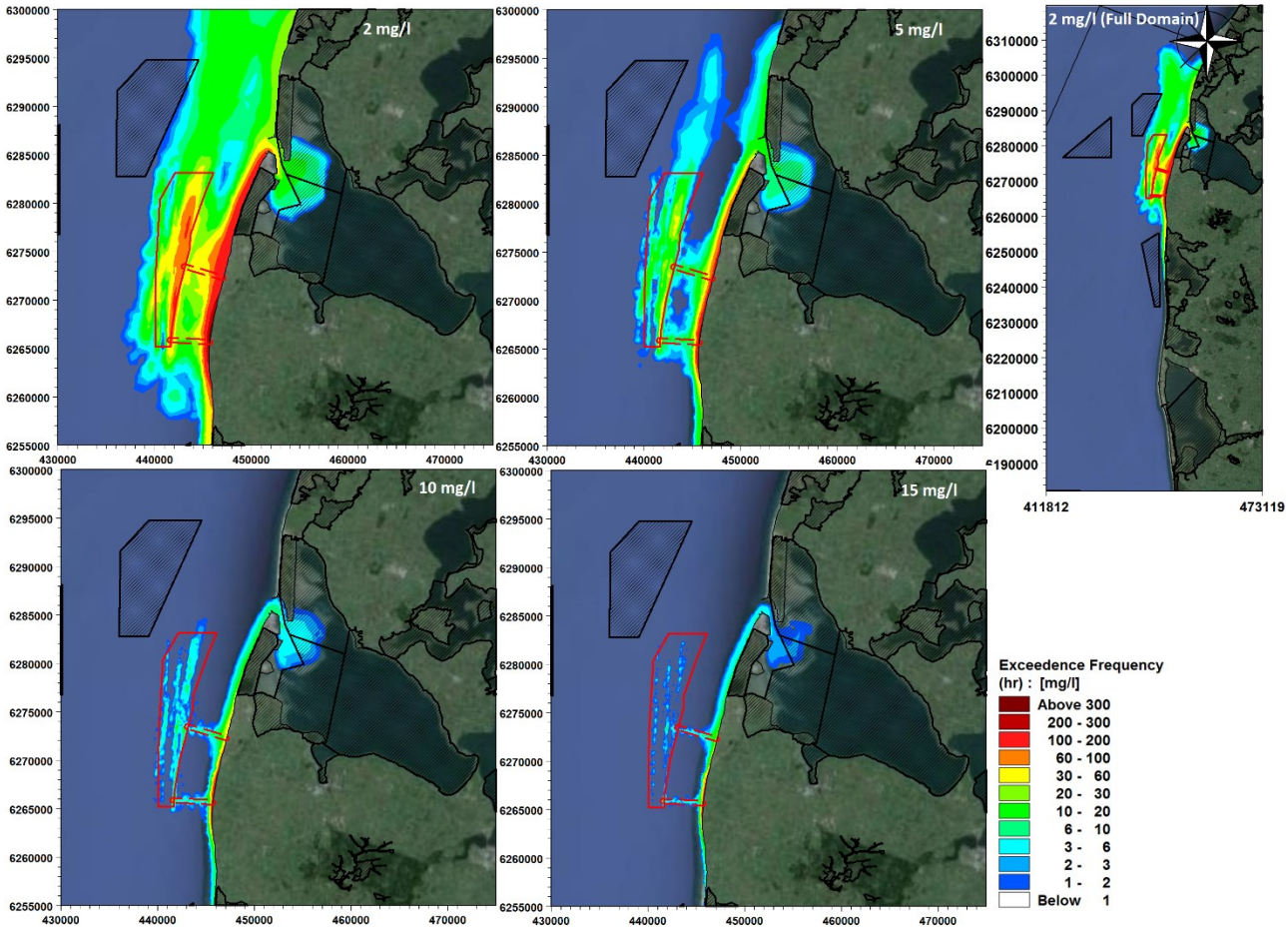

Figure 5.3 *Exceedance frequency of depth averaged total suspended sediment concentrations (TSSC) in excess of 2, 5, 10 and 15 mg/l, during the jetting of cables. Left: zoomed, and right: full domain. Hatched areas with black frames are Nature 2000 areas.*

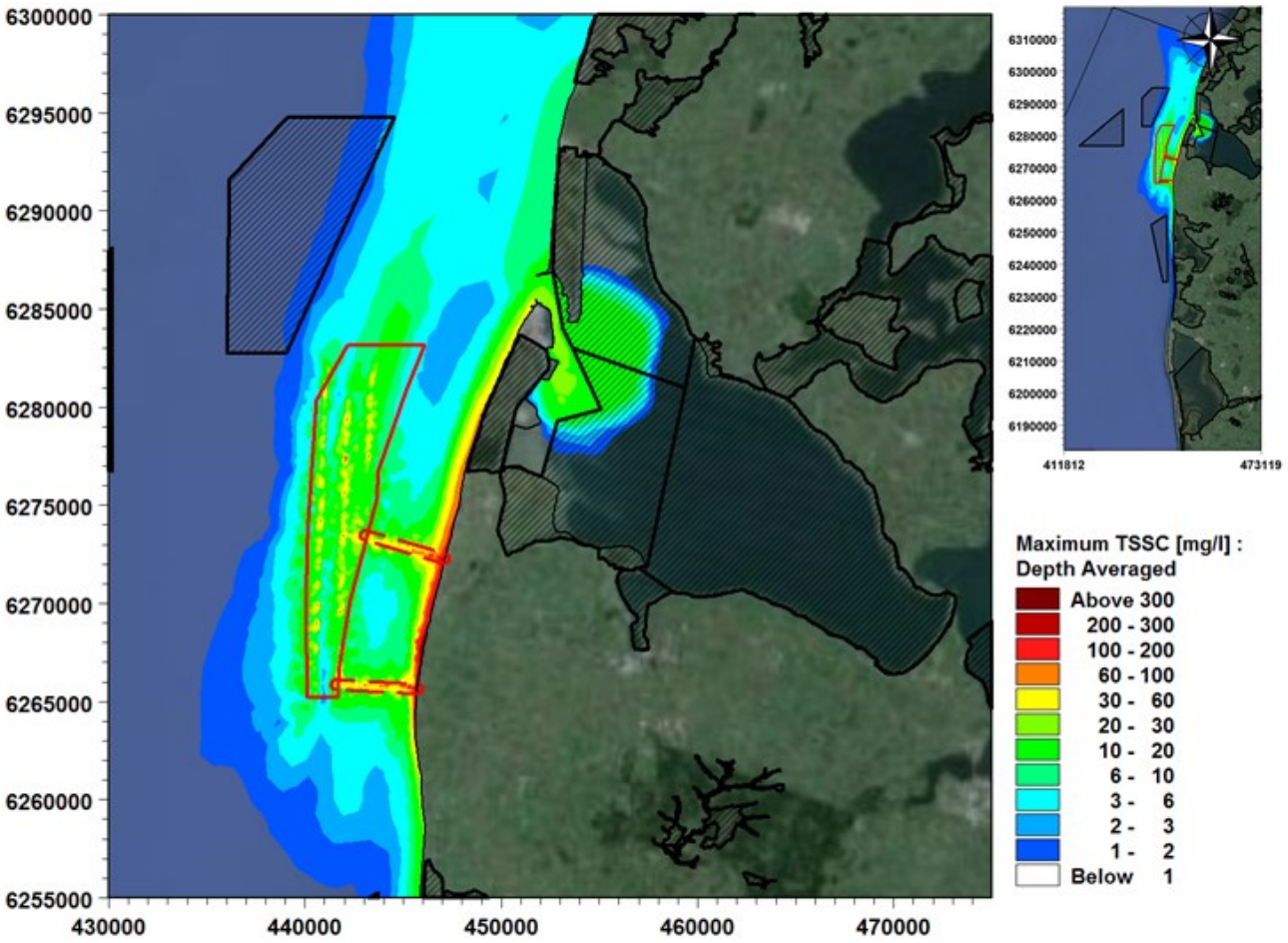

Figure 5.4 *Maximum depth average suspended sediment concentrations at any given location during jetting of cables. Hatched areas with black frames are Nature 2000 areas.*

Figure 5.4 indicates a maximum increase in sediment concentrations within the wind farm in the order of 6 to 30 mg/l. Locally inside the OWF sediment concentrations reach 100 mg/l and at the landfall of the cable corridors the sediment concentrations reach 200 mg/l. Concentrations of 30-60 mg/l are observed up to Thyborøn Kanal north of the OWF within less than 4 m water depth, and 10 mg/l are predicted along the coast as far as 30 km north of the OWF. An exceedance of 2 and 5 mg/l will occur for up to 100-400 hours (4-16 days) whereas an exceedance of 10 and 15 mg/l will only occur in local areas for 30 to 60 hours within the 36 day period where jetting works are performed. When compared to natural variations of SPM concentrations (see section 4.8.4) it is found that suspended sediment concentrations due to jetting of cables will be of the same order of magnitude as the natural variability in the region.

5.1.3 Summary of increase in total suspended sediment concentration during construction

The results of the modelling show that seabed preparation for installation of gravity based foundations (scenario 1) will result in minor increases in sediment concentrations (increased turbidity); less than 5 mg/l within most of the OWF area and very short periods with concentration of up to 10 mg/l in limited areas. It is also

found that maximum concentrations outside the OWF area are less than 5 mg/l at all times.

Jetting of cables (scenario 2) is expected to cause larger sediment spill volumes and affects wider areas than dredging/excavation works at foundations (scenario 1). Model results predict maximum concentrations reaching the order of 60 mg/l in the cable corridors and 200 mg/l at the landfall. Concentrations of 30-60 mg/l are observed along the coast up to Thyborøn Kanal to the north. Up to 10 mg/l is predicted along the coast as fare as 30 km north of the OWF because some of the spilled sediment is caught and transported by the strong littoral current and kept in suspension by wave breaking. Within the OWF area jetting of inter-array cables is predicted to cause concentrations of up to the order of 30 mg/l. Outside the wind farm and cable corridors maximum concentrations are less than 20 mg/l at all times during jetting operations except in shallow waters along the coastline. In the near vicinity along the coast of where jetting is being performed concentrations greater than 2 mg/l occur for up to 100 to 400 hours, whereas concentrations of 5 mg/l are experienced for up to 20-200 hours.

Natural variations in sediment concentrations are caused by bed sediments brought in suspension by large waves and/or suspended particular matter from the North-German rivers which gets carried up the West Coast by the coastal current at regular intervals. These natural variations in sediment concentrations, which occur at regular intervals, are of the same order of magnitude as the concentrations of spilled sediments during dredging/excavation and jetting operations. It is considered unlikely that the a high input of suspended particular matter from the North-German rivers should affect the waters at the OWF in conjunction with the 8-16 day period where sediment concentrations are higher than 2-5 mg/l due to construction activities. And in the unlikely event that this should take place the combined pressure will be very short Consequently, the transitory influence of the OWF on light attenuation at the seabed is considered within the range of the natural variations. The environmental pressures caused by increased turbidity - during and after construction – is considered to be *minor*.

5.2 Sediment spill deposition

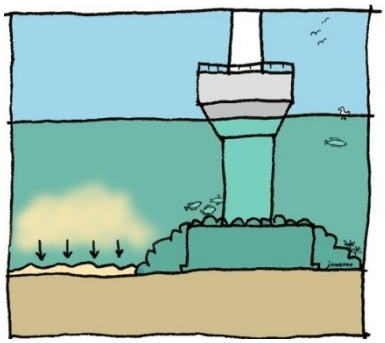

The sediment released during seabed preparation will deposit on the seabed near the dredging/excavation and jetting activities. The material may deposit and get re-suspended several times before it deposits more permanently in a location where the waves and currents are not able to re-suspend it. The following description is based on the net deposition two weeks after dredging/excavation and jetting activities have been finalised. It is assumed that spilled material will have deposited in a relatively permanent location after two weeks. However, as mentioned in section 5.1.2 some of the fines caught in the turbulent near shore waters along the West Coast may remain in suspension of several weeks before settling in sheltered bays (i.e. Nissum Bredning) or in deep waters. It is highlighted that the model only describes the transport, deposition and erosion of spilled sediments and not the natural sediment transport, deposition and erosion rates.

5.2.1 Installation of foundations

The total deposition of spilled sediment two weeks after end of foundation dredging/excavation works is shown in Figure 5.5. Inside the OWF area the spilled sediment will deposit in quantities of around 50-100 g/m^2 with a very few exceptions near individual foundations, where of up to 400 g/m^2 will deposit. Only very little sedimentation is found outside the OWF area (up to 50 g/m^2 north of the OWF), and Figure 5.6 shows that the threshold sedimentation rate of 2.5 g/m^2/hour (or 60 g/m^2/day) is not exceeded during the dredging/excavation works for foundations.

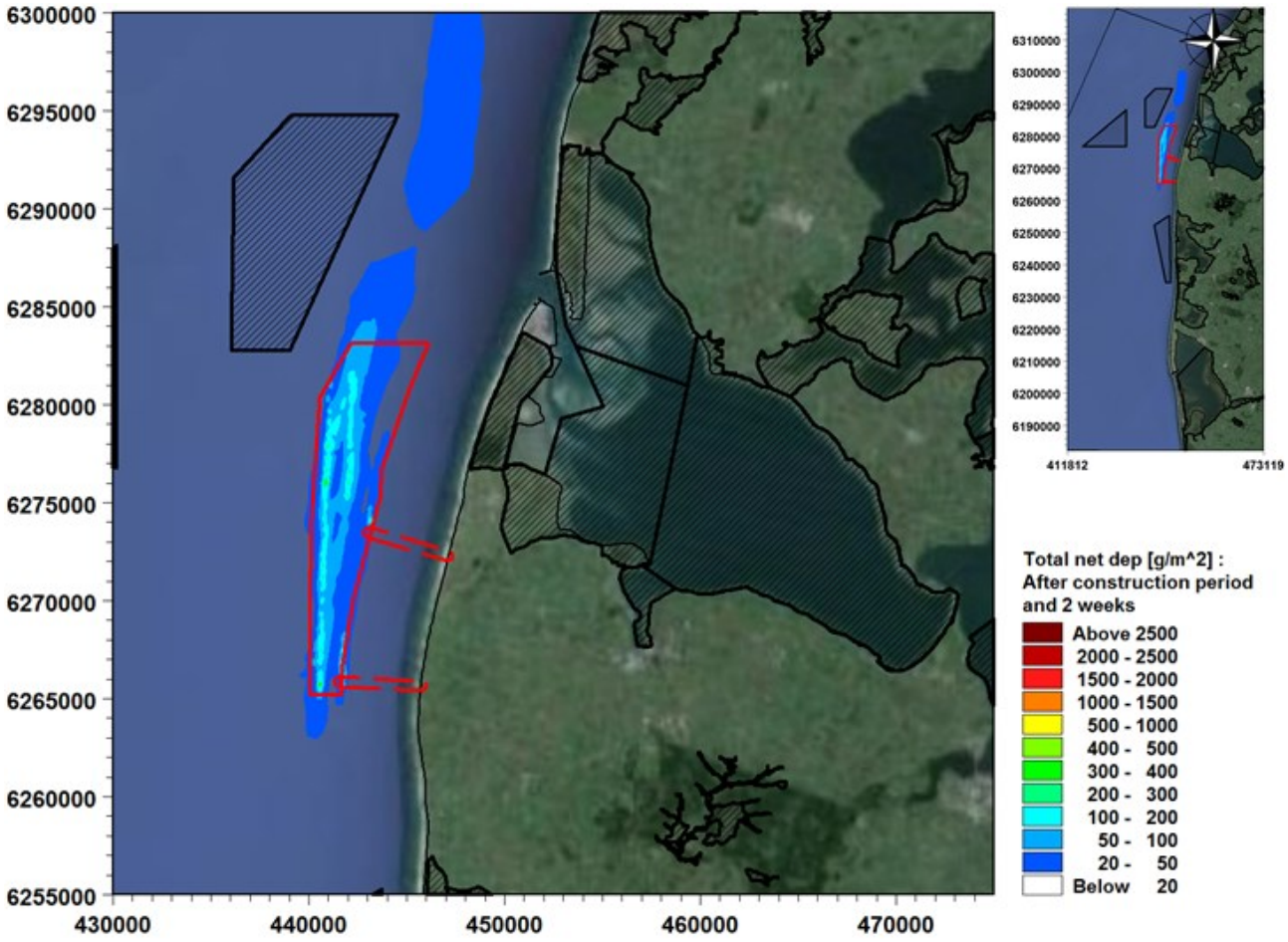

Figure 5.5 Total net deposition of spilled sediment two weeks after end of dredging/excavation works for foundations. Hatched areas with black frames are Nature 2000 areas.

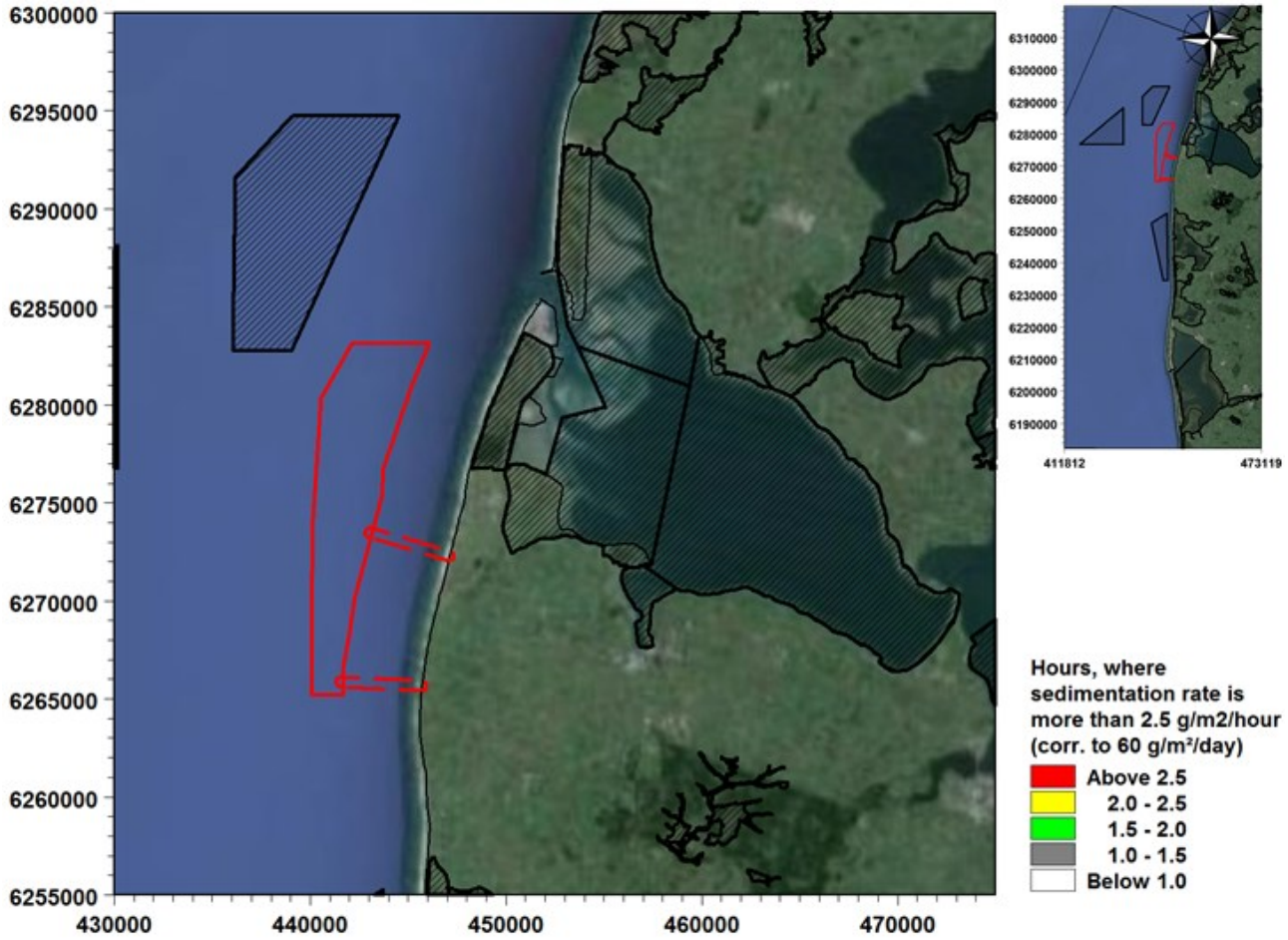

Figure 5.6 *Hours with sediment rate more than 2.5 g/m^2/hour (or 60 g/m^2/day), during dredging/exca foundations. Hatched areas with black frames are Nature 2000 areas.*

Figure 5.7 and Figure 5.8 shows the maximum deposition rate and erosion rate of spilled material during the foundation dredging/excavation works. While being below the threshold sedimentation rate (of 2.5 g/m^2/hour) highest depositions rates are predicted near all foundations whereas erosion is most predominant near foundations located along the nearshore boundary of the OWF. In this area the fine material is less likely to deposit due to wave action and higher bottom shear stresses.

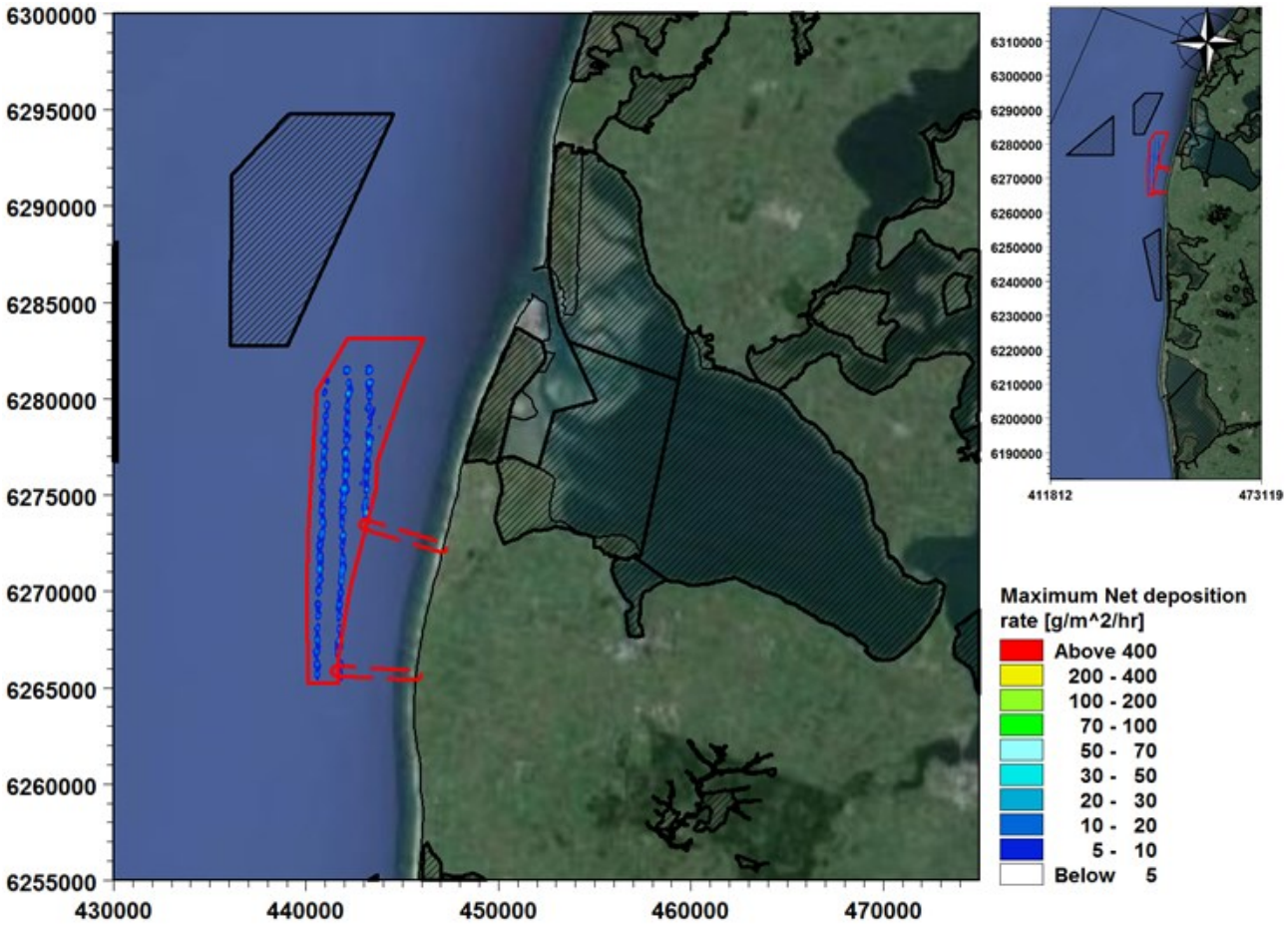

Figure 5.7 *Maximum net deposition rate of spilled sediment during the foundation dredging/excavation works. Hatched areas with black frames are Nature 2000 areas.*

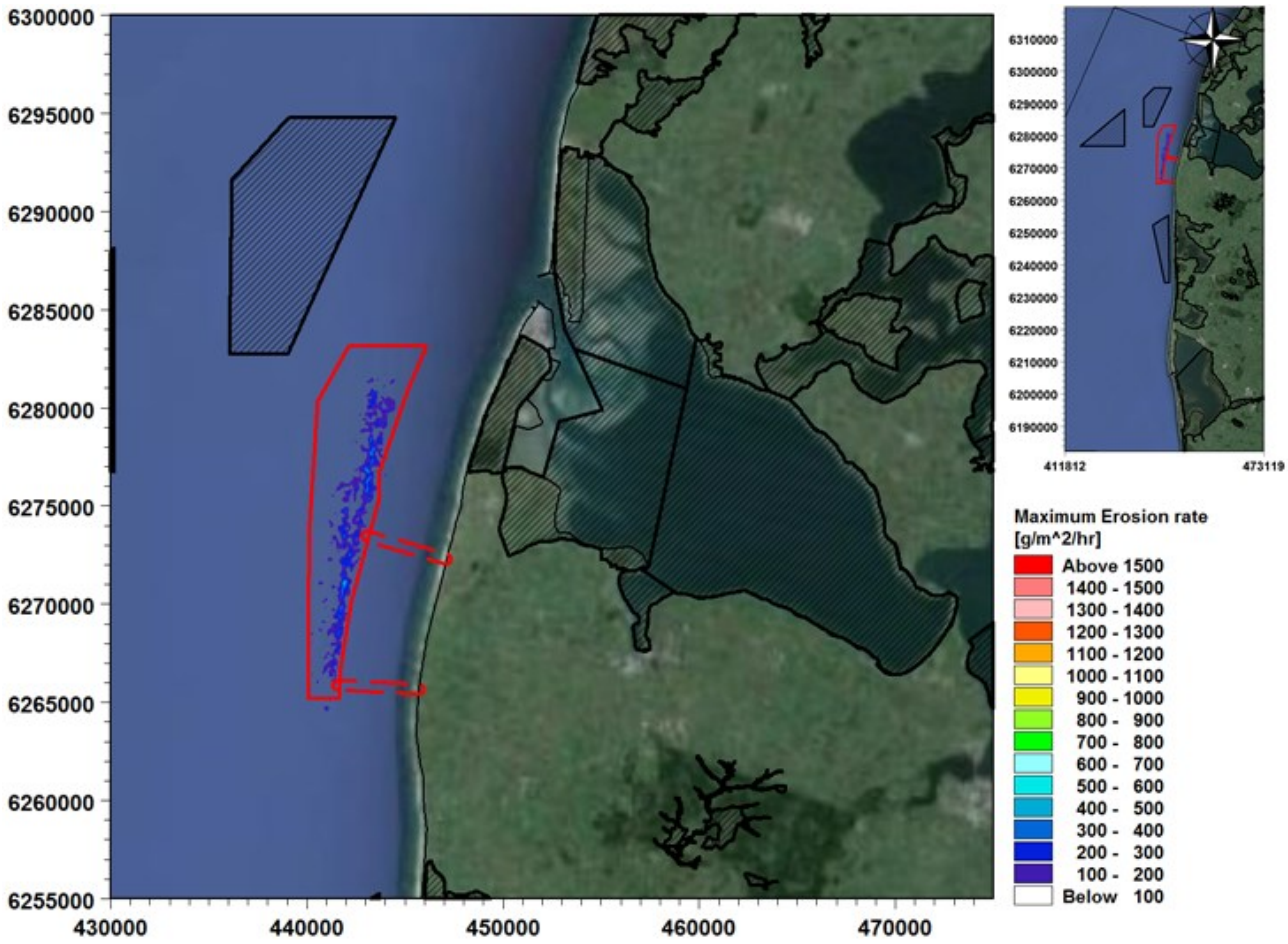

Figure 5.8 *Maximum erosion rate of spilled sediment during the foundation dredging/excavation works. Hatched areas with black frames are Nature 2000 areas.*

5.2.2 Jetting of cables

The total deposition of spilled sediment two weeks after end of jetting of inter-array and export cables is found in Figure 5.9. It is found that inside the OWF area the sediment will deposit in quantities of around 300-500 g/m^2. However, in a few local areas inside the OWF, along the cable corridors and between the cable corridors the model shows quantities of up to 10 kg/m^2. Outside these areas sedimentation is limited to less than 200 g/m^2. Figure 5.10 sedimentation rates of 2.5 g/m^2/hour (or 60 g/m^2/day) are not exceeded.

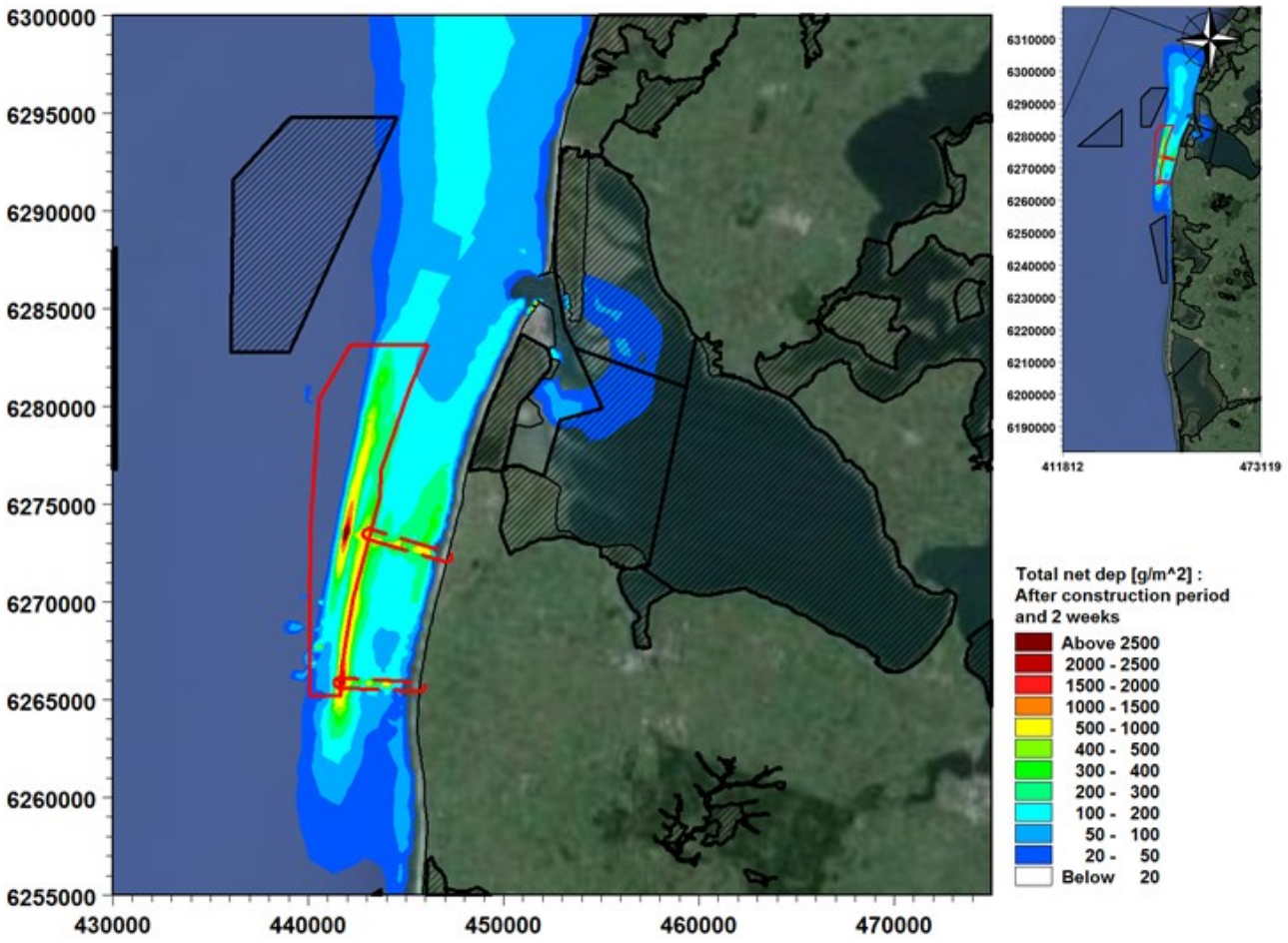

Figure 5.9 *Total net deposition of spilled sediment two weeks after end of cable jetting. Hatched areas with black frames are Nature 2000 areas.*

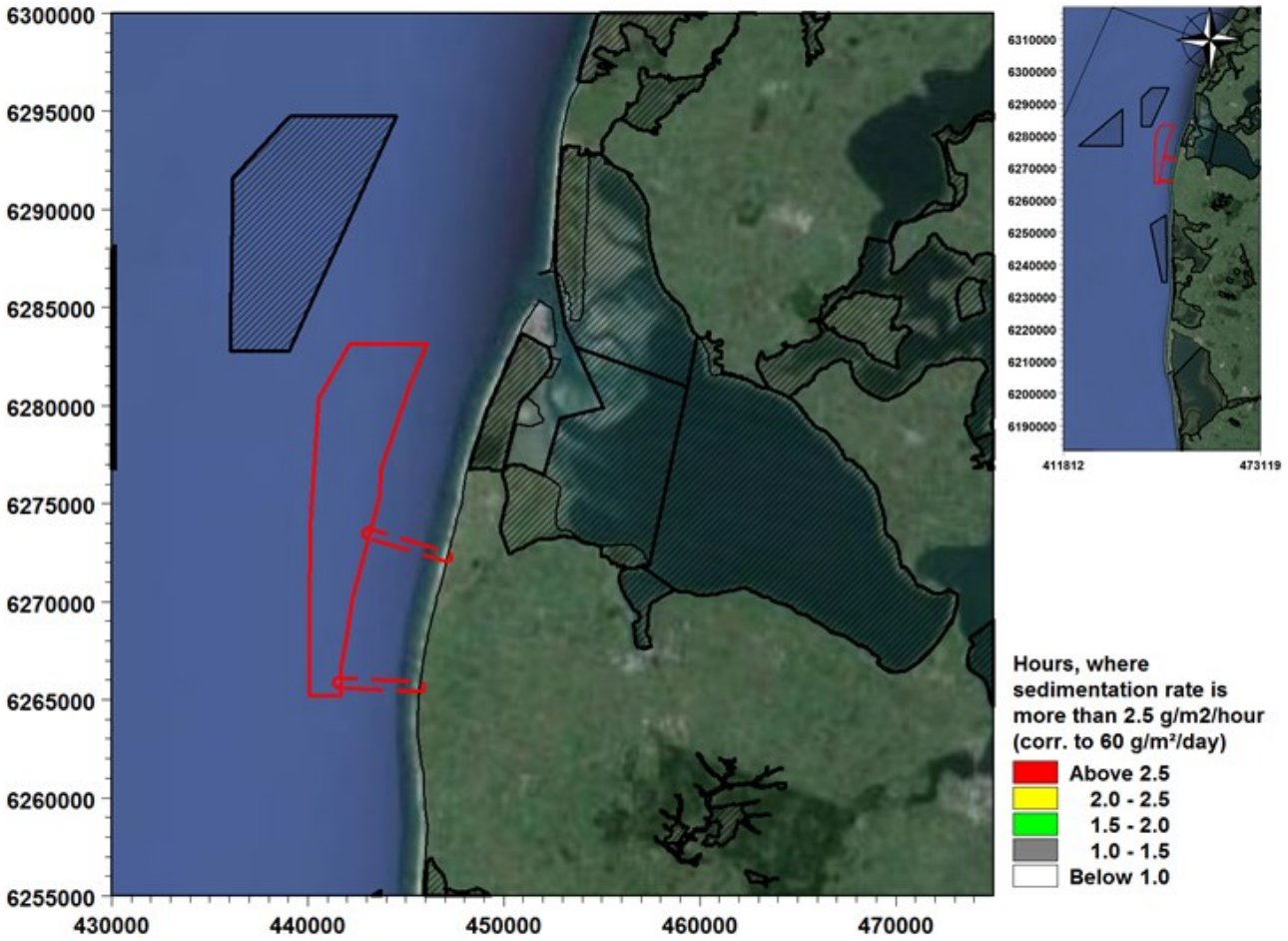

Figure 5.10 *Hours with sediment rate more than 2.5 g/m^2/hour (or 60 g/m^2/day) during jetting of cables. Hatched areas with black frames are Nature 2000 areas.*

Figure 5.11 and Figure 5.12 show the maximum net deposition rate and erosion rate during jetting of cables. It is found that there is only very local deposition around the cables and that erosion rates are highest is shallow areas along the coast and in areas where larger sedimentation occurs.

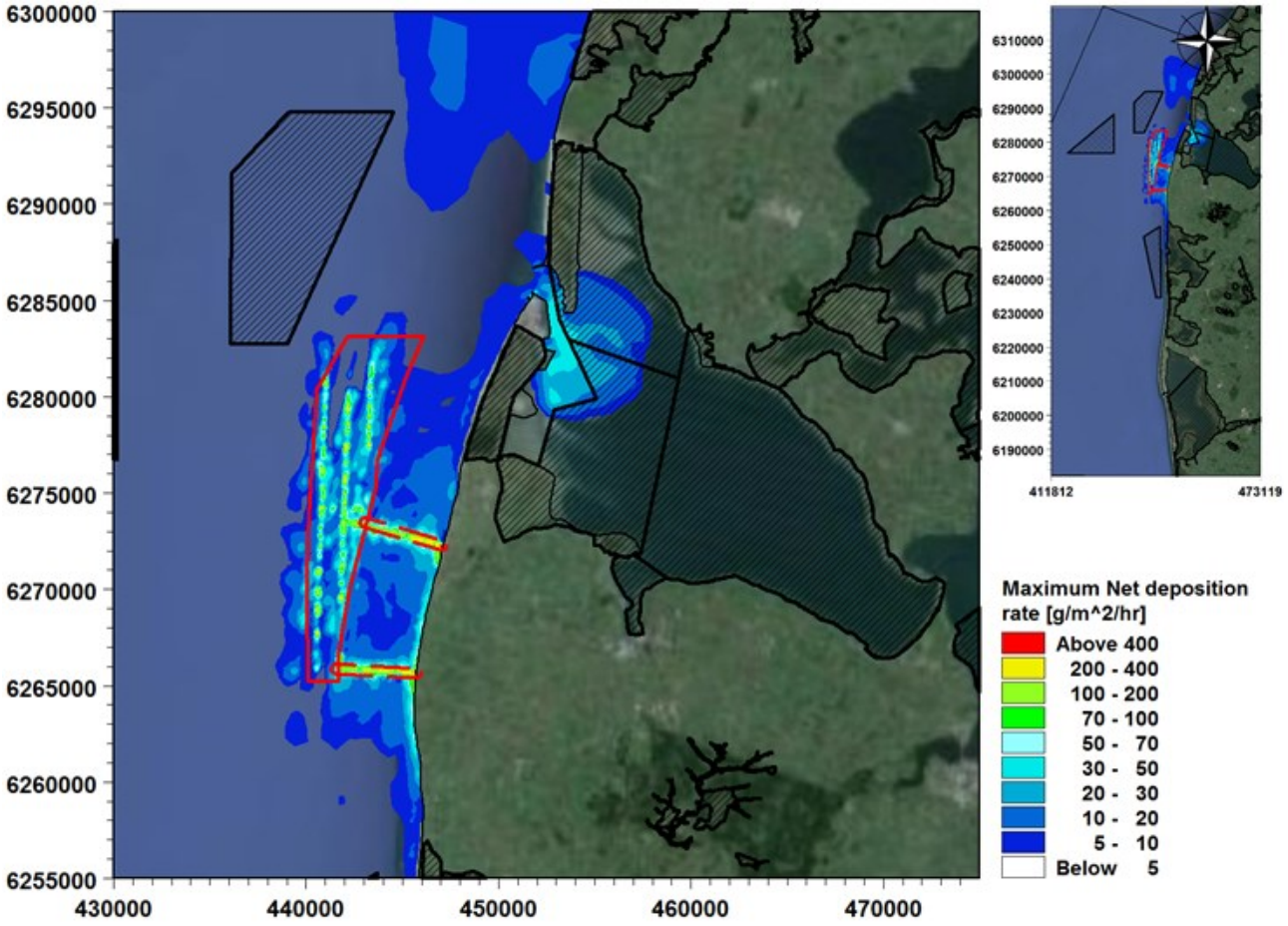

Figure 5.11 *Maximum net deposition rate of spilled sediment during jetting of cables. Hatched areas with black frames are Nature 2000 areas.*

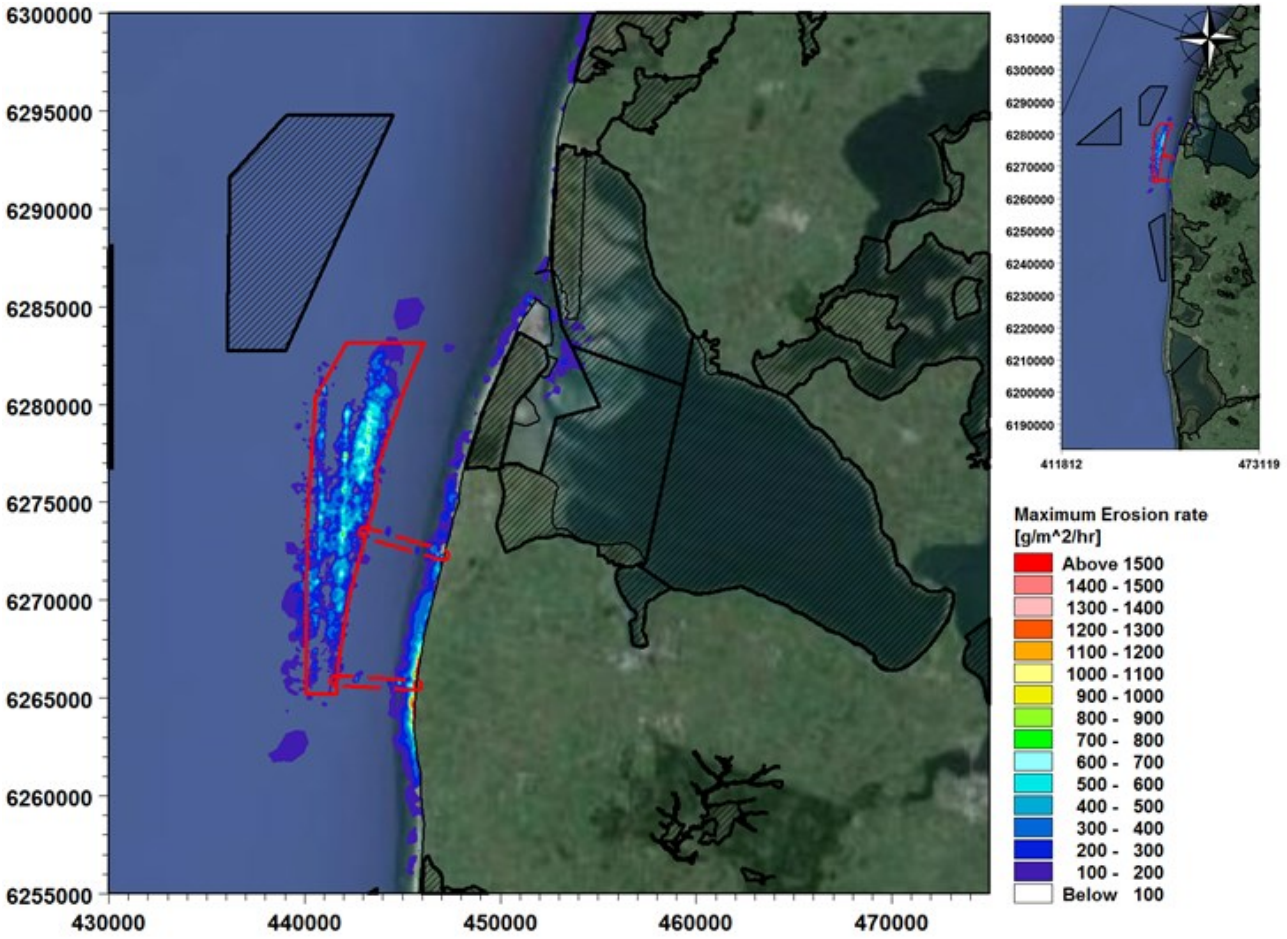

Figure 5.12 *Maximum erosion rate of spilled sediment during jetting of cables. Hatched areas with black frames are Nature 2000 areas.*

5.2.3 Summary of sediment spill deposition during construction

Figure 5.13 shows the combined total deposition of spilled sediment of scenario 1 and 2. The figure shows that spilled sediments will generally deposit in and near the OWF and associated cable corridors, and close to the coast north and south of the OWF. In the cable corridors up to maximum 10 kg/m^2 will deposit, whereas sedimentation values of up to 200 g/m^2 are predicted in the nearby surrounding areas and in the OWF area itself. In a minor part of the Natura 2000 area inside Nissum Bredning sedimentation of up to maximum 50 g/m^2 may occur. The predicted sedimentation values are very small and will be expected to result in local seabed accretion in the order of only a few millimetres. Consequently, the pressure on the environment due to deposition of spilled sediments is expected to be *minor*.

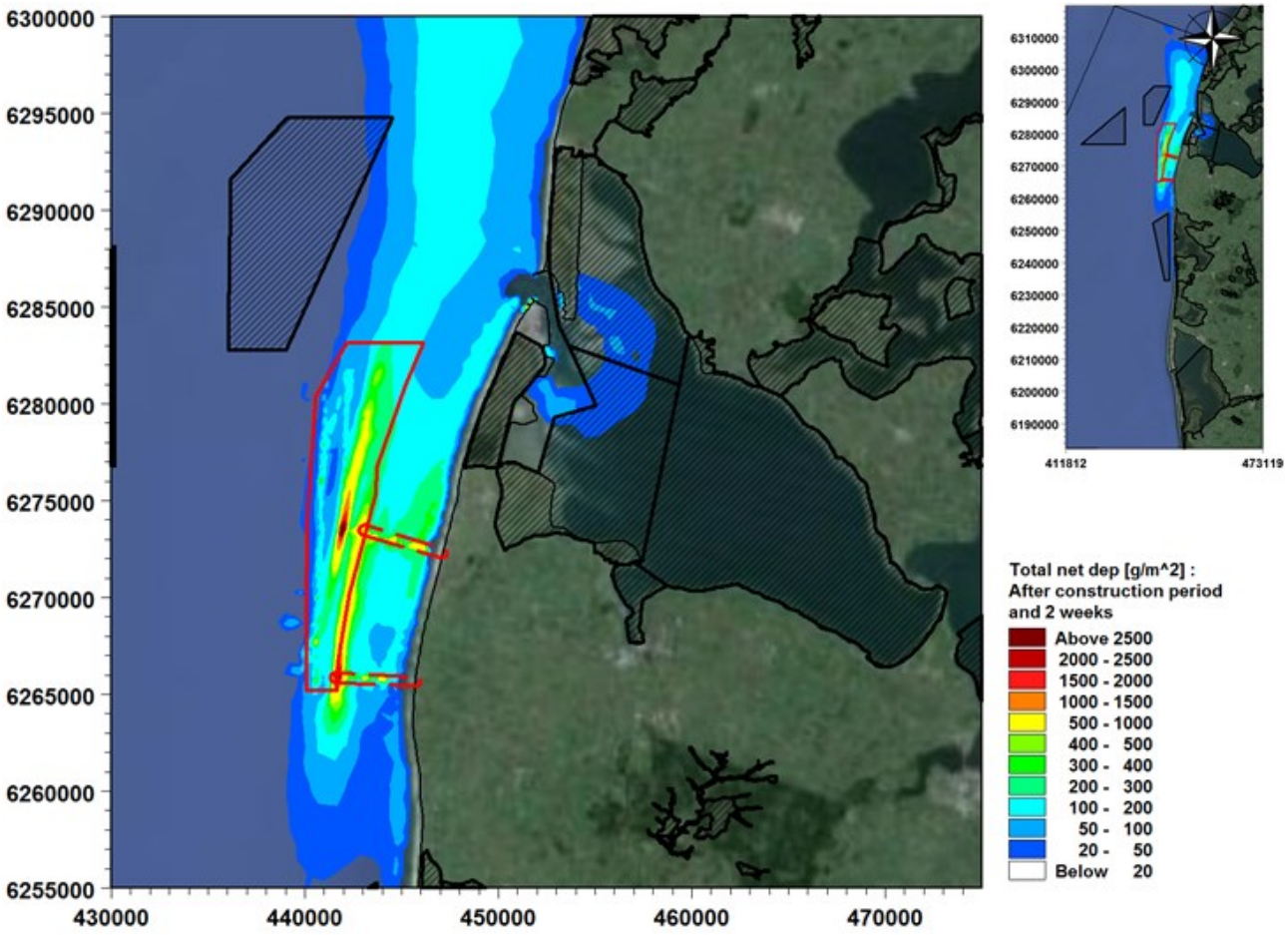

Figure 5.13 *Total net deposition of spilled sediment two weeks after end of construction period of both foundation dredging/excavation works and jetting of cables. Hatched areas with black frames are Nature 2000 areas.*

6 Potential pressures during operation

6.1 Wave conditions

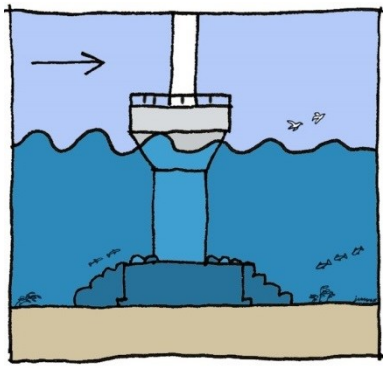

The regional effects on the wave climate have been examined based on changes to the significant wave heights relative to the baseline without wind farm (year 2012). The foundation layout used in the simulation is shown in Figure 1.1 and comprises 66 foundations (3 MW turbines) installed across the OWF area.

Figure 6.1 to Figure 6.3 shows the damping/reduction of the average significant wave height and reduction of highest significant wave height during a typical year (2012) with and without the OWF. The wave height damping is defined as the reduction of the average significant wave height relative to the average significant wave height before construction of the OWF:

$$\overline{c_w} = \frac{\frac{1}{T}\sum\left[H_{m0,existing}(t)\,\Delta t\right] - \frac{1}{T}\sum\left[H_{m0,future}(t)\,\Delta t\right]}{\frac{1}{T}\sum\left[H_{m0,existing}(t)\,\Delta t\right]}\,[\%]$$

The changes in average and maximum significant wave heights are defined as:

$$\Delta H_{m0,max} = \max\left(H_{m0,future}(t)\right) - \max\left(H_{m0,existing}(t)\right)\,[m]$$

$$\Delta H_{m0,average} = \frac{1}{T}\sum\left[H_{m0,future}(t)\,\Delta t\right] - \frac{1}{T}\sum\left[H_{m0,existing}(t)\,\Delta t\right]\,[m]$$

The figures show that effect on the significant wave height is largest at the centre of the OWF and decreasing radially outwards from the OWF, mainly to the north and south, with the average wave height reductions ranging from 4 cm locally in the OWF to 0.5 cm within 10 km south of to 12 km north of the offshore wind farm.

Along the west coast the largest waves will occur during storms from north-westerly directions. Figure 6.3 shows that the wave heights during storm events of 2012 of 7-7.5 m are reduced by up to 5-6 cm inside the OWF and up to 2-3 cm locally at the coast due to the presence of the Vesterhav Nord OWF. The largest reduction of storm wave heights is observed inside the OWF itself.

In conclusion, the changes to the wave climate are in the order of 1-3.5 % in the coastal area. This reduction of the wave heights is considered *minor* compared to the yearly variations of the wave climate.

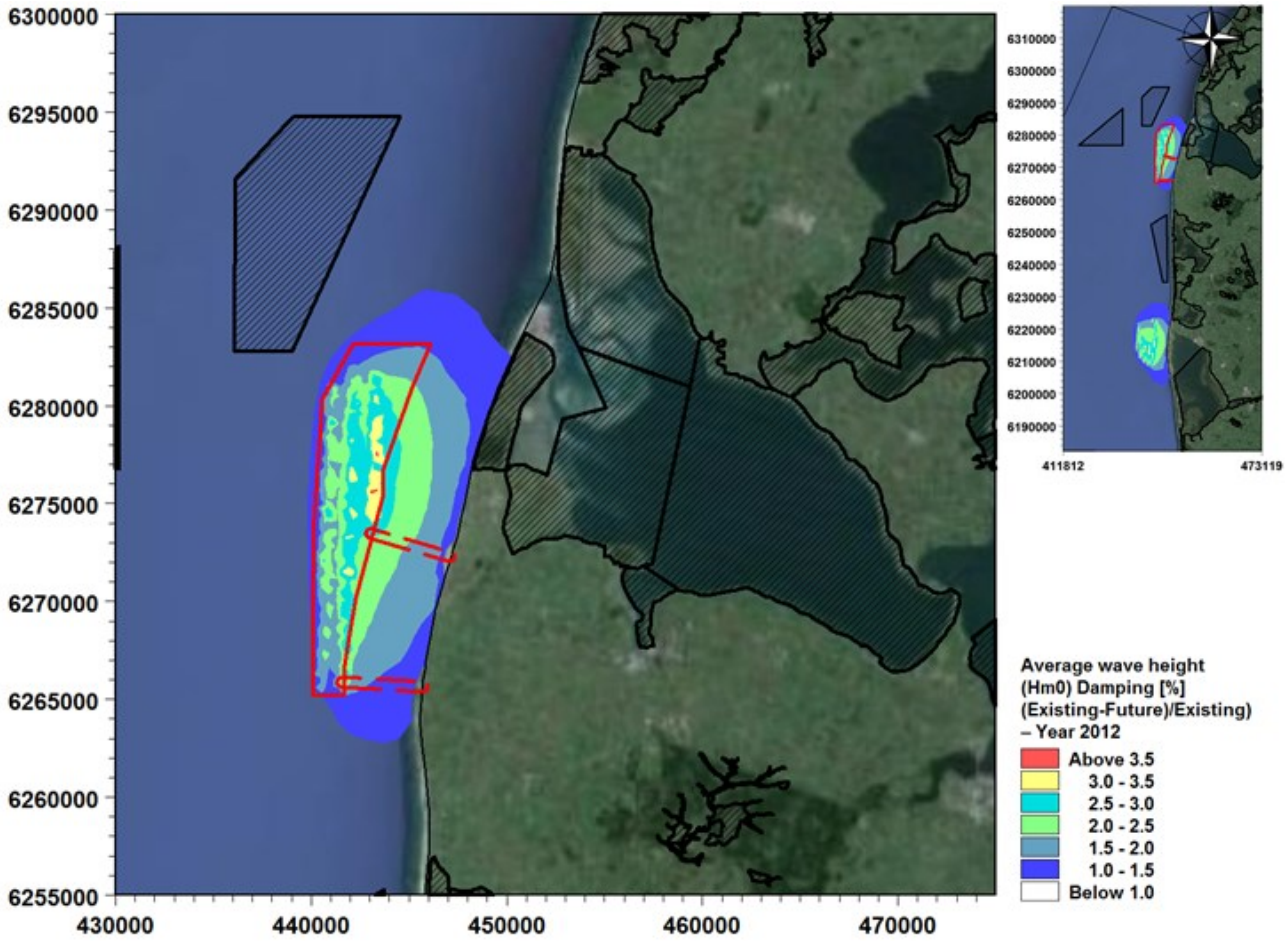

Figure 6.1 *Yearly average wave height (H_{m0}) damping, $\overline{c_w}$ [%] due to the presence of the Vesterhav Nord OWF. Hatched areas with black frames are Nature 2000 areas.*

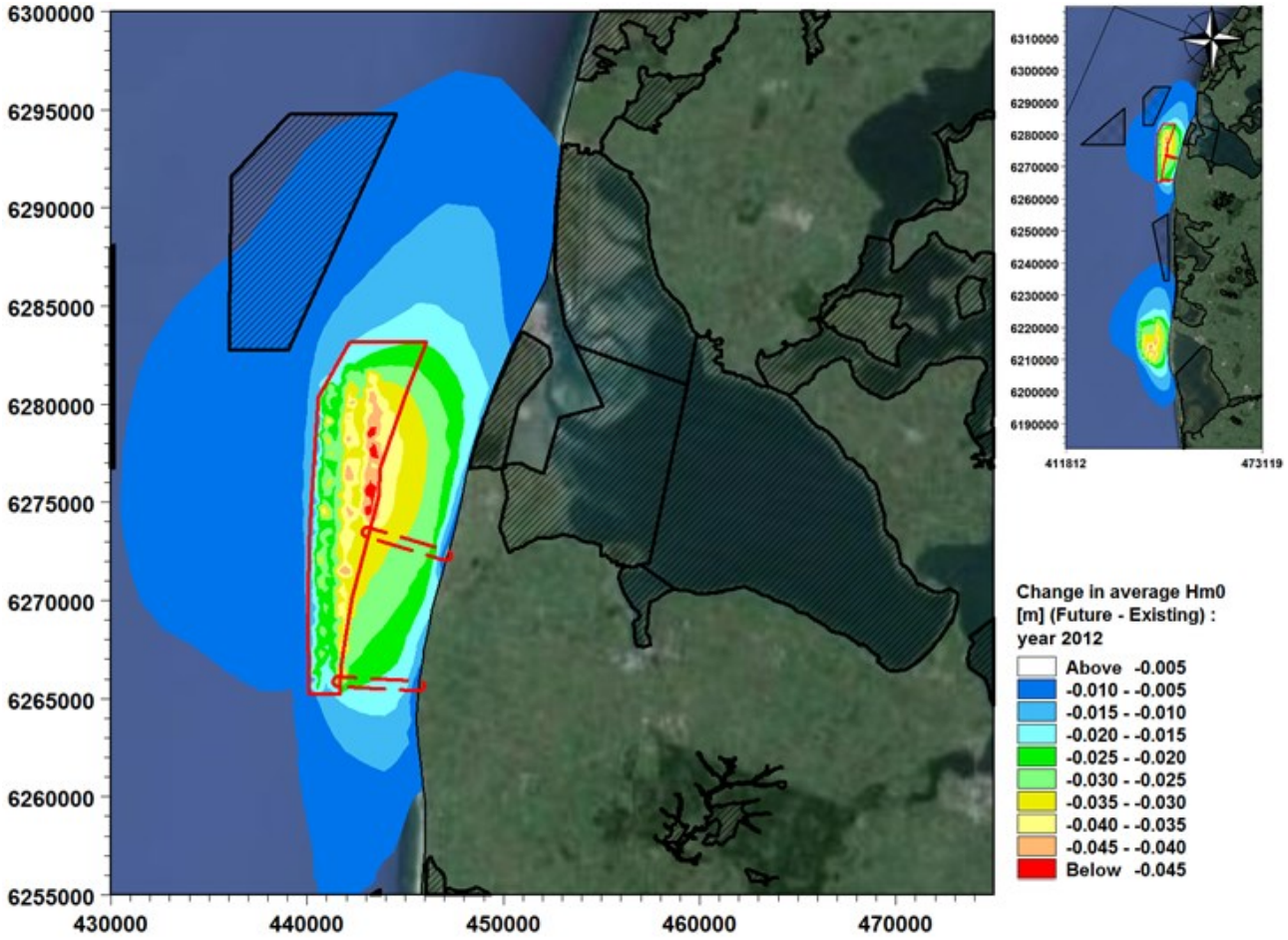

Figure 6.2 *Change of yearly average significant wave height, $\Delta H_{m0,,average}$ in meters due to the presence of the Vesterhav Nord OWF. Hatched areas with black frames are Nature 2000 areas.*

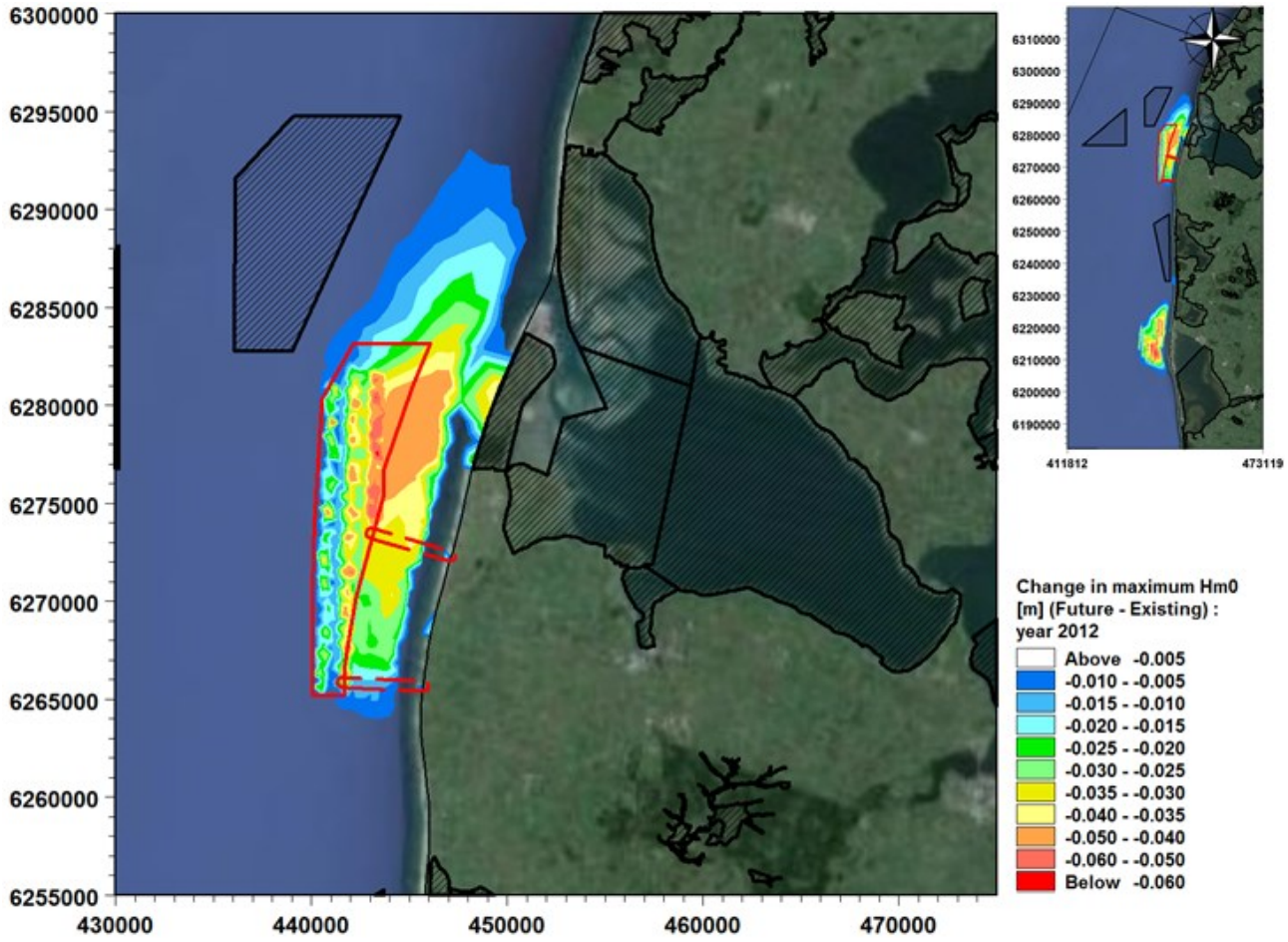

Figure 6.3 *Change of yearly maximum significant wave heights $\Delta H_{m0,max}$ in meters due to presence of Vesterhav Nord OWF. Hatched areas with black frames are Nature 2000 areas.*

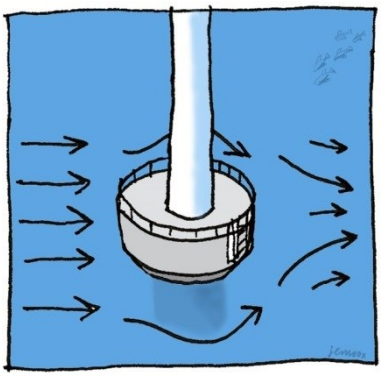

6.2 Currents

The regional effects on tidal and wind driven currents of the Vesterhav Nord OWF is studied based on the depth-averaged current velocity relative to the baseline. The foundation layout used in the simulation is shown in Figure 1.1 and comprises 66 3 MW foundations installed across the pre-investigation area.

The results of the hydrodynamic modelling are presented as a series of maps showing changes to depth-averaged current velocity relative to the baseline during the baseline period 01.06.2012 to 30.08.2012.

The damping of the average current speed is defined as the reduction of the average current speed relative to the average current speed before construction of the OWF:

$$\bar{c_u} = \frac{\frac{1}{T}\, U_{existing} \sum[(t)\, \Delta t] - \frac{1}{T} \sum[U_{future}(t)\, \Delta t]}{\frac{1}{T} \sum[U_{existing}(t)\, \Delta t]}\ [\%]$$

The changes in average and maximum depth average current velocity are defined as:

$$\Delta U_{max} = \max\left(U_{future}(t)\right) - \max\left(U_{existing}(t)\right)\,[m/s]$$

$$\Delta U_{average} = \frac{1}{T}\sum\left[U_{future}(t)\,\Delta t\right] - \frac{1}{T}\,\Sigma\left[U_{existing}(t)\,\Delta t\right]\,[m/s]$$

Figure 6.4 to Figure 6.6 describe the effect of the offshore wind farm on current velocities during normal and high current speeds. As shown the largest effect is observed locally near the individual foundations where average currents are reduced by up to 0.003 m/s (0.8 %). Strong currents of around 0.8 m/s are reduced by up to 0.015 m/s.

The predicted very limited effect of the Vesterhav Nord OWF has en extent of approximately 5 km towards north of the OWF, but there is no effect along the coast.

The predicted effect of the OWF on currents is considered to be of the same order of magnitude as the modelling uncertainty. It is thus concluded that the effect of the wind farm on currents is *neutral*.

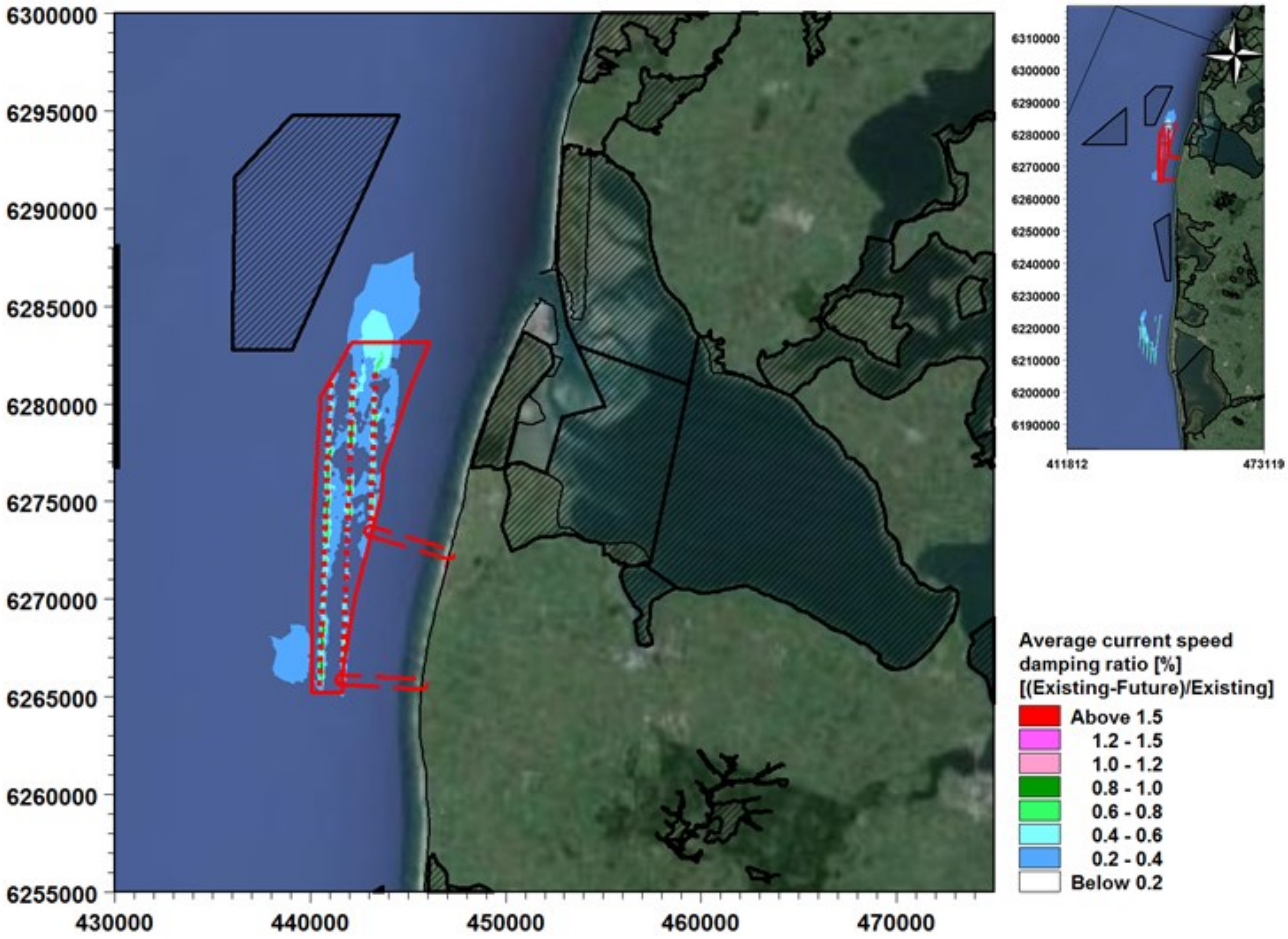

Figure 6.4 *Average damping of current speed caused by the Vesterhav Nord OWF in %. Positive values mean that the current speed is reduced. Hatched areas with black frames are Nature 2000 areas.*

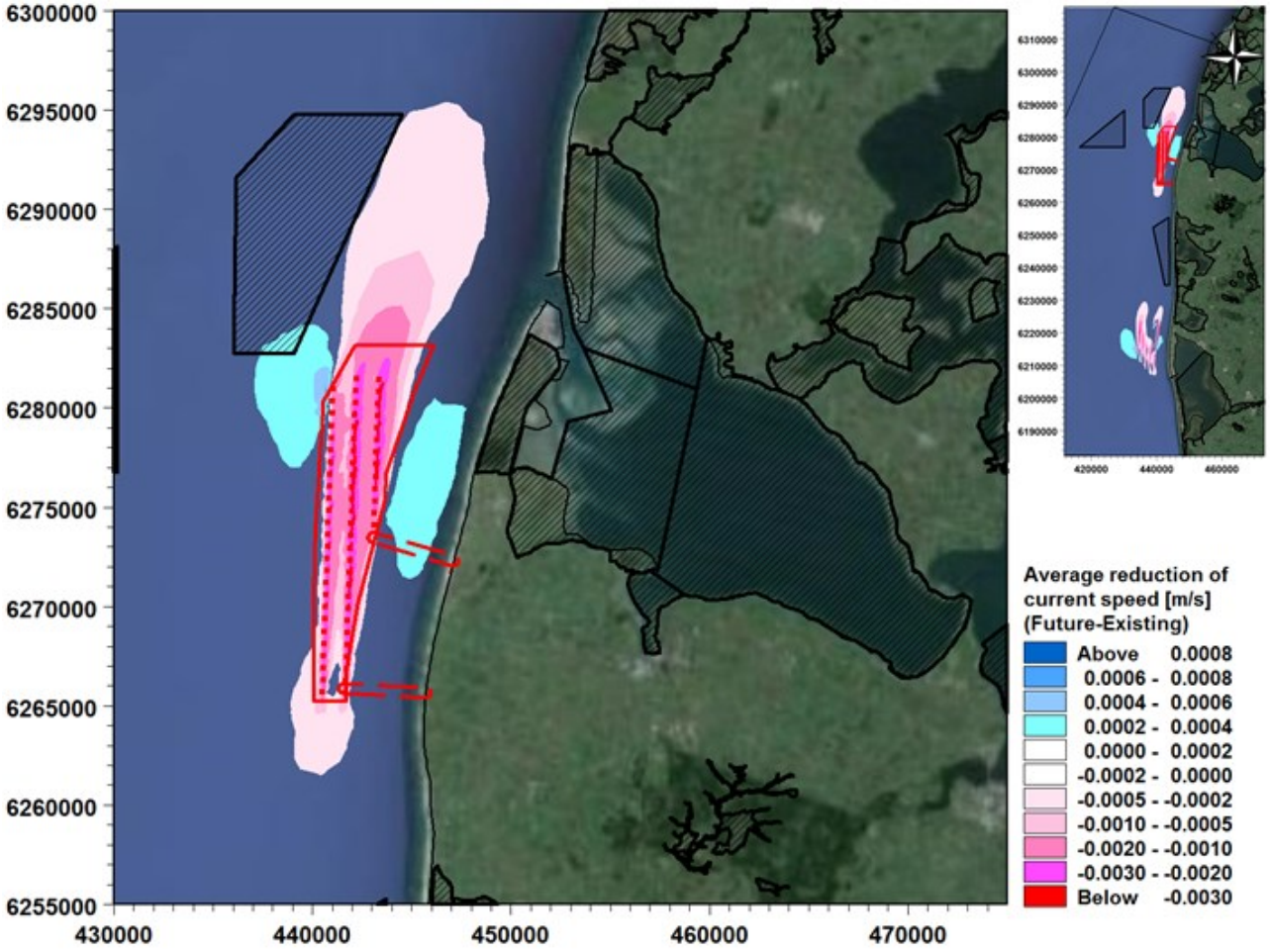

Figure 6.5 *Average reduction of current speed [m/s] future-existing. Positive values mean that the current speed is increased and vice versa. Hatched areas with black frames are Nature 2000 areas.*

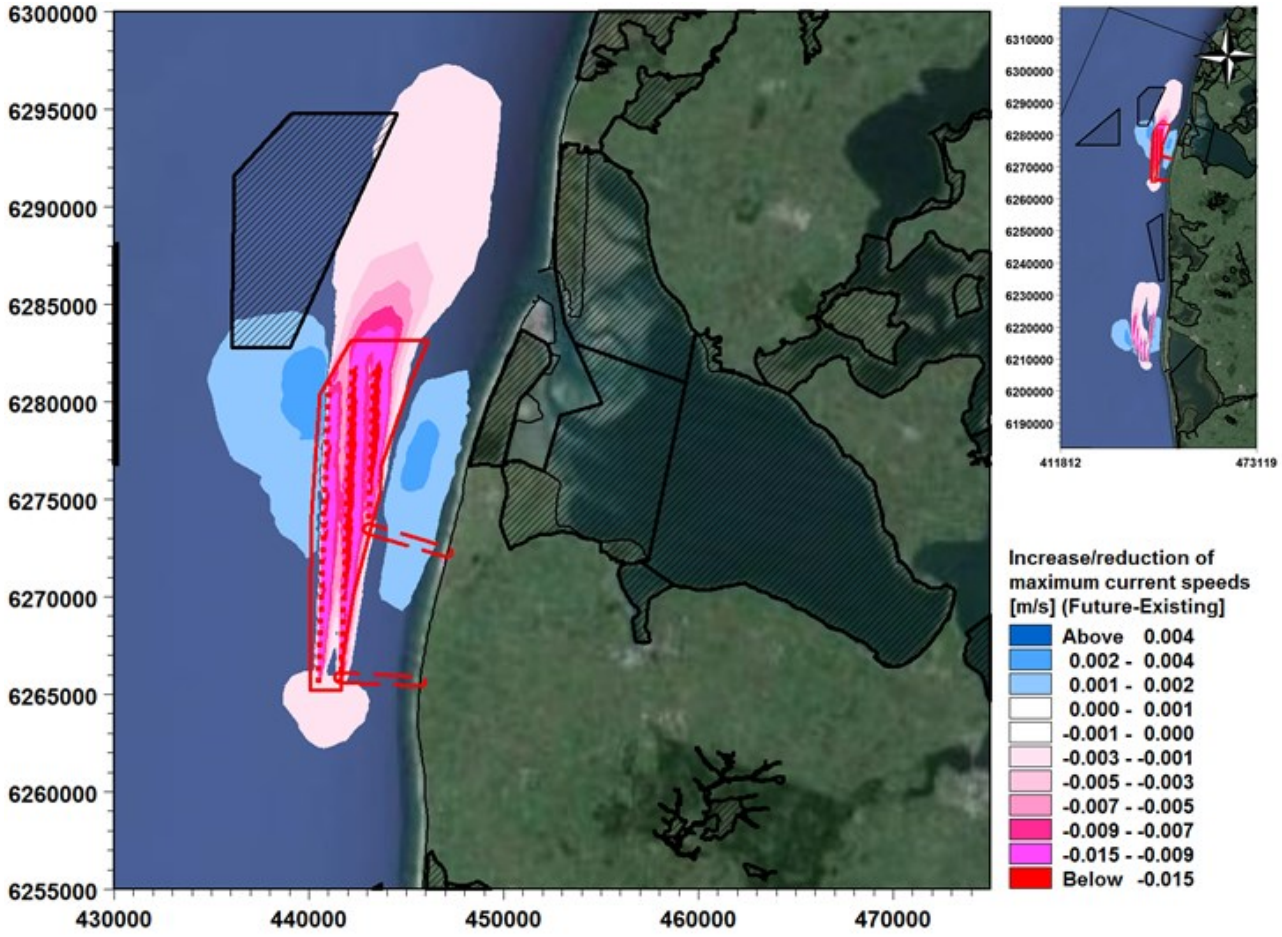

Figure 6.6 *Increase/reduction of maximum current speeds [m/s] caused by Vesterhav Nord OWF. Positive values mean that the maximum currents are increased and vice versa. Hatched areas with black frames are Nature 2000 areas.*

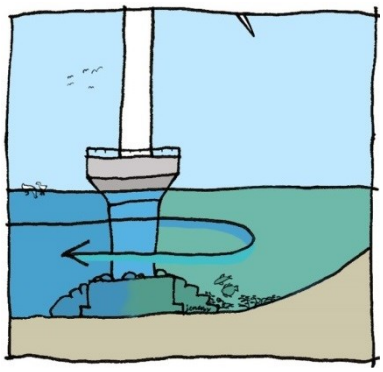

6.3 Water exchange and fluxes

On a small scale, the modelling of the pressures on water exchange and fluxes quantifies the reduction of the flow speed at the position of each wind turbine. On a larger scale, i.e. within the scale of the wind farm, the flow speed is also reduced, but much less, see Figure 6.4.

Figure 6.5 shows, that the average current speed is reduced by 0.001-0.002 m/s within the OWF and by up to 0.003 m/s near the individual foundations and. The typical background speed is around 0.5 m/s and the changes are therefore of the order of 0.5 % compared to background speed, which is to be considered to be of the same order of magnitude as the modelling accuracy.

The pressure on water flux is given as a blocking value. The blocking calculation has been made for one cross section for the Vesterhav Nord OWF to assess the impact of the proposed wind farm on the discharge after the construction of proposed wind farm (Figure 6.7).

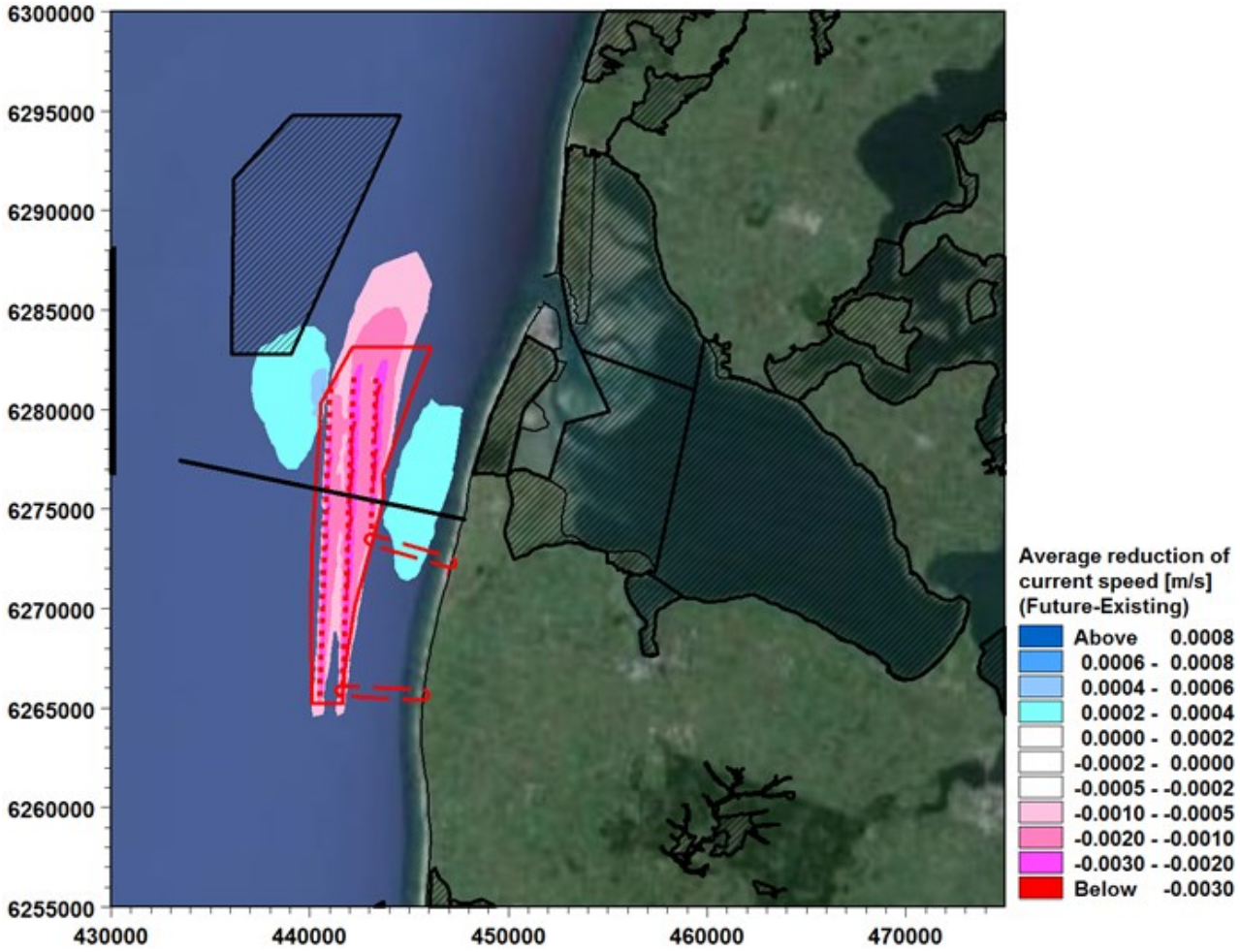

Figure 6.7 *Cross section selected for the discharge calculation through the wind farm. Hatched areas with black frames are Nature 2000 areas.*

The calculated discharge blocking at the location are 0.12 %.

The uncertainty for achieving a zero effect solution for the Great belt crossing was found to be 0.07 % ±0.20 % where the 0,07 % are the central estimate on the blocking and the ±0.20% is the confidence interval [ref. /21/].

Therefore, the calculated blocking values for the OWF are considered to be of negligible importance for the environmental conditions. It is thus concluded that the effect of the wind farm on water exchange and fluxes is *neutral*.

6.4 Stratification and mixing

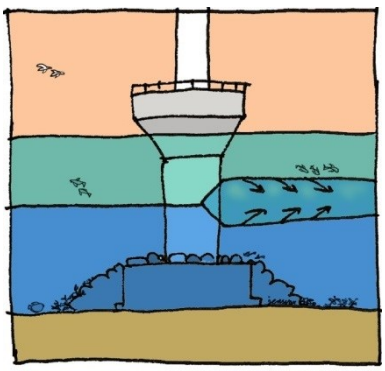

Stratification of flow, where water masses with different properties form layers separated from each other, occurs rarely at positions close to the wind farm Vesterhav Nord since the stratification is very weak.

The pressure on stratification and hence on mixing is therefore not of practical relevance for this site. Therefore, no calculations of mixing effects are conducted for Vesterhav Nord.

It is thus concluded that the effect of the wind farm on stratification and mixing is *neutral*.

6.5 Coastal impact

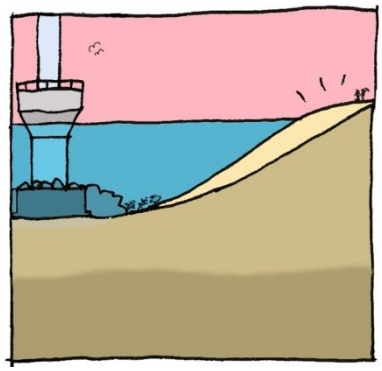

Downwind of the wind farm, the coastline could retreat or advance as a result of OWF induced changes in wave conditions due.

As described in section 6.1 the OWF will reduce the average wave height by approximately 2-3 cm (1.0-1.5 %) along adjacent coastlines and up to 3.5 % inside the OWF.

Large waves of 7-7.5 m are reduced by up to approximately 0.05 m at the OWF. However, along the coast the impact of the OWF cannot be identified, as the maximum significant wave height is governed by depth induced wave breaking and bathymetry, which is identical with and without the OWF.

The coastline and beaches will experience a more extensive variability due to natural changes in wave climate compared to the expected impact of the wind farm, which is assessed in more detail in the following.

6.5.1 Littoral sediment drift

The influence of the OWF on the net littoral drift capacity at the coast at Vejlby is studied in LITDRIFT, based on a typical beach profile from Vejlby and wave conditions before and after construction of the OWF, see Figure 3.12. There are no groynes at the locations of the assessed beach profile.

Figure 6.8 shows the modelled wave roses (year 2012) at the east side of the OWF with and without the OWF. The wave climates are extracted from the MIKE 21 SW model at 22.2 m water depth at Point 1 (see Figure 3.12) and thus outside the littoral zone in the alongshore location where the OWF is assessed to have the largest impact on the wave climate and coastline.

Figure 6.9 shows the modelled distribution of the littoral drift capacity across the beach profile for the existing and future situation (2012). The figure and calculations show, that the active depth[8] of the littoral zone is around 9.5 m at this location. A small difference is observed in the littoral drift when comparing the existing and future situation. The littoral drift is proportional to ~ $H_{m0}^{2.5}$, which means that a small reduction in wave height can cause a relatively larger reduction in littoral drift capacity.

Figure 6.10 shows the impact of the OWF on the littoral drift for a series of beach orientations. The orientation of coast normal is around 290°N at Vejlby.

[8] The depth where 97.5 % of the littoral drift is found inside.

The results show that the OWF causes a reduction of the *gross littoral drift capacity* by in the order of 50,000 m³/year or 5%. The *net littoral drift capacity* is reduced by in the order of 20,000 m³/year or 4 % (depending on the shoreline orientation).

As shown in Figure 4.21 the natural variability in net littoral drift capacity varies by more than 500,000 m³/year from year to year. Therefore a reduction by in the order of 20,000 m³/year is well within the yearly variations, and the coastal impact of the wind farm is thus assessed to be *minor.*

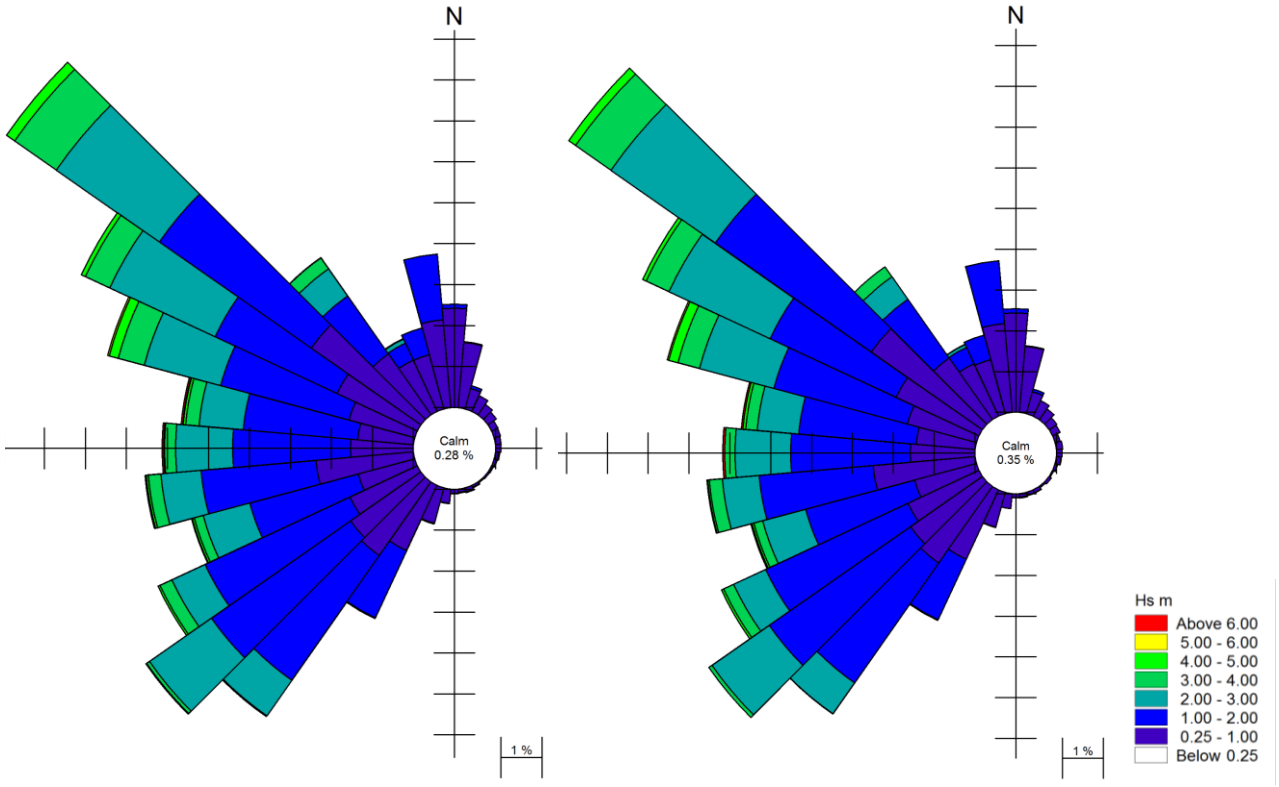

Existing conditions

Without OWF (2012)

Future conditions

With OWF (2012)

Figure 6.8 Modelled wave rose for 2012 at Point 1, Vejlby (see Figure 3.12) with and without influence of the OWF.

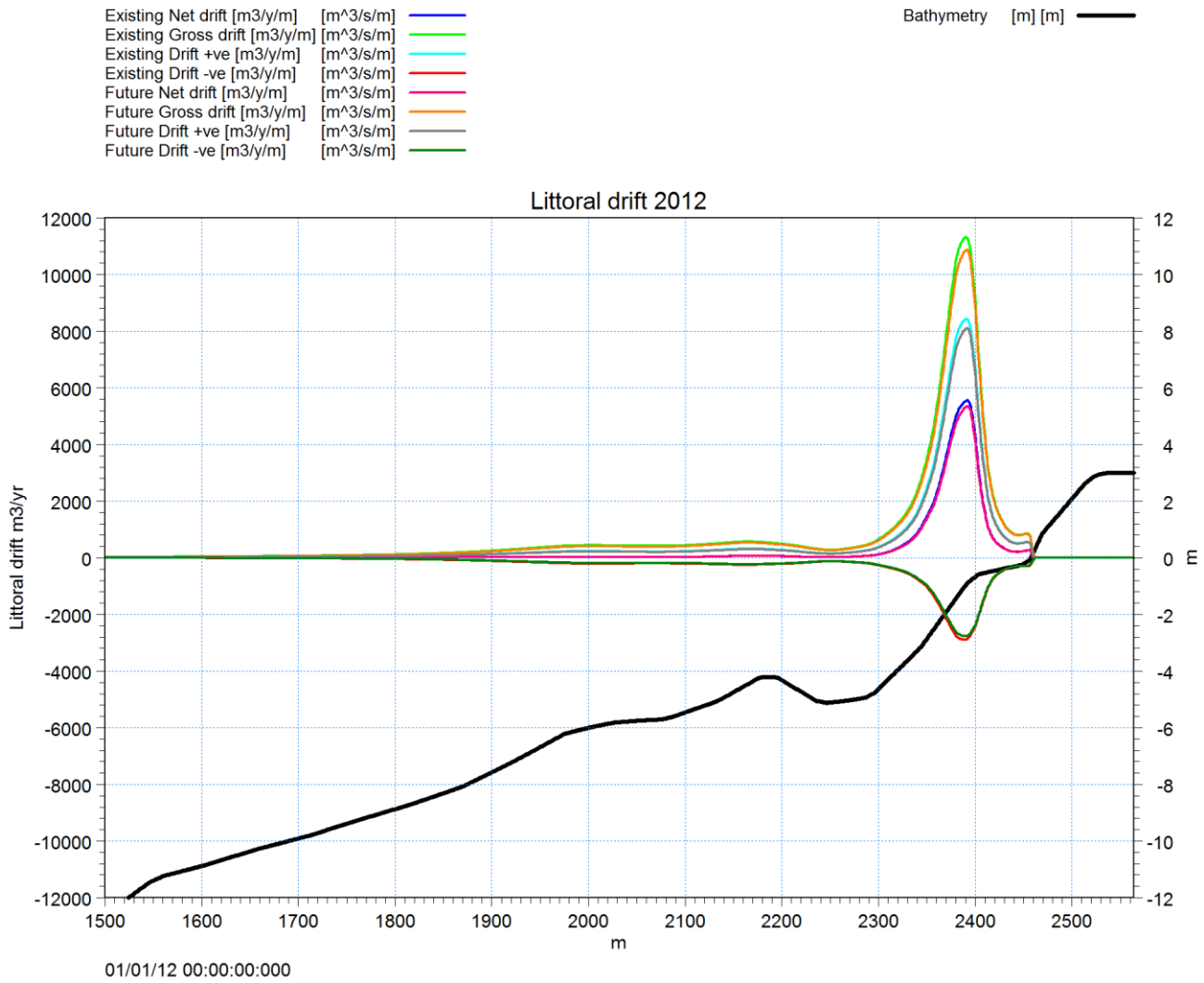

Figure 6.9 Modelled distribution of littoral drift across Beach Profile 1 for 2012 with and without the OWF.

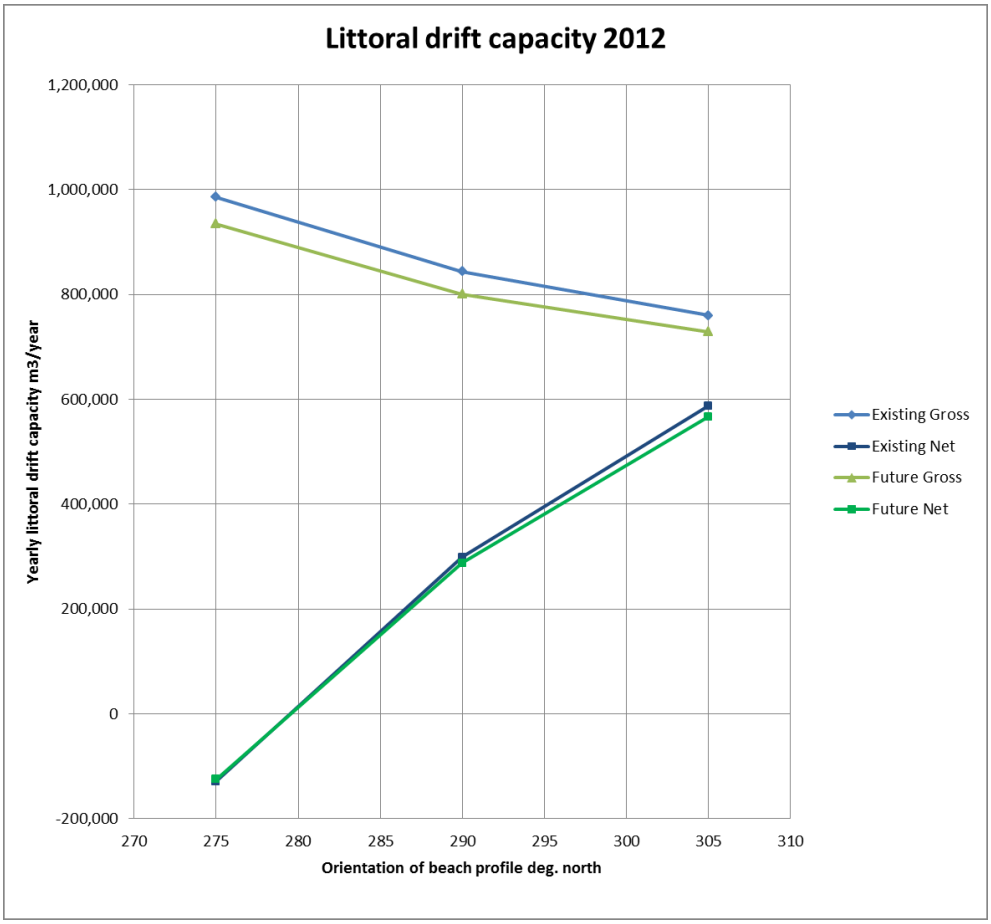

Figure 6.10 *Modelled littoral drift for 2012 with and without OWF for varying orientation of Beach Profile 1, Vejlby.*

Table 6.1 *Modelled littoral drift for 2012 with and without OWF for varying orientation of Beach Profile 1, Vejlby.*

Shoreline orientation Deg. north	Existing Gross m³/year	Existing Net m³/year	Future Gross m³/year	Future Net m³/year	Change Gross m³/year	Change Net m³/year	Change Gross %	Change Net %
275	990,000	-130,000	930,000	-130,000	50,000	0	-5.2	-3.0
290	840,000	300,000	800,000	290,000	40,000	10,000	-5.1	-3.8
305	760,000	590,000	730,000	570,000	30,000	20,000	-4.1	-3.5

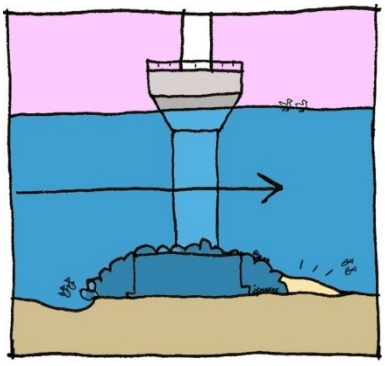

6.6 Morphological impact on seabed

The sediment transport patterns and morphology at the seabed in and near the OWF area may be affected by the presence of wind turbines. Near the individual foundations the currents are amplified and horseshoe vortices (eddies) develop at the seabed. This leads to the development of local scour, which is often mitigated through the installation of scour protection around the turbine foundations.

Studies have shown that the maximum scour-depth for gravity based foundations is in the order of 1 times the diameter of the base, dependent on the shape and geometry of the GBF [ref. /22/]. The scour-hole will have a horizontal extend, based on the friction angle of the sediment surrounding the foundation, with a radius of approx. 3 times the depth of the scour-hole. A scour hole of this size

would however not be allowed to develop, because it would reduce the geotechnical stability of the foundation. Hence, in locations where there is a severe risk of scour at a GBF foundation this will most probably be mitigated with scour protection. Scour it thus considered local and/or minor where not mitigated with scour protection.

As discussed in section 4.4 the sediment transport in the OWF area (in water depths ranging from 15-28 m) is governed by the northbound coastal current and less by waves. The coastal current is responsible for the migration and development of bed forms such as sandwaves found across most of the OWF area. A reduction of the coastal current caused by the OWF may thus influence the migration, orientation and geometry of the natural sand waves as well as reduce the general sediment transport capacity inside the park area. However, as noted in section 6.2 the influence of the wind farm on strong currents is less than 0.015 m/s. A change of this magnitude is within the uncertainties of the numerical model and it is thus concluded that seabed morphology will be unaffected by the presence of the offshore wind farm. Compared to the natural variations and variations caused by sand mining in adjacent areas the impact to seabed morphology is rated *neutral*.

7 Potential pressures during decommissioning

The lifetime of the wind farm is expected to be around 25-30 years [ref. /1/]. Prior to expiry of the production time a decommissioning plan for the wind farm should be prepared. Currently, the decommissioning approach has not been defined, and therefore this assessment of potential pressures uses a worst case consideration of complete removal of the structures.

The pressures during removal of foundations and cables are likely to include short-term increases in suspended sediment concentration and sediment deposition from the plume caused by foundation cutting, dredging or excavation and seabed disturbance caused by removal of cables and scour protection. Limited impacts on water quality are anticipated as the sediments are not contaminated. Although there is no evidence on these potential effects, the effects during decommissioning are considered to be less than or comparable with those effects described during the construction phase, because the volumes of soil to be handled during decommissioning will be equal or smaller than during construction. This is because there will be no need for seabed preparation and there is a possibility that cables are left in situ with no consequential increase in suspended sediment concentration or changes to water quality.

During decommissioning of both the turbine components and foundations, all fluids and substances will need to be removed. The effects during decommissioning are considered to be similar to those described during the construction phase.

The pressure during decommissioning is thus considered to be *minor*.

8 Cumulative pressures

The assessment of cumulative effects evaluates the extent of the environmental effects of the wind farm in terms of intensity and geographic extent compared with other projects in the area. The assessment of the cumulative conditions includes activities associated with existing utilised and un-utilised permits or approved plans for projects. When projects within the same region affect the same environmental conditions simultaneously, they are defined to have cumulative impacts. Cumulative effects can potentially occur on a local scale, such as within the wind farm area, and on a regional scale.

One project has been identified in the offshore region that could potentially give rise to cumulative impacts on sediments, water quality and/or hydrographical conditions:

› Vesterhav Syd OWF (VHS)

VHS is located 42-60 km south of the Vesterhav Nord OWF (see Figure 8.1). The status of the project is, that pre-investigation permits have been obtained from the Danish Energy Agency and that EIA studies are ongoing. The project is planned to go into operation in 2019-2020.

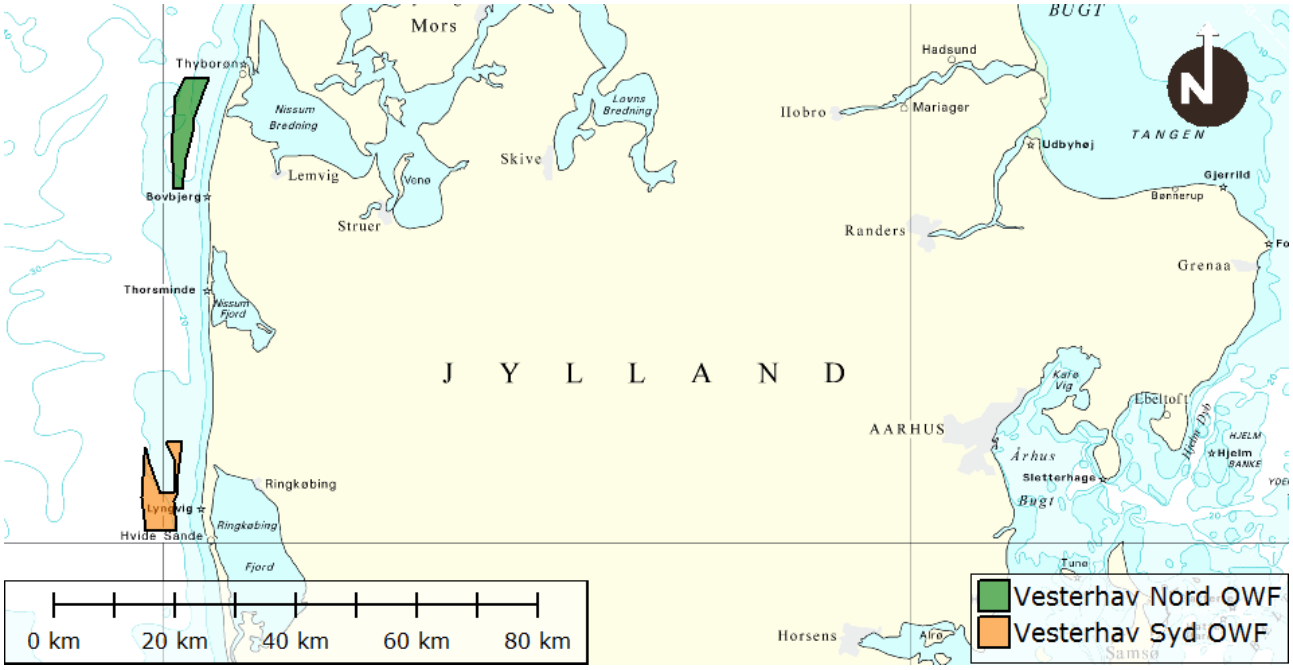

Figure 8.1 Location of Vesterhav Syd OWF relative to Vesterhav Nord OWF.

Based on the studies performed cumulative effects are not expected during operation or construction phases.

› During construction, simultaneous activities at the neighbouring site could potentially cause higher sediment concentrations in the adjacent areas due to overlapping sediment plumes. This is however considered highly unlikely because the effects of sediment spill are relatively short in duration, and occur locally near the OWF and cable corridors.

› During operation, the effects on water quality, hydrography and morphology occur within a radius of the order of 2-5 km from the OWF. Therefore, cumulative effects are not expected due the VHS OWF more than 40 km away.

In addition to the VHS OWF, sand mining in designated offshore sites close to the proposed Vesterhav Nord OWF (see Figure 4.12) may cause cumulative effects.

Simultaneous activities at these sites during construction of the offshore wind farm are however considered unlikely and the additional pressure under such circumstances is not expected to be significant. The EIA for the continued use of *562-AD, Ferring* [ref. /23/] shows that sandmining is expected to increase sediment concentrations by more than 5 mg/l within an area of 11 km^2. This concentration will be exceeded for 5% of the 5-7 week period where sand mining is conducted (~40-60 hours). The increase in sediment concentrations is primarily within the bounds of the sand mining site. By comparison the sediment spill during construction of the OWF will cause an increase in sediment concentration by 5 mg/l near the cable alignments and foundations for 30-60 hours, and in the unlikely event that sediment plumes from these activities should mix, the concentration in the mixed plume would be around 10 mg/l. This concentration would not be

exceeded for more than 30-60 hours, and the additional pressure is thus not considered significant.

9 Mitigation measures

Mitigation measures are divided into the phases of construction, operation and decommissioning. The decommissioning phase is similar to the construction phase and the same mitigation measures are applicable – no explicit description is therefore given for this phase.

9.1 Mitigation measures during construction

During construction the spill of dredged material is considered to give rise to the most severe impacts. Therefore, the mitigation is concentrated on the:

- Equipment type for marine earth works (spill percentage),
- Dredging/Jetting intensity (spill rate),
- Dredging/Jetting period (environmentally sensitive periods can be avoided) and
- Sediment pressure on fjords and estuaries

Equipment type

It is proposed to apply equipment that gives rise to as little sediment spill as possible. Backhoe or grab equipment usually give rise to environmental friendly marine earth works.

Dredging/Jetting intensity

The intensity in terms of m^3/day determines the concentration in the water column and sedimentation rates. Therefore, it is advisable to use small equipment or to stretch the earth works over a long period.

Dredging/Jetting period

An important factor is to coordinate the dredging activities with seasons that are environmentally particular sensitive.

Fjords and estuary

The possible sediment pressure on Sdr. Nissum Fjord can be mitigated at the sluices/locks at Thorsminde, which may be closed during construction activities.

9.2 Mitigation measures during operation

During operation the processes that give environmental consequences are related to maintenance activities. For these activities, best practices and environmental friendly procedures shall be applied.

Impacts on currents and waves can only be mitigated by design mitigation, see next chapter, e.g. by choosing smaller diameters for the foundations.

Other processes are not expected to give rise to significant long term environmental effects and can consequently not be mitigated.

9.3 Design mitigation

As described in section 3.2, the present study adopts a “worst case approach” to park layouts as well as turbine and foundation types. Although the identified pressures and impacts during construction, operation and decommission are minor, they can be further reduced by design measures, for example by:

- Selecting larger turbines (i.e. 10 MW instead of 3 MW), which will lead to fewer structures and lower impacts
- Placing turbines further from shore, which will lead to less wave reduction along the coastline and thus a reduction in coastal impacts
- Selecting smaller foundations (i.e. monopiles instead of gravity based foundations), which will lead to a reduction of current/wave damping and thus reduced impacts.

10 Lack of information of relevance for derived assessments

The present chapter gives an indication of any difficulties (technical deficiencies or lack of know-how) encountered in compiling the required information needed to predict and evaluate environmental impacts:

Project description

The present study adopts a “worst case” approach to the layout of the OWF, the type foundation, the rated power of the turbines to be installed etc. The “worst case” approach is deemed necessary because project specific details are not available at the present stage of the project. The assumptions applied in the study are expected to cause an overestimation of the environmental pressures and impacts presented in this study.

Corridors location

At the present stage of the project it has not been decided if the Vesterhav Nord OWF should use a northern or southern cable corridor. Therefore, sediment spill modelling is based on the assumption that both cable corridors are used. Therefore, sediment spill quantities and effects are overestimated in the present study.

Jetting of cables

The landing point of the export cable is considered to be jetted right onto shore. Practically, this method cannot be applied on shallow water, and therefore alternative dredging/excavation works are to be applied. Furthermore, coastal erosion and the highly dynamic morphology observed in shallow water of less than ~6-7 m is likely to expose the export cables unless these are protected and/or jetted more than 2 m into the seabed. It is expected that this might give rise to local effects such as high sediment concentration in the surf zone along the coast. This effect is not covered in this study. Besides being locally confined, the impact will be of temporary character.

Geophysics

Beach profiles and sediments have not been made available in shallow water along the coastline. Consequently, the coastal impact assessment presented in this study is based expert judgment and overall assessments about sediment characteristics, beach profiles and bed roughness. Consequently, the study is based on the relative increases/decreases of sediment transport capacities and not absolute values. This is considered justifiable because impacts are considered minor and because absolute coastal retreat of accretion is not required in the present study to quantify loss of property and vice versa.

11 Impact assessment summary

The impact assessments based on the potential pressures from section 5 to 7 (construction, operation and decommissioning) are summarised in Table 11.1, with remarks to the overall impact assessment. It should be noted, that the worst case approach has not considered every possible layout (spatial distribution of the turbines) of the OWF, but employed a realistic layout based on an optimized energy yield analysis respecting the site conditions. The final layout of the Vesterhav Nord OWF defined by the appointed concessionary may most likely differ from the one applied in this report. However, considering the hydrographical regimes, seabed morphology and sediment characteristics of the Vesterhav Nord OWF, layouts with approximated comparative distances between turbines, but different orientation within the OWF, is by expert judgment expected to be enveloped in the span of predicted environmental impacts presented in this EIA technical report.

Table 11.1 Summary of overall impacts.

	Overall impact	Remarks
Wave climate	Minor impact	Impact is regionally confined to Vesterhav Nord OWF and with average reduction in wave height ranging between 2 and 4 cm (1-3.5%).
Currents	No impact	The largest effect is observed locally near the individual foundations where average currents are reduced by up to 0.003 m/s (0.8 %). Strong currents of around 0.8 m/s are reduced by up to 0.015 m/s.
Water quality	No impact	Water quality is not affected since flow blocking is close to zero. Stratification and mixing conditions are also not affected, since additional turbulence is < 1% than natural background.
Sediment spill: Sediment concentration	Minor impact	Sediment concentrations are relatively low during the construction phase and environmental thresholds are only exceeded for very short periods of time during construction. Furthermore, the spilled sediment enters into a highly dynamic environment with significant natural suspended sediment transport.
Sediment spill: Sedimentation	Minor impact	Sedimentation occurs locally within the Vesterhav Nord OWF area and along the coast. Environmental threshold sedimentation rates are not exceeded.
Sediment spill: Light Attenuation	No impact	Light attenuation at the seabed is frequently affected by wave action and particulate material from the North-German rivers, which is carried up along the Danish West Coast by the coastal current. These natural variations are considered to contribute more to light attenuation at the seabed than the temporary effects of increased sediments during construction.
Seabed and coastal morphology	Minor impact	The effects on the wave and current climate by the Vesterhav Nord OWF are minor and the subsequent effects on both coastal and seabed morphology are thus found to be equally minor to negligible (within model accuracy or yearly variations).

12 References

/1/ **NIRAS** for Energinet.dk
TECHNICAL PROJECT DESCRIPTION FOR THE NEARSHORE WIND FARMS (450 MW)
Doc. no. 1210677820, rev. 1, 21 March 2014.

/2/ **E.ON Energy**
Online: https://www.eonenergy.com/About-eon/our-company/generation/planning-for-the-future/wind/offshore/Rampion/project-information/offshore-elements, accessed April 2014.

/3/ **DHI** for Energinet.dk
Anholt Offshore Wind Farm - Hydrography, sediment spill, water quality, geomorphology and coastal morphology
Doc. no. 11803332-3 , rev. 6, October 2009.

/4/ **Christiansena, M. B. and Hasagera, C. B.**
Wake studies around a large offshore wind farm using satellite and airborne SAR
RISØ, http://isprsserv.ifp.uni-stuttgart.de/proceedings/2005/ISRSE/html/papers/272.pdf, 2005.

/5/ **Christensen, E. D. *et al.***
Transmission of wave energy through an offshore wind turbine farm Coastal Engineering, p. 25–46, Coastal Engineering 82 (2013), August 2013.

/6/ **DHI**
MIKE 21/3 HD FM Reference Manual, 2014th edition
2014.

/7/ **Smed, P.**
Landskabskort over Danmark, Blad 4, Sjælland, Lolland, Falster, Bornholm
Brenderup : Geografforlaget, 1981.

/8/ **Danish Coastal Authorities**
Historic shoreline development in Denmark ~1900 to ~2000
2014.

/9/ **EGS** for Energinet.dk
DANISH WIND FARM SITE SURVEYS - SITE 2 – VESTERHAV NORD
Volume 2 - INTERPRETATIVE REPORT, rev. 2 (Final), December 2013.

/10/ **GEO** for Energinet.dk
Cable Route Survey Vesterhav Nord - Geophysical and geotechnical investigations
Interpretative Report, Doc. no. 1047, v1, 2014-02-24, rev. 1, GEO project no. 36692, 24 February 2014.

/11/ **Lorenz, R.**
Spill from Dredging Activities
Øresund Link Dredging & Reclamation Conference, pp. 309-324, May 1999.

/12/ **Danish Pilot Guide**
Den danske havnelods
Online: http://www.danskehavnelods.dk/, April 2014.

/13/ **Knudsen, S. B. . L. C. . M. H. t. &. C. E. D.**
Sediment transport in the outer part of the coastal profile
in *28th International Conference on Coastal Engineering*, pp. 1-13, Cardiff, Wales, 2002.

/14/ **Danish Coastal Authorities**
Variationer i kystprofilet
2005.

/15/ **OSPAR**
http://www.ospar.org/eng/doc/pdfs/r2c2.pdf
.

/16/ **NIRAS**
Vurdering af behovet for kemiske analyser, Kystnære havmøller; Vesterhav Nord, Vesterhav Syd og Bornholm
Document no. 129984731, version 1, 2014.

/17/ **DMU**
http://www.dmu.dk/vand/havmiljoe/mads/ctd/data
, 2014.

/18/ **Lund-Hansen, L. C.**
Diffuse attenuation coefficients Kd(PAR) at the estuarin North Sea–Baltic Sea transition
Coastal and Shelf Science 61, no. time-series, partitioning, absorption, and scattering. Estuarine, pp. 251-259, 2004.

/19/ **Devlin, M. J. *et al.***
Relationships between suspended particulate material,light attenuation and Secchi depth in UK marine waters
Estuarine, Coastal and Shelf Science 79 (2008), p. 429–439, 2008.

/20/ **Dobrynin M., G. H. . G. G.**
Assimilation of satellite data in a Suspended Particulate Matter transport model
2008.

/21/ **Sund & Belt**
Storebælt og miljøet
1999.

/22/ **Whitehouse, R. J. S., Sutherland, J. and Harris, J. M.**
Evaluating scour at marine gravity foundations
2011.

/23/ **Orbicon**
VVM-Redegørelse for indvinding af sand til kystfodring
Indvindingsområde 562-AD, Ferring, Kystdirektoratet, 2013.

/24/ **Poulsen, J. W. and Berg, P.** for DMI
More details on HBM - general modelling theory and
Doc. no. Technical Report 12-16,
http://beta.dmi.dk/fileadmin/Rapporter/TR/tr12-16.pdf, 2012.

/25/ **COWI** for Energinet.dk
Vesterhav Syd - Laboratory Test Report
Report no. 1, Doc. no. A037055-37.1.1, rev. 2, 08 January 2014.

/26/ **Wentworth, C. K.**
Udden-Wentworth grain-size classification scheme (Wentworth, 1922)
Online: http://www-odp.tamu.edu/publications/200_IR/chap_02/c2_f7.htm, accessed 26 February 2014.

/27/ **Whitehouse, R. S. R. R. W. a. M. H.**
Dynamics of estuarine muds. A manual for practical applications
Thomas Telford, 2000.

/28/ **DHI**
MIKE 21/3 MT reference manual, 2014th edition
2014.

/29/ **Yang, C. T.**
Erosion and Sedimentation Manual
U.S. Department of the Interior,
http://www.usbr.gov/pmts/sediment/kb/ErosionAndSedimentation/,
November 2006.

/30/ **van Rijn, L.**
Principles of Sediment Transport in Rivers, Estuaries and Coastal Seas
The Netherlands : Aqua Publications, 1993.

/31/ **Miljøministeriet**
Naturplaner 2011
Online: http://miljoegis.mim.dk/cbkort?profile=miljoegis_naturplaner2011, accessed 2014.

/32/ **Aarup, T.**
Transparency of the North Sea and Batic Sea - a Secchi depth data mining study
Oceanologia, vol. 44, no. 3, pp. 323-337, 2002.

/33/ **Danish Coastal Authorities**
Direction of net littoral drift in Denmark
Online: http://kysterne.kyst.dk/sedimenttransport.html, 2011.

/34/ **Leth, J. O., Larsen, B. and Authony, D.**
Sediment distribution and transport in the shallow coastal waters along the west coast of Denmark
Geological survey of Denmark and Greenland Bulletin 4, 41-44, 2004.

/35/ **Leth, J. O. and Authony, D.**
Large-scale bedforms, sediment distribution and sand mobility in the eastern North Sea off the Danish west coast
Marine Geology 182, pp. 247-263, Geological Survey of Denmark and Greenland (GEUS), August 2001.

Appendix A Model description

A.1 Wave modelling using MIKE21 SW

MIKE 21 Wave Modelling

MIKE 21 SW – Spectral Waves FM

Short Description

Software for **WATER ENVIRONMENTS**

DHI headquarters
Agern Allé 5
DK-2970 Hørsholm
Denmark

+45 4516 9200 Telephone
+45 4516 9333 Support
+45 4516 9292 Telefax

mikebydhi@dhigroup.com
www.mikebydhi.com

MIKE21_SW_FM_Short_Description_.docx / HKH /EBR/ 2013-09-19

MIKE 21 SW - SPECTRAL WAVE MODEL FM

MIKE 21 SW is a state-of-the-art third generation spectral wind-wave model developed by DHI. The model simulates the growth, decay and transformation of wind-generated waves and swells in offshore and coastal areas.

MIKE 21 SW includes two different formulations:

- Fully spectral formulation
- Directional decoupled parametric formulation

The fully spectral formulation is based on the wave action conservation equation, as described in e.g. Komen et al (1994) and Young (1999). The directional decoupled parametric formulation is based on a parameterisation of the wave action conservation equation. The parameterisation is made in the frequency domain by introducing the zeroth and first moment of the wave action spectrum. The basic conservation equations are formulated in either Cartesian co-ordinates for small-scale applications and polar spherical co-ordinates for large-scale applications.

The fully spectral model includes the following physical phenomena:

- Wave growth by action of wind
- Non-linear wave-wave interaction
- Dissipation due to white-capping
- Dissipation due to bottom friction
- Dissipation due to depth-induced wave breaking
- Refraction and shoaling due to depth variations
- Wave-current interaction
- Effect of time-varying water depth
- Effect of ice coverage on the wave field

The discretisation of the governing equation in geographical and spectral space is performed using cell-centred finite volume method. In the geographical domain, an unstructured mesh technique is used. The time integration is performed using a fractional step approach where a multi-sequence explicit method is applied for the propagation of wave action.

MIKE 21 SW is a state-of-the-art numerical modelling tool for prediction and analysis of wave climates in offshore and coastal areas. © BIOFOTO/Klaus K. Bentzen

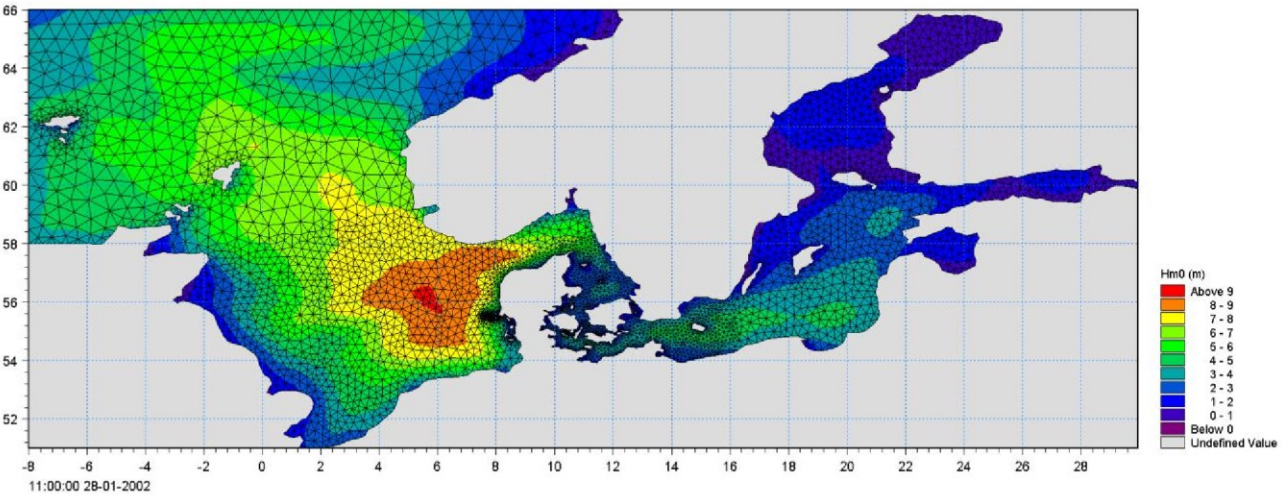

A MIKE 21 SW forecast application in the North Sea and Baltic Sea. The chart shows a wave field (from the NSBS model) illustrated by the significant wave height in top of the computational mesh. See also www.waterforecast.com

Computational Features

The main computational features of MIKE 21 SW - Spectral Wave Model FM are as follows:

- Fully spectral and directionally decoupled parametric formulations
- Source functions based on state-of-the-art 3rd generation formulations
- Instationary and quasi-stationary solutions
- Optimal degree of flexibility in describing bathymetry and ambient flow conditions using depth-adaptive and boundary-fitted unstructured mesh
- Coupling with hydrodynamic flow model for modelling of wave-current interaction and time-varying water depth
- Flooding and drying in connection with time-varying water depths
- Cell-centred finite volume technique
- Fractional step time-integration with an multi-sequence explicit method for the propagation
- Extensive range of model output parameters (wave, swell, air-sea interaction parameters, radiation stress tensor, spectra, etc.)

Application Areas

MIKE 21 SW is used for the assessment of wave climates in offshore and coastal areas - in hindcast and forecast mode.

A major application area is the design of offshore, coastal and port structures where accurate assessment of wave loads is of utmost importance to the safe and economic design of these structures.

Illustrations of typical application areas of DHI's MIKE 21 SW – Spectral Wave Model FM

Measured data are often not available during periods long enough to allow for the establishment of sufficiently accurate estimates of extreme sea states.

In this case, the measured data can then be supplemented with hindcast data through the simulation of wave conditions during historical storms using MIKE 21 SW.

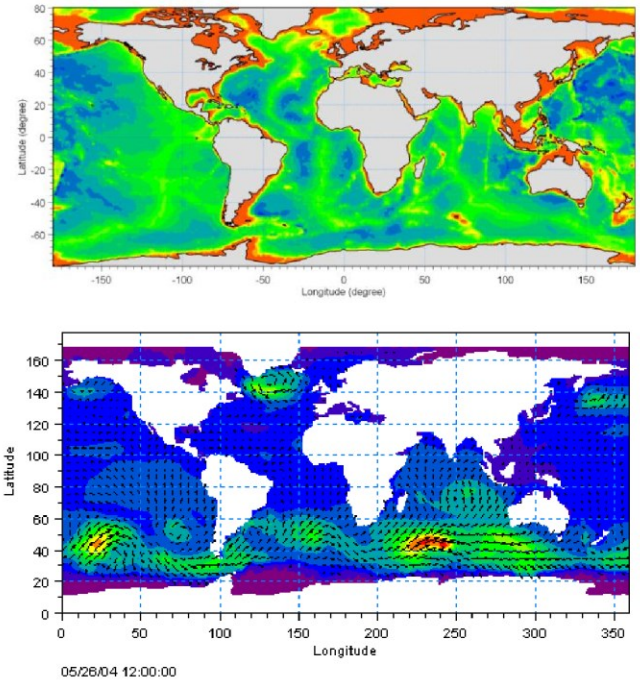

Example of a global application of MIKE 21 SW. The upper panel shows the bathymetry. Results from such a model (cf. lower panel) can be used as boundary conditions for regional scale forecast or hindcast models. See http://www.waterforecast.com for more details on regional and global modelling

MIKE 21 SW is particularly applicable for simultaneous wave prediction and analysis on regional scale and local scale. Coarse spatial and temporal resolution is used for the regional part of the mesh and a high-resolution boundary and depth-adaptive mesh is describing the shallow water environment at the coastline.

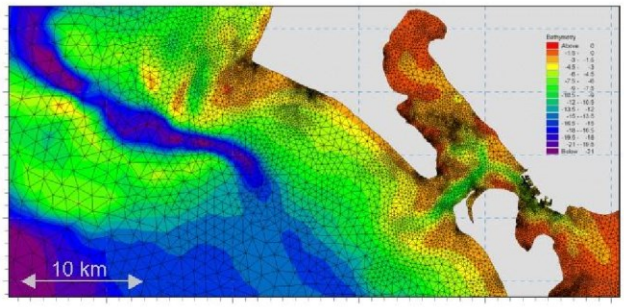

Example of a computational mesh used for transformation of offshore wave statistics using the directionally decoupled parametric formulation

MIKE 21 SW is also used for the calculation of the sediment transport, which for a large part is determined by wave conditions and associated wave-induced currents. The wave-induced current is generated by the gradients in radiation stresses that occur in the surf zone.

MIKE 21 SW can be used to calculate the wave conditions and associated radiation stresses. The long-shore currents and sediment transport are then calculated using the flow and sediment transport models available in the MIKE 21 package. For such type of applications, the directional decoupled parametric formulation of MIKE 21 SW is an excellent compromise between the computational effort and accuracy.

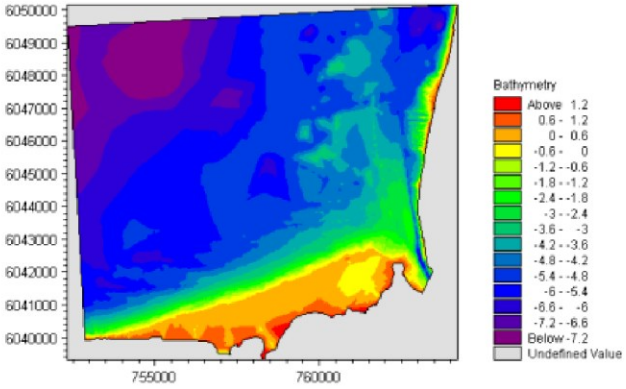

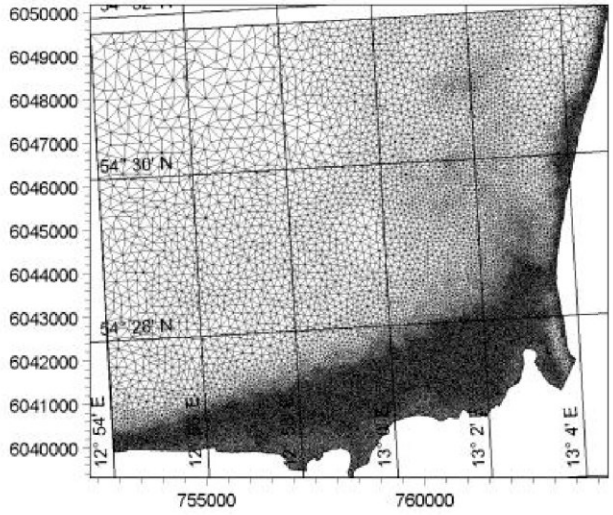

Bathymetry (upper) and computational mesh (lower) used in a MIKE 21 SW application on wave induced currents in Gellen Bay, Germany

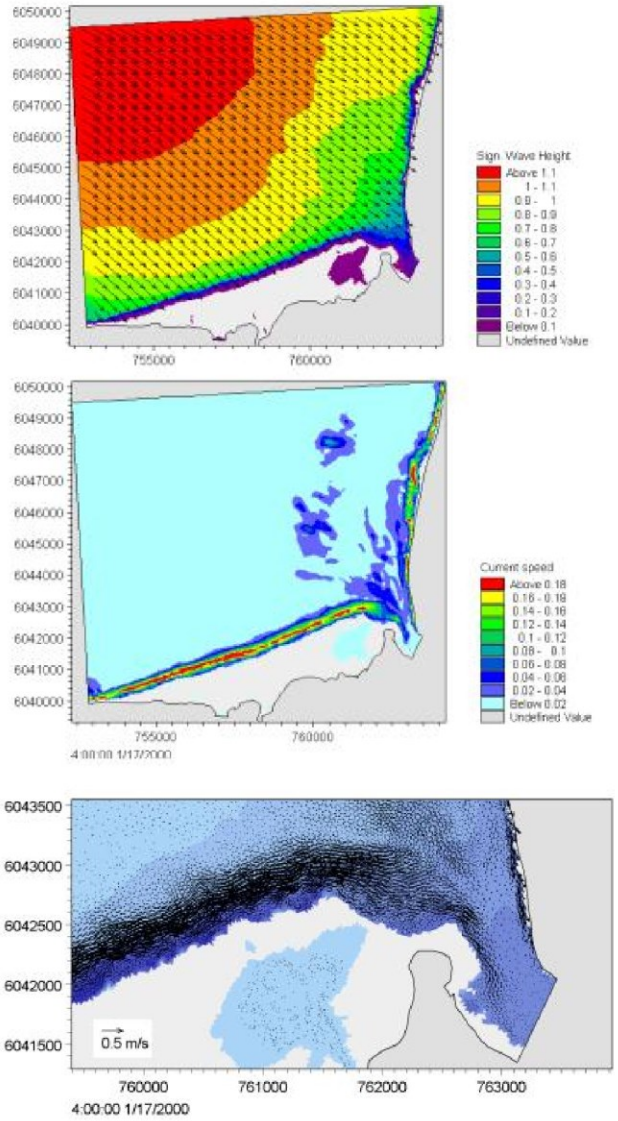

Map of significant wave height (upper), current field (middle) and vector field (lower). The flow field is simulated by DHI's MIKE 21 Flow Model FM, which is dynamically coupled to MIKE 21 SW

Model Equations

In MIKE 21 SW, the wind waves are represented by the wave action density spectrum $N(\sigma,\theta)$. The independent phase parameters have been chosen as the relative (intrinsic) angular frequency, $\sigma = 2\pi f$ and the direction of wave propagation, θ. The relation between the relative angular frequency and the absolute angular frequency, ω, is given by the linear dispersion relationship

$$\sigma = \sqrt{gk\tanh(kd)} = \omega - \bar{k}\cdot\bar{U}$$

where g is the acceleration of gravity, d is the water depth and $\bar{U}$ is the current velocity vector and $\bar{k}$ is the wave number vector with magnitude k and direction θ. The action density, $N(\sigma,\theta)$, is related to the energy density $E(\sigma,\theta)$ by

$$N = \frac{E}{\sigma}$$

Fully Spectral Formulation

The governing equation in MIKE 21 SW is the wave action balance equation formulated in either Cartesian or spherical co-ordinates. In horizontal Cartesian co-ordinates, the conservation equation for wave action reads

$$\frac{\partial N}{\partial t} + \nabla\cdot(\bar{v}N) = \frac{S}{\sigma}$$

where $N(\bar{x},\sigma,\theta,t)$ is the action density, t is the time, $\bar{x} = (x,y)$ is the Cartesian co-ordinates, $\bar{v} = (c_x, c_y, c_\sigma, c_\theta)$ is the propagation velocity of a wave group in the four-dimensional phase space $\bar{x}$, σ and θ. S is the source term for energy balance equation. ∇ is the four-dimensional differential operator in the $\bar{x}$, σ, θ-space. The characteristic propagation speeds are given by the linear kinematic relationships

$$(c_x, c_y) = \frac{d\bar{x}}{dt} = \bar{c}_g + \bar{U} = \frac{1}{2}\left(1 + \frac{2kd}{\sinh(2kd)}\right)\frac{\sigma}{k} + \bar{U}$$

$$c_\sigma = \frac{d\sigma}{dt} = \frac{\partial\sigma}{\partial d}\left[\frac{\partial d}{\partial t} + \bar{U}\cdot\nabla_{\bar{x}} d\right] - c_g\bar{k}\cdot\frac{\partial\bar{U}}{\partial s}$$

$$c_\theta = \frac{d\theta}{dt} = -\frac{1}{k}\left[\frac{\partial\sigma}{\partial d}\frac{\partial d}{\partial m} + \bar{k}\cdot\frac{\partial\bar{U}}{\partial m}\right]$$

Here, s is the space co-ordinate in wave direction θ and m is a co-ordinate perpendicular to s. $\nabla_{\bar{x}}$ is the two-dimensional differential operator in the $\bar{x}$-space.

Source Functions

The source function term, S, on the right hand side of the wave action conservation equation is given by

$$S = S_{in} + S_{nl} + S_{ds} + S_{bot} + S_{surf}$$

Here S_{in} represents the momentum transfer of wind energy to wave generation, S_{nl} the energy transfer due non-linear wave-wave interaction, S_{ds} the dissipation of wave energy due to white-capping (deep water wave breaking), S_{bot} the dissipation due to bottom friction and S_{surf} the dissipation of wave energy due to depth-induced breaking.

The default source functions S_{in}, S_{nl} and S_{ds} in MIKE 21 SW are similar to the source functions implemented in the WAM Cycle 4 model, see Komen et al (1994).

The wind input is based on Janssen's (1989, 1991) quasi-linear theory of wind-wave generation, where the momentum transfer from the wind to the sea not only depends on the wind stress, but also the sea state itself. The non-linear energy transfer (through the resonant four-wave interaction) is approximated by the DIA approach, Hasselmann et al (1985). The source function describing the dissipation due to white-capping is based on the theory of Hasselmann (1974) and Janssen (1989). The bottom friction dissipation is modelled using the approach by Johnson and Kofoed-Hansen (2000), which depends on the wave and sediment properties. The source function describing the bottom-induced wave breaking is based on the well-proven approach of Battjes and Janssen (1978) and Eldeberky and Battjes (1996).

A detailed description of the various source functions is available in Komen et al (1994) and Sørensen et al (2003), which also includes the references listed above.

Directional Decoupled Parametric Formulation

The directionally decoupled parametric formulation is based on a parameterisation of the wave action conservation equation. Following Holthuijsen et al (1989), the parameterisation is made in the frequency domain by introducing the zeroth and first moment of the wave action spectrum as dependent variables.

A similar formulation is used in the MIKE 21 NSW Near-shore Spectral Wind-Wave Model, which is one of the most popular models for wave transformation in coastal and shallow water environment. However, with MIKE 21 SW it is not necessary to set up a number of different orientated bathymetries to cover varying wind and wave directions.

The parameterisation leads to the following coupled equations

$$\frac{\partial(m_0)}{\partial t}+\frac{\partial(c_x m_0)}{\partial x}+\frac{\partial(c_y m_0)}{\partial y}+\frac{\partial(c_\theta m_0)}{\partial \theta}=T_0$$

$$\frac{\partial(m_1)}{\partial t}+\frac{\partial(c_x m_1)}{\partial x}+\frac{\partial(c_y m_1)}{\partial y}+\frac{\partial(c_\theta m_1)}{\partial \theta}=T_1$$

where $m_0(x, y, \theta)$ and $m_1(x, y, \theta)$ are the zeroth and first moment of the action spectrum $N(x, y, \sigma, \theta)$, respectively. $T_0(x, y, \theta)$ and $T_1(x, y, \theta)$ are source functions based on the action spectrum. The moments $m_n(x, y, \theta)$ are defined as

$$m_n(x,y,\theta)=\int_0^\infty \omega^n N(x,y,\omega,\theta)d\omega$$

The source functions T_0 and T_1 take into account the effect of local wind generation (stationary solution mode only) and energy dissipation due to bottom friction and wave breaking. The effects of wave-current interaction are also included. The source functions for the local wind generation are derived from empirical growth relations, see Johnson (1998) for details.

Numerical Methods

The frequency spectrum (fully spectral model only) is split into a prognostic part for frequencies lower than a cut-off frequency σ_{max} and an analytical diagnostic tail for the high-frequency part of the spectrum

$$E(\sigma,\theta)=E(\sigma_{\max},\theta)\left(\frac{\sigma}{\sigma_{\max}}\right)^{-m}$$

where m is a constant (= 5) as proposed by Komen et al (1994).

The directional decoupled parametric formulation in MIKE 21 SW is used extensively for calculation of the wave transformation from deep-water to the shoreline and for wind-wave generation in local areas

Space Discretisation

The discretisation in geographical and spectral space is performed using cell-centred finite volume method. In the geographical domain an unstructured mesh is used. The spatial domain is discretised by subdivision of the continuum into non-overlapping elements. Triangle and quadrilateral shaped polygons are presently supported in MIKE 21 SW. The action density, $N(\sigma,\theta)$ is represented as a piecewise constant over the elements and stored at the geometric centres.

In frequency space either an equidistant or a log-arithmic discretisation is used. In the directional space, an equidistant discretisation is used for both types of models. The action density is represented as piecewise constant over the discrete intervals, $\Delta\sigma$ and $\Delta\theta$, in the frequency and directional space.

Integrating the wave action conservation over an area A_i, the frequency interval $\Delta\sigma_l$ and the directional interval $\Delta\theta_m$ gives

$$\frac{\partial}{\partial t}\int_{\Delta\theta_m}\int_{\Delta\sigma_l}\int_{A_i} N d\Omega d\sigma d\theta - \int_{\Delta\theta_m}\int_{\Delta\sigma_l}\int_{A_i}\frac{S}{\sigma}d\Omega d\sigma d\theta$$
$$= \int_{\Delta\theta_m}\int_{\Delta\sigma_l}\int_{A_i}\nabla\cdot(\bar{v}N)d\Omega d\sigma d\theta$$

where Ω is the integration variable defined on A_i. Using the divergence theorem and introducing the convective flux $\bar{F} = \bar{v}N$, we obtain

$$\frac{\partial N_{i,l,m}}{\partial t} = -\frac{1}{A_i}\left[\sum_{p=1}^{NE}(F_n)_{p,l,m}\Delta l_p\right]$$
$$-\frac{1}{\Delta\sigma_l}\left[(F_\sigma)_{i,l+1/2,m} - (F_\sigma)_{i,l-1/2,m}\right]$$
$$-\frac{1}{\Delta\theta_m}\left[(F_\theta)_{i,l,m+1/2} - (F_\theta)_{i,l,m-1/2}\right] + \frac{S_{i,l,m}}{\sigma_l}$$

where NE is the total number of edges in the cell, $(F_n)_{p,l,m} = (F_x n_x + F_y n_y)_{p,l,m}$ is the normal flux trough the edge p in geographical space with length Δl_p. $(F_\sigma)_{i,l+1/2,m}$ and $(F_\theta)_{i,l,m+1/2}$ is the flux through the face in the frequency and directional space, respectively.

The convective flux is derived using a first-order upwinding scheme. In that

$$F_n = c_n\left(\frac{1}{2}(N_i + N_j) - \frac{1}{2}\frac{c}{|c|}(N_i - N_j)\right)$$

where c_n is the propagation speed normal to the element cell face.

Time Integration

The integration in time is based on a fractional step approach. Firstly, a propagation step is performed calculating an approximate solution N^* at the new time level (n+1) by solving the homogenous wave action conservation equation, i.e. without the source terms. Secondly, a source terms step is performed calculating the new solution N^{n+1} from the estimated solution taking into account only the effect of the source terms.

The propagation step is carried out by an explicit Euler scheme

$$N^*_{i,l,m} = N^n_{i,l,m} + \Delta t\left(\frac{\partial N_{i,l,m}}{\partial t}\right)^n$$

To overcome the severe stability restriction, a multi-sequence integration scheme is employed. The maximum allowed time step is increased by employing a sequence of integration steps locally, where the number of steps may vary from point to point.

A source term step is performed using an implicit method (see Komen et al, 1994)

$$N^{n+1}_{i,l,m} = N^*_{i,l,m} + \Delta t\left[\frac{(1-\alpha)S^*_{i,l,m} + \alpha S^{n+1}_{i,l,m}}{\sigma_l}\right]$$

where α is a weighting coefficient that determines the type of finite difference method. Using a Taylor series to approximate S^{n+1} and assuming the off-diagonal terms in $\partial S/\partial E = \gamma$ are negligible, this equation can be simplified as

$$N^{n+1}_{i,l,m} = N^n_{i,l,m} + \frac{(S^*_{i,l,m}/\sigma_l)\Delta t}{(1-\alpha\gamma\Delta t)}$$

For growing waves ($\gamma > 0$) an explicit forward difference is used ($\alpha = 0$), while for decaying waves ($\gamma < 0$) an implicit backward difference ($\alpha = 1$) is applied.

MIKE 21 SW is also applied for wave forecasts in ship route planning and improved service for conventional and fast ferry operators

Model Input

The necessary input data can be divided into following groups:

- Domain and time parameters:
  - computational mesh
  - co-ordinate type (Cartesian or spherical)
  - simulation length and overall time step
- Equations, discretisation and solution technique
  - formulation type
  - frequency and directional discretisation
  - number of time step groups
  - number of source time steps
- Forcing parameters
  - water level data
  - current data
  - wind data
  - ice data
- Source function parameters
  - non-linear energy transfer
  - wave breaking (shallow water)
  - bottom friction
  - white capping
- Initial conditions
  - zero-spectrum (cold-start)
  - empirical data
  - data file
- Boundary conditions
  - closed boundaries
  - open boundaries (data format and type)

Providing MIKE 21 SW with a suitable mesh is essential for obtaining reliable results from the model. Setting up the mesh includes the appropriate selection of the area to be modelled, adequate resolution of the bathymetry, flow, wind and wave fields under consideration and definition of codes for essential and land boundaries.

Furthermore, the resolution in the geographical space must also be selected with respect to stability considerations.

As the wind is the main driving force in MIKE 21 SW, accurate hindcast or forecast wind fields are of utmost importance for the wave prediction.

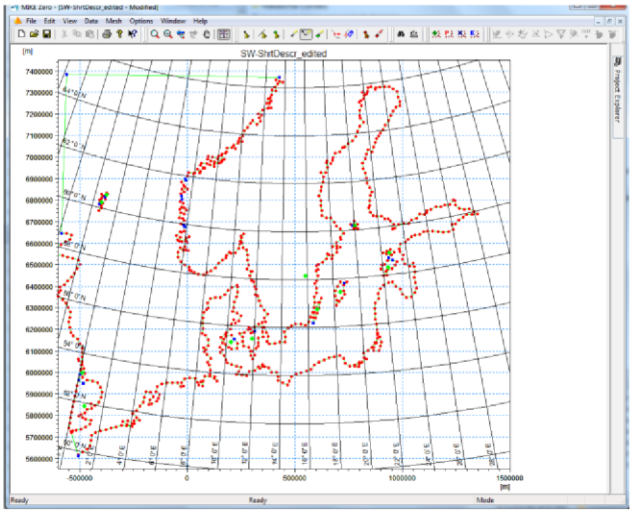

The Mesh Generator is an efficient MIKE Zero tool for the generation and handling of unstructured meshes, including the definition and editing of boundaries

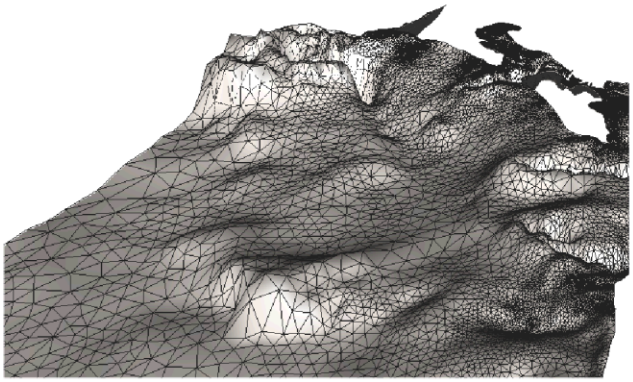

3D visualisation of a computational mesh

If wind data is not available from an atmospheric meteorological model, the wind fields (e.g. cyclones) can be determined by using the wind-generating programs available in MIKE 21 Toolbox.

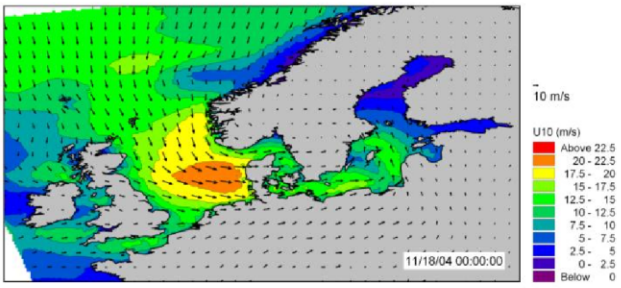

The chart shows an example of a wind field covering the North Sea and Baltic Sea as wind speed and wind direction. This is used as input to MIKE 21 SW in forecast and hindcast mode

Model Output

At each mesh point and for each time step four types of output can be obtained from MIKE 21 SW:

- Integral wave parameters divided into wind sea and swell such as
  - significant wave height, H_{m0}
  - peak wave period, T_p
  - averaged wave period, T_{01}
  - zero-crossing wave period, T_{02}
  - wave energy period, T_{-10}
  - peak wave direction, θ_p
  - mean wave direction, θ_m
  - directional standard deviation, σ
  - wave height with dir., $H_{m0} cos\theta_m$, $H_{m0} sin\theta_m$
  - radiation stress tensor, S_{xx}, S_{xy} *and* S_{yy}

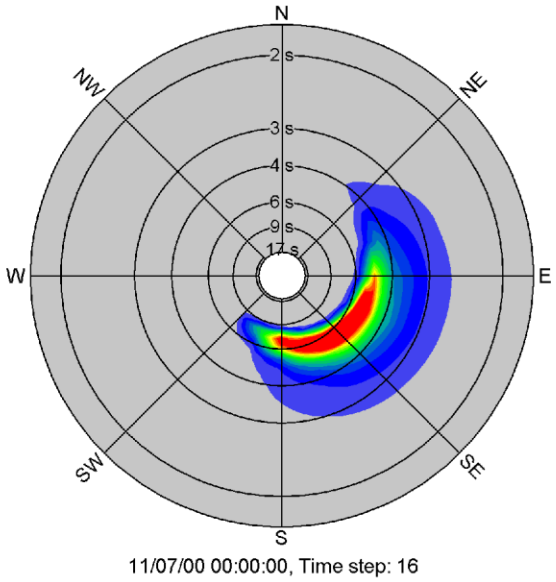

Example of model output (directional-frequency wave spectrum) processed using the Polar Plot control in the MIKE Zero Plot Composer

The distinction between wind-sea and swell can be calculated using either a constant threshold frequency or a dynamic threshold frequency with an upper frequency limit.

- Input parameters
  - water level, h
  - current velocity, $\overline{U}$
  - wind speed, U_{10}
  - wind direction, θ_w

- Model parameters
  - bottom friction coefficient, C_f
  - breaking parameter, γ
  - Courant number, Cr
  - time step factor, α
  - characteristic edge length, Δl
  - area of element, a
  - wind friction speed, u_*
  - roughness length, z_0
  - drag coefficient, C_D
  - Charnock parameter, z_{ch}

- Directional-frequency wave spectra at selected grid points and or areas as well as direction spectra and frequency spectra

Output from MIKE 21 SW is typically post-processed using the Data Viewer available in the common MIKE Zero shell. The Data Viewer is a tool for analysis and visualisation of unstructured data, e.g. to view meshes, spectra, bathymetries, results files of different format with graphical extraction of time series and line series from plan view and import of graphical overlays.

Various other editors and plot controls in the MIKE Zero Composer (e.g. Time Series Plot, Polar Plot, etc.) can be used for analysis and visualisation.

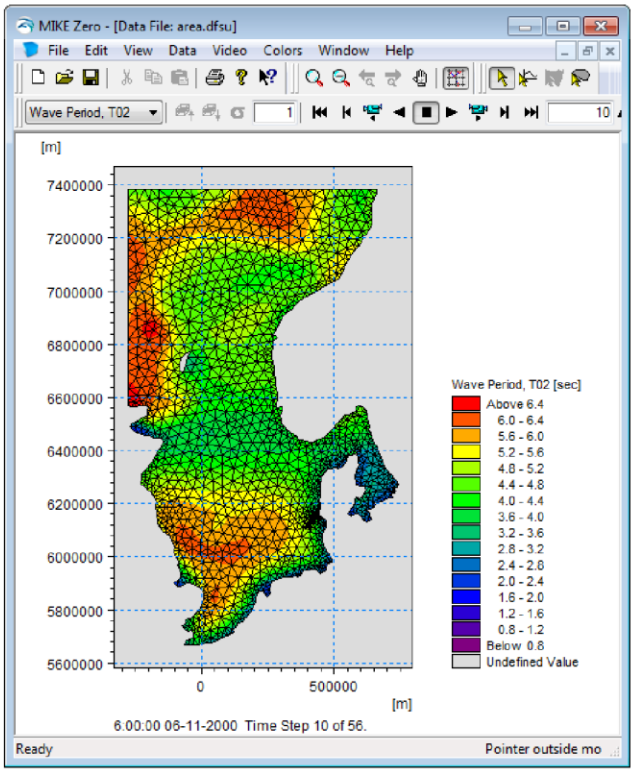

The Data Viewer in MIKE Zero – an efficient tool for analysis and visualisation of unstructured data including processing of animations

Validation

The model has successfully been applied to a number of rather basic idealised situations for which the results can be compared with analytical solutions or information from the literature. The basic tests covered fundamental processes such as wave propagation, depth-induced and current-induced shoaling and refraction, wind-wave generation and dissipation.

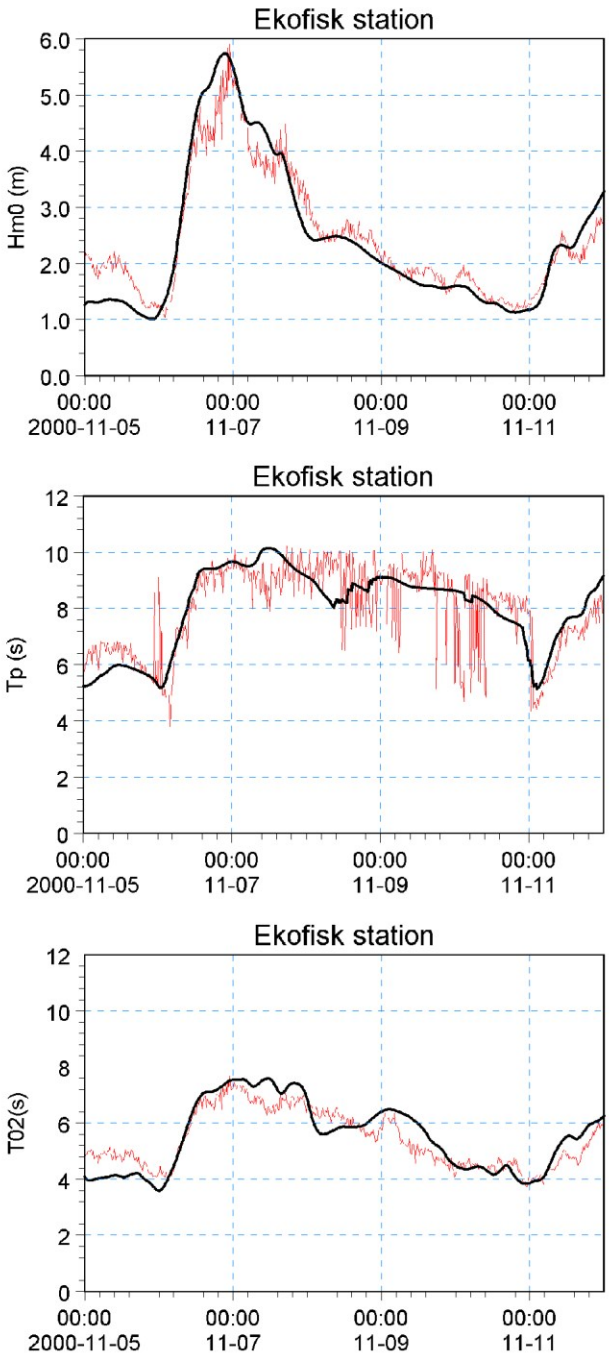

Comparison between measured and simulated significant wave height, peak wave period and mean wave period at the Ekofisk offshore platform (water depth 70 m) in the North Sea). (——) calculations and (——) measurements

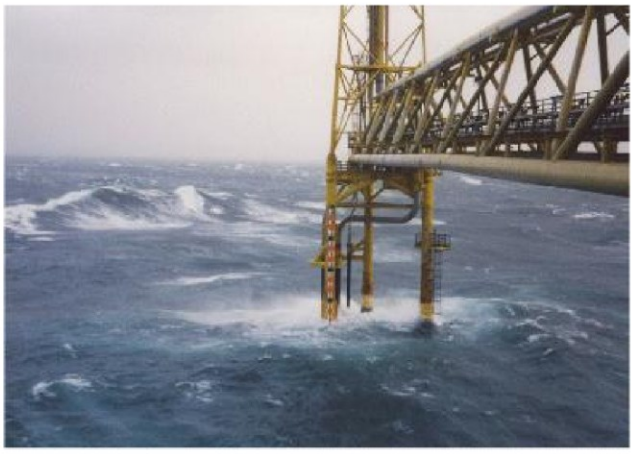

A major application area of MIKE 21 SW is in connection with design and maintenance of offshore structures

The model has also been tested in natural geophysical conditions (e.g. in the North Sea, the Danish West Coast and the Baltic Sea), which are more realistic and complicated than the academic test and laboratory tests mentioned above.

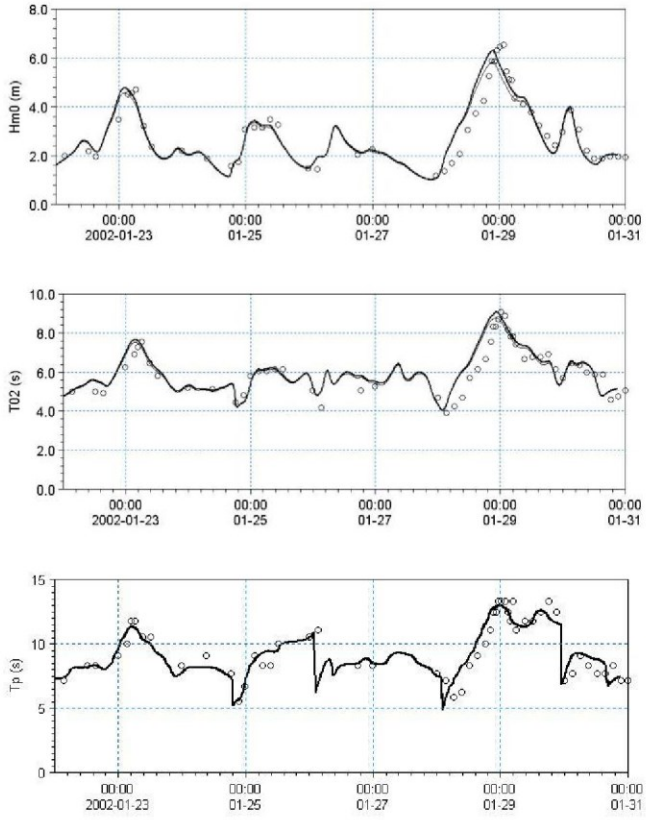

Comparison between measured and simulated significant wave height, peak wave period and mean wave period at Fjaltring located at the Danish west coast (water depth 17.5 m).(——) calculations and (o) measurements

The Fjaltring directional wave rider buoy is located offshore relative to the depicted arrow

MIKE 21 SW is used for prediction of the wave conditions at the complex Horns Rev (reef) in the southeastern part of the North Sea. At this site, a 168 MW offshore wind farm with 80 turbines has been established in water depths between 6.5 and 13.5 m.

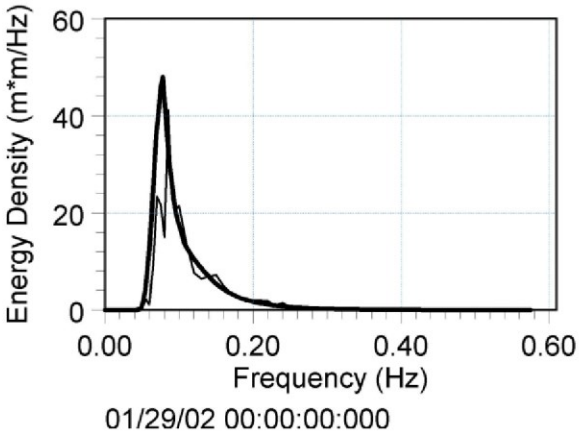

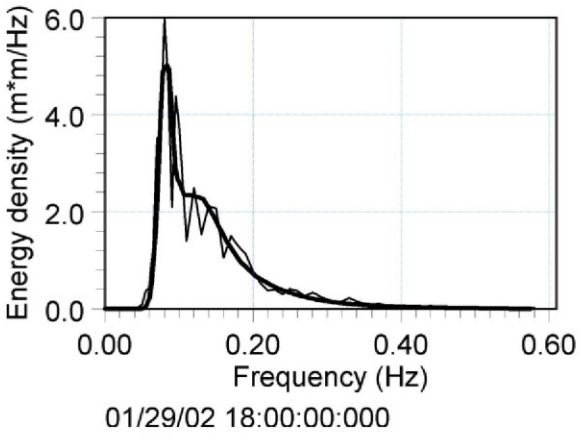

Comparison of frequency spectra at Fjaltring. (——) calculations and (——)measurements

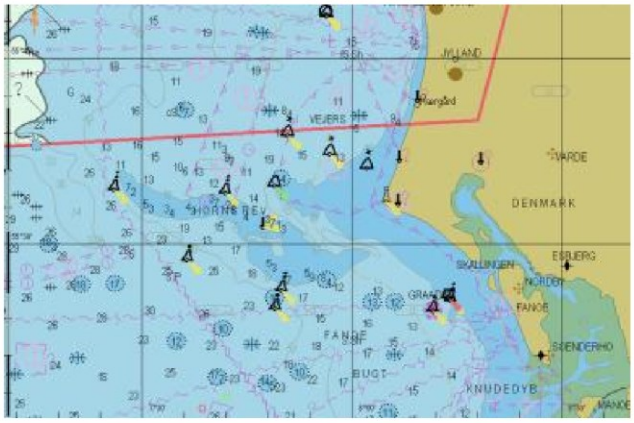

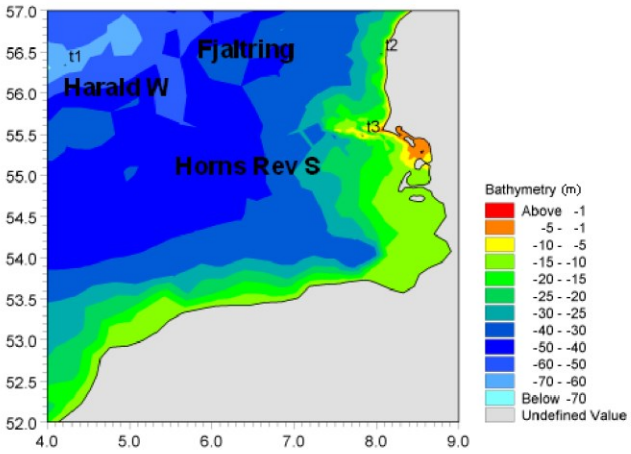

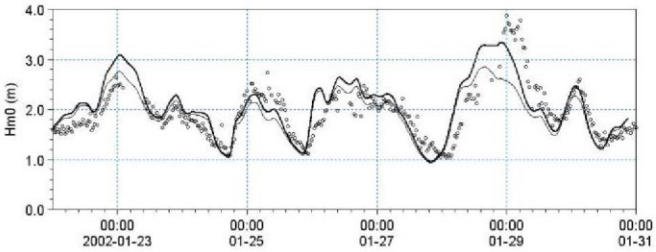

The upper panels show the Horns Rev offshore wind farm and MIKE C-map chart. 'The middle panel shows a close-up of the mesh near the Horns Rev S wave rider buoy (t3, 10 m water depth. The lower panel shows a comparison between measured and simulated significant wave height at Horns Rev S, (——) calculations including tide and surge and (——-) calculations excluding including tide and surge, (o) measurements

The predicted nearshore wave climate along the island of Hiddensee and the coastline of Zingst located in the micro-tidal Gellen Bay, Germany have been compared to field measurements (Sørensen et al, 2004) provided by the MORWIN project. From the illustrations it can be seen that the wave conditions are well reproduced both offshore and in more shallow water near the shore. The RMS values (on significant wave height) are less than 0.25m at all five stations.

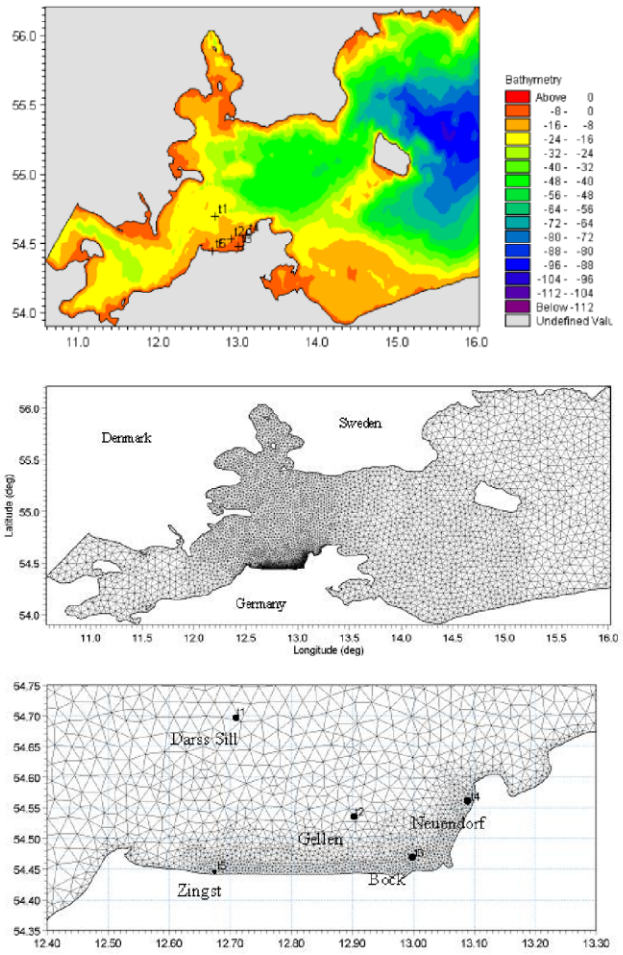

A MIKE 21 SW hindcast application in the Baltic Sea. The upper chart shows the bathymetry and the middle and lower charts show the computational mesh. The lower chart indicates the location of the measurement stations

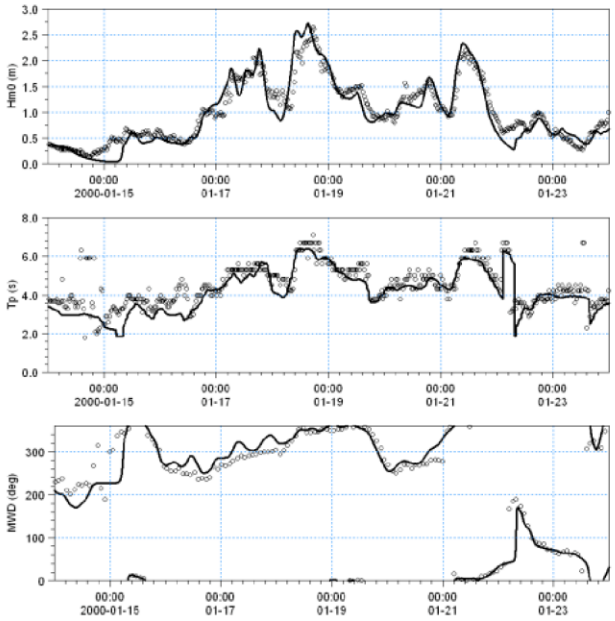

Time series of significant wave height, H_{m0}, peak wave period, T_p , and mean wave direction, MWD, at Darss sill (Offshore, depth 20.5 m). (——) Calculation and (o) measurements. The RMS value on H_{m0} is approximately 0.2 m

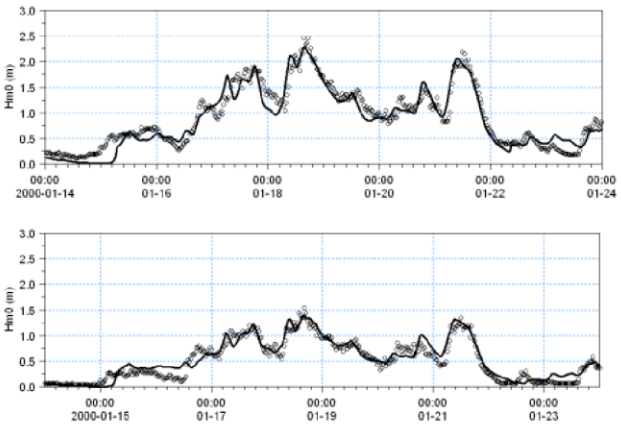

Time series of significant wave height, H_{m0}, at Gellen (upper, depth 8.3m) and Bock (lower, depth 5.5 m). (——) Calculation and (o) measurements. The RMS value on H_{m0} is approximately 0.15 m

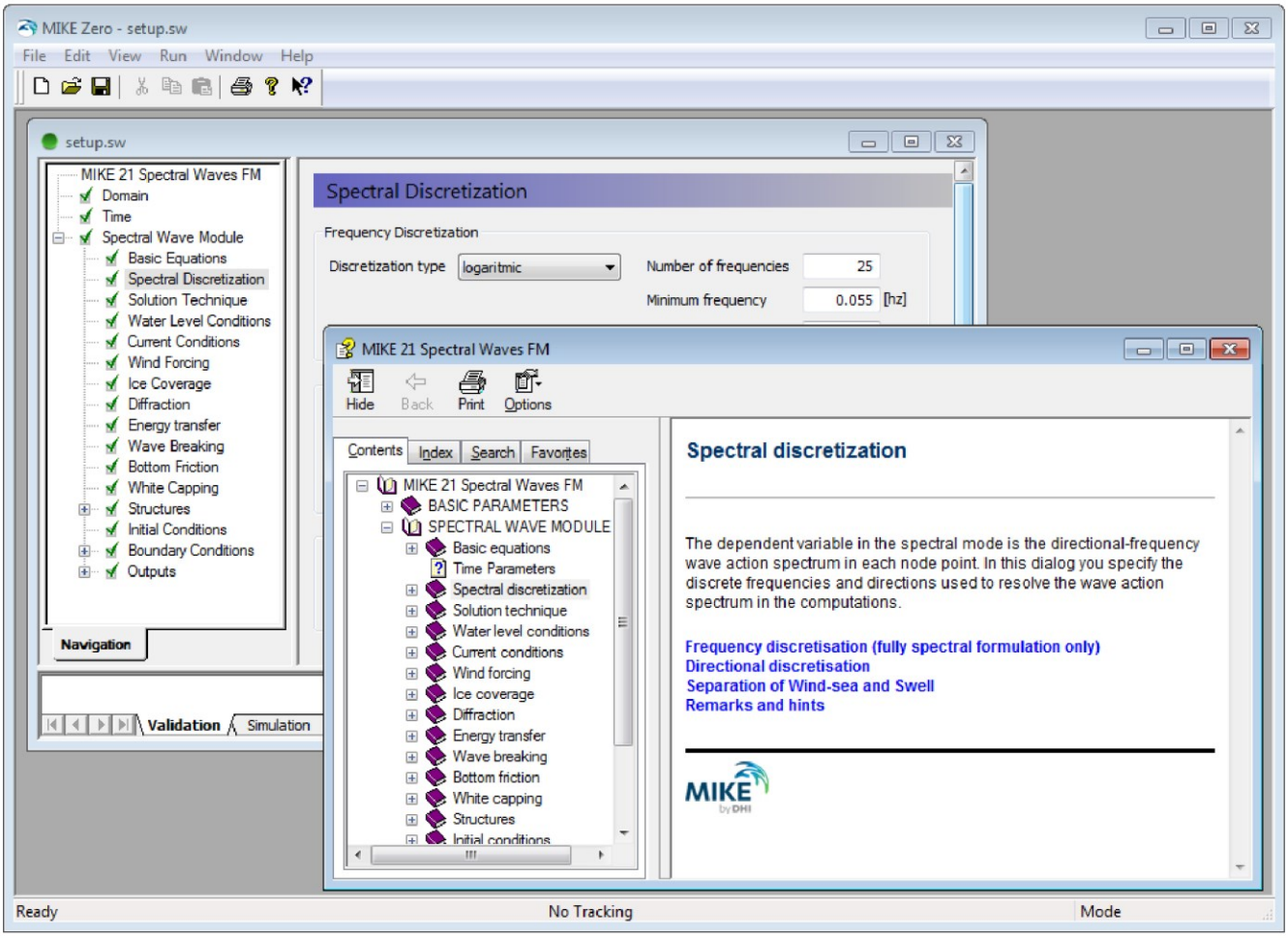

Graphical user interface of MIKE 21 SW, including an example of the Online Help System

Graphical User Interface

MKE 21 SW is operated through a fully Windows integrated Graphical User Interface (GUI). Support is provided at each stage by an Online Help System.

The common MIKE Zero shell provides entries for common data file editors, plotting facilities and a toolbox for/utilities as the Mesh Generator and Data Viewer.

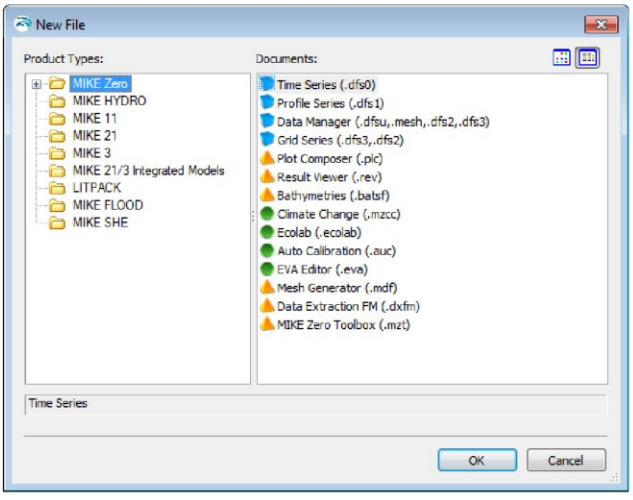

Overview of the common MIKE Zero utilities

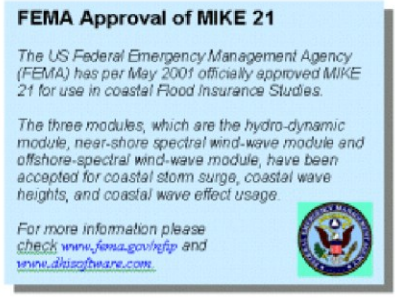

FEMA approval of the MIKE 21 package

Parallelisation

The computational engines of the MIKE 21/3 FM series are available in versions that have been parallelised using both shared memory (OpenMP) as well as distributed memory architecture (MPI). The result is much faster simulations on systems with many cores.

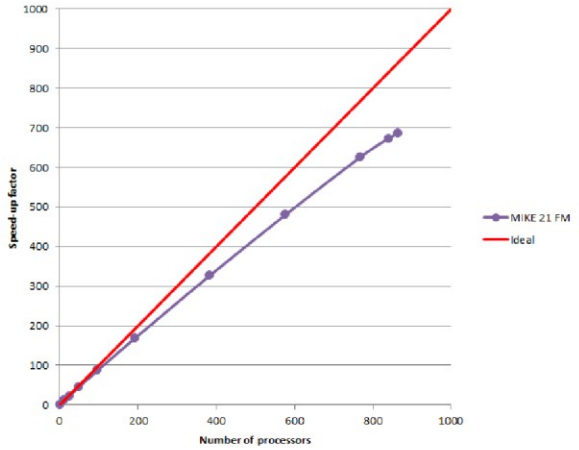

MIKE 21 FM speed-up using a HPC Cluster for Release 2012 with distributed memory architecture (purple)

Hardware and Operating System Requirements

Release 2012 version of the MIKE 21 SW Module supports Microsoft Windows XP Professional Edition (32 and 64 bit), Microsoft Windows Vista Business (32 and 64 bit) and Microsoft Windows 7 Enterprise (32 and 64 bit). Release 2014 version will only support Microsoft Windows 7 Professional SP1 (32 and 64 bit) and Microsoft Windows 8 Professional (64 bit). Microsoft Internet Explorer 6.0 (or higher) is required for network license management as well as for accessing the Online Help.

The recommended minimum hardware requirements for executing MIKE 21 SW are:

Processor:	3 GHz PC (or higher)
Memory (RAM):	4 GB (or higher)
Hard disk:	160 GB (or higher)
Monitor:	SVGA, resolution 1024x768
Graphic card:	64 MB RAM (or higher), 32 bit true colour
Media:	DVD drive compatible with dual layer DVDs

Support

News about new features, applications, papers, updates, patches, etc. are available here:

www.mikebydhi.com/Download/DocumentsAndTools.aspx

For further information on MIKE 21 SW, please contact your local DHI office or the Software Support Centre:

MIKE by DHI
DHI
Agern Allé 5
DK-2970 Hørsholm
Denmark

Tel: +45 4516 9333
Fax: +45 4516 9292

www.mikebydhi.com
mikebydhi@dhigroup.com

Documentation

The MIKE 21 & MIKE 3 modules are provided with comprehensive user guides, online help, scientific documentation, application examples and step-by-step training examples.

References

Sørensen, O. R., Kofoed-Hansen, H., Rugbjerg, M. and Sørensen, L.S., 2004: A Third Generation Spectral Wave Model Using an Unstructured Finite Volume Technique. In Proceedings of the 29th International Conference of Coastal Engineering, 19-24 September 2004, Lisbon, Portugal.

Johnson, H.K., and Kofoed-Hansen, H., (2000). Influence of bottom friction on sea surface roughness and its impact on shallow water wind wave modelling. *J. Phys. Oceanog.,* **30,** 1743-1756.

Johnson, H.K., Vested, H.J., Hersbach, H. Højstrup, J. and Larsen, S.E., (1999). On the coupling between wind and waves in the WAM model. *J. Atmos. Oceanic Technol.,* **16,** 1780-1790.

Johnson, H.K. (1998). On modeling wind-waves in shallow and fetch limited areas using the method of Holthuijsen, Booij and Herbers. *J. Coastal Research,* **14**, 3, 917-932.

Young, I.R., (1999). Wind generated ocean waves, in Elsevier Ocean Engineering Book Series, Volume 2, Eds. R. Bhattacharyya and M.E. McCormick, Elsevier.

Komen, G.J., Cavaleri, L., Doneland, M., Hasselmann, K., Hasselmann S. and Janssen, P.A.E.M., (1994). Dynamics and modelling of ocean waves. Cambridge University Press, UK, 560 pp.

Holthuijsen, L.H, Booij, N. and Herbers, T.H.C. (1989). A prediction model for stationary, short-crested waves in shallow water with ambient currents, *Coastal Engr.*, **13**, 23-54.

References on Applications

Kofoed-Hansen, H., Johnson, H.K., Højstrup, J. and Lange, B., (1998). Wind-wave modelling in waters with restricted fetches. In: Proc of 5th International Workshop on Wave Hindcasting and Forecasting, 27-30 January 1998, Melbourne, FL, USA, pp. 113-127.

Kofoed-Hansen, H, Johnson, H.K., Astrup, P. and Larsen, J., (2001). Prediction of waves and sea surface roughness in restricted coastal waters. In: Proc of 27th International Conference of Coastal Engineering, pp.1169-1182.

Al-Mashouk, M.A., Kerper, D.R. and Jacobsen, V., (1998). Red Sea Hindcast study: Development of a sea state design database for the Red Sea.. *J Saudi Aramco Technology*, **1**, 10 pp.

Rugbjerg, M., Nielsen, K., Christensen, J.H. and Jacobsen, V., (2001). Wave energy in the Danish part of the North Sea. In: Proc of 4th European Wave Energy Conference, 8 pp.

A.2 Hydrodynamic modelling using MIKE21 HDFM

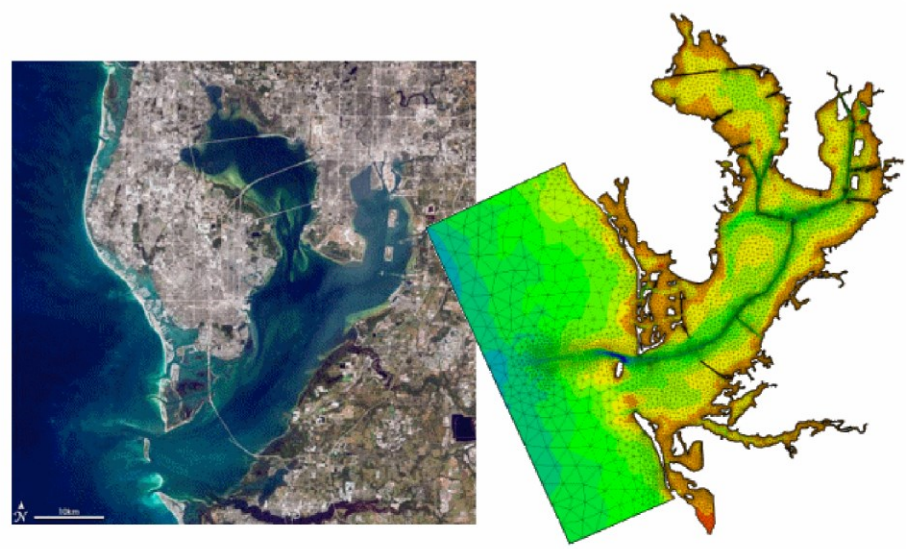

MIKE 21 & MIKE 3 Flow Model FM

Hydrodynamic Module

Short Description

Software for **WATER ENVIRONMENTS**

DHI headquarters
Agern Allé 5
DK-2970 Hørsholm
Denmark

+45 4516 9200 Telephone
+45 4516 9333 Support
+45 4516 9292 Telefax

mikebydhi@dhigroup.com
www.mikebydhi.com

MIKE213_HD_FM_Short_Description_.docx / AJS/EBR / 2013-09-19

MIKE 21 & MIKE 3 Flow Model FM

The Flow Model FM is a comprehensive modelling system for two- and three-dimensional water modelling developed by DHI. The 2D and 3D models carry the same names as the classic DHI model versions MIKE 21 & MIKE 3 with an 'FM' added referring to the type of model grid - Flexible Mesh.

The modelling system has been developed for complex applications within oceanographic, coastal and estuarine environments. However, being a general modelling system for 2D and 3D free-surface flows it may also be applied for studies of inland surface waters, e.g. overland flooding and lakes or reservoirs.

MIKE 21 & MIKE 3 Flow Model FM is a general hydrodynamic flow modelling system based on a finite volume method on an unstructured mesh

The Modules of the Flexible Mesh Series

DHI's Flexible Mesh (FM) series includes the following modules:

Flow Model FM modules

- Hydrodynamic Module, HD
- Transport Module, TR
- Ecology Module, ECO Lab
- Oil Spill Module, ELOS
- Sand Transport Module, ST
- Mud Transport Module, MT
- Particle Tracking Module, PT

Wave module

- Spectral Wave Module, SW

The FM Series meets the increasing demand for realistic representations of nature, both with regard to 'look alike' and to its capability to model coupled processes, e.g. coupling between currents, waves and sediments. Coupling of modules is managed in the Coupled Model FM.

All modules are supported by advanced user interfaces including efficient and sophisticated tools for mesh generation, data management, 2D/3D visualization, etc. In combination with comprehensive documentation and support, the FM series forms a unique professional software tool for consultancy services related to design, operation and maintenance tasks within the marine environment.

An unstructured grid provides an optimal degree of flexibility in the representation of complex geometries and enables smooth representations of boundaries. Small elements may be used in areas where more detail is desired, and larger elements used where less detail is needed, optimising information for a given amount of computational time.

The spatial discretisation of the governing equations is performed using a cell-centred finite volume method. In the horizontal plane an unstructured grid is used while a structured mesh is used in the vertical domain (3D).

This document provides a short description of the Hydrodynamic Module included in MIKE 21 & MIKE 3 Flow Model FM.

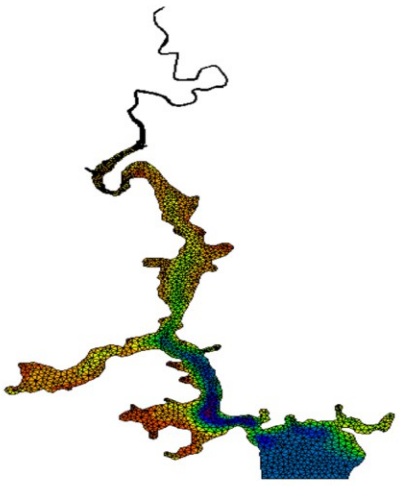

Example of computational mesh for Tamar Estuary, UK

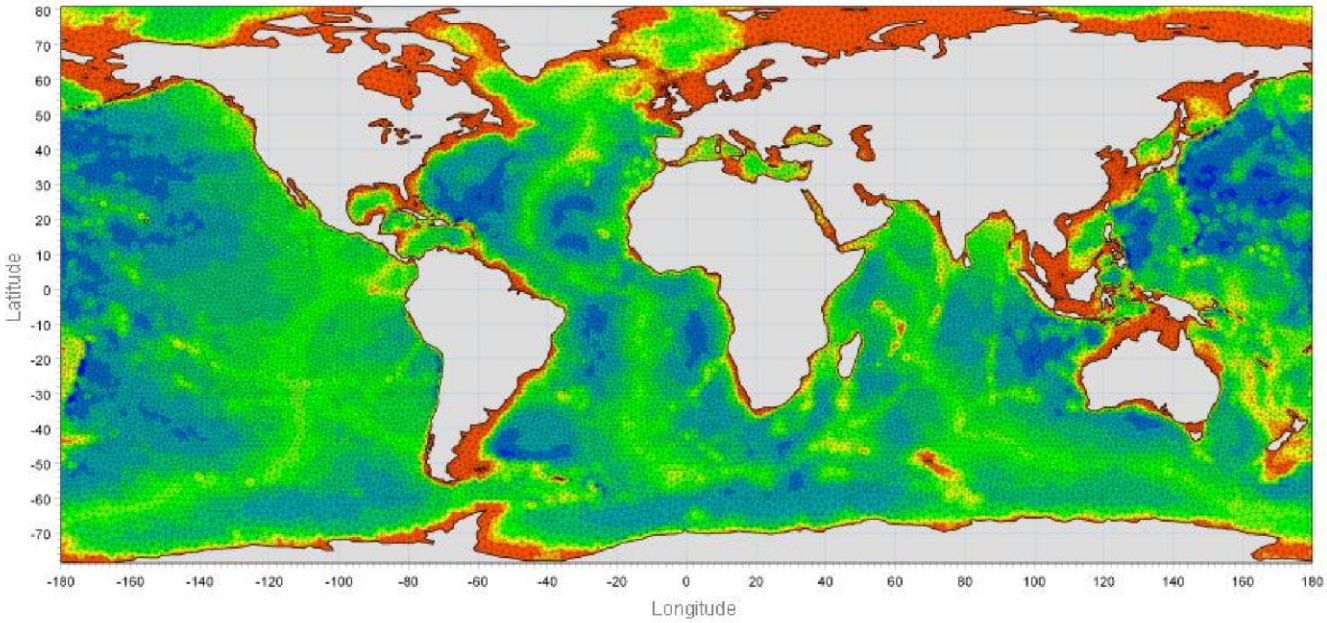

MIKE 21 & MIKE 3 FLOW MODEL FM supports both Cartesian and spherical coordinates. Spherical coordinates are usually applied for regional and global sea circulation applications. The chart shows the computational mesh and bathymetry for the planet Earth generated by the MIKE Zero Mesh Generator

MIKE 21 & MIKE 3 Flow Model FM - Hydrodynamic Module

The Hydrodynamic Module provides the basis for computations performed in many other modules, but can also be used alone. It simulates the water level variations and flows in response to a variety of forcing functions on flood plains, in lakes, estuaries and coastal areas.

Application Areas

The Hydrodynamic Module included in MIKE 21 & MIKE 3 Flow Model FM simulates unsteady flow taking into account density variations, bathymetry and external forcings.

The choice between 2D and 3D model depends on a number of factors. For example, in shallow waters, wind and tidal current are often sufficient to keep the water column well-mixed, i.e. homogeneous in salinity and temperature. In such cases a 2D model can be used. In water bodies with stratification, either by density or by species (ecology), a 3D model should be used. This is also the case for enclosed or semi-enclosed waters where wind-driven circulation occurs.

Typical application areas are

- Assessment of hydrographic conditions for design, construction and operation of structures and plants in stratified and non-stratified waters
- Environmental impact assessment studies
- Coastal and oceanographic circulation studies
- Optimization of port and coastal protection infrastructures
- Lake and reservoir hydrodynamics
- Cooling water, recirculation and desalination
- Coastal flooding and storm surge
- Inland flooding and overland flow modelling
- Forecast and warning systems

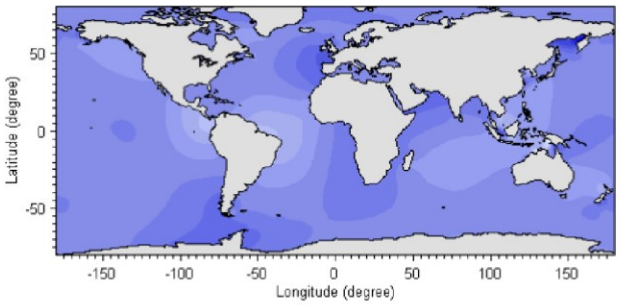

Example of a global tide application of MIKE 21 Flow Model FM. Results from such a model can be used as boundary conditions for regional scale forecast or hindcast models

The MIKE 21 & MIKE 3 Flow Model FM also support spherical coordinates, which makes both models particularly applicable for global and regional sea scale applications.

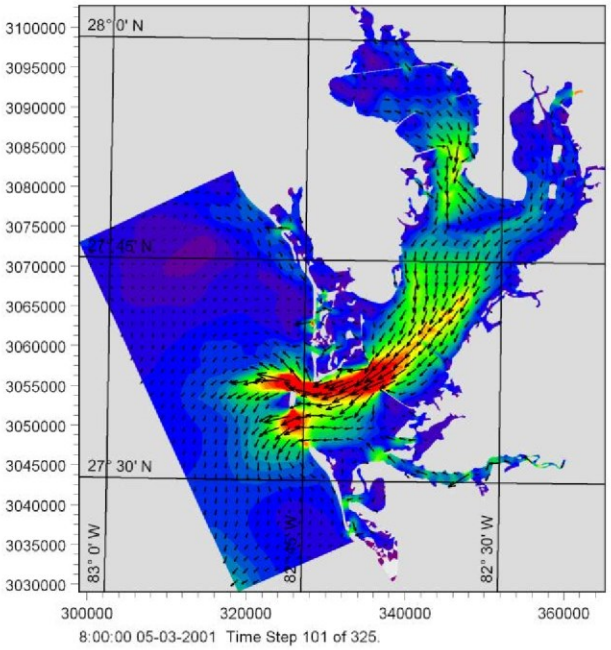

Example of a flow field in Tampa Bay, FL, simulated by MIKE 21 Flow Model FM

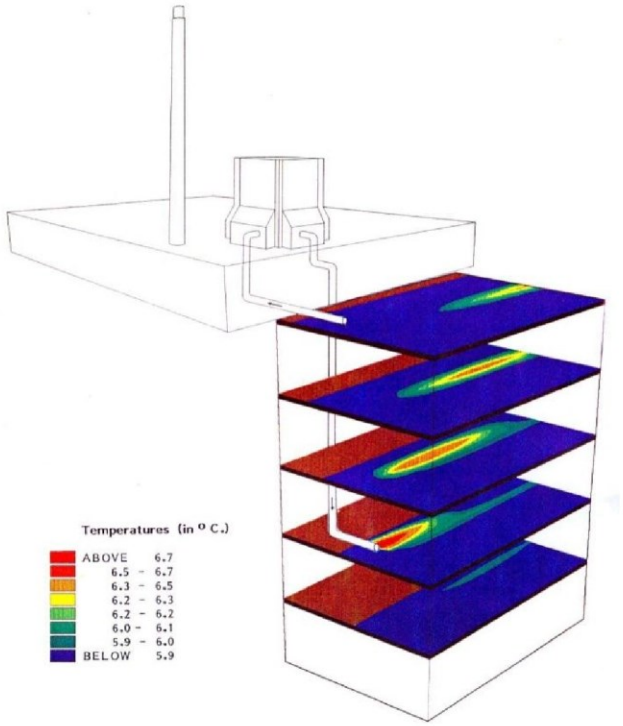

Study of thermal recirculation

Typical applications with the MIKE 21 & MIKE 3 Flow Model FM include cooling water recirculation and ecological impact assessment (eutrophication)

The Hydrodynamic Module is together with the Transport Module (TR) used to simulate the spreading and fate of dissolved and suspended substances. This module combination is applied in tracer simulations, flushing and simple water quality studies.

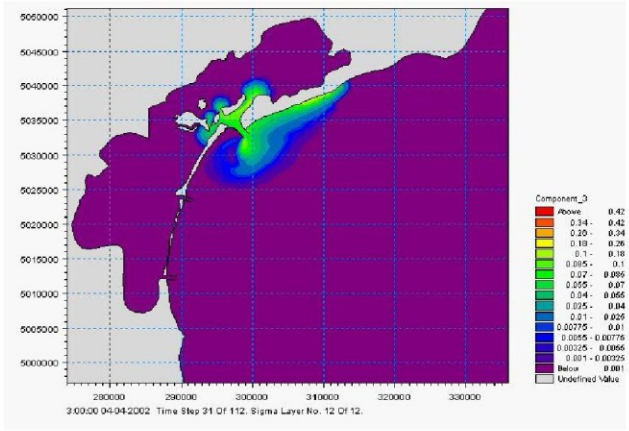

Tracer simulation of single component from outlet in the Adriatic, simulated by MIKE 21 Flow Model FM HD+TR

Prediction of ecosystem behaviour using the MIKE 21 & MIKE 3 Flow Model FM together with ECO Lab

The Hydrodynamic Module can be coupled to the Ecological Module (ECO Lab) to form the basis for environmental water quality studies comprising multiple components.

Furthermore, the Hydrodynamic Module can be coupled to sediment models for the calculation of sediment transport. The Sand Transport Module and Mud Transport Module can be applied to simulate transport of non-cohesive and cohesive sediments, respectively.

In the coastal zone the transport is mainly determined by wave conditions and associated wave-induced currents. The wave-induced currents are generated by the gradients in radiation stresses that occur in the surf zone. The Spectral Wave Module can be used to calculate the wave conditions and associated radiation stresses.

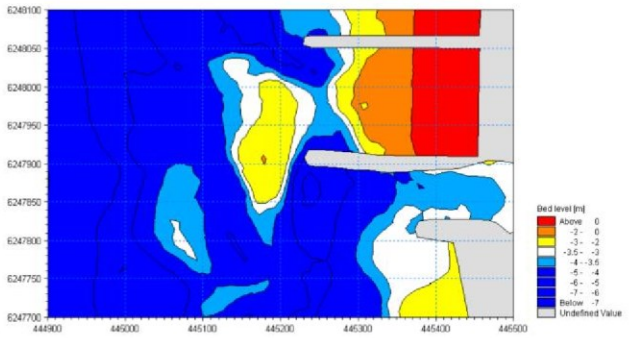

Coastal application (morphology) with coupled MIKE 21 HD, SW and ST, Torsminde harbour Denmark

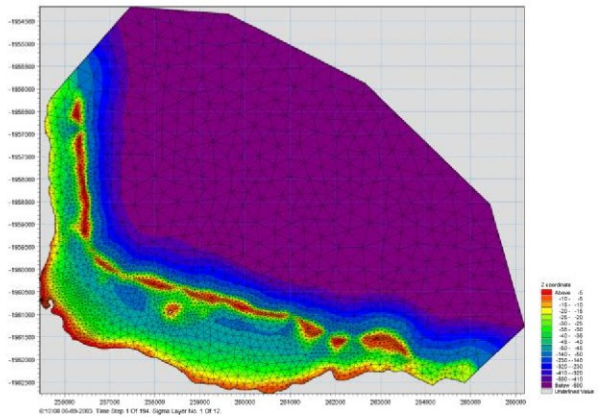

Model bathymetry of Taravao Bay, Tahiti

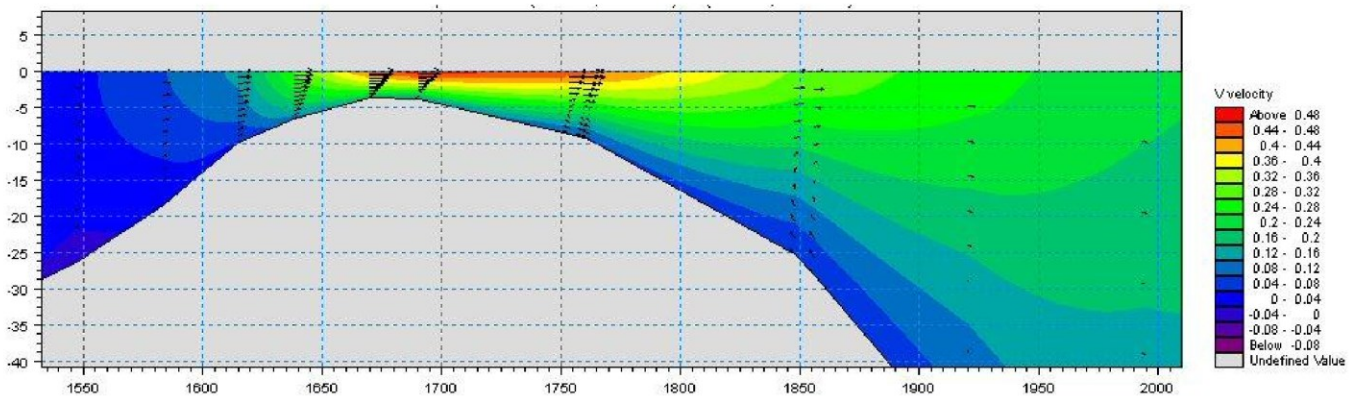

Example of Cross reef currents in Taravao Bay, Tahiti simulated with MIKE 3 Flow Model FM. The circulation and renewal of water inside the reef is dependent on the tides, the meteorological conditions and the cross reef currents, thus the circulation model includes the effects of wave induced cross reef currents

Computational Features

The main features and effects included in simulations with the MIKE 21 & MIKE 3 Flow Model FM – Hydrodynamic Module are the following:

- Flooding and drying
- Momentum dispersion
- Bottom shear stress
- Coriolis force
- Wind shear stress
- Barometric pressure gradients
- Ice coverage
- Tidal potential
- Precipitation/evaporation
- Wave radiation stresses
- Sources and sinks

Model Equations

The modelling system is based on the numerical solution of the two/three-dimensional incompressible Reynolds averaged Navier-Stokes equations subject to the assumptions of Boussinesq and of hydrostatic pressure. Thus, the model consists of continuity, momentum, temperature, salinity and density equations and it is closed by a turbulent closure scheme. The density does not depend on the pressure, but only on the temperature and the salinity.

For the 3D model, the free surface is taken into account using a sigma-coordinate transformation approach or using a combination of a sigma and z-level coordinate system.

Below the governing equations are presented using Cartesian coordinates.

The local continuity equation is written as

$$\frac{\partial u}{\partial x}+\frac{\partial v}{\partial y}+\frac{\partial w}{\partial z}=S$$

and the two horizontal momentum equations for the x- and y-component, respectively

$$\frac{\partial u}{\partial t}+\frac{\partial u^2}{\partial x}+\frac{\partial vu}{\partial y}+\frac{\partial wu}{\partial z}=fv-g\frac{\partial \eta}{\partial x}-\frac{1}{\rho_0}\frac{\partial p_a}{\partial x}-\frac{g}{\rho_0}\int_z^\eta \frac{\partial \rho}{\partial x}dz+F_u+\frac{\partial}{\partial z}\left(\nu_t\frac{\partial u}{\partial z}\right)+u_sS$$

$$\frac{\partial v}{\partial t}+\frac{\partial v^2}{\partial y}+\frac{\partial uv}{\partial x}+\frac{\partial wv}{\partial z}=-fu-g\frac{\partial \eta}{\partial y}-\frac{1}{\rho_0}\frac{\partial p_a}{\partial y}-\frac{g}{\rho_0}\int_z^\eta \frac{\partial \rho}{\partial y}dz+F_v+\frac{\partial}{\partial z}\left(\nu_t\frac{\partial v}{\partial z}\right)+v_sS$$

Temperature and salinity

In the Hydrodynamic Module, calculations of the transports of temperature, *T*, and salinity, *s* follow the general transport-diffusion equations as

$$\frac{\partial T}{\partial t}+\frac{\partial uT}{\partial x}+\frac{\partial vT}{\partial y}+\frac{\partial wT}{\partial z}=F_T+\frac{\partial}{\partial z}\left(D_v\frac{\partial T}{\partial z}\right)+\widehat{H}+T_sS$$

$$\frac{\partial s}{\partial t}+\frac{\partial us}{\partial x}+\frac{\partial vs}{\partial y}+\frac{\partial ws}{\partial z}=F_s+\frac{\partial}{\partial z}\left(D_v\frac{\partial s}{\partial z}\right)+s_sS$$

Unstructured mesh technique gives the maximum degree of flexibility, for example: 1) Control of node distribution allows for optimal usage of nodes 2) Adoption of mesh resolution to the relevant physical scales 3) Depth-adaptive and boundary-fitted mesh. Below is shown an example from Ho Bay Denmark with the approach channel to the Port of Esbjerg

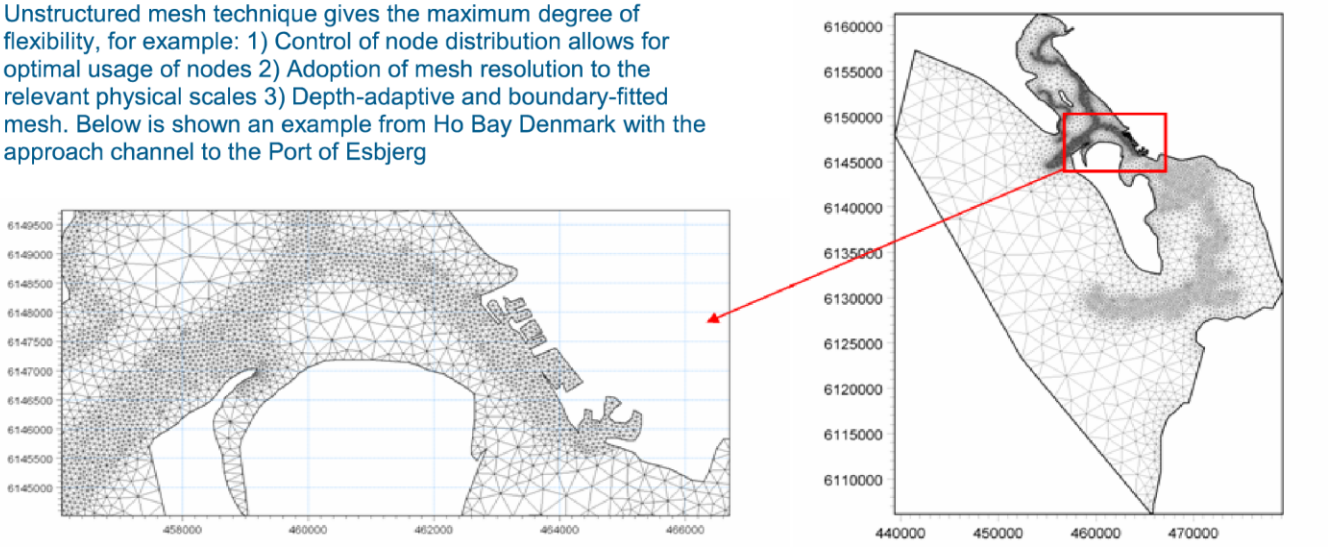

The horizontal diffusion terms are defined by

$$(F_T, F_s) = \left[\frac{\partial}{\partial x}\left(D_h \frac{\partial}{\partial x} \right) + \frac{\partial}{\partial y}\left(D_h \frac{\partial}{\partial y} \right) \right](T, s)$$

The equations for two-dimensional flow are obtained by integration of the equations over depth.

Heat exchange with the atmosphere is also included.

Symbol list

t	time
x, y, z	Cartesian coordinates
u, v, w	flow velocity components
T, s	temperature and salinity
D_v	vertical turbulent (eddy) diffusion coefficient
$\hat{H}$	source term due to heat exchange with atmosphere
S	magnitude of discharge due to point sources
T_s, s_s	temperature and salinity of source
F_T, F_s, F_c	horizontal diffusion terms
D_h	horizontal diffusion coefficient
h	depth

Solution Technique

The spatial discretisation of the primitive equations is performed using a cell-centred finite volume method. The spatial domain is discretised by subdivision of the continuum into non-overlapping elements/cells.

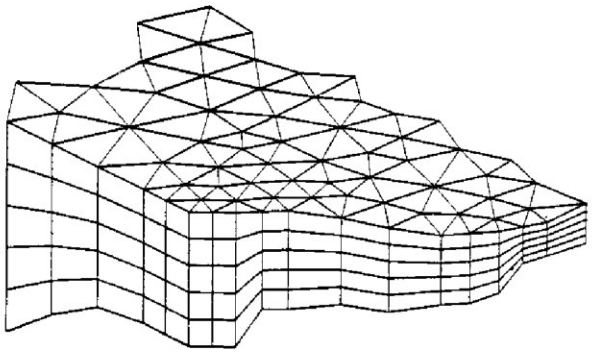

Principle of 3D mesh

In the horizontal plane an unstructured mesh is used while a structured mesh is used in the vertical domain of the 3D model. In the 2D model the elements can be triangles or quadrilateral elements. In the 3D model the elements can be prisms or bricks whose horizontal faces are triangles and quadrilateral elements, respectively.

Model Input

Input data can be divided into the following groups:

- Domain and time parameters:
  - computational mesh (the coordinate type is defined in the computational mesh file) and bathymetry
  - simulation length and overall time step
- Calibration factors
  - bed resistance
  - momentum dispersion coefficients
  - wind friction factors
- Initial conditions
  - water surface level
  - velocity components
- Boundary conditions
  - closed
  - water level
  - discharge
- Other driving forces
  - wind speed and direction
  - tide
  - source/sink discharge
  - wave radiation stresses

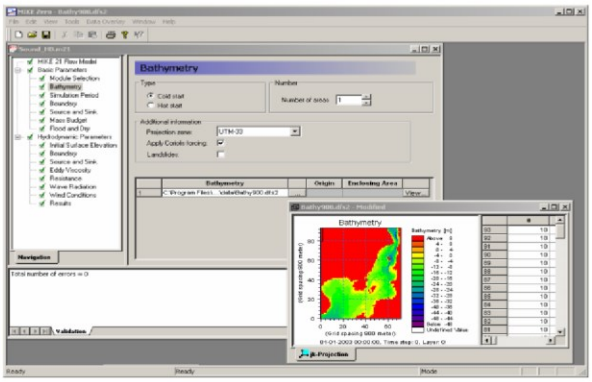

View button on all the GUIs in MIKE 21 & MIKE 3 FM HD for graphical view of input and output files

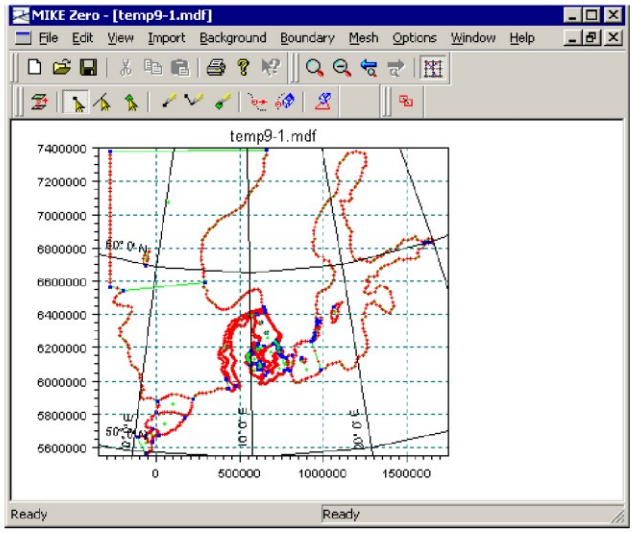

The Mesh Generator is an efficient MIKE Zero tool for the generation and handling of unstructured meshes, including the definition and editing of boundaries

Providing MIKE 21 & MIKE 3 Flow Model FM with a suitable mesh is essential for obtaining reliable results from the models. Setting up the mesh includes the appropriate selection of the area to be modelled, adequate resolution of the bathymetry, flow, wind and wave fields under consideration and definition of codes for defining boundaries.

2D visualization of a computational mesh (Odense Estuary)

Bathymetric values for the mesh generation can e.g. be obtained from the MIKE by DHI product MIKE C-Map. MIKE C-Map is an efficient tool for extracting depth data and predicted tidal elevation from the world-wide Electronic Chart Database CM-93 Edition 3.0 from Jeppesen Norway.

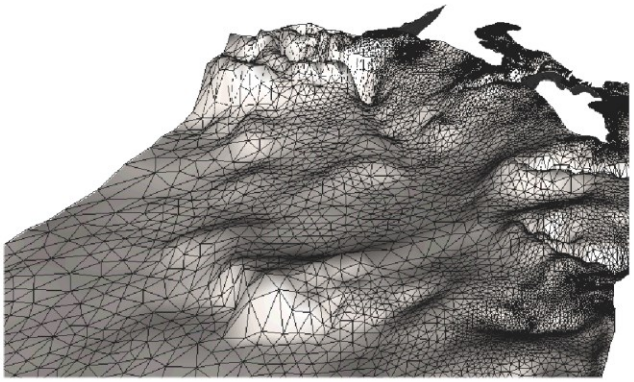

3D visualization of a computational mesh

If wind data is not available from an atmospheric meteorological model, the wind fields (e.g. cyclones) can be determined by using the wind-generating programs available in MIKE 21 Toolbox.

Global winds (pressure & wind data) can be downloaded for immediate use in your simulation. The sources of data are from GFS courtesy of NCEP, NOAA. By specifying the location, orientation and grid dimensions, the data is returned to you in the correct format as a spatial varying grid series or a time series. The link is:

www.mikebydhi.com/Download/DocumentsAndTools/Tools/AvailableData.aspx

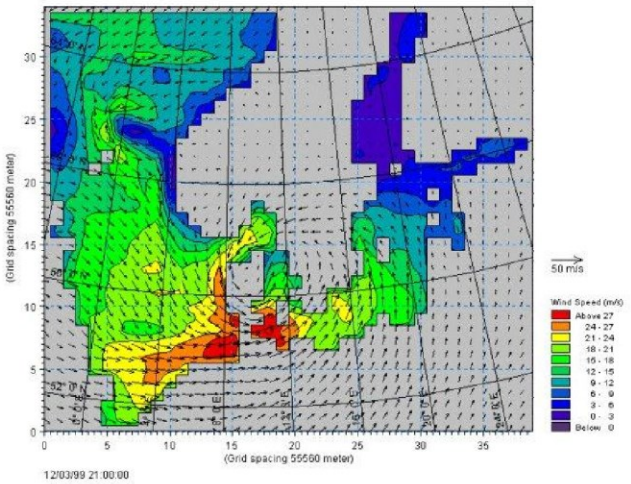

The chart shows a hindcast wind field in the North Sea and Baltic Sea as wind speed and wind direction

Model Output

Computed output results at each mesh element and for each time step consist of:

- Basic variables
  - water depth and surface elevation
  - flux densities in main directions
  - velocities in main directions
  - densities, temperatures and salinities
- Additional variables
  - Current speed and direction
  - Wind velocities
  - Air pressure
  - Drag coefficient
  - Precipitation/evaporation
  - Courant/CFL number
  - Eddy viscosity
  - Element area/volume

The output results can be saved in defined points, lines and areas. In the case of 3D calculations the results are saved in a selection of layers.

Output from MIKE 21 & MIKE 3 Flow Model FM is typically post-processed using the Data Viewer available in the common MIKE Zero shell. The Data Viewer is a tool for analysis and visualization of unstructured data, e.g. to view meshes, spectra, bathymetries, results files of different format with graphical extraction of time series and line series from plan view and import of graphical overlays.

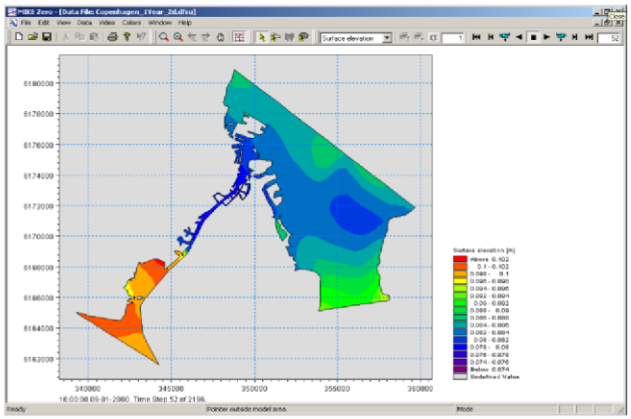

The Data Viewer in MIKE Zero – an efficient tool for analysis and visualization of unstructured data including processing of animations. Above screen dump shows surface elevations from a model setup covering Port of Copenhagen

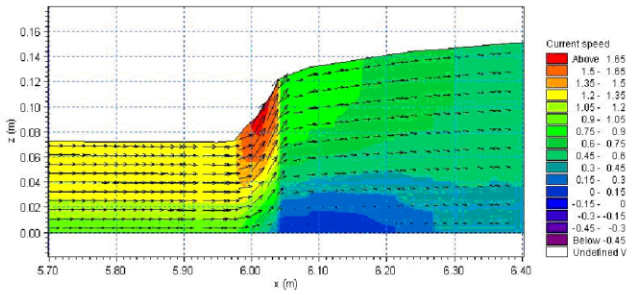

Vector and contour plot of current speed at a vertical profile defined along a line in Data Viewer in MIKE Zero

Validation

Prior to the first release of MIKE 21 & MIKE 3 Flow Model FM the model has successfully been applied to a number of rather basic idealized situations for which the results can be compared with analytical solutions or information from the literature.

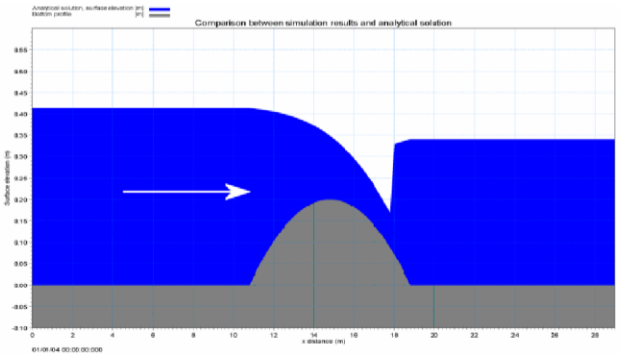

The domain is a channel with a parabola-shaped bump in the middle. The upstream (western) boundary is a constant flux and the downstream (eastern) boundary is a constant elevation. Below: the total depths for the stationary hydraulic jump at convergence. Red line: 2D setup, green line: 3D setup, black line: analytical solution

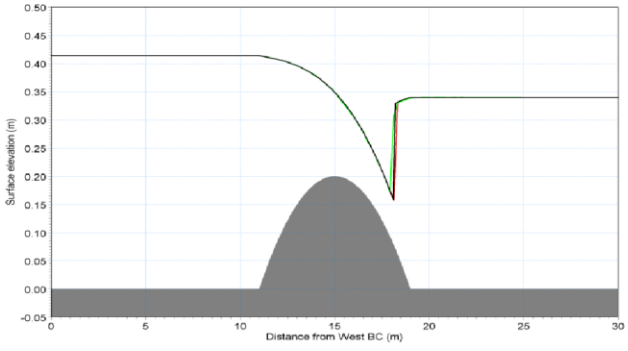

A dam-break flow in an L-shaped channel (a, b, c):

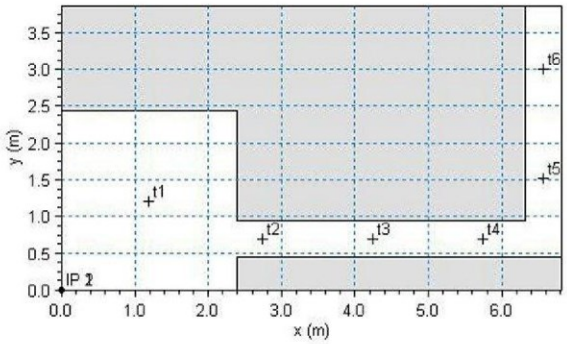

a) Outline of model setup showing the location of gauging points

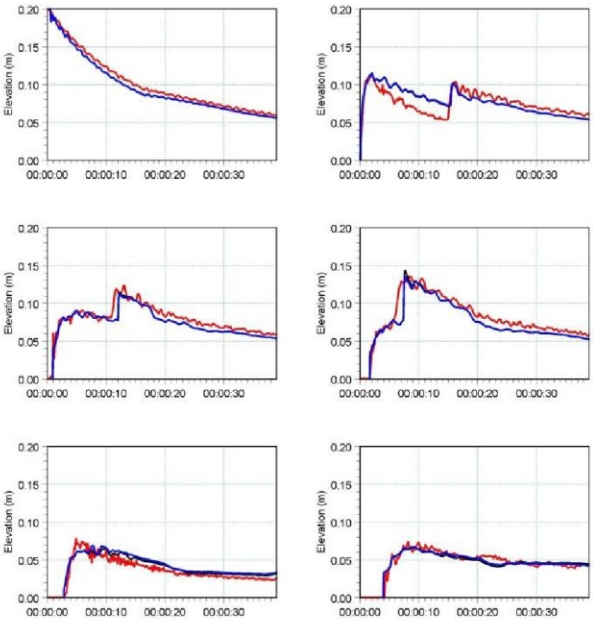

b) Comparison between simulated and measured water levels at the six gauge locations.
(Blue) coarse mesh (black) fine mesh and (red) measurements

The model has also been applied and tested in numerous natural geophysical conditions; ocean scale, inner shelves, estuaries, lakes and overland, which are more realistic and complicated than academic and laboratory tests.

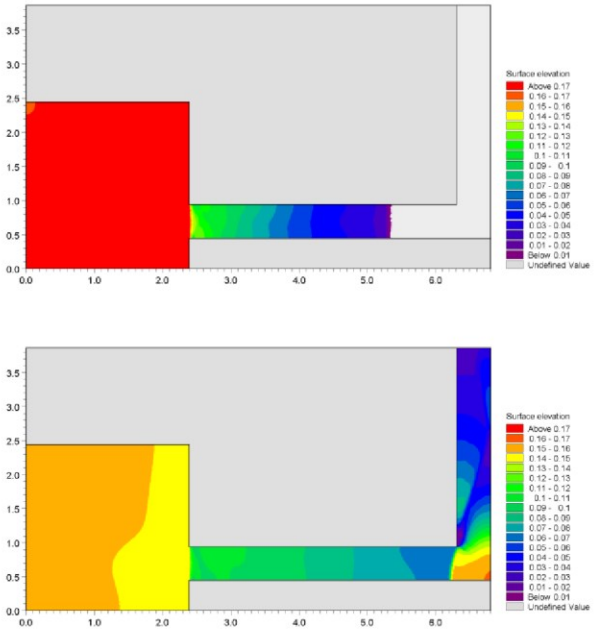

c) Contour plots of the surface elevation at T = 1.6 s (top) and T = 4.8 s (bottom)

Example from Ho Bay, a tidal estuary (barrier island coast) in South-West Denmark with access channel to the Port of Esbjerg. Below: Comparison between measured and simulated water levels

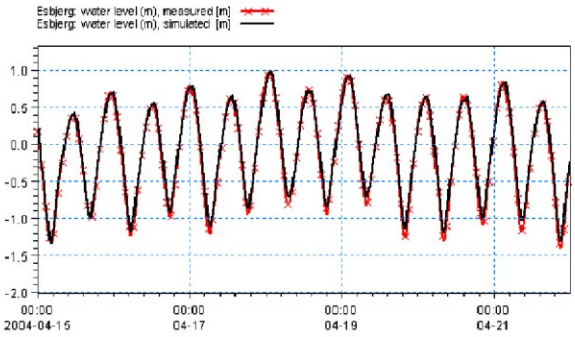

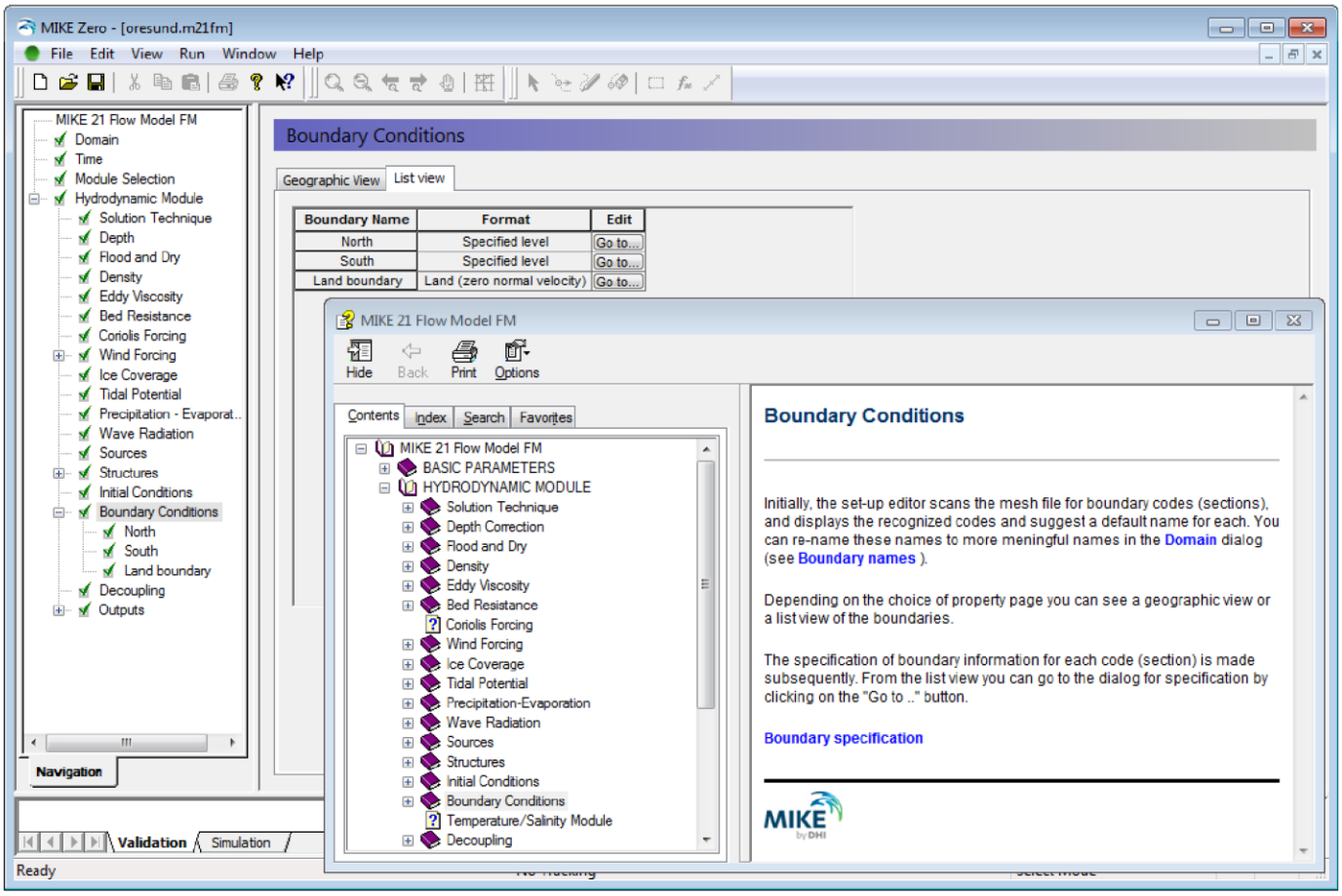

The user interface of the MIKE 21 and MIKE 3 Flow Model FM (Hydrodynamic Module), including an example of the extensive Online Help system

Graphical User Interface

The MIKE 21 & MIKE 3 Flow Model FM Hydrodynamic Module is operated through a fully Windows integrated graphical user interface (GUI). Support is provided at each stage by an Online Help system.

The common MIKE Zero shell provides entries for common data file editors, plotting facilities and utilities such as the Mesh Generator and Data Viewer.

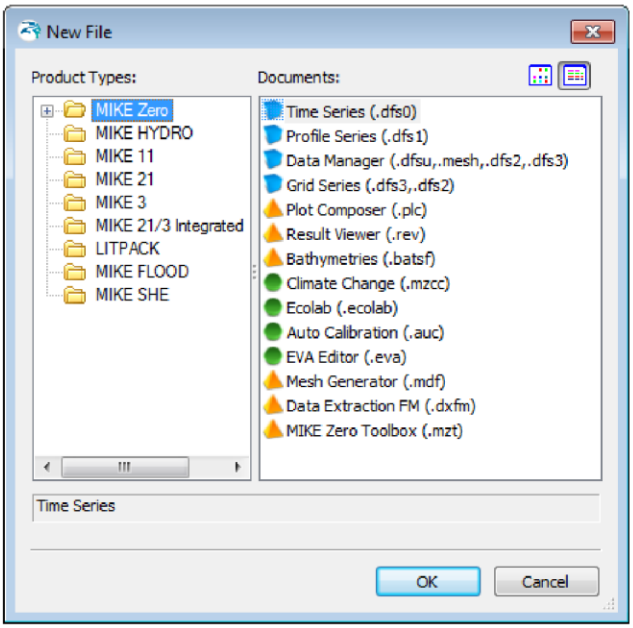

Overview of the common MIKE Zero utilities

Parallelisation

The computational engines of the MIKE 21/3 FM series are available in versions that have been parallelised using both shared memory (OpenMP) as well as distributed memory architecture (MPI). The result is much faster simulations on systems with many cores.

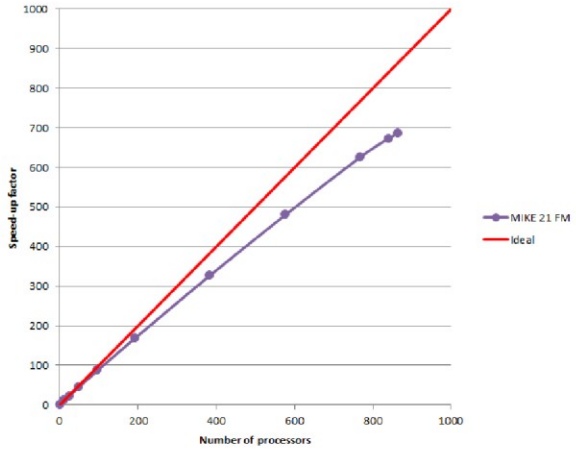

MIKE 21 FM speed-up using a HPC Cluster for Release 2012 with distributed memory architecture (purple)

Hardware and Operating System Requirements

Release 2012 version of the MIKE 21 and MIKE 3 Flow Model FM Hydrodynamic Module supports Microsoft Windows XP Professional Edition (32 and 64 bit), Microsoft Windows Vista Business (32 and 64 bit) and Microsoft Windows 7 Enterprise (32 and 64 bit). Release 2014 version will only support Microsoft Windows 7 Professional SP1 (32 and 64 bit) and Microsoft Windows 8 Professional (64 bit). Microsoft Internet Explorer 6.0 (or higher) is required for network license management as well as for accessing the Online Help.

The recommended minimum hardware requirements for executing MIKE 21 & MIKE 3 Flow Model FM Hydrodynamic Module are:

Processor:	3 GHz PC (or higher)
Memory (RAM):	4 GB (or higher)
Hard disk:	160 GB (or higher)
Monitor:	SVGA, resolution 1024x768
Graphic card:	64 MB RAM (or higher), 32 bit true colour
Media:	DVD drive compatible with dual layer DVDs

Support

News about new features, applications, papers, updates, patches, etc. are available here:

www.mikebydhi.com/Download/DocumentsAndTools.aspx

For further information on MIKE 21 & MIKE 3 Flow Model FM software, please contact your local DHI office or the Software Support Centre:

MIKE by DHI
DHI
Agern Allé 5
DK-2970 Hørsholm
Denmark

Tel: +45 4516 9333
Fax: +45 4516 9292

www.mikebydhi.com
mikebydhi@dhigroup.com

Documentation

The MIKE 21 & MIKE 3 Flow Model FM modules are provided with comprehensive user guides, online help, scientific documentation, application examples and step-by-step training examples.

References

Petersen, N.H., Rasch, P. “Modelling of the Asian Tsunami off the Coast of Northern Sumatra”, presented at the 3rd Asia-Pacific DHI Software Conference in Kuala Lumpur, Malaysia, 21-22 February, 2005

French, B. and Kerper, D. Salinity Control as a Mitigation Strategy for Habitat Improvement of Impacted Estuaries. 7th Annual EPA Wetlands Workshop, NJ, USA 2004.

DHI Note, “Flood Plain Modelling using unstructured Finite Volume Technique” January 2004 – download from

www.mikebydhi.com/Download/DocumentsAndTools/PapersAndDocs/Hydrodynamics.aspx

A.3 Sediment transport modelling using MIKE21 MT

MIKE 21 & MIKE 3 FLOW MODEL FM

Mud Transport Module

Short Description

Agern Allé 5
DK-2970 Hørsholm
Denmark

Tel: +45 4516 9200
Support: +45 4516 9333
Fax: +45 4516 9292

E-mail: software@dhigroup.com
Web: www.dhigroup.com

WATER • ENVIRONMENT • HEALTH

MIKE213_MT_FM_ShortDescription_.doc/AJS/HKH/ULU/KAE/2007Short_Descriptions.lsm/2007-11-19

MIKE 21 & MIKE 3 Flow Model FM – Mud Transport Module

This document describes the Mud Transport Module (MT) under the new comprehensive modelling system for two- and three-dimensional flows, the Flexible Mesh series, developed by DHI.

The MT module includes a state-of-the-art mud transport model that simulates the erosion, transport, settling and deposition of cohesive sediment in marine, brackish and freshwater areas. The module also takes into account fine-grained non-cohesive material.

Example of spreading of dredged material in Øresund, Denmark

The MT module is an add-on module to MIKE 21 & MIKE 3 Flow Model FM. It requires a coupling to the hydrodynamic solver and to the transport solver for passive components (Advection Dispersion module). The hydrodynamic basis is obtained with the MIKE 21 or MIKE 3 FM HD module. The influence of waves on the erosion/deposition patterns can be included by applying the Spectral Wave module, MIKE 21 FM SW.

With the FM series it is possible to combine and run the modules dynamically. If the morphological changes within the area of interest are within the same order of magnitude as the variation in the water depth, then it is possible to take the morphological impact on the hydrodynamics into consideration. This option for dynamic feedback between update of seabed and flow may be relevant to apply in shallow areas, for example, where long term effects are being considered. Furthermore it may be relevant in shallow areas where capital or considerable maintenance dredging is planned and similarly at sites where disposal of the dredged material takes place.

Example of sediment plume from a river near Malmö, Sweden

Application Areas

The MT module is used in a variety of cases where the erosion, dispersion, and deposition of cohesive sediments are of interest. Fine-grained sediment may cause impacts in different ways. In suspension, the fines may shadow areas over a

time span, which can be critical for the survival of light-depending benthic fauna and flora. The fine-grained sediment may deposit in areas where deposition is unwanted, for instance in harbour inlets. Furthermore, pollutants such as heavy metals and TBT are prone to adhere to the cohesive sediment. If polluted sediment is deposited in ecologically sensitive areas it may heavily affect local flora and fauna and water quality in general.

Example of resuspension in the nearshore zone. Caravelas, Brazil. Assessment of resuspension may be relevant in for example dredging projects to identify sources and levels of background turbidity

The estimation of siltation rates is an area where the MT module often is applied and also an important aspect to consider when designing new approach channels or deepening existing channels to allow access for larger vessels to the ports. Simulations of fine-grained sediment dynamics may contribute to optimise the design with regard to navigation and manoeuvrability on one hand and minimising the need for maintenance dredging on the other.

The MT module has many application areas and some of the most frequently used are listed below:

- Dispersion of dredged material
- Optimisation of dredging operations
- Siltation of harbours
- Siltation in access channels
- Cohesive sediment dynamics and morphology
- Dispersion of river plumes
- Erosion of fine-grained material under combined waves and currents
- Studies of dynamics of contaminated sediments

Example of muddy estuary. Caravelas, Brazil

Computational Features

The main features of the MIKE 21 & MIKE 3 Flow Model FM Mud Transport module are:

- Multiple sediment fractions
- Multiple bed layers
- Flocculation
- Hindered settling
- Inclusion of non-cohesive sediments
- Bed shear stress from combined currents and waves
- Waves included as wave database or 2D time series.
- Consolidation
- Morphological update of bed

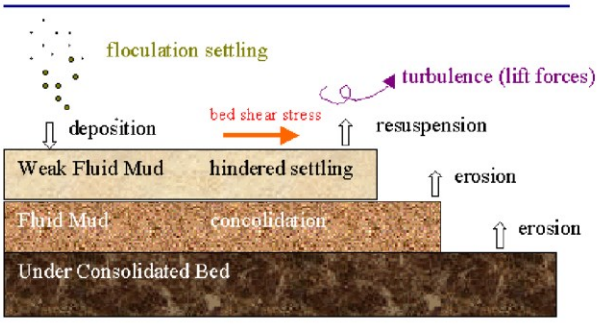

Example of modelled physical processes

Model Equations

The governing equations behind the MT module are essentially based on Mehta et al. (1989). The impact of waves is introduced through the bed shear stress.

The cohesive sediment transport module or mud transport (MT) module deals with the movement of mud in a fluid and the interaction between the mud and the bed.

The transport of the mud is generally described by the following equation (e.g. Teisson, 1991):

$$\frac{\partial c^i}{\partial t} + \frac{\partial u c^i}{\partial x} + \frac{\partial v c^i}{\partial y} + \frac{\partial w c^i}{\partial z} - \frac{\partial w_s c^i}{\partial z} =$$

$$\frac{\partial}{\partial x}\left(\frac{\upsilon_{Tx}}{\sigma^i_{Tx}}\frac{\partial c^i}{\partial x}\right) + \frac{\partial}{\partial y}\left(\frac{\upsilon_{Ty}}{\sigma^i_{Ty}}\frac{\partial c^i}{\partial y}\right) + \frac{\partial}{\partial z}\left(\frac{\upsilon_{Tz}}{\sigma^i_{Tz}}\frac{\partial c^i}{\partial z}\right) + S^i$$

Symbol list	
t	*time*
x, y, z:	*Cartesian co-ordinates*
u, v, w:	*flow velocity components*
D_v :	*vertical turbulent (eddy) diffusion coefficient*
c^i:	*the i'th scalar component (defined as the mass concentration)*
w_s^i:	*fall velocity*
σ_{Tx}^i :	*turbulent Schmidt number*
ν_{Tx} :	*anisotropic eddy viscosity*
S^i:	*source term*

The transport of the cohesive sediment is handled by a transport solver for passive components (AD-module). The settling velocity w_s is a sedimentological process and as such it is described separately with the extra term $\frac{\partial w_s c^i}{\partial z}$ using an operator splitting technique.

The bed interaction/update and the settling velocity terms are handled in the MT module.

The sedimentological effects on the fluid density and viscosity (concentrated near-bed suspensions) are not considered as part of the mud process module. Instead they are provided as separate sub-modules as they are only relevant for higher suspended sediment concentrations (SSC).

Mud plains in Loire river, France

Settling velocity

The settling velocity of the suspended sediment may be specified as a constant value. Flocculation is described as a relationship with the suspended sediment concentration as given in Burt (1986). Hindered settling can be applied if the suspended sediment concentration exceeds a certain level. To distinguish between three different settling regimes, two boundaries are defined, c_{floc} and $c_{hindered}$, being the concentrations where flocculation and hindered settling begins, respectively.

Constant settling velocity

Below a certain suspended sediment concentration the flocculation may be negligible and a constant settling velocity can be applied:

$$w_s = k \qquad c < c_{floc}$$

where w_s is the settling velocity and k is the constant.

Flocculation

After reaching c_{floc}, the sediment will begin to flocculate. Burt (1986) found the following relationship:

$$w_s = k \times \left(\frac{c}{\rho_{sediment}}\right)^{\gamma} \qquad c_{floc} > c > c_{hindered}$$

In which k is a constant, $\rho_{sediment}$ is the sediment density, and γ is a coefficient termed settling index.

Hindered settling

After a relatively high sediment concentration ($c_{hindered}$) is reached, the settling columns of flocs begin to interfere and hereby reducing the settling velocity. Formulations given by Richardson and Zaki (1954) and Winterwerp (1999) are implemented.

Deposition

The deposition is described as (Krone, 1962):

$$S_D = w_s c_b p_D$$

where w_s is the settling velocity of the suspended sediment (m s^{-1}), c_b is the suspended sediment concentration near the bed, and p_d is an expression of the probability of deposition:

$$p_d = 1 - \frac{\tau_b}{\tau_{cd}}$$

In the three-dimensional model, c_b is simply equal to the sediment concentration in the water cell just above the sediment bed.

In the two-dimensional model, two different approaches are available for computing c_b. If the Rouse profile is applied, the near bed sediment concentration is related to the depth averaged sediment concentration by multiplying with a constant centroid height:

$$c_b = \bar{c} \times (\text{centroid height})$$

Teeter (1986) related the near bed concentrations to the Peclet number (P_e), the bed fluxes, and the depth averaged suspended sediment concentrations. In this case, the near bed sediment concentration is described as:

$$c_b = \bar{c} \times \left(1 + \left(\frac{P_e}{1.25 + 4.75\left(p_d^{2.5}\right)}\right)\right)$$

where P_e is the Peclet number:

$$P_e = \frac{w_s h}{D_z}$$

where h is the water depth, D_z is the eddy diffusivity, both computed by the hydrodynamic model.

Erosion

Erosion features the following two modes.

Hard bed

For a consolidated bed the erosion rate can be written as (Partheniades, 1965):

$$S_E = E\left(\frac{\tau_b}{\tau_{ce}} - 1\right)^n \qquad \tau_b > \tau_c$$

Where E is the erodibility (kg m^{-2} s^{-1}), n is the power of erosion, τ_b is the bed shear stress (N m^{-2}) and τ_{ce} is the critical shear stress for erosion (N m^{-2}). S_E is the erosion rate (kg m^{-2} s^{-1}).

Soft bed

For a soft, partly consolidated bed the erosion rate can be written as (Parchure and Mehta, 1985):

$$S_E = E\left(e^{\alpha\sqrt{(\tau_b - \tau_c)}}\right) \qquad \tau_b > \tau_c$$

Consolidation

When long term simulations are performed consolidation of deposited sediment may be an important process. If several bed layers are used a transition rate (T_i) can be applied. This will cause sediment from the top layers to be transferred to the subsequently lower layers.

Solution Technique

The solution of the transport equations is closely linked to the solution of the hydrodynamic conditions.

The spatial discretisation of the primitive equations is performed using a cell-centred finite volume method. The spatial domain is discretised by subdivision of the continuum into non-overlapping elements/cells. In the horizontal plane an unstructured grid is used while in the vertical domain in the 3D model a structured mesh is used. In the 2D model the elements can be triangles or quadrilateral elements. In the 3D model the elements can be prisms or bricks whose horizontal faces are triangles and quadrilateral elements, respectively.

The time integration is performed using an explicit scheme.

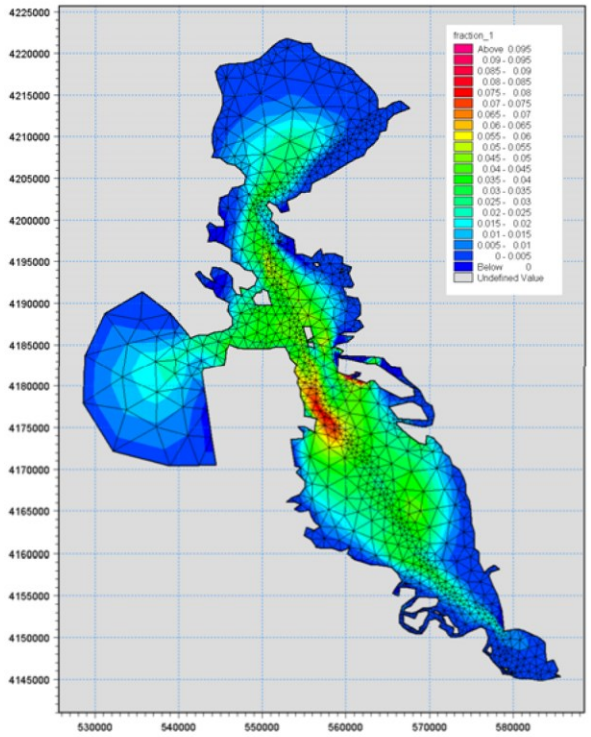

The MT module is a tool for estuary sediment management in complex estuaries like San Francisco bay, California, USA

Model Input

The generic nature of cohesive sediment dynamics reveals a numerical model that will always call for tremendous field work or calibration due to measurements performed. The following input parameters have to be given:

- Settling velocity
- Critical shear stress for erosion
- Critical shear stress for deposition
- Erosion coefficients
- Power of erosion
- Suspended sediment
- Concentration at open boundaries
- Dispersion coefficients
- Thickness of bed layers or estimate of total amount of active sediment in the system
- Transition coefficients between bed layers
- Dry density of bed layers

Model Output

The main output possibilities are listed below:

- Suspended sediment concentrations in space and time
- Sediment in bed layers given as masses or heights
- Net sedimentation rates
- Computed bed shear stress
- Computed settling velocities
- Updated bathymetry

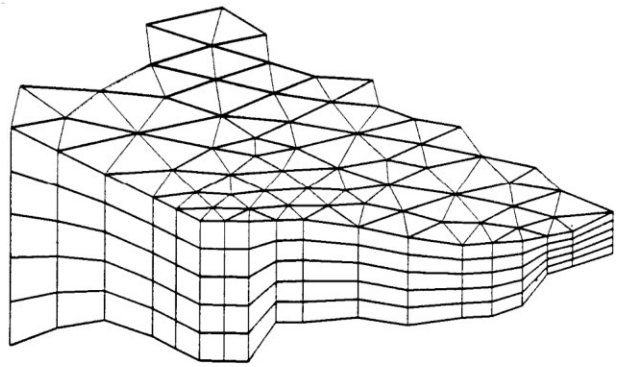

Principle of 3D mesh

Validation

The model engine is well proven in numerous studies throughout the world:

The Rio Grande estuary, Brazil

In 2001, the model was applied for a 3D study in the Rio Grande estuary (Brazil). The study focused on a number of hydrodynamic issues related to changing the Rio Grande Port layout. In addition the possible changes in sedimentation patterns and dredging requirements were investigated.

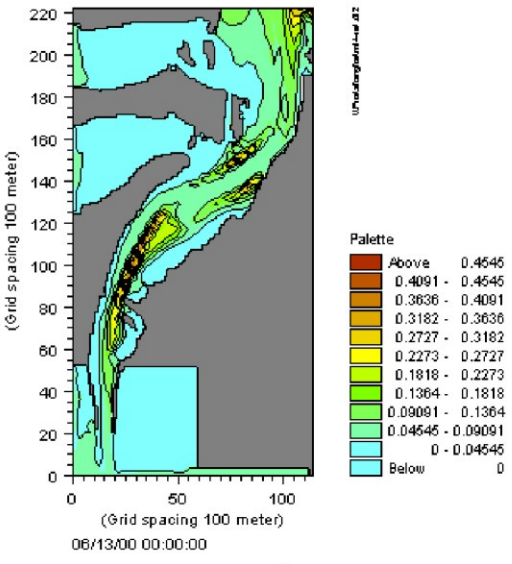

SSC in surface layer (kg/m^3), Rio Grande, Brazil

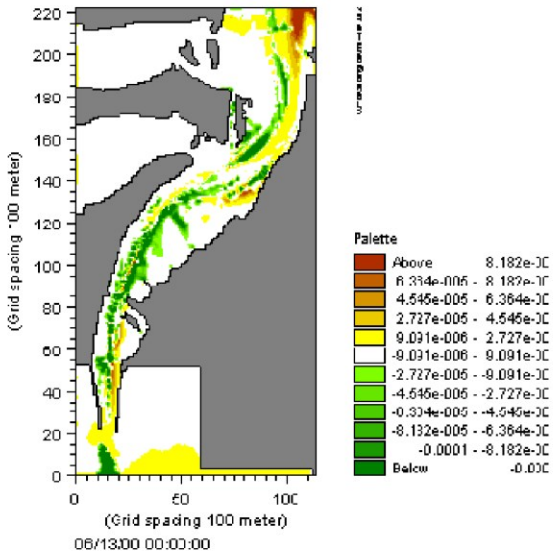

Instantaneous erosion (kg/m^2/s), Rio Grande, Brazil

The figure below shows the most common calibration parameter, which is the suspended sediment concentration (SSC). The results are reasonable given the large uncertainties connected with mud transport modelling.

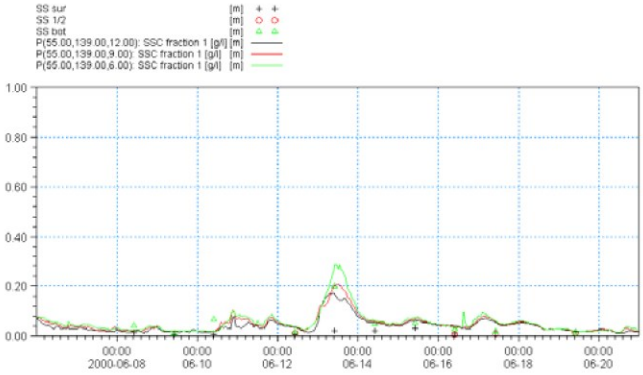

Suspended sediment concentrations, Rio Grande, Brazil

The Graadyb tidal inlet, Denmark

The MT module has also been used in the Graadyb tidal inlet located in the Danish part of the Wadden Sea. In this area, the highest tidal range reaches 1.7 m at springs, but the storm surge in the area can be as high as 2-4 metres.

The maximum current in the navigation channel leading to the harbour of Esbjerg is in the range of 1-2 m/s. The depth in the channel is 10-12 m at mean sea level.

Graadyb tidal inlet (Skallingen), Denmark

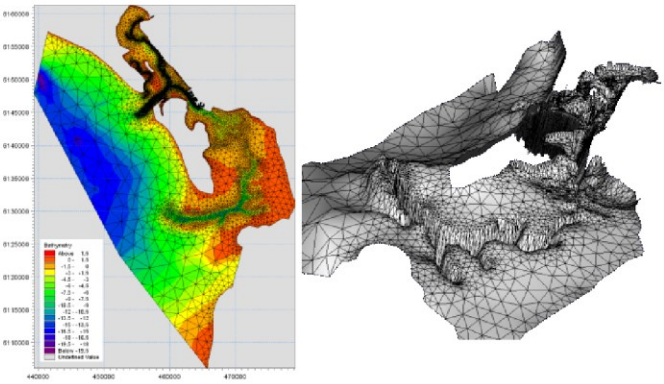

Bathymetry and computational mesh for the Graadyb tidal inlet, Denmark

A comparison between measured and simulated SSC time series is shown below. The overall comparison is excellent.

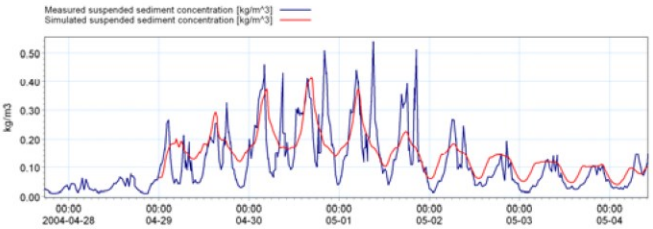

Comparison between measured and simulated suspended sediment concentrations, Graadyb tidal inlet, Denmark

Graphical User Interface

The MIKE 21 & MIKE 3 Flow Model FM, Mud Transport module is operated through a fully Windows integrated Graphical User Interface (GUI). Support is provided at each stage by an Online Help System. The common MIKE Zero shell provides entries for common data file editors, plotting facilities and a toolbox for/utilities as the Mesh Generator, the Data Viewer and the Data Manager.

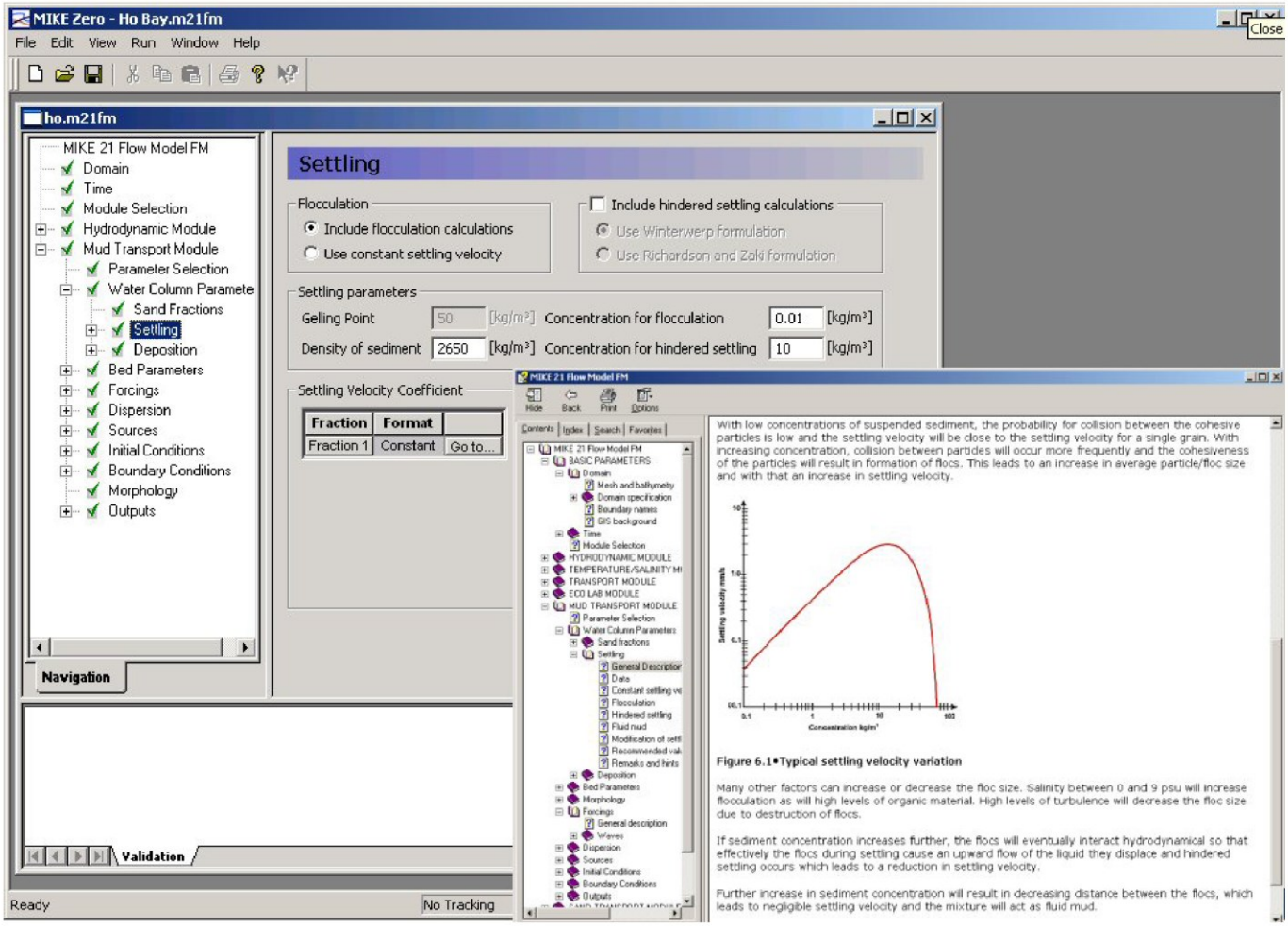

The graphical user interface of the MIKE 21 & MIKE 3 Flow Model FM MT module including an example of the Online Help

Hardware and Operating System Requirements

The MIKE 21 & MIKE 3 Flow Model FM Mud Transport Module supports Microsoft Windows XP and Microsoft Windows Vista. Microsoft Internet Explorer 5.0 (or higher) is required for network license management as well as for accessing the Online Help.

The recommended minimum hardware requirements for executing MIKE 21 & MIKE 3 Flow Model FM Mud Transport Module are:

Processor:	2 GHz PC (or higher)
Memory (RAM):	1 GB (or higher)
Hard disk:	40 GB (or higher)
Monitor:	SVGA, resolution 1024x768
Graphic card:	32 MB RAM (or higher), 24 bit true colour
Media:	CD-ROM/DVD drive, 20 x speed (or higher)

Support

News about new features, applications, papers, updates, patches, etc. are available here:

http://www.dhigroup.com/Software/Download/DocumentsAndTools.aspx

For further information on MIKE 21 & MIKE 3 Flow Model FM software, please contact your local DHI agent or the Software Support Centre:

Software Support Centre
DHI
Agern Allé 5
DK-2970 Hørsholm
Denmark
Tel: +45 4516 9333
Fax: +45 4516 9292
http://dhigroup.com/Software.aspx
software@dhigroup.com

References

Burt, N., 1986. Field settling velocities of estuary muds. In: Estuarine Cohesive Sediment Dynamics, edited by Mehta, A.J. Springer-Verlag, Berlin, Heidelberg, NewYork, Tokyo, 126–150.

Krone, R.B., 1962. Flume Studies of the Transport of Sediment in Estuarine Shoaling Processes. Final Report to San Francisco District U. S. Army Corps of Engineers, Washington D.C.

Mehta, A.J., Hayter, E.J., Parker, W.R., Krone, R.B. and Teeter, A.M., 1989. Cohesive sediment transport. I: Process description. Journal of Hydraulic Engineering – ASCE 115 (8), 1076–1093.

Parchure, T.M. and Mehta, A.J., 1985. Erosion of soft cohesive sediment deposits. Journal of Hydraulic Engineering – ASCE 111 (10), 1308–1326.

Partheniades, E., 1965. Erosion and deposition of cohesive soils. Journal of the hydraulics division Proceedings of the ASCE 91 (HY1), 105–139.

Richardson, J.F and Zaki, W.N., 1954. Sedimentation and fluidization, Part I, Transactions of the institution Chemical Engineers 32, 35–53.

Teeter, A.M., 1986. Vertical transport in fine-grained suspension and newly deposited sediment. In: Estuarine Cohesive Sediment Dynamics, edited by Mehta, A.J. Springer-Verlag, Berlin, Heidelberg, NewYork, Tokyo, 170–191.

Teisson, C., 1991. Cohesive suspended sediment transport: feasibility and limitations of numerical modelling. Journal of Hydraulic Research 29 (6), 755–769.

Winterwerp, J.C. (1999) "Flocculation and settling velocity", TU delft. pp 10-17.

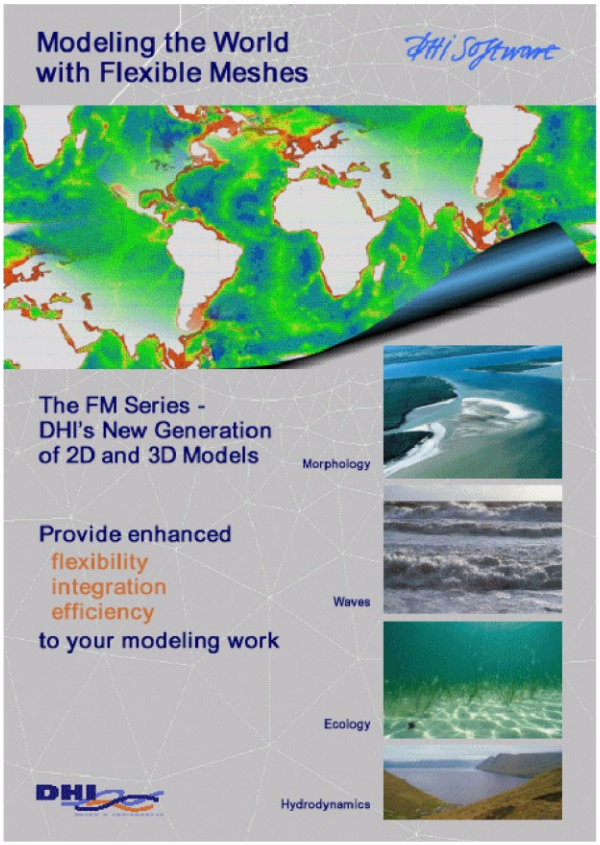

References on applications

Edelvang, K., Lund-Hansen, L.C., Christiansen, C., Petersen, O.S., Uhrenholdt, T., Laima, M. and Berastegui, D.A., 2002. Modelling of suspended matter transport from the Oder River. Journal of Coastal Research 18 (1), 62–74.

Lumborg, U., Andersen, T.J. and Pejrup, M., 2006. The effect of *Hydrobia ulvae* and microphytobenthos on cohesive sediment dynamics on an intertidal mudflat described by means of numerical modelling. Estuarine, Coastal and Shelf Science 68 (1-2), 208–220.

Lumborg, U. and Pejrup, M., 2005. Modelling of cohesive sediment transport in a tidal lagoon – An annual budget. Marine Geology 218 (1-4), 1–16.

Petersen, O. and Vested, H.J., 2002. Description of vertical exchange processes in numerical mud transport modelling. In: Fine Sediment Dynamics in the Marine Environment, edited by Winterwerp, J.C. and Kranenburg, C. Elsevier, Amsterdam, 375–391.

Petersen, O., Vested, H.J., Manning, A.J., Christie, M. and Dyer, K., 2002. Numerical modelling of mud transport processes in the Tamar Estuary. In: Fine Sediment Dynamics in the Marine Environment, edited by Winterwerp, J.C. and Kranenburg, C. Elsevier, Amsterdam, 643–654.

Valeur, J.R., 2004. Sediment investigations connected with the building of the Øresund bridge and tunnel. Danish Journal of Geography 104 (2), 1–12.

A.4 DMI-HIRLAM (DMI's weather model)

The goal of the HIRLAM (High Resolution Limited Area Model) forecasting system is to analyse and forecast small-scale variability in the atmosphere with high precision. To make this possible, many ingredients are required: At first observational data from the atmosphere are pre-processed for the data-assimilation. Many types of observational data are used, e.g., data from radio sondes measuring vertical profiles of basic meteorological variables, surface observations from land and sea, air craft measurements and many data from satellites used in the analysis of the atmospheric state.

An advanced data-assimilation system has been developed specifically for operational use (e.g. Gustafsson et al., 2012).The data combines information from observations with a model state from the forecast model in order to produce an optimal description of the atmosphere. The forecast model is based on the equations of motion governing atmospheric flow and a comprehensive set of parameterisations describing the physical processes of the atmosphere, e.g. radiation, turbulence, surface fluxes of heat, moisture and momentum, and cloud processes including precipitation (e.g., Unden et al., 2002). Figure A.1 shows the different model domains of DMI-HIRLAM. The HIRLAM system T15 has a horizontal resolution of 15 km and is using hourly lateral boundary information from the ECMWF global model. ECMWF (European Centre for Medium range Weather Forecasts) is the world leading model system for global weather forecasts. The DMI-HIRLAM systems K05 and SKA receive lateral boundary conditions from T15 and have horizontal resolutions of 5 km and 3 km, respectively.

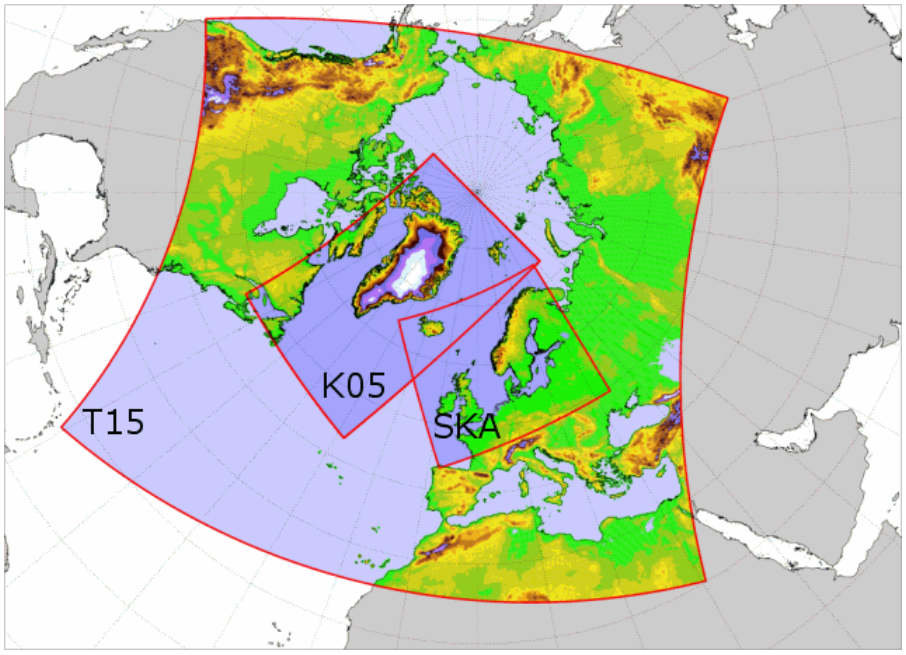

Figure A.1 DMI-HIRLAM model domains: SKA 3 km grid, K05 5 km grid and T15 15 km grid.

DMI has a long record of operational verification quantifying significant quality improvements over the years. The model is subject to extensive validation and verification.

A.5 DMI-WAM (DMI's surface wave model)

DMI's operational ocean surface wave model DMI-WAM is based on the third generation spectral wave model WAM Cycle 4.5 (WAMDI Group, 1988; Günther et al., 1992; Komen et al., 1994). WAM is an acronym for WAve prediction Model and is maintained by the Helmholz- Zentrum Geesthacht in Germany. WAM computes the directional wave energy spectrum. From this, wave parameters (height, period, direction) are derived. The wave parameters are computed for total sea, for wind sea and for swell.

The energy source is the surface wind which is obtained from DMI-HIRLAM. The sink terms are wave energy dissipation through wave breaking (white capping), wave breaking in shallow seas (depth-induced wave breaking) and friction against the sea bed. DMI-WAM includes non-linear wave interaction which accounts for the redistribution of wave energy across wave periods. DMI-WAM includes effects of sea ice where present. The model is continually updated to include the latest results of research.

DMI-WAM is running operationally four times a day to produce five day forecasts. Model output is produced with hourly resolution. At present, DMI-WAM has five geographical domains which are coupled (nested) so that swells generated far away are included into regions where their effect may be of importance. The full wave energy spectrum is transferred along the model domain interfaces. The geographical domains are: the North Atlantic, the North Sea and Baltic Sea, the inner Danish waters (Figure A.2), besides the Mediterranean Sea and the Red Sea. The spatial resolution of the North Atlantic model domain is 0.5 degrees (around 55 km), of the western part of the North Sea the resolution is about 10 km, and in the eastern part of the North Sea, including the inner Danish waters and eastern Baltic Sea (including the area around Bornholm), the resolution is 1.85 km. The model describes wind waves with periods ranging from 1.25 to 24 seconds and within 24 compass directions.

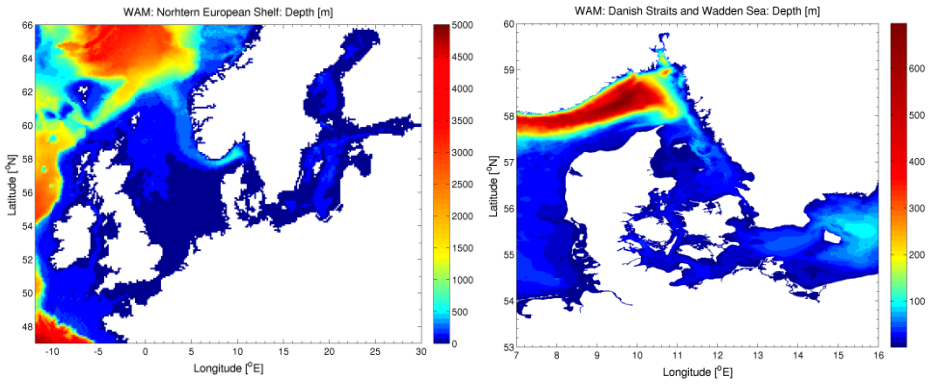

Figure A.2 *Left: WAM model domain with coarse resolution of 10 and 55 km . Right: WAM model with high resolution of 1.85 km.*

DMI-WAM is validated on a regular basis against other operational wave forecasting systems and observations.

A.6 HBM (DMI's hydrodynamic model)

DMI's operational hydrodynamic model is based on the 3D model HBM (HIROMB-BOOS-Model[9]). The origin of the HBM code dates back to the BSHcmod hydrodynamic model (Dick et al., 2001), the development of which was initiated in the 1990'es at Bundesamt für Seeschifffahrt und Hydrographie (BSH) in Germany. HBM is managed by DMI and is developed in a consortium with DMI, BSH and other Baltic Sea operational centres (Berg and Poulsen, 2012; Poulsen and Berg, 2012).

The vertical dynamics in the model assumes hydrostatic balance and incompressibility of sea water. Horizontal dynamics is modelled using the Boussinesq approximation. Higher order contributions to the dynamics are parameterised following Smagorinsky (1963) in the horizontal direction and a higher-order turbulence closure scheme in the vertical (Berg, 2012) which includes both the effects of breaking surface waves (Craig and Banner, 1994) and internal waves (Axell, 2002).

The model is two-way coupled with a sea ice model that handles both ice dynamics and thermodynamics (Dick et al., 2001). The model is further coupled to an ecosystem model (e.g., Wan et al., 2011; Wan et al., 2012; Wan et al., 2013) and to an oil drift and fate module. The system used in this study has a horizontal grid spacing of 3 nm (5.6 km) in the western part of the North Sea, 1 nm (1.85 km) in the eastern part of the North Sea including the Wadden Sea and Skagerrak, 0.5 nm (0.93 km) in inner Danish waters and the western Baltic Sea (including the area around Bornholm). The eastern Baltic Sea is resolved with a grid resolution of 1 nm (1.85 km) (Figure A.3). In the vertical the model has up to 122 levels. Top-layer thickness is 2 m. Below the top-layer and to a depth of 100 m the layer-thickness is 1 m. Layer thickness increases gradually to 40 m between 100 m and the deepest part in the model domain.

[9] HIROMB is an abbreviation for High Resolution Oceanographic Model for the Baltic. BOOS stands for the Baltic Operational Oceanographic System.

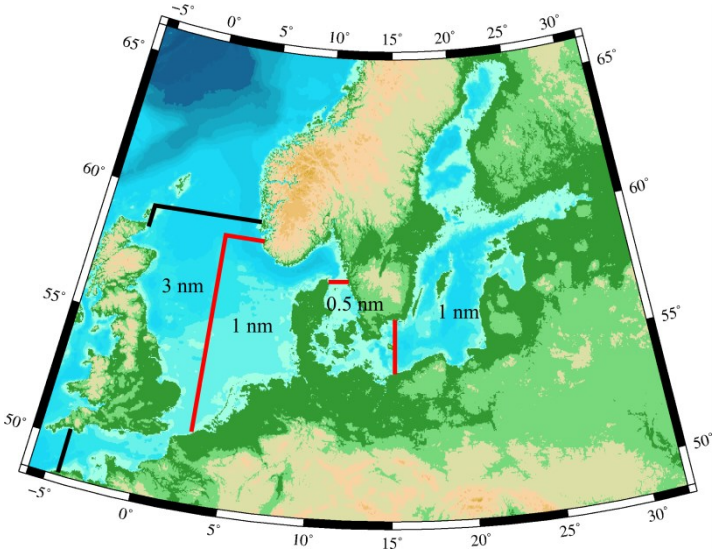

Figure A.3 *HBM model domain. Open model boundaries are located between Scotland and Norway and in the English Channel (black lines). Along the open model boundaries the model is coupled to a model of the North Atlantic. Two-way nested domains are indicated in the figure, bounded by the red lines. See text for further details.*

At open model boundaries between Scotland and Norway and in the English Channel, tides composed of the 17 major constituents and pre-calculated surges of DMI's North Atlantic Model (NOAMOD) (Dick et al., 2001) is applied. In this way, large scale features generated far away from the North Sea but which may be of importance for the local circulation is included.

Freshwater runoff in the model is obtained from 79 major rivers in the region. At the sea surface, the model is forced with winds, atmospheric pressure and heat flux obtained from DMI-HIRLAM. The model allows for 3D-variational data-assimilation (Fu et al., 2011a; Fu et al., 2011b; Fu et al., 2012; Zhang et al., 2011) of both surface (e.g., satellite derived sea surface temperature and sea level) and profile data (e.g., temperature, salinity, nutrients) The model is validated on a regular basis – both in real time and in hindcast see [ref. /24/].

References

Axell, L. B., 2002. Wind-driven internal waves and Langmuir circulations in a numerical model of the southern Baltic Sea. J. Geophys. Res. 107, C11, 3204.

Berg, P., 2012. Mixing in HBM. Scientific Report 12-03, Danish Meteorological Institute, pp. 21, http://www.dmi.dk/dmi/sr12-03.pdf.

Berg P. and J. W. Poulsen, 2012. Implementation details for HBM. Technical Report 12-11, Danish Meteorological Institute, pp. 149, http://www.dmi.dk/dmi/tr12-11.pdf.

Craig, P. D. and M. L. Banner, 1994. Modelling Wave-Enhanced Turbulence in the Ocean Surface Layer. J. Phys. Ocean. 24, 2546-2559.

Dick S., E. Kleine and S. Müller-Navarra, 2001. The operational circulation model of BSH (BSH cmod). Model description and validation. Berichte des Bundesamtes für Seeschifffahrt und Hydrographie. 29/2001. Hamburg, Germany, 48 pp.

Fu W., J. L. Høyer and J. She, 2011a. Assessment of the three dimensional temperature and salinity observational networks in the Baltic Sea and North Sea. Ocean Science, 7, 75-90.

Fu W., J. She and S. Zhuang, 2011b. Application of an Ensemble Optimal Interpolation in a North/Baltic Sea model: Assimilating temperature and salinity profiles. Ocean Modelling, 40, 227-245.

Fu W., J. She and M. Dobrynin, 2012. A 20-year reanalysis experiment in the Baltic Sea using three-dimensional variational (3DVAR) method. Ocean Science, 8, 827-844.

Gustafsson, N., X-Y. Huang, X. Yang, K. Mogensen, M. Lindskog, O. Vignes, T. Wilhelmsson and S. Thorsteinsson, 2012. Four-dimensional variational data assimilation for a limited area model. Tellus A, 64 , 14985.

Günther, H., S. Hasselmann and P.A.E.M. Janssen, 1991. Wamodel cycle 4. DKRZ report no. 4, Hamburg, http://www.mad.zmaw.de/fileadmin/extern/documents/reports/ReportNo.04.pdf.

Komen,G.J., L.Cavaleri, M.Donelan, K.Hasselmann, S.Hasselmann, and P.A.E.M.Janssen, 1994.Dynamics and Modelling of Ocean Waves.Cambridge University Press, 532 pp.

Poulsen, J. W. and P. Berg, 2012. More details on HBM - general modelling theory and survey of recent studies. Technical Report 12-16, Danish Meteoro-logical Institute, pp. 115, http://www.dmi.dk/dmi/tr12-16.pdf.

Sass B. H. and X. Yang, 2013. Verifi cation score for high resolution NWP:Idealized and preoperational tests. HIRLAM Technical Report, 69, 2012. 29 pp.

http://www.hirlam.org/index.php?option=com_docman&task=doc_download&gid=1429&Itemid=70

Smagorinsky, J., 1963. General circulation experiments with the primitive equations: I. The basic experiment. Monthly Weather Review, 91, 99 -164.

Undén, P., L. Rontu, H. Järvinen, P. Lynch, J. Calvo, G. Cats, J. Cuxart, K. Eerola, C. Fortelius, J. A. Garcia-Moya, C. Jones, G. Lenderlink, A. McDonald, R. McGrath, B. Navascues, N. Woetman Nielsen, V. ¬degaard, E. Rodriguez, M. Rummukainen, R. Rõõm, K. Sattler, B. H. Sass, H. Savijärvi, B. Wichers Schreur, R. Sigg, H. The and A. Tijm, 2002. HIRLAM-5 Scientific Documentation. HIRLAM Scientific Report, 2002, 146 pp.
http://hirlam.org/index.php?option=com_docman&task=doc_download&gid=270&Itemid=70

WAMDI Group (S. Hasselmann, K.Hasselmann, E.Bauer, P.A.E.M.Janssen, G.J.Komen, L.Bertotti, P.Lionello, A.Guillaume, V.C.Cardone, J.A.Greenwood, M.Reistad, L.Zambresky, J.A.Ewing), 1988.The WAM model – A third genera-tion wave prediction model,J. Phys.Oceanography., 18,1775-1810.

Wan, Z., L. Jonasson and H. Bi, 2011. N/P ratio of nutrient uptake in the Baltic Sea. Ocean Science, 7, 693 - 704.

Wan, Z., J. She, M. Maar, L. Jonasson, J. Baasch-Larsen, 2012. Assessment of a physical-biogeochemical coupled model system for operational service in the Baltic Sea. Ocean Science, 8, 683 - 701.

Wan, Z., H. Bi and J. She, 2013. Comparison of two light attenuation parame-terisaton focusing on timing of spring bloom and primary production in the Baltic Sea. Ecological Modelling, 259, 40 - 49.

Zhuang S. Y., W. Fu and J. She, 2011. A pre-operational three Dimensional variational data assimilation system in the North/Baltic Sea. Ocean Science, 7, 771-781.

On-line validation links etc.:

http://ocean.dmi.dk/validations/waves
http://ocean.dmi.dk/validations/surges
http://www.ecmwf.int/products/forecasts/d/charts/medium/verification/wave/intercomparison and select North Sea under the tab Area
http://ocean.dmi.dk/validations/surges/index.php
http://catalogue.myocean.eu.org/static/resources/myocean/quid/MYO2-BAL-QUID-003-006-007-V1.3.pdf
http://dmi.dk/hav/prognoser/havprognoser.
http://www.ecmwf.int/products/forecasts/d/charts/medium/verification/wave/intercomparison/

Appendix B Wave modelling

Wave modelling is performed with a high resolution MIKE 21 SW FM model. The model is forced with high resolution wind fields from the atmospheric DMI-HIRLAM model and with wave boundary conditions from the regional hindcast wave model DMI-WAM (See descriptions in Appendix A).

The wave model is used to study the influence of the offshore wind farm on the wave climate, and provides the basis for assessing the potential impact to the adjacent coastline and seabed morphology. Furthermore, the wave climate is implemented in the hydrodynamic modelling performed in MIKE 21 HD FM and sediment plume modelling performed in MIKE 21 MT FM.

Wave modelling for the two offshore wind farms Vesterhav Nord OWF and Vesterhav Syd OWF is performed in one model domain that covers both sites.

B.1 Data collection

Met-ocean data including water level and wave measurements have been collated from a variety of stations located near the Vesterhav Nord OWF, see Table B.1.

Table B.1 Data points in the vicinity of the OWF areas and details. See Figure 4.12 for location of data points.

Observation location name	Type of data	Time series		Data owner	Position (lat, lon)
		Start	End		
Hvidesande-1	Water level	01-01-2003	31-01-2014	DMI	8.128977; 56.000458
Hvidesande-2	Water level	01-01-2003	01-02-2014	DMI	8.1412; 56.0072
Fjaltring (Wave Rider)	Waves	01-01-2011	31-12-2012	ENDK	56.475; 8.048
Nymindgeb (Wave Rider)	Waves	01-01-2011	31-12-2012	ENDK	55.810; 7.941

In addition to the above measurements, synoptic wind and wave conditions from DMI regional model DMI-HIRLAM and DMI-WAM are used as forcing of the MIKE 21 SW FM wave model, see Table B.2.

Table B.2 Synoptic wind and wave data used in the wave modelling.

Synoptic dataset	Parameters	Time step	Resolution	Time series	
				Start	End
DMI-HIRLAM 2D wind	Wind components at z = 10 m (U, V) [m/s]	Δt=1 hr	0.03 ° (Δx = 1.9 km, Δx = 3.3 km)	01-01-2005	01-01-2013
DMI-WAM 1D waves along 4 open boundaries	Hm0 [m], Tp [s], MWD [°], DWD [°]	Δt=1 hr	~ Δx' =4.5-5 km	01-01-2005	01-01-2013

B.2 Model bathymetry

The model bathymetry is based on the following datasets:

- Project Area survey: Bathymetric survey performed by ESG International Ltd in October 2013. Resolution 5 x 5 m. The survey data has an approximate extent of 5 x 10 km covering the OWF area.
- Cable corridor survey: Bathymetric survey performed by ESG International Ltd in October 2013. Resolution 5 x 5 m. The survey covers the two cable corridors connecting Sejerø Bugt OWF to the shoreline.
- Other surveys: Danish Coastal Authorities (KDI) line and profile surveys from 2008-2013 within 8 km from the West Coast.
  Geo Technical Institute (GEO) line surveys conducted 10-20 km from shore in 2010.
- DK-Bathymetry from FRV (Danish Maritime Safety Administration): 50 x 50 m bathymetry of the Danish waters.

The model domain is divided into several zones with different resolution. A coarse mesh is used in the offshore regions near the model boundaries and a gradually finer mesh in the vicinity of the project site. The spatial resolution of the mesh varies from an average element size of ~4,000 m in the offshore regions to a minimum of ~300 m at the OWF area where 66 turbines (3 MW each) are proposed.

Figure B.1 presents various bathymetry data used to establish the bathymetry and Figure B.3-Figure B.4 show the flexible mesh bathymetry (overall and magnified to the project site).

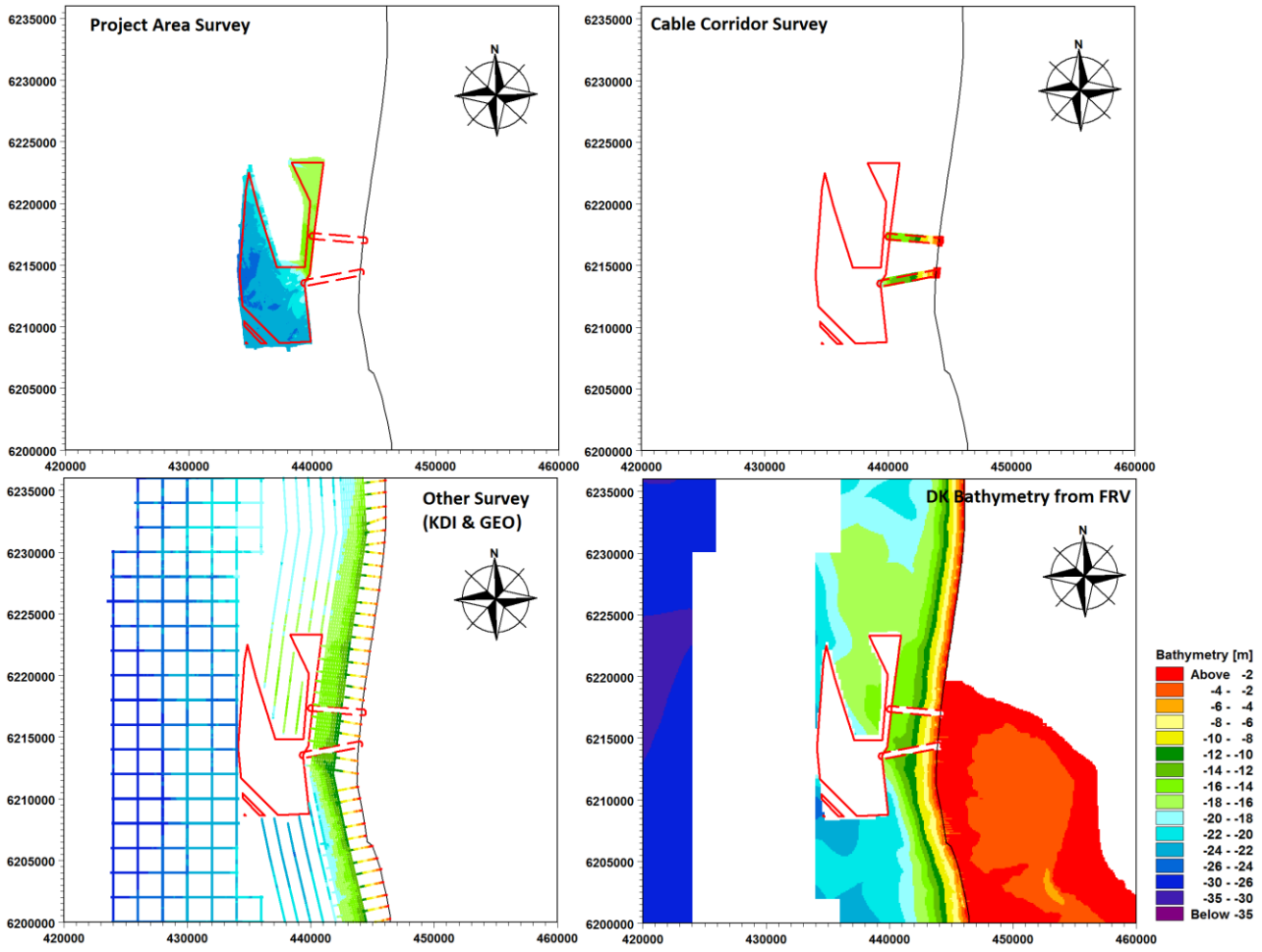

Figure B.1 Various datasets used to derive the model bathymetry at Vesterhav Syd OWF.

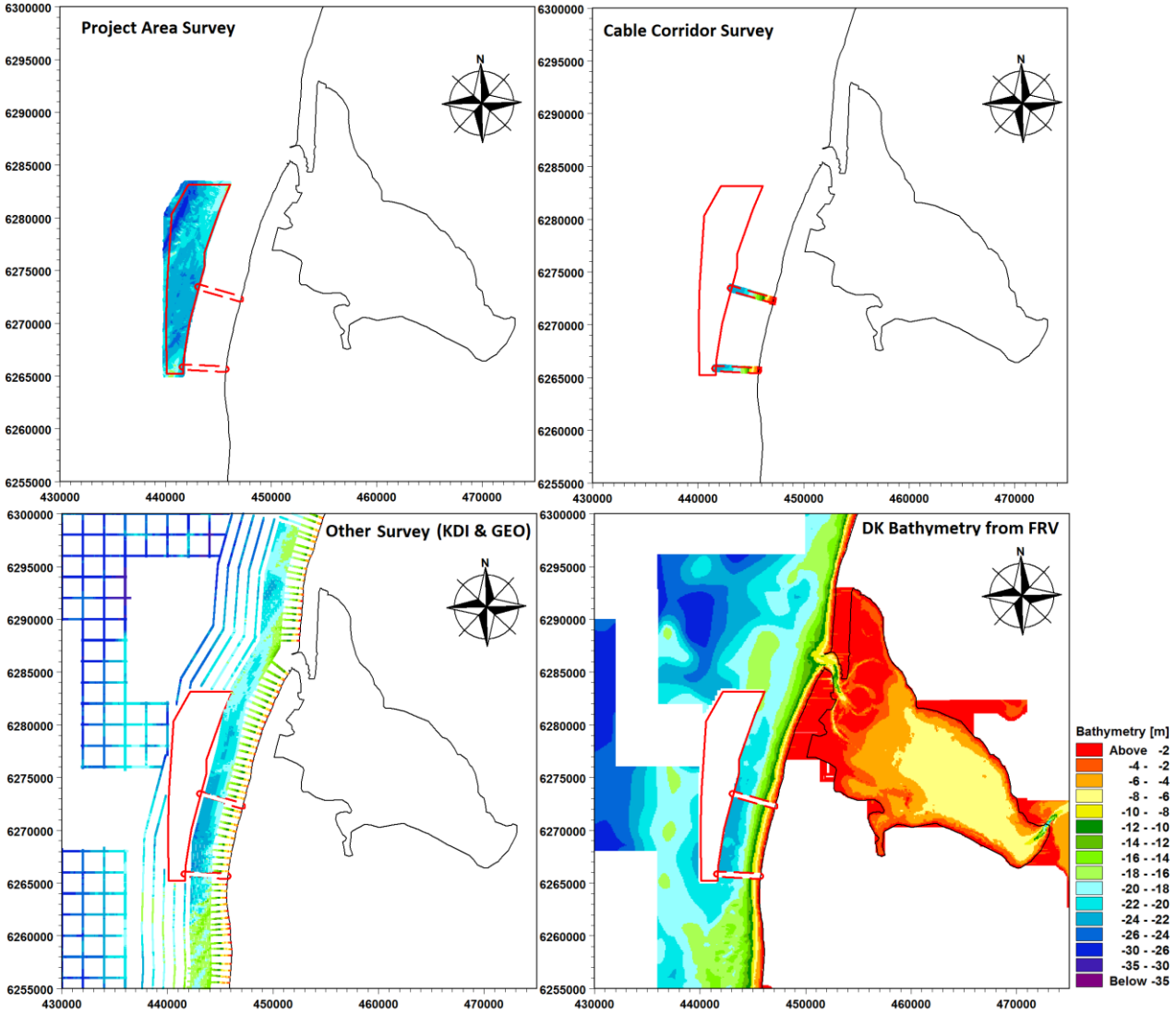

Figure B.2 Various datasets used to derive the model bathymetry.

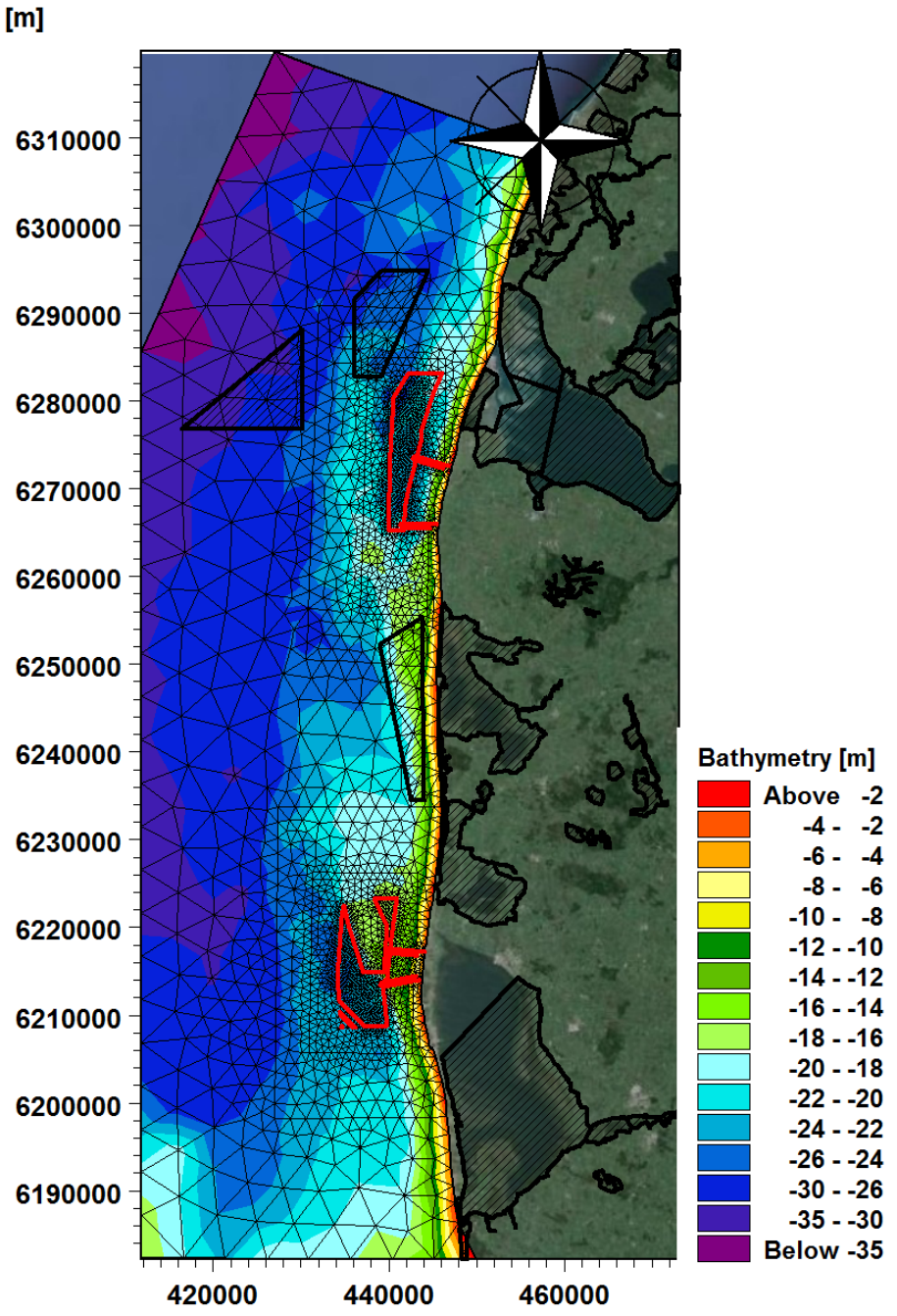

Figure B.3 *Flexible mesh bathymetry for the wave modelling study; overall model. Depth relative to DVR90. The spatial resolution of the mesh varies from an average element size of ~4,000 m in the offshore regions to a minimum of ~300 m at the OWF area.*

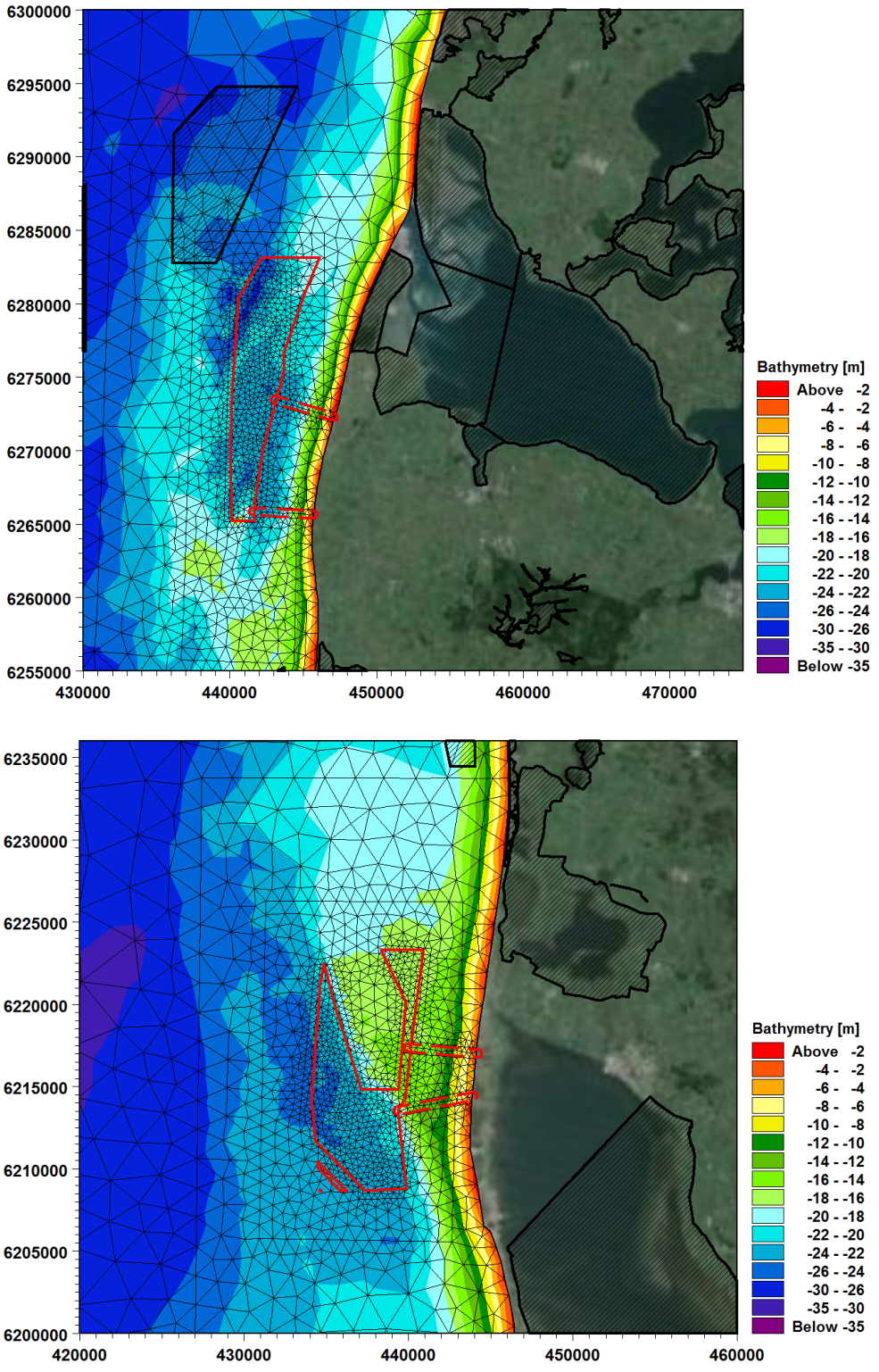

Figure B.4 *Flexible mesh bathymetry for the wave modelling study; zoomed to the Vesterhav Nord (top) and Vesterhav Syd (bottom). Depth relative to DVR90. The spatial resolution of the mesh varies from an average element size of ~4,000 m in the offshore regions to a minimum of ~300 m at the OWF area.*

B.3 Boundary conditions

The input parameters for the wave model are the wind forcing and wave conditions at the open boundaries of the model domain shown in Figure B.5. Wave conditions are applied as integrated wave parameters (H_{m0}, T_p and M_{dir}) from DMI-WAM along the four open boundaries of the model. Wind conditions are applied as 2D wind fields in a 0.03° grid (1.9 km horizontal and 3.3km vertical resolution) from the DMI-HILRAM model.

Water level variations are included in the wave modelling based on measurements at Hvide Sande.

The additional model parameters which will influence the wave characteristics in the nearshore waters include wave breaking, white capping, bottom friction and wind/sea friction parameters. These are used as calibration parameters.

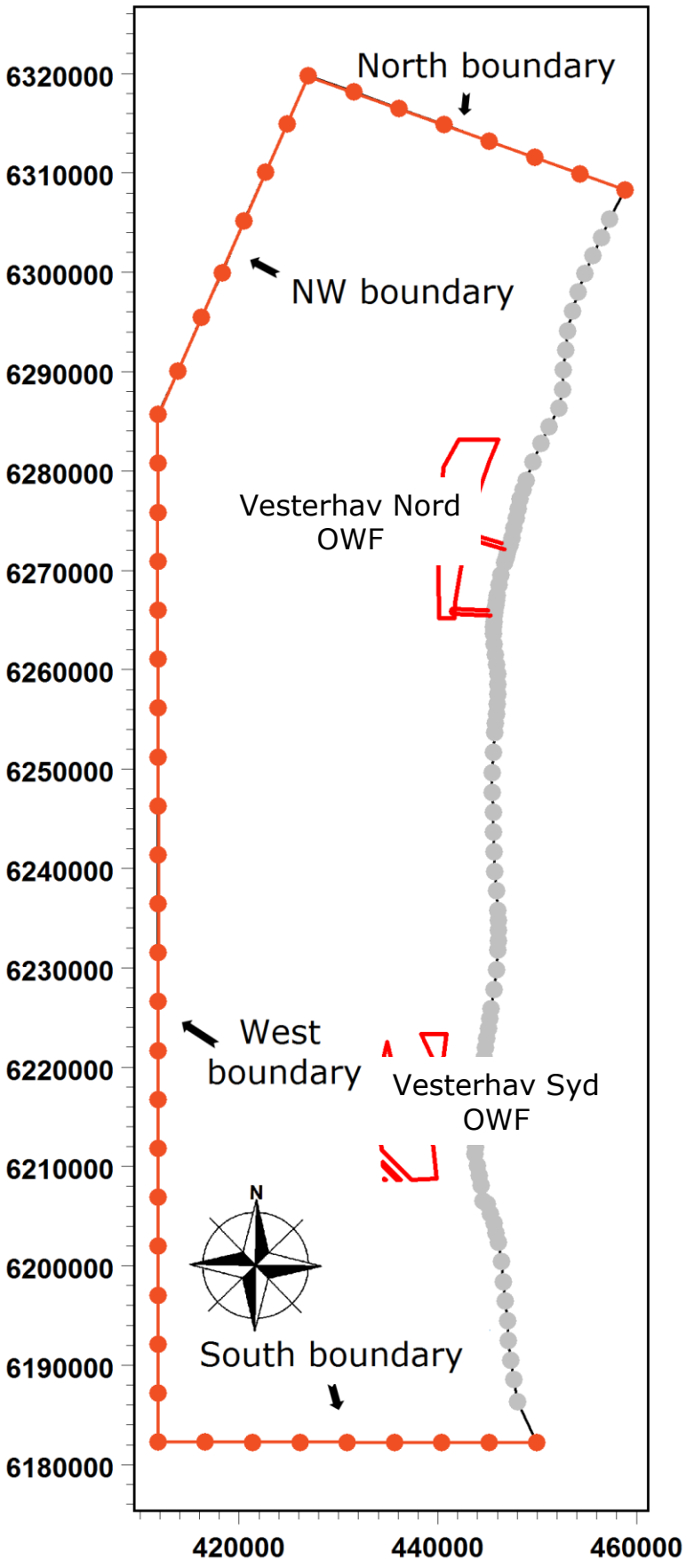

Figure B.5 *Definition of boundaries in the model domain.*

B.4 Offshore wind farm

The influence of the wind turbines is included in the form of the *wind effect* and *diffraction/reflection*.

The *wind effect* is caused by the wind wake in lee of the wind turbines. Studies by RISØ of SAR[10] wind maps in and downstream of offshore wind farms have shown wind velocity deficits[11] of up to 10% and wake persistency of at least 10 km [ref. /4/]. Figure B.6 shows the wind velocity deficit in and downstream of the Horns Reef offshore wind farm based on 19 satellite SAR wind maps. It is noted that the wind velocity deficit increases gradually inside the wind farm and peaks at around 10% 2-3 km downstream of the wind farm after which the wake declines gradually with increasing distance to the wind farm.

The *wind effect* is included in the wave model by reducing the wind speed in the 2D wind field (from DMI-HIRLAM) by 10 % inside the wind farm and 10 km downstream, as shown in Figure 3.5. This approach is considered conservative.

The implementation of the *wind effect* in the 2D wind climate is illustrated in Figure B.7.

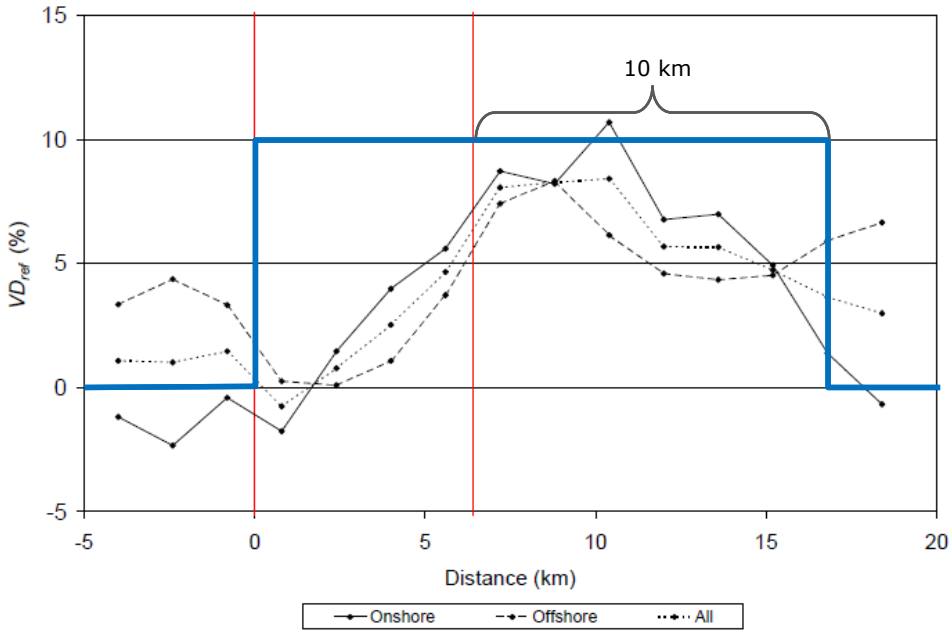

Figure B.6 *Average wind velocity deficit (VD) at Horns Reef 1 wind farm obtained from 19 satellite SAR wind maps. Vertical red lines indicate maximum wind farm boundaries [ref. /4/]. The blue line indicates the wind velocity deficit applied in the wave model.*

[10] SAR = Synthetic Aperture Radar

[11] Velocity Deficit (VD) = $(U_{freestream} – U_{wake})/U_{freestream}$ x 100%

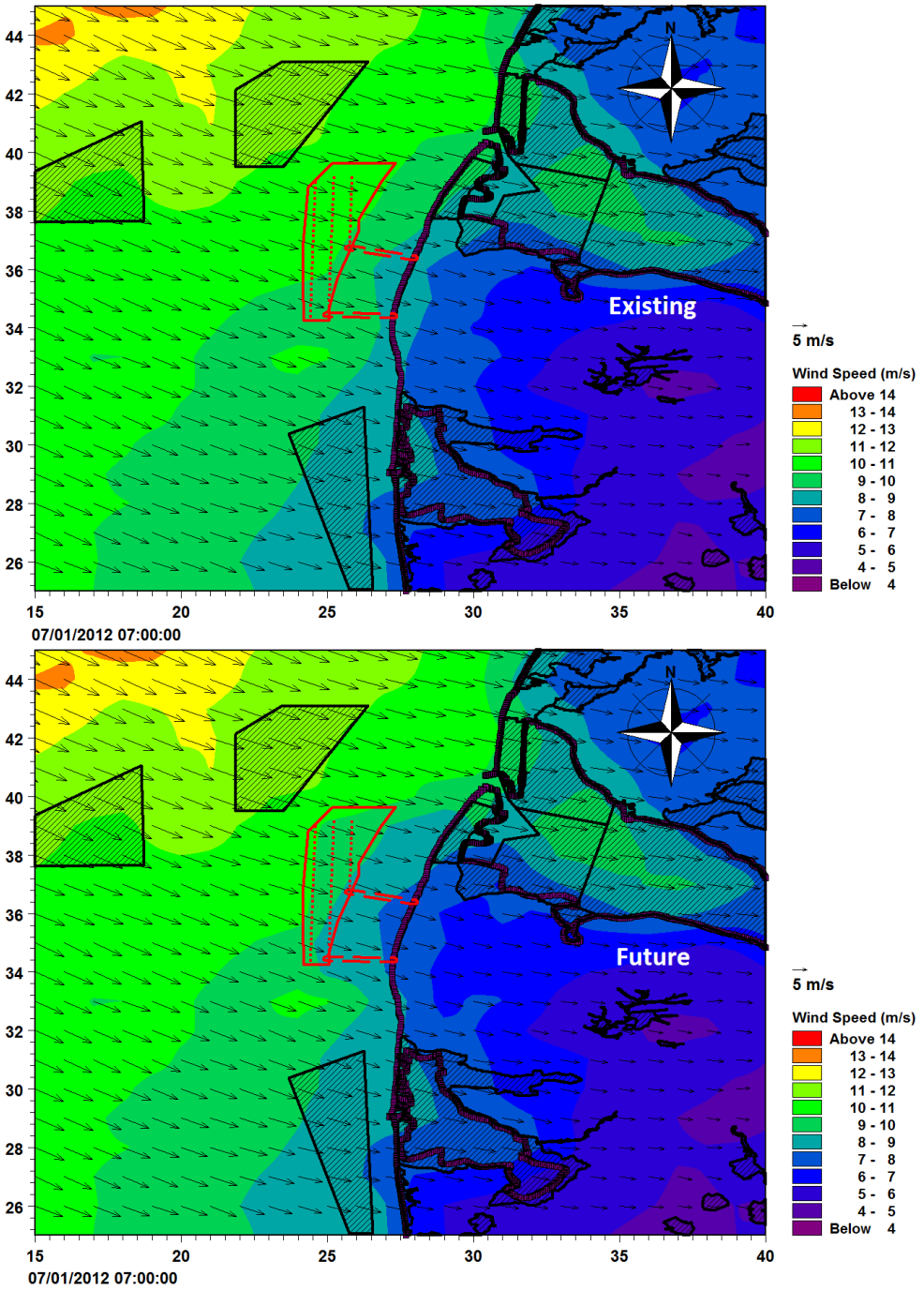
Existing
Future
N
5 m/s
Wind Speed (m/s)
Above 14
13 - 14
12 - 13
11 - 12
10 - 11
9 - 10
8 - 9
7 - 8
6 - 7
5 - 6
4 - 5
Below 4
44
42
40
38
36
34
32
30
28
26
15
20
25
30
35
40
07/01/2012 07:00:00

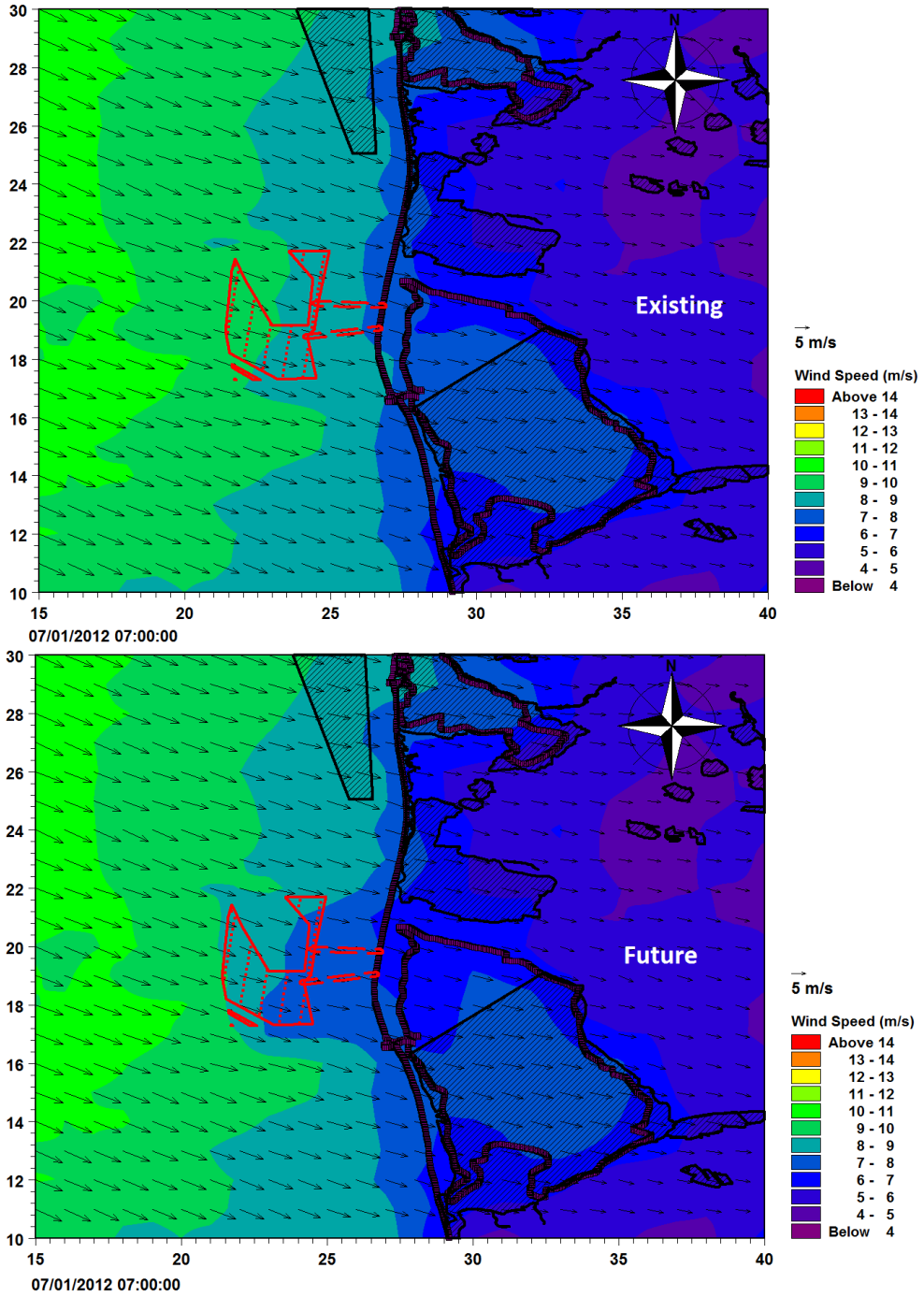

Figure B.7 *Spatially varying wind across the model domain; Existing (Top) and Future (Bottom) situation. Brown points representing coastline and Pink line indicates OWF project area.*
Vesterhav Nord shown at the first figure, and Vesterhav Syd shown at the last figures.

The *diffraction/reflection effect* is caused by the physical presence of the wind turbine foundations. The effects of the foundations are implemented in the MIKE 21 SW as energy dissipation at each wind turbine position [ref. /5/].

The geometry of the gravity based foundations is simplified to a circular structure of 18 m diameter. This corresponds to the average diameter of the shaft, base and ice-cone of the gravity based foundation described in section 2.3.

B.5 Model setup and calibration

The fully spectral and in-stationary formulation of the MIKE 21 SW code is used. Wave energy dissipation is described with wave breaking, white capping and bottom friction parameters. These parameters are calibration parameters which are fine tuned in order to attain a satisfactory comparison between the model results and wave measurements at the project site (May 2012 to October 2012).

Measurements at Fjaltring and Nymindegab include significant wave height (H_{mo}), peak wave period (T_p), mean wave period (T_m) and mean wave direction (MWD). The measurements were conducted by KDI in 15.5-17.5 m water depths with wave rider buoys (see Figure B.8).

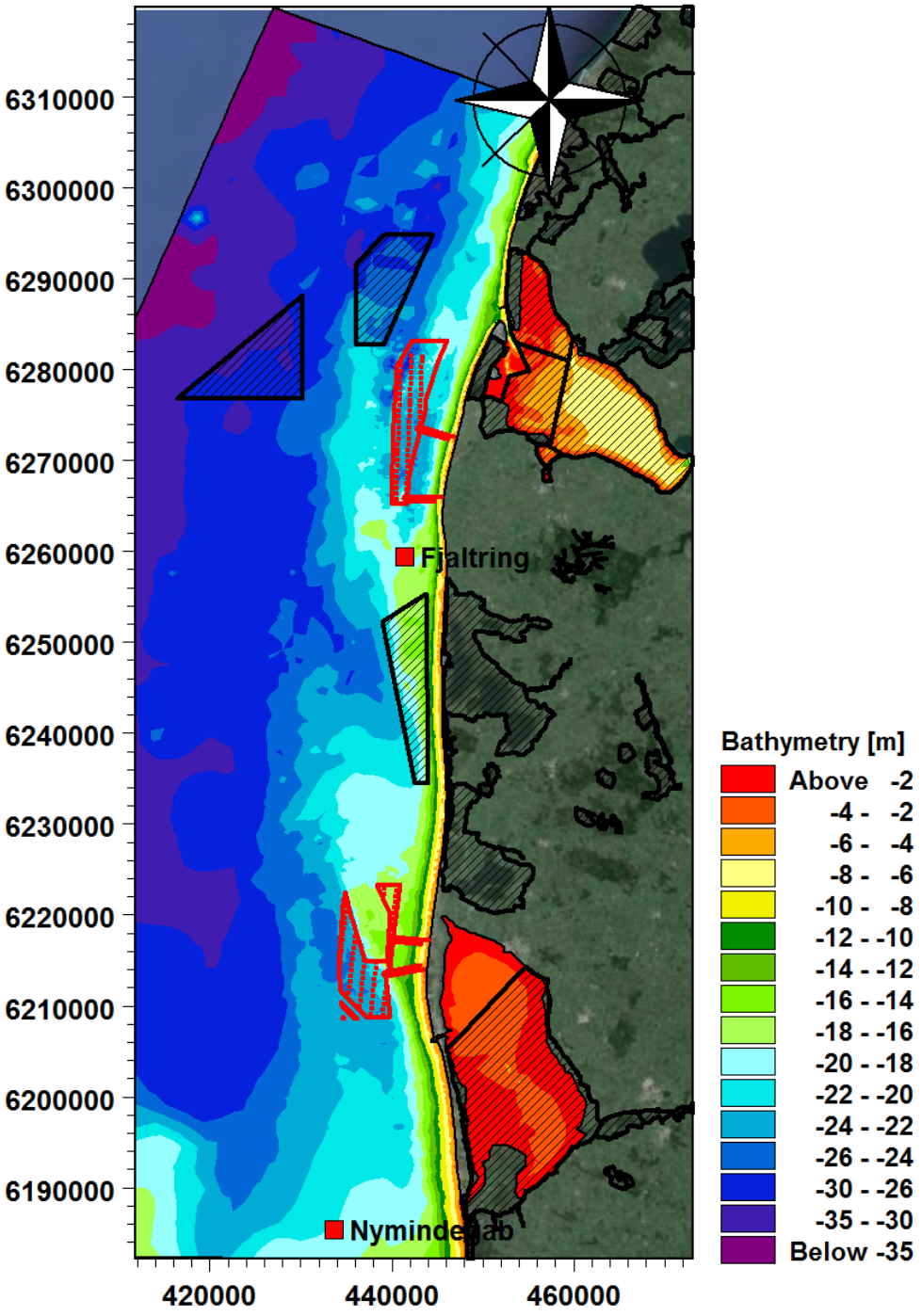
6310000
6300000
6290000
6280000
6270000
6260000
6250000
6240000
6230000
6220000
6210000
6200000
6190000
420000
440000
460000
Fjaltring
Nymindegab
Bathymetry [m]
Above -2
-4 - -2
-6 - -4
-8 - -6
-10 - -8
-12 - -10
-14 - -12
-16 - -14
-18 - -16
-20 - -18
-22 - -20
-24 - -22
-26 - -24
-30 - -26
-35 - -30
Below -35

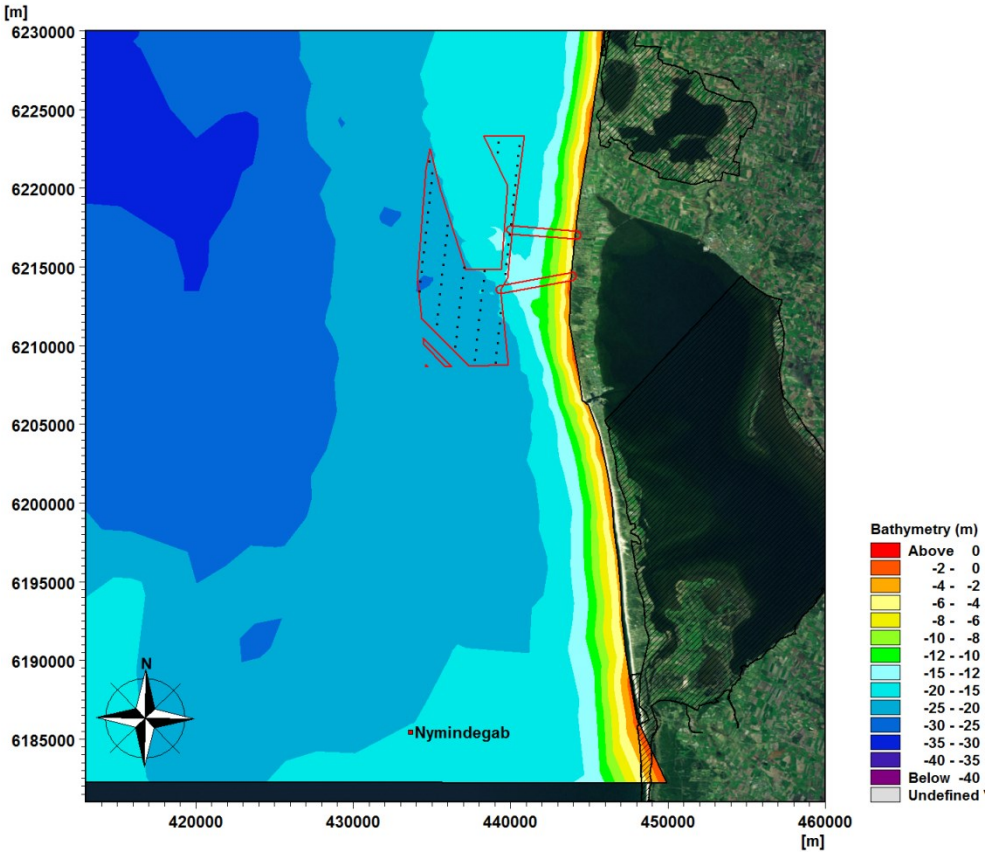

Figure B.8 *Location of measurements near the Vesterhav Nord [56.475 N,8.048 E] and Vesterhav Syd [55.810 N,7.941 E] OWF.*

A satisfactory calibration is obtained with model dissipation parameters provided in Table B.3. The calibration is presented in Figure B.9 to Figure B.12 and shows a very good fit. The calibration of the wave height shows a correlation coefficient of 0.97, a scatter index of 0.14 and a BIAS of -0.02 m and RMS-Error of 0.18 m for Nymindegab and a correlation coefficient of 0.98, a scatter index of 0.11 and a BIAS of 0.01 m and RMS-Error of 0.16 m for Fjaltring.

Table B.3 *Model parameters applied in the MIKE 21 SW FM model.*

Parameters	Value
Bottom Friction, K_n	4 mm
Wave Breaking, γ	0.8
Wave Breaking, α (wave steepness)	1
Air-sea interaction, Charnock Parameter (uncoupled)	0.01
White Capping, dissipation coefficient, C_{dis}	1.5
White Capping, dissipation coefficient, Δ_{dis}	0.5

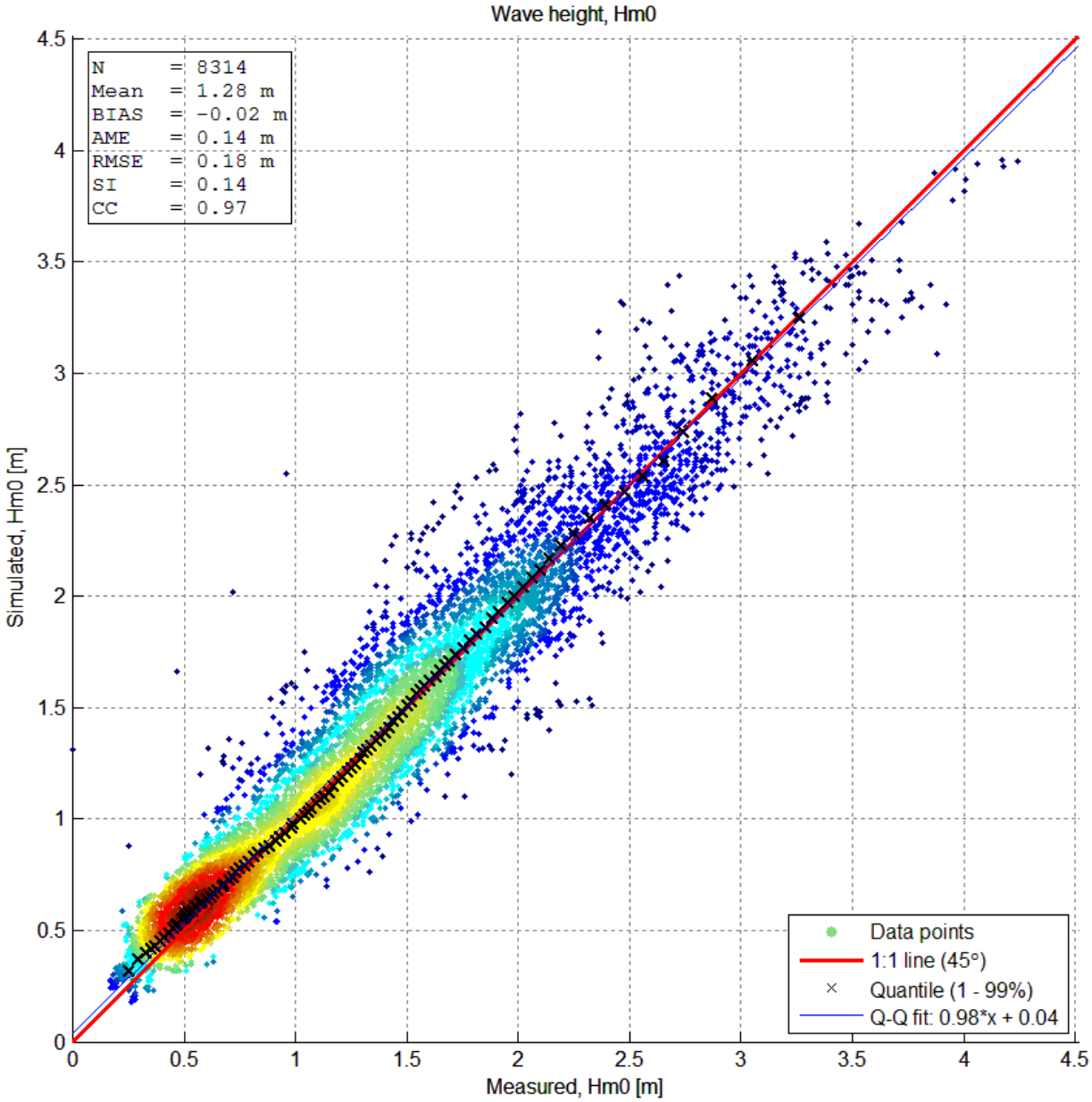

Figure B.9 *Scatter analysis showing the measured and simulated significant wave height at ADCP location during May 2012 – Oct 2012, Nymindegab.*

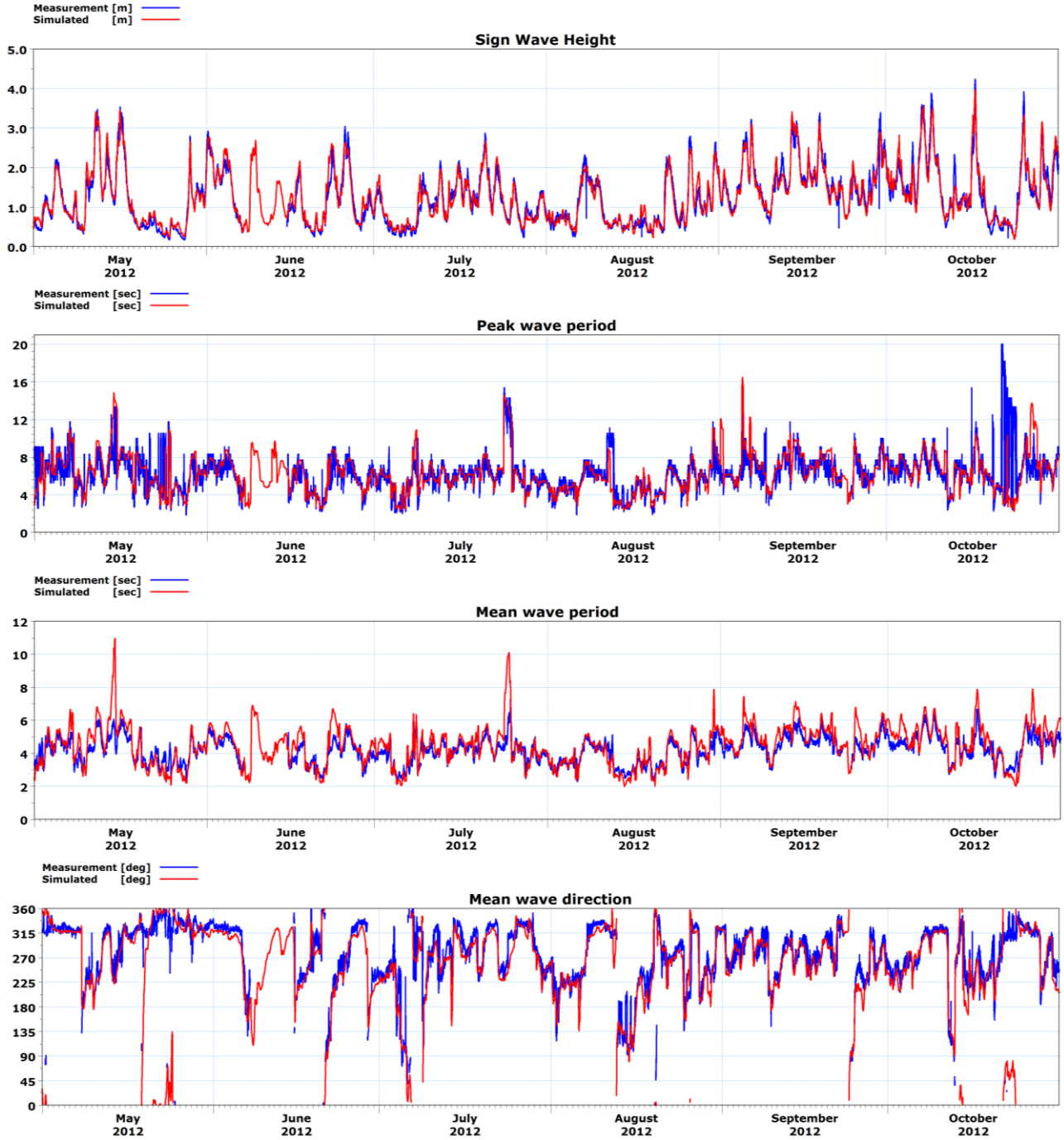

Figure B.10 *Comparison of H_{m0} (Top), T_p (Second from Top), T_m (Third from top) and MWD (Bottom) between buoy measurement and MIKE 21 SW wave propagation model during May 2012 – Oct 2012, Nymindegab.*

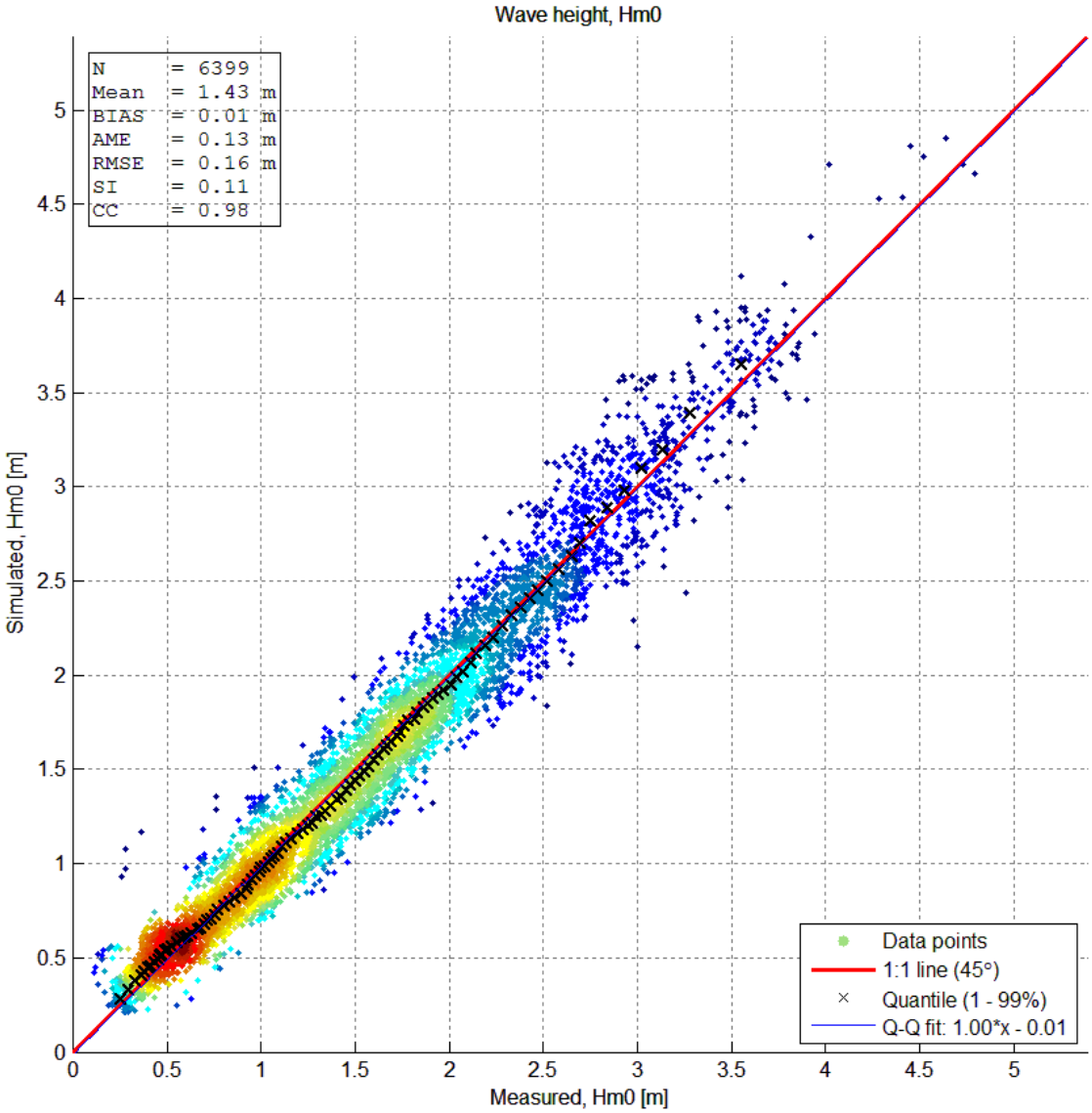

Figure B.11 *Scatter analysis showing the measured and simulated significant wave height at ADCP location during May 2012 – Oct 2012, Fjaltring.*

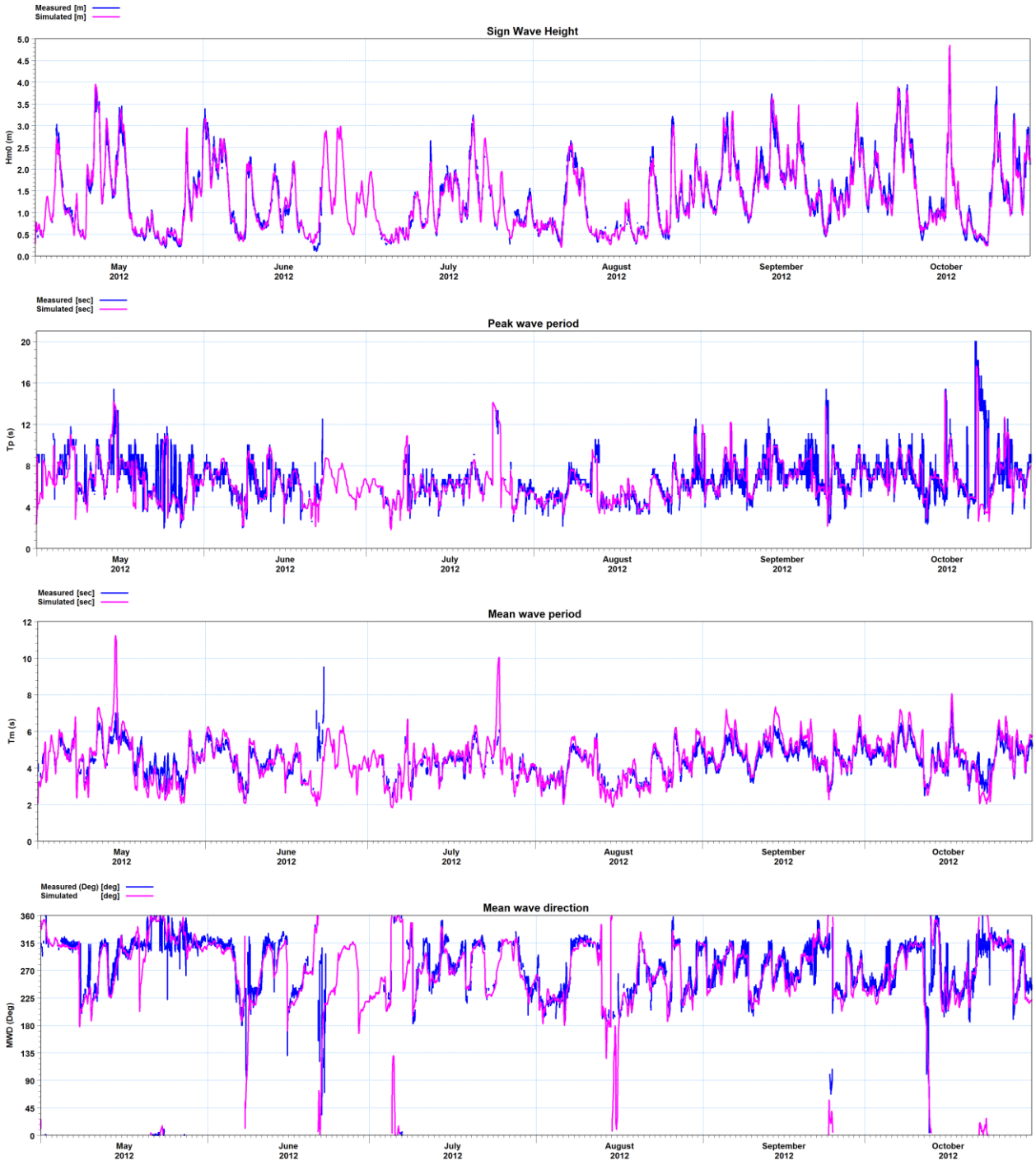

Figure B.12 *Comparison of H_{m0} (Top), T_p (Second from Top), T_m (Third from top) and MWD (Bottom) between buoy measurement and MIKE 21 SW wave propagation model during May 2012 – Oct 2012, Fjaltring.*

Appendix C Hydrodynamic modelling

The current model MIKE 21 HD FM is driven by wind and pressure fields from DMI's atmospheric model DMI-HIRLAM and boundary conditions from DMI's regional current model DMI-HBM. Further, because the waves at the west coast of Jutland will give rise to significant wave induced currents compared to tide and meteorological induced currents; waves (radiation stresses) from the MIKE SW model is included in the hydrodynamic model. It is noted that the effect of wave induced currents are only relevant in the nearshore coastal areas – the surf zone; i.e. at water depths from approximately 5 m and more shallow, and thus not present at the location of the OWF it selves.

The hydrodynamic model is used to study the influence of the OWF on currents and water levels, and form the basis of evaluating the seabed morphology and water quality. Furthermore the results are applied in the sediment transport model (MIKE 21 MT).

Current modelling for the two offshore wind farms Vesterhav Nord OWF and Vesterhav Syd OWF is performed in one model domain that covers both sites.

C.1 Data collection

Met-ocean data including water level and tidal current measurements have been collated from a variety of stations located near the two offshore wind farms; Vesterhav Nord OWF and Vesterhav Syd OWF, see Table C.1

Table C.1 Measurements in the vicinity of the OWF areas and details. See Figure D.1 for location of data points.

Observation location name	Type of data	Time series		Data owner	Position (lat, lon)
		Start	End		
Ferring	Water level	01-01-2003	29-01-2013	DMI	56.524593; 8.115164
Thyborøn	Water level	01-01-2003	01-02-2014	DMI	56.707733; 8.208776
Thorsminde	Water level	01-01-2003	01-02-2014	DMI	56.372643; 8.113573
Hvide Sande, 1	Water level	01-01-2003	31-01-2014	DMI	56.000458; 8.128977
Hvide Sande, 2	Water level	01-01-2003	01-02-2014	DMI	56.0072; 8.1412;
Fjaltring (Wave Rider)	Waves	01-01-2011	31-12-2012	KDI	56.475; 8.048
Nymindegab (Wave Rider)	Waves	01-01-2011	31-12-2012	KDI	55.810; 7.941

In addition to the above measurements, synoptic wind and water level conditions from DMI regional model DMI-HIRLAM and DMI-HBM, see Table C.2, are used as forcing of the MIKE 21 HD FM model.

Table C.2 Hindcast data used as boundary conditions.

SYNOPTIC DATASET	PARAMETERS	TIME STEP	RESOLUTION	TIME SERIES	
				Start	End
DMI-HIRLAM 2D wind	Wind components (U, V) [m/s]	Δt=1 hr	0.03 ° (Δx = 1.9 km, Δx = 3.3 km)	01-01-2005	01-01-2013
DMI-HBM 1D Water levels along 4 open boundaries	h[x]	Δt=1 hr	~ Δx' =4.5-5 km	01-01-2011	31-12-2012

C.2 Model bathymetry

Various bathymetry datasets are utilised for developing the flexible mesh model for the hydrodynamic modelling study, which is explained in section B.2.

The hydrodynamic model domain is created using an unstructured flexible mesh approach, whereby the domain is divided into several zones, in which the resolution becomes progressively higher in the vicinity of the project sites. The model uses an unstructured mesh of triangular elements to discretise the domain and represent the bathymetry, thereby allowing a higher resolution in areas of interest such as the OWF and natural channels, etc. The flexibility associated with the triangular elements in the mesh also allows for a smoother representation of land/water boundaries.

The spatial resolution of the computational mesh varies from an average element size of ~1800 m in the offshore regions to a minimum of ~100 m inside the wind farm areas (Figure C.1 and Figure C.2).

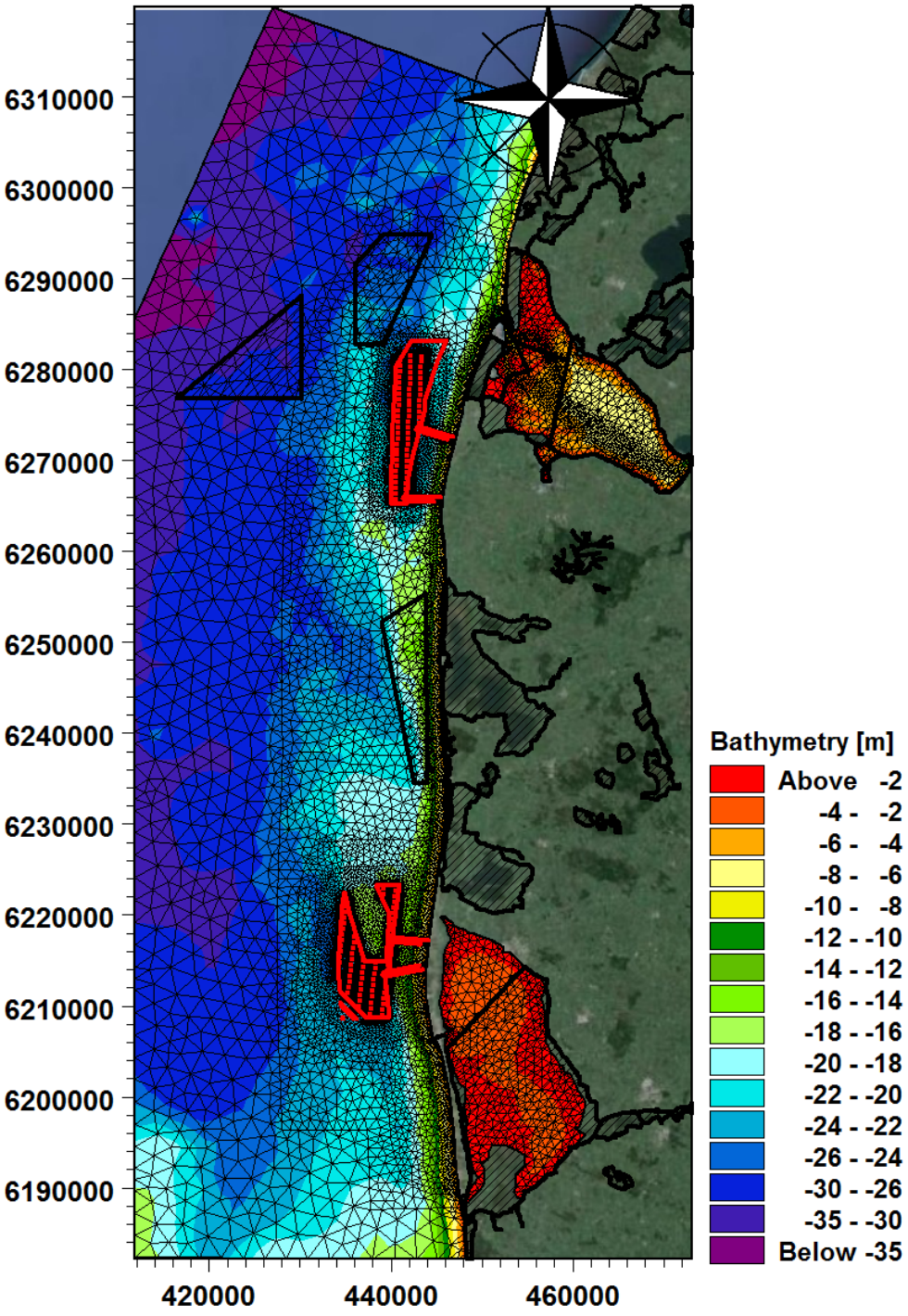

Figure C.1 *Flexible mesh bathymetry for the hydrodynamic modelling study; overall model. Depth relative to DVR90.*

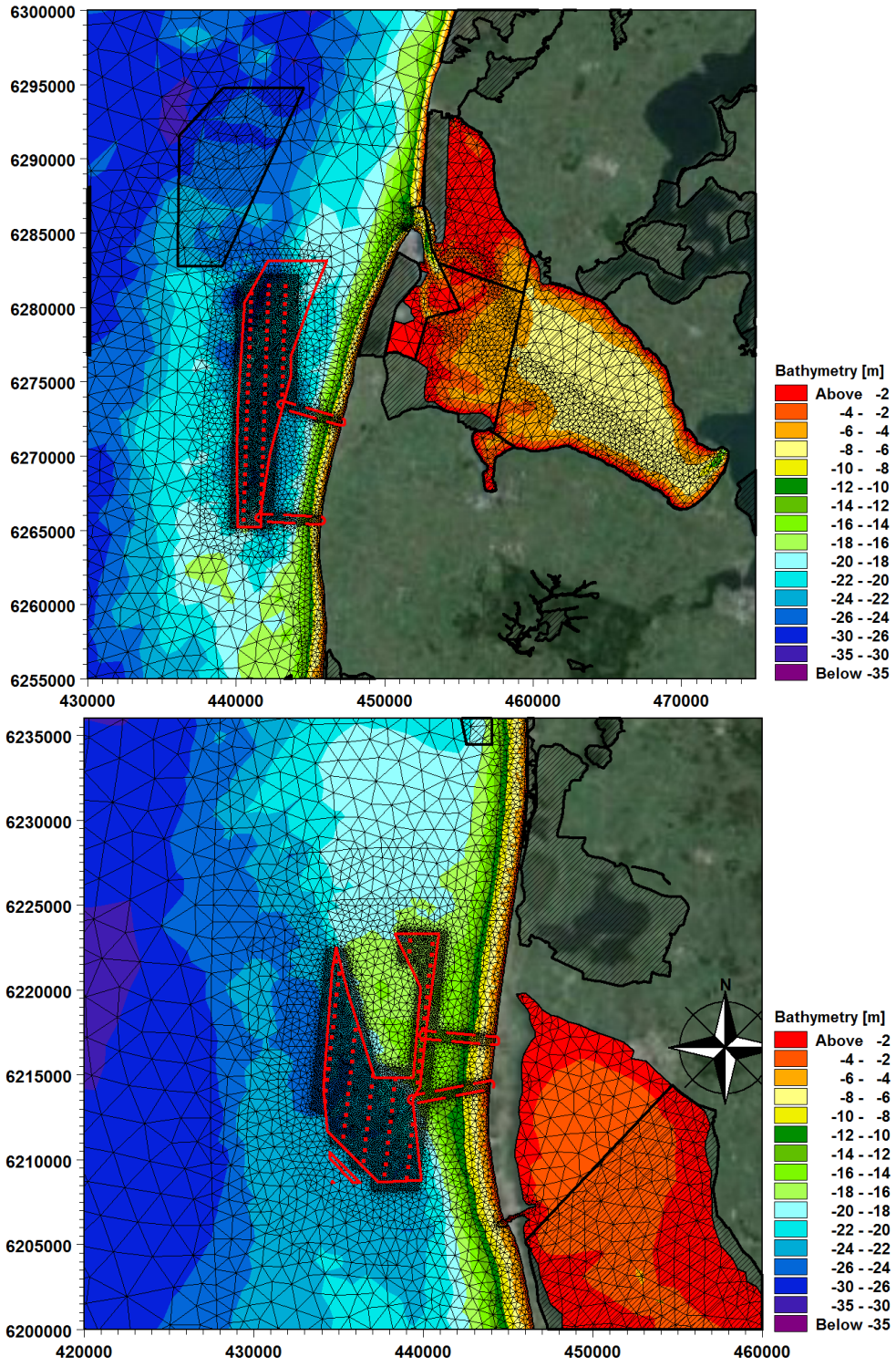

Figure C.2 *Flexible mesh bathymetry for the hydrodynamic modelling study; zoomed to the Vesterhav Nord (top) and Vesterhav Syd (bottom). Depth relative to DVR90.*

C.3 Boundary conditions

The forcing of the hydrodynamic model comprises wind forcing, barometric pressure and water levels at the open boundaries of the model domain.

Water level variations along the four open boundaries (see Figure B.5) are applied from DMI's regional hydrodynamic model (DMI-HBM) at 4.5-5 km intervals. Wind/pressure fields are applied in a 2D grid from DMI's atmospheric model DMI-HIRLAM in 0.03° grid spacing.

C.4 Offshore wind farm

The offshore wind turbines influence on the hydrodynamic conditions (currents and water levels) is modelled in MIKE 21 HD FM as pier-resistance [ref. /6/].

The geometry of the gravity based foundations is implemented based on the dimensions provided in section 2.3 and the geometric scheme shown in Figure C.3. Hence, the varying diameters and the influence of water depth at the location of individual turbines are implemented in the geometric representation of the foundation in the model.

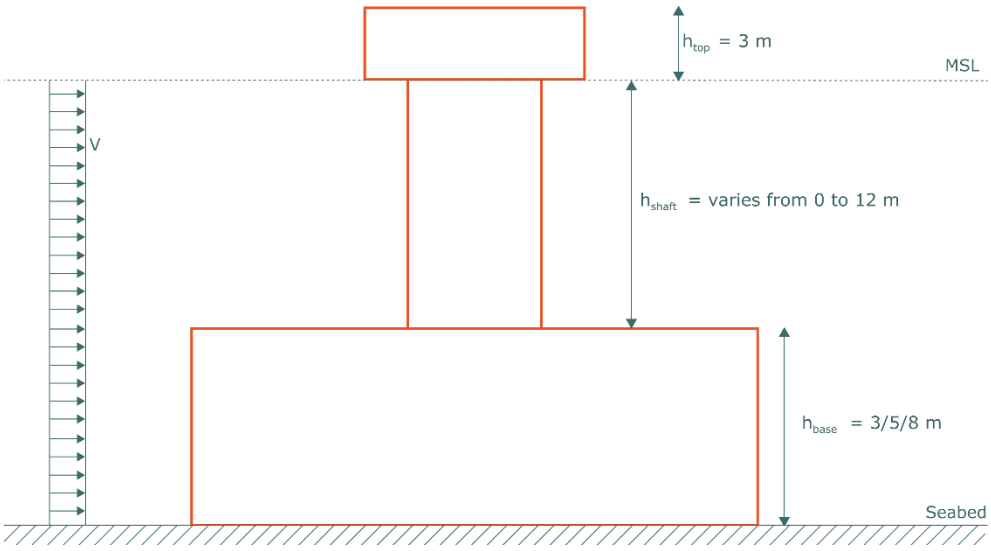

Figure C.3 Geometric scheme of gravity based foundations.

The resistance to the flow due to the turbine foundations is included in terms of the drag force, *F*, which acts against the current direction:

$$F = \frac{1}{2}\rho_w \gamma C_D A_e U^2$$

Where,

- γ : Streaming factor, γ = 1.02
- C_D : Drag coefficient
- A_e : Cross area of pier exposed to current
- ρ_w: Water Density
- U : Current speed

C.5 Model setup and calibration

The hydrodynamic model is calibrated against water level measurements from four locations (Thyborøn, Ferring, Torsminde and Hvide Sande) for a period of three months (June to August 2012), see Figure C.4.

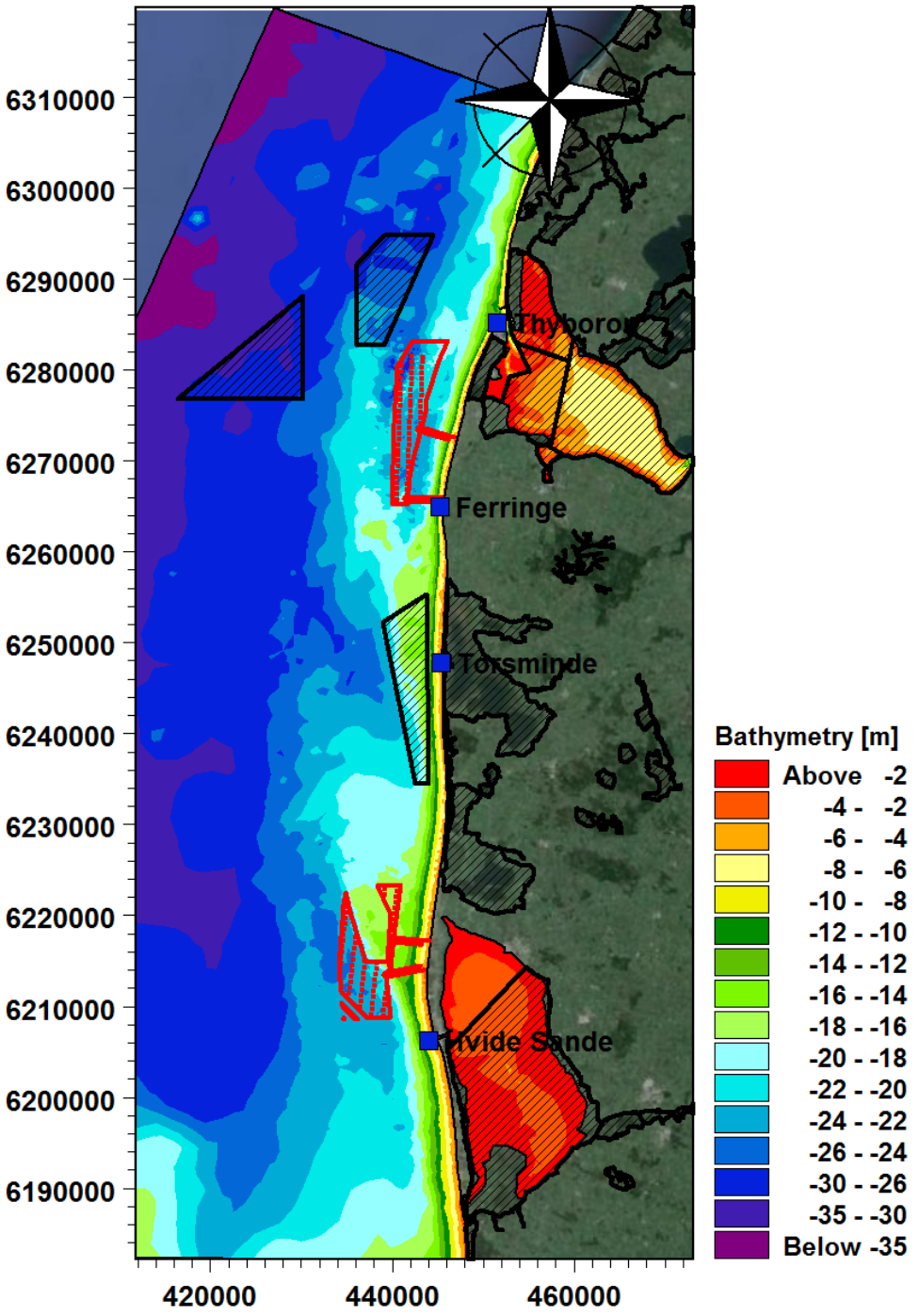

Figure C.4 Location of water level measurements near the OWF.

A satisfactory calibration is obtained by minimizing the deviation between the measured and modelled values through iterative adjustment of the uniform bed resistance and wind friction within physically reasonable limits. Best calibration was achieved by applying a constant Manning coefficient of 42 $m^{1/3}/s$ and a varying wind friction proportional to the wind speed (see Figure C.5)

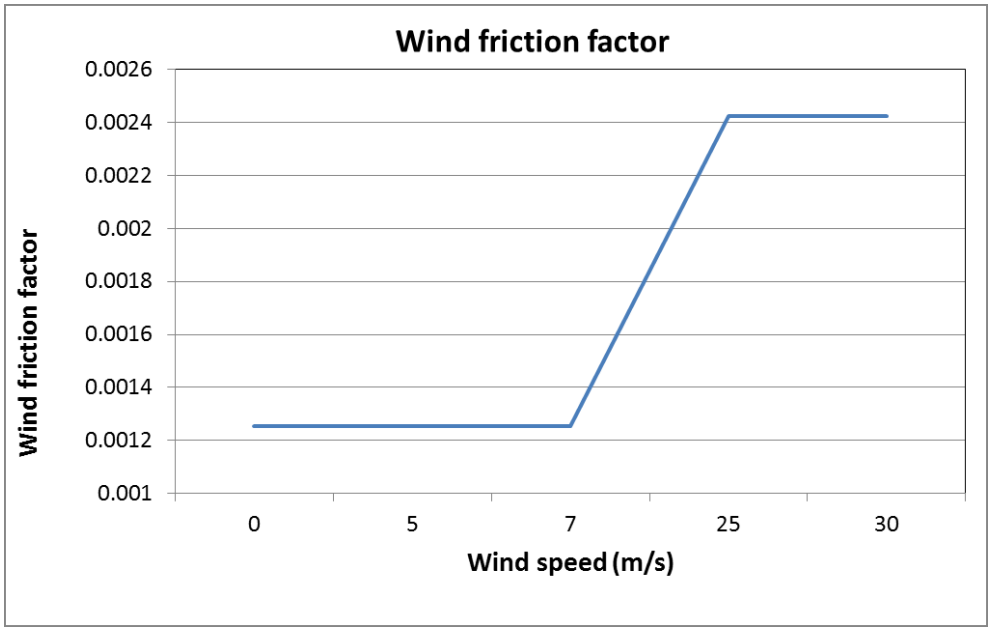

Figure C.5 Applied wind friction factor.

C.5.1 Calibration

Water level

Figure C.6 to Figure C.9 shows the comparison between the measured and modelled water level at four locations (Thyborøn, Ferring, Thorsminde and Hvide Sande) for the calibration period.

The calibration results indicate that the simulated water levels at the four locations were in good agreement with the measured data (see Table C.3). The results show a bias of ~0.07 m or less between the measured and simulated water levels. The same bias is observed in the boundary water level inputs from DMI-HBM.

Table C.3 Measured and simulated water level comparison at three locations.

Statistical parameters	Thyborøn	Ferring	Torsminde	Hvide sande
Bias	-0.07	-0.06	0.01	-0.03
AME	0.09	0.08	0.07	0.09
RMSE	0.1	0.1	0.09	0.11
SI	2.45	1.75	1.36	1.33
CC	0.96	0.96	0.95	0.95

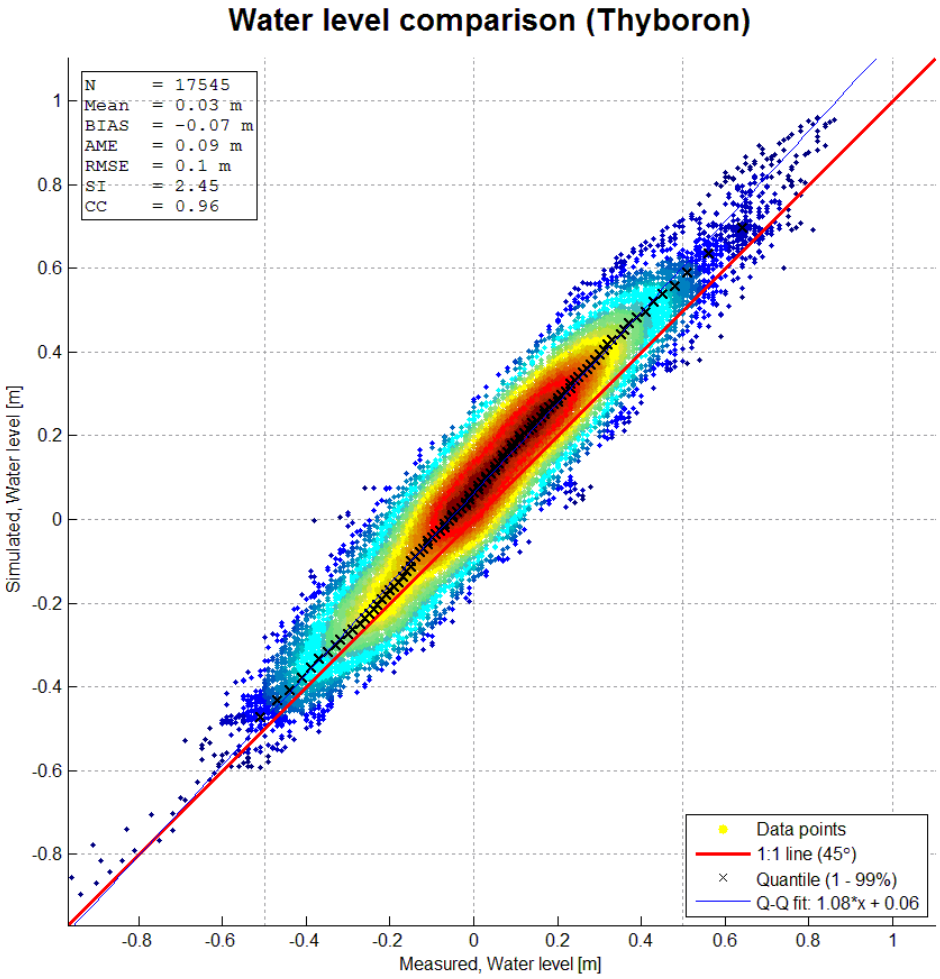

Figure C.6 Scatter plot showing the measured and modelled water level at Thyborøn.

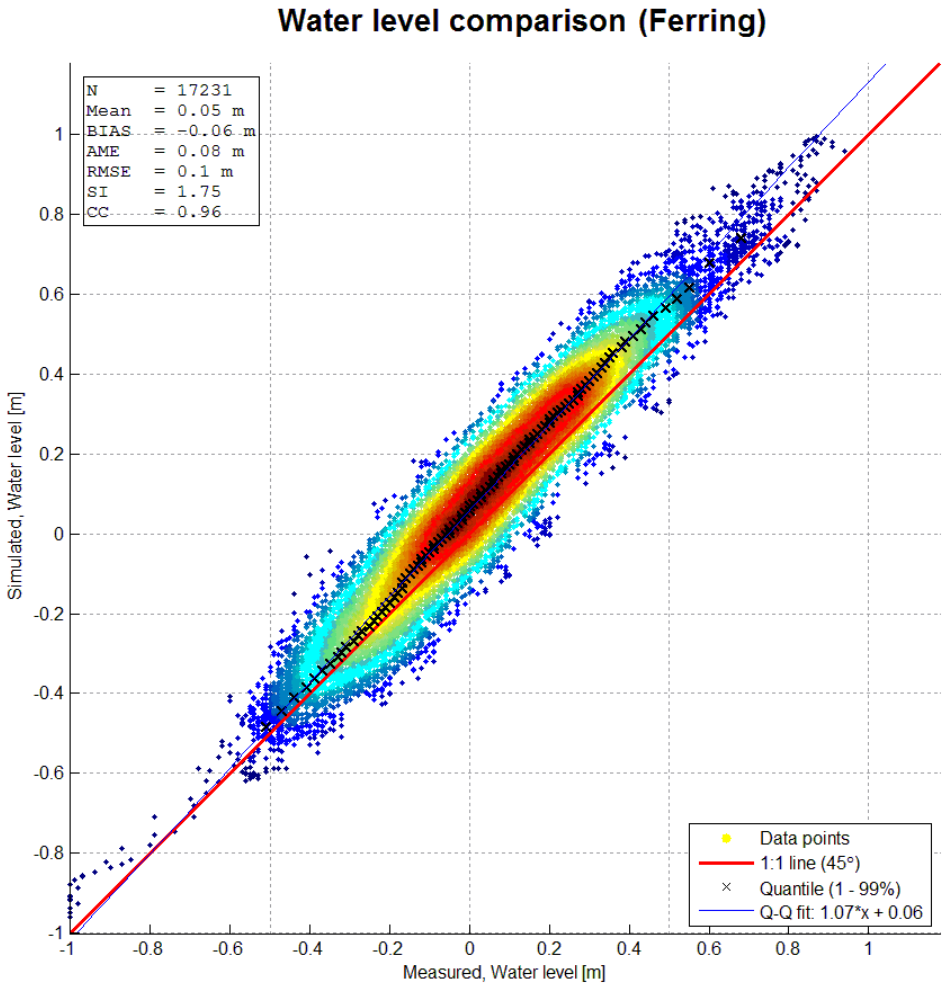

Figure C.7 Scatter plot showing the measured and modelled water level at Ferring.

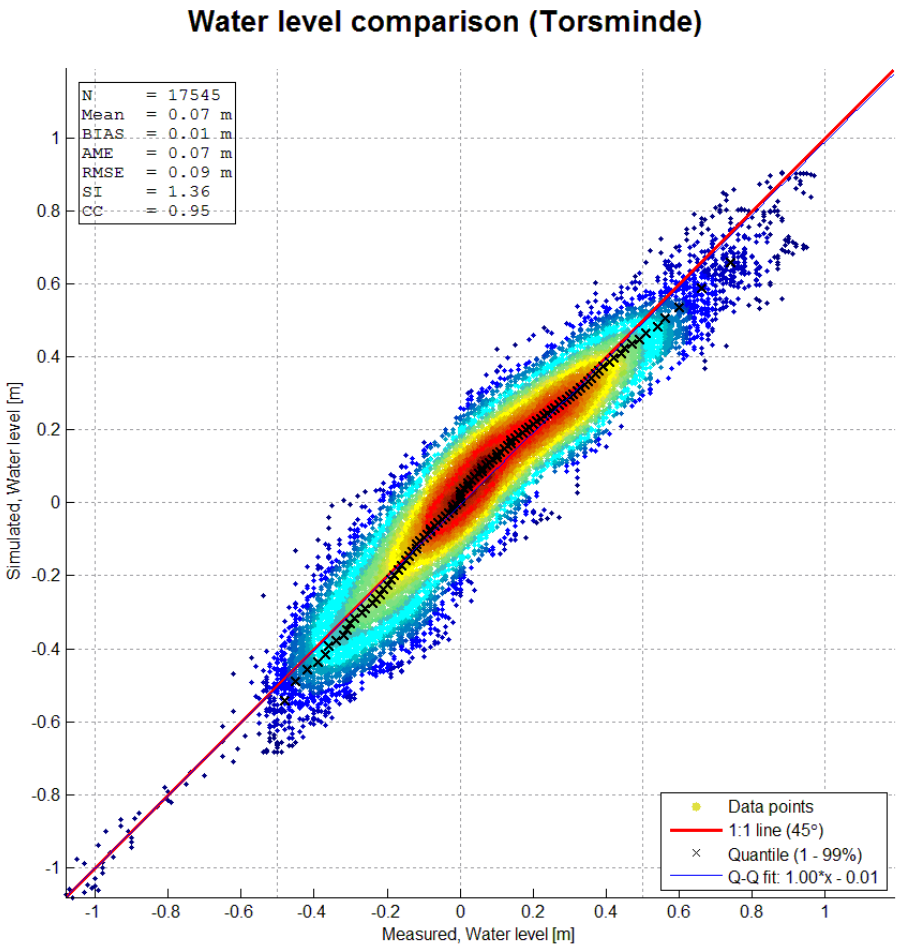

Figure C.8 Scatter plot showing the measured and modelled water level at Torsminde.

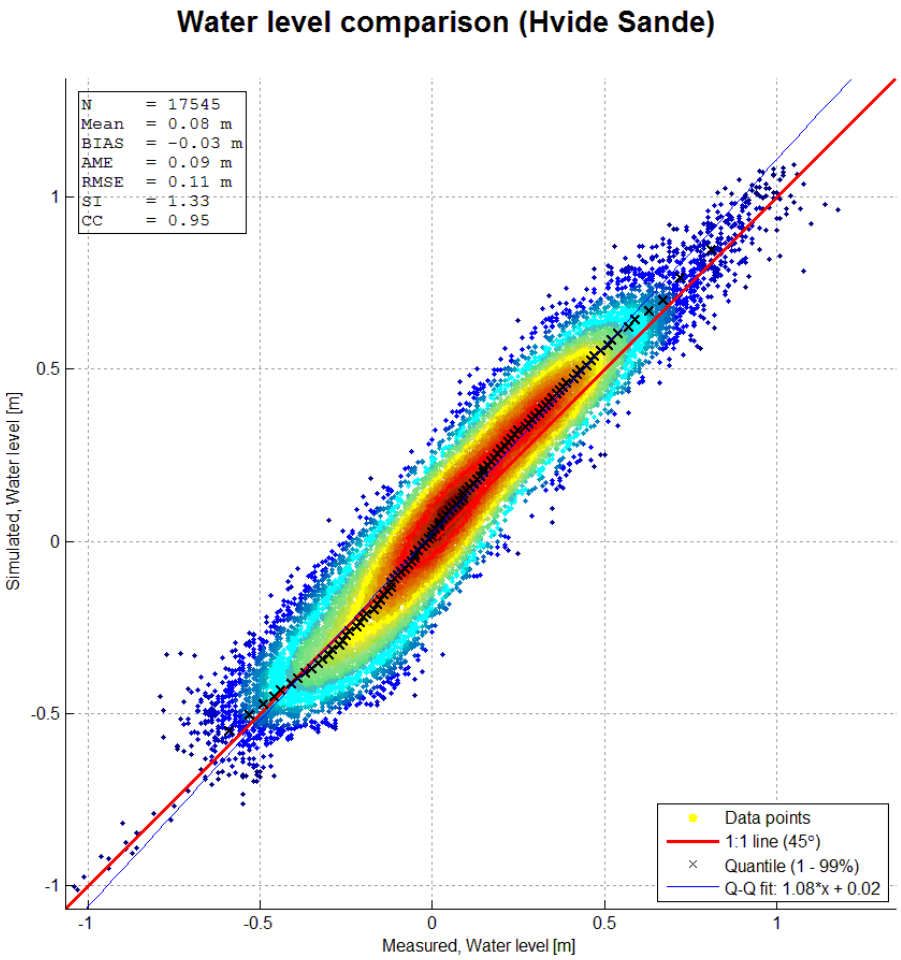

Figure C.9 Scatter plot showing the measured and modelled water level at Hvide Sande.

Figure C.10 to Figure C.13 shows the time series comparison between the measured and modelled water levels at Thyborøn, Ferring, Thorsminde and Hvide Sande. The results show some bias which may be caused by physics not implemented in the model like sluice control, wave set-up, storm water run-off. It is thus considered that the simulated water levels is in good agreement with the measurements.

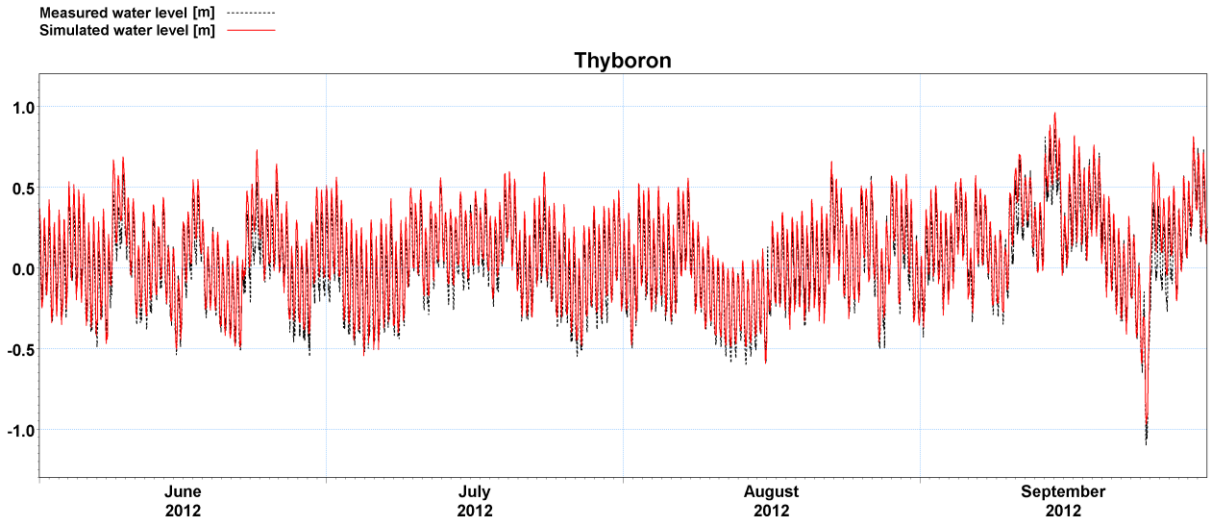

Figure C.10 Measured and modelled water level at Thyborøn.

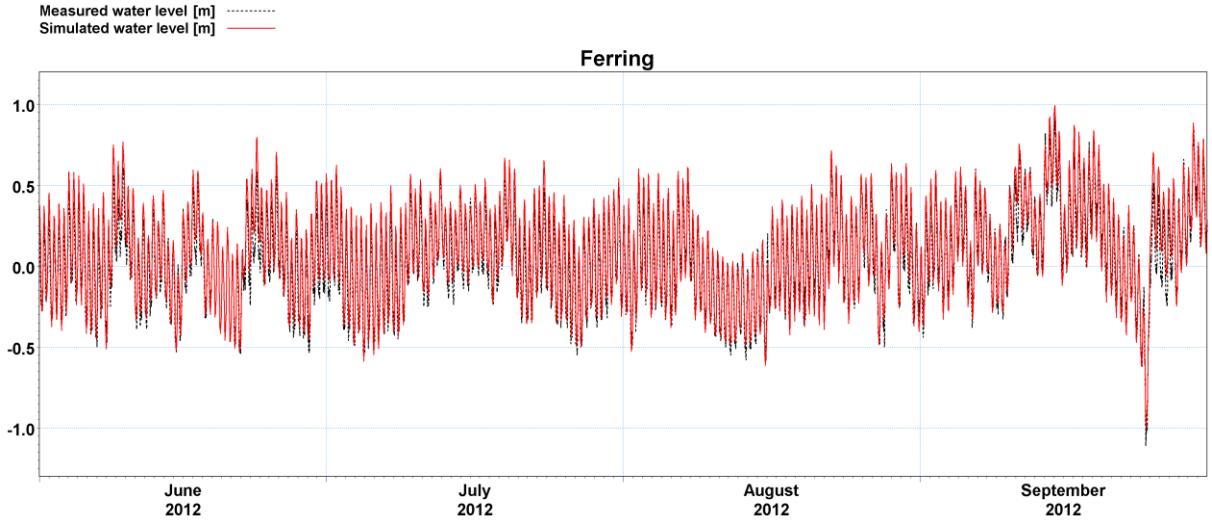

Figure C.11 Measured and modelled water level at Ferring.

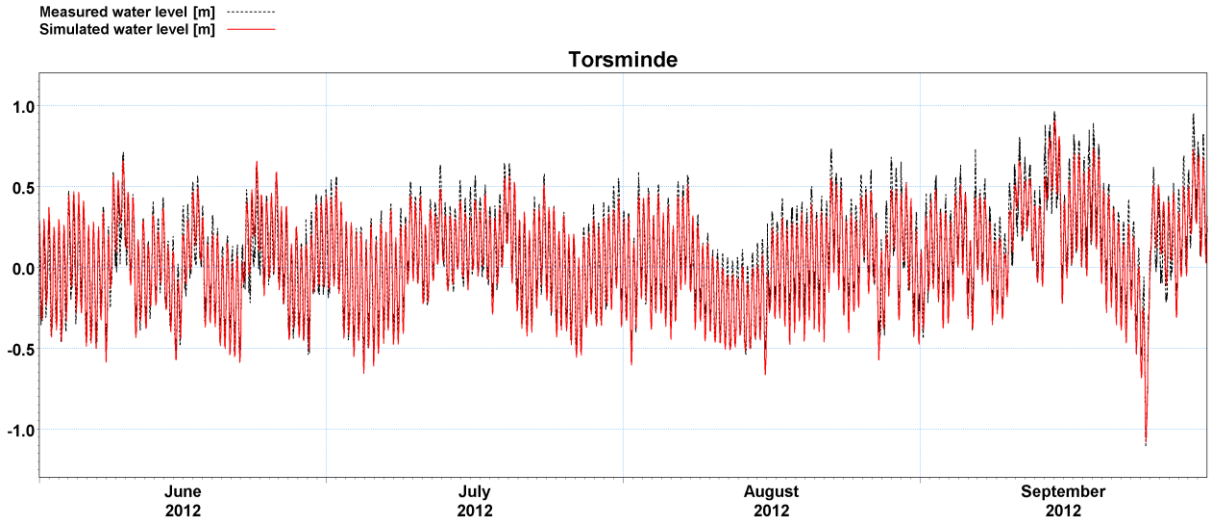

Figure C.12 Measured and modelled water level at Torsminde.

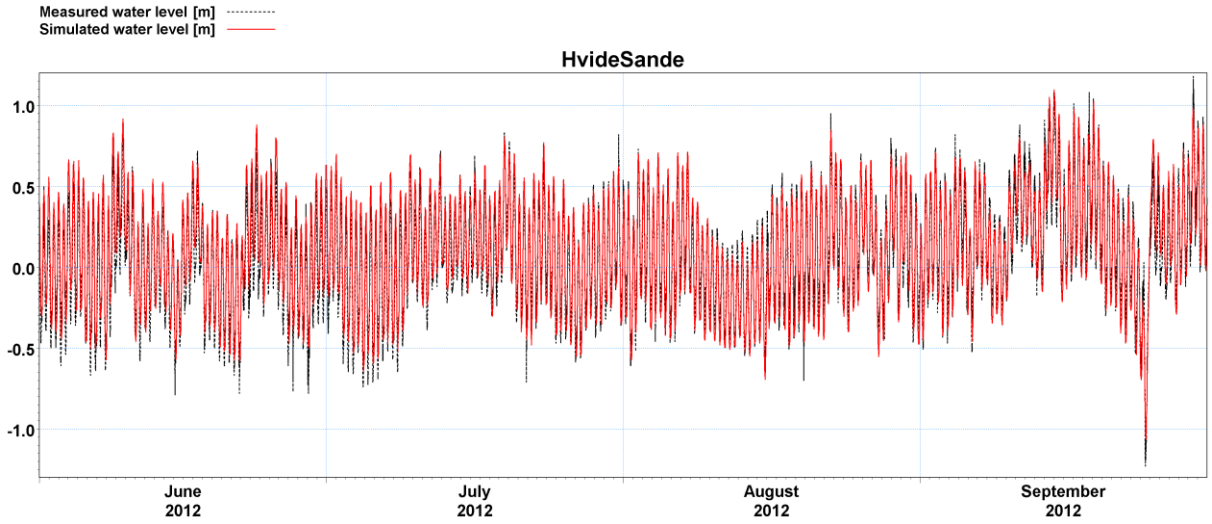

Figure C.13 Measured and modelled water level at Hvide Sande.

Current Velocities

The currents along the West coast of Jutland and inside the OWF's run parallel to the shore in the north-south direction. As shown in Table D.4 the currents are oriented in the directions 180-210° and 0-30° (+/-15°) most of the time.

Figure C.16 to Figure C.19 show the comparison of the depth-averaged current velocities (V-component) of the MIKE 21 HD FM model and DMI's operational DMI-HBM model in the two offshore wind farms (Vesterhav Nord and Vesterhav Syd). It is noted, that the DMI-HBM model is based on a simplistic model bathymetry, whereas the MIKE 21 HD FM model uses a detailed bathymetry based on recent surveys. Therefore, the MIKE 21 HD FM model is expected to provide a more correct representation of the current pattern inside the project area than the DMI-HBM model. Figure C.14 and Figure C.15 shows the location of the model comparison. The comparison shows a good agreement between the two models, though peak currents are generally slightly higher in the DMI-HBM model than in the MIKE 21 HD FM model.

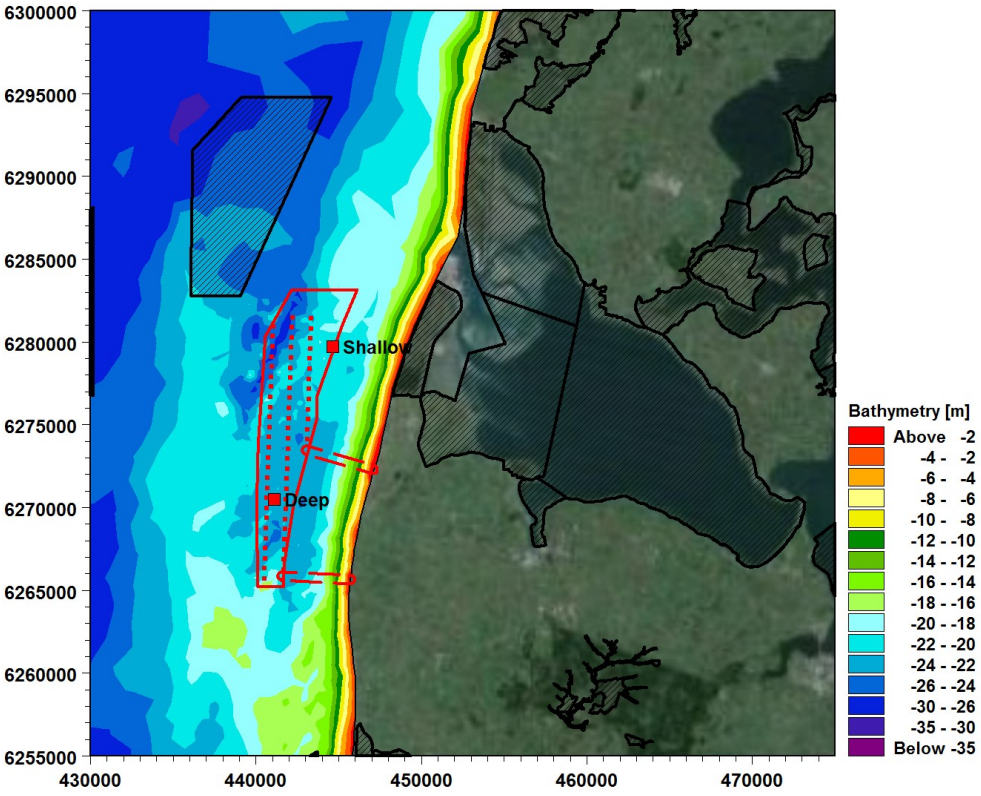

Figure C.14 *Location selected for the current velocity comparison: Vesterhav Nord. Deep point: 56.575°N, 8.042°E, depth: 22.5 mDVR90 Shallow point: 56.658°N, 8.097°E, depth: 17.3 mDVR90*

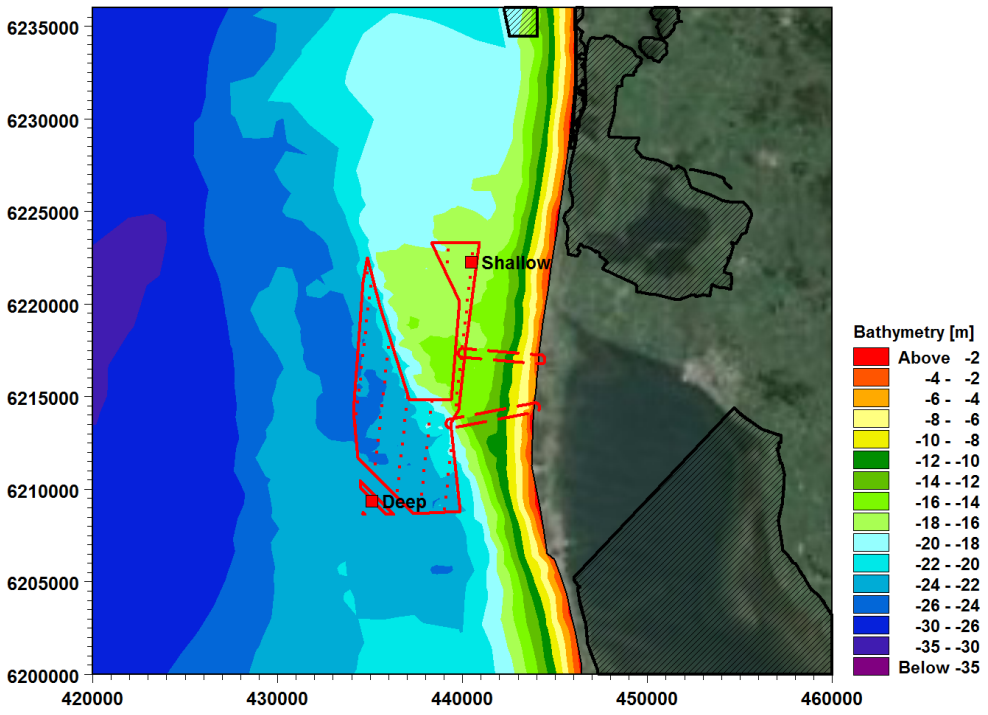

Figure C.15 *Location selected for the current velocity comparison: Vesterhav Syd. Deep point: 56.025°N, 7.958°E, depth: 26.1 mDVR90. Shallow point: 56.142°N, 8.042°E, depth: 14.6 mDVR90*

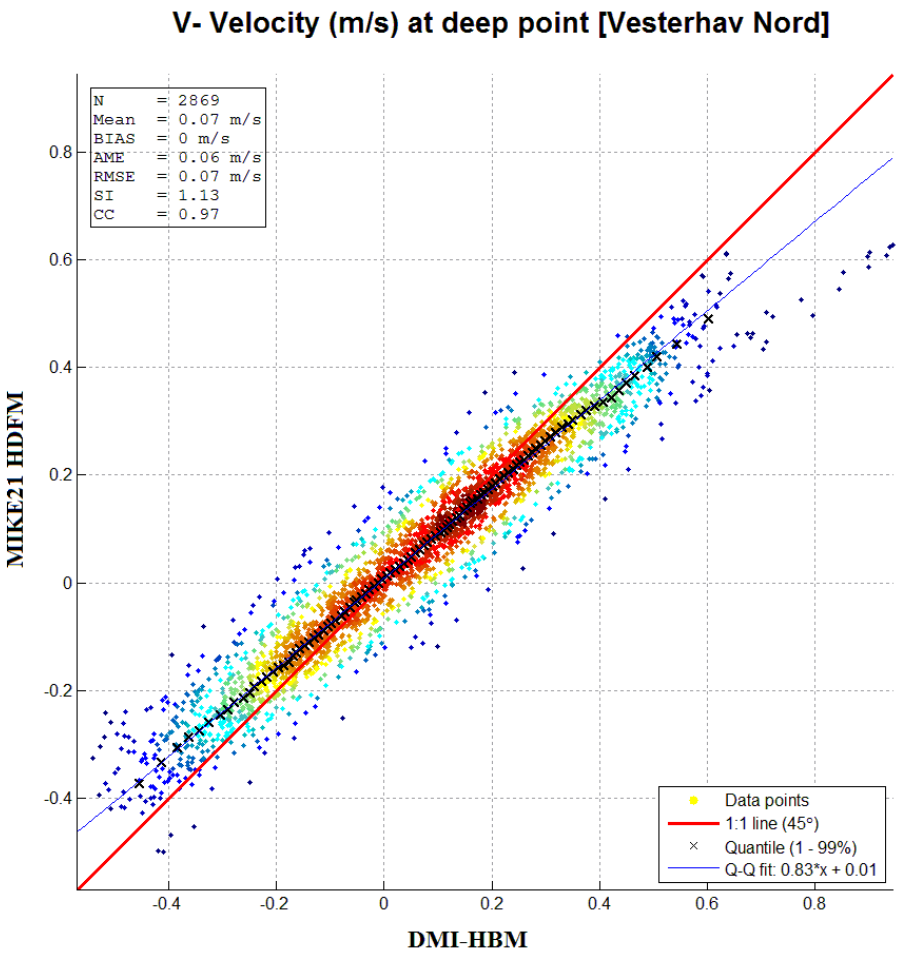

Figure C.16 Comparison of MIKE 21 HD model and DMI-HBM model (V-velocity); Deep point (Vesterhav Nord) [56.575N, 8.042E].

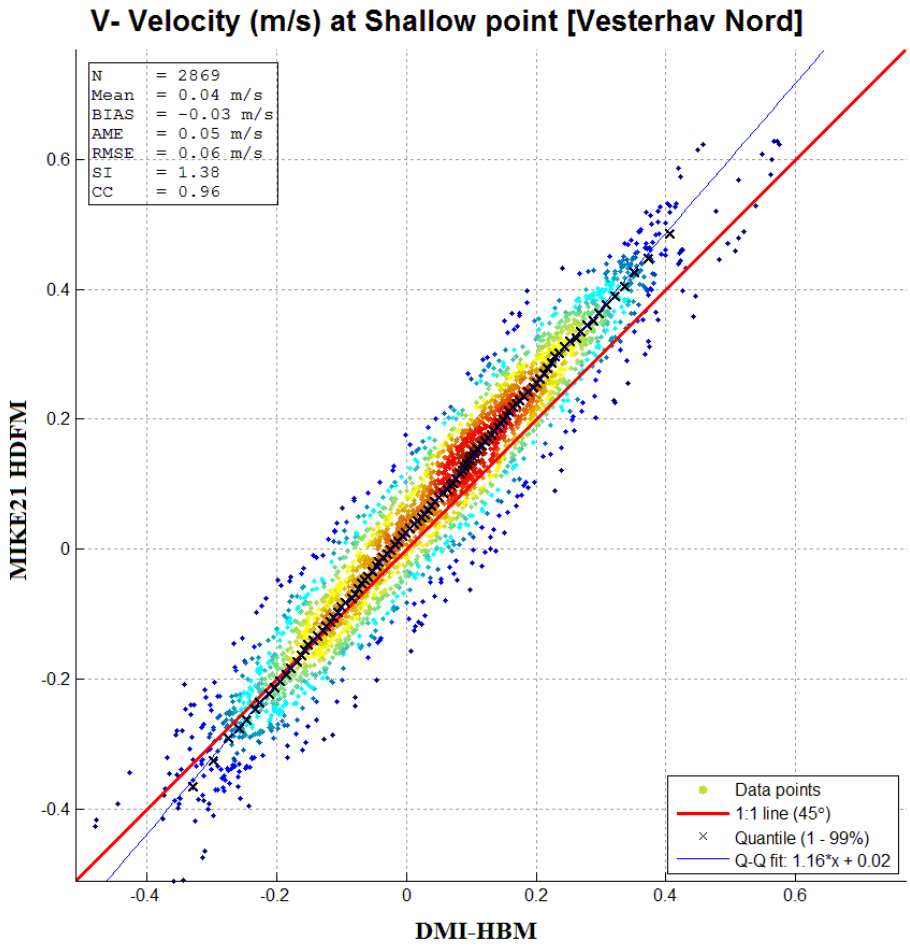

Figure C.17 Comparison of MIKE 21 HD FM model and DMI-HBM model (V-velocity); Shallow point (Vesterhav Nord) [56.658N, 8.097E].

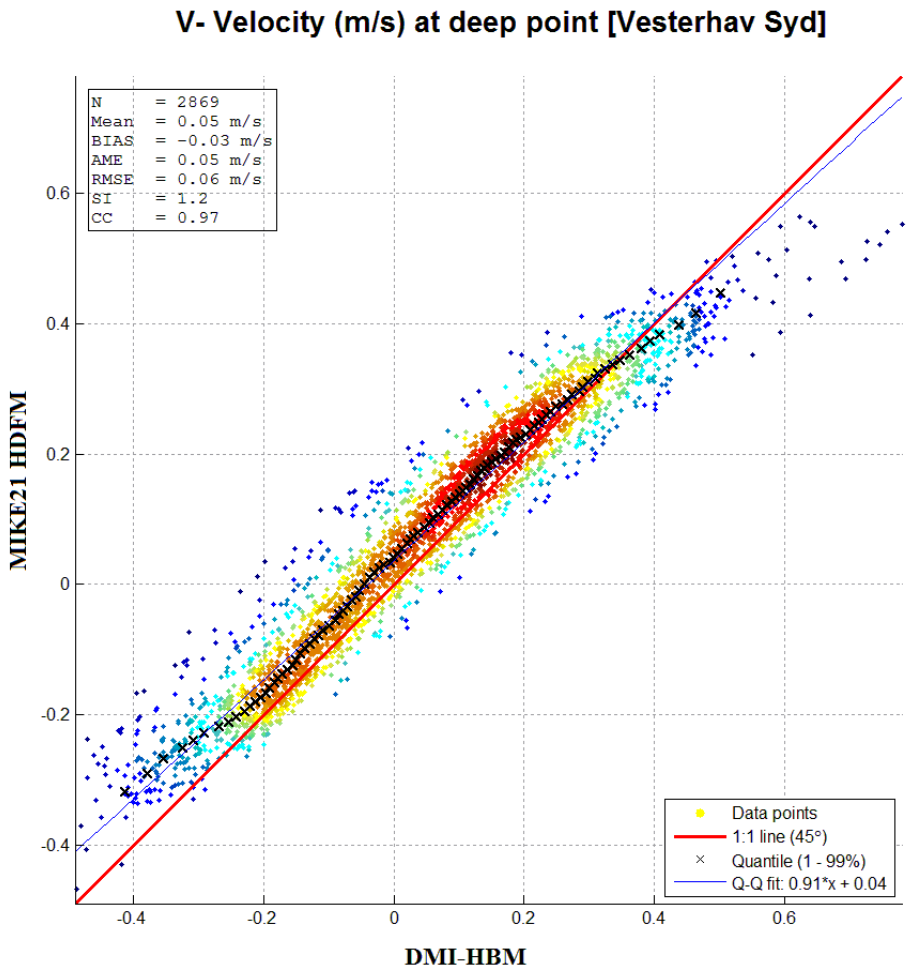

Figure C.18 *Comparison of MIKE 21 HD FM model and DMI-HBM model (V-velocity); Deep point (Vesterhav Syd) [56.025N, 7.958E].*

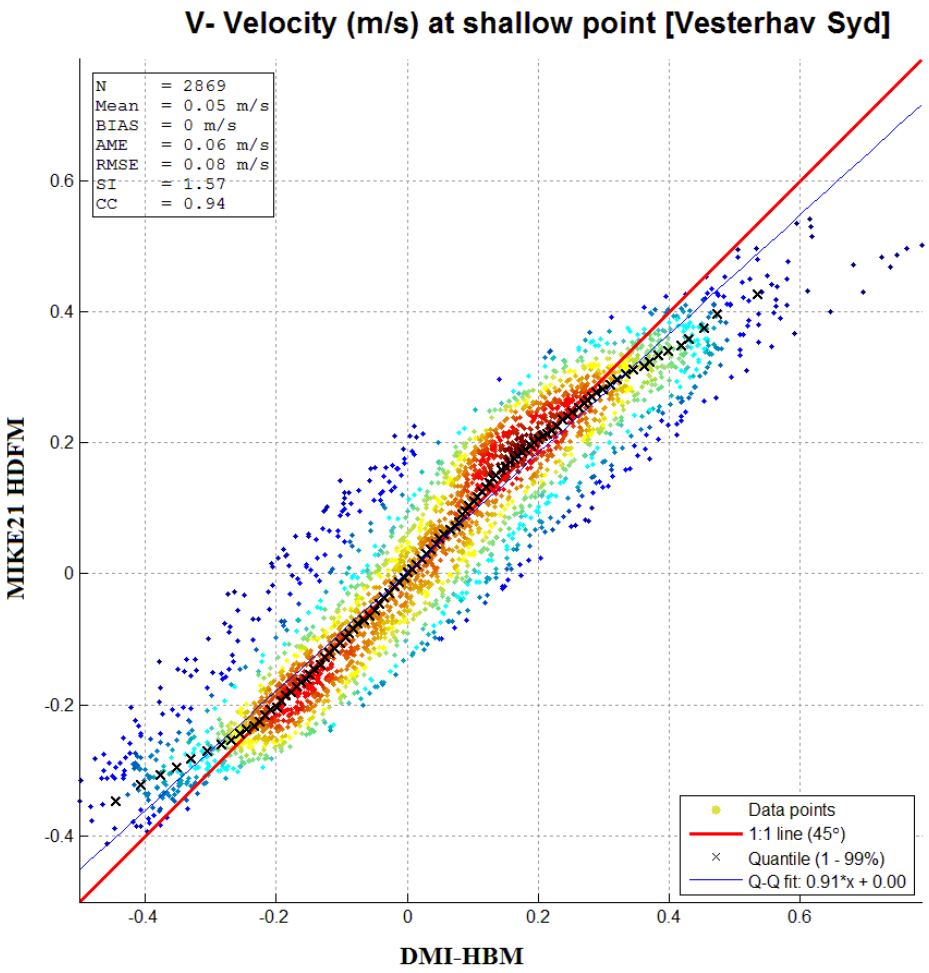

Figure C.19 Comparison of MIKE 21 HD FM model and DMI-HBM model (V-velocity); Shallow point (Vesterhav Syd) [56.142N, 8.042E].

A time series comparison between the DMI and simulated V-velocity components at two locations are presented in Figure C.21 and Figure C.23.

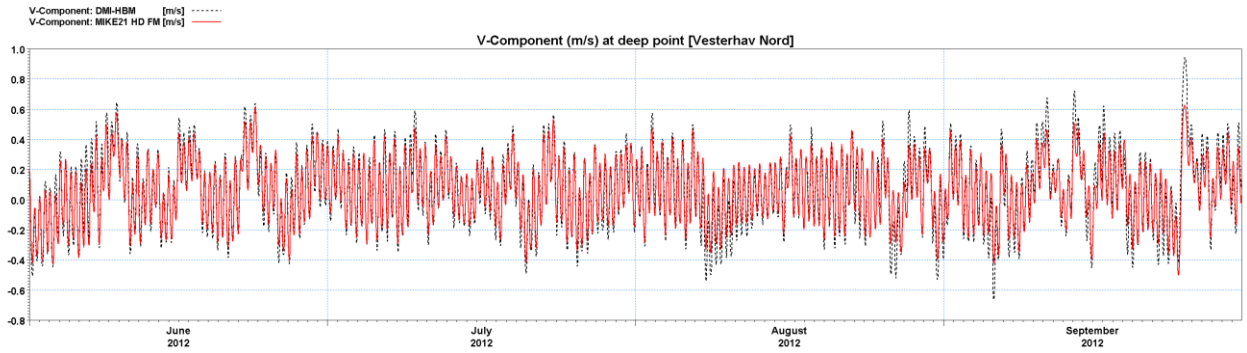

Figure C.20 Comparison of MIKE 21 HD FM model and DMI-HBM model (V-velocity); Deep point (Vesterhav Nord) [56.575N, 8.042E].

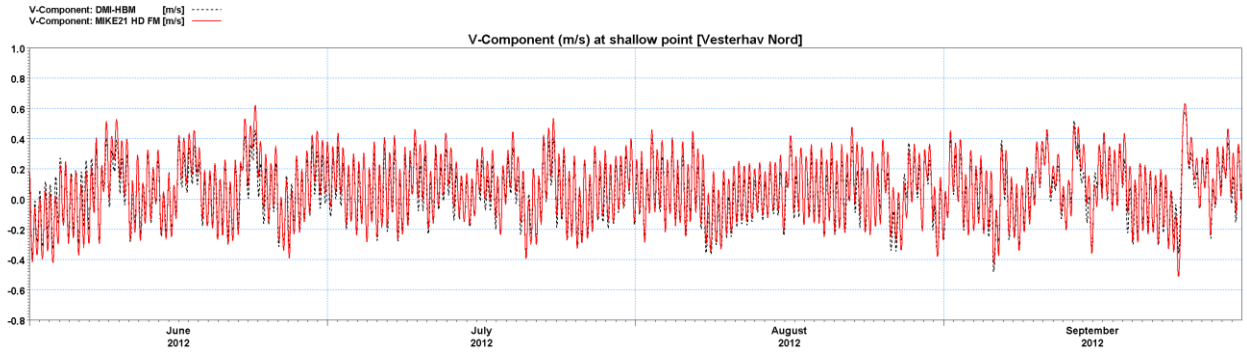

Figure C.21 Comparison of MIKE 21 HD FM model and DMI-HBM model (V-velocity); Shallow point (Vesterhav Nord) [56.658N, 8.097E].

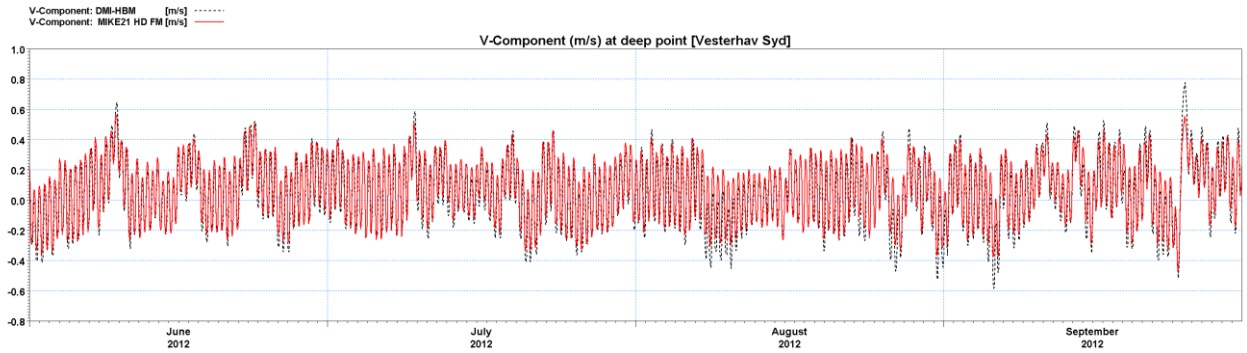

Figure C.22 Comparison of MIKE 21 HD FM model and DMI-HBM model (V-velocity); Deep point (Vesterhav Syd) [56.025N, 7.958E].

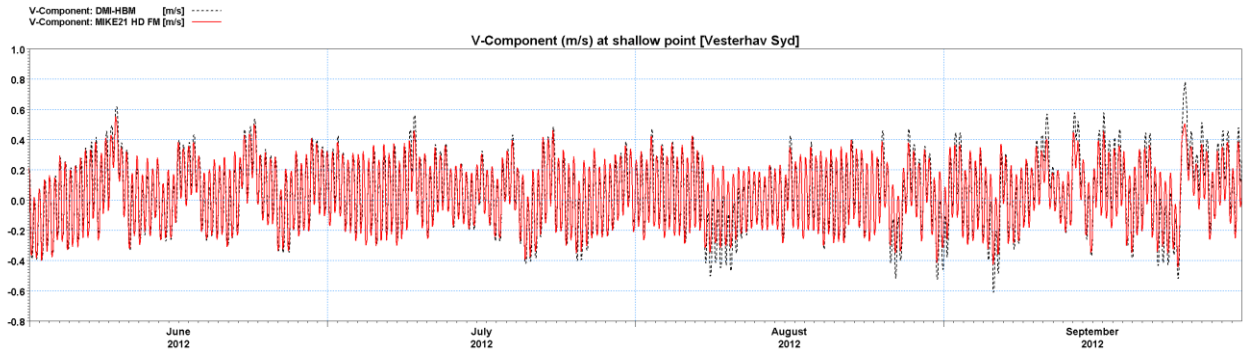

Figure C.23 Comparison of MIKE 21 HD FM model and DMI-HBM model (V-velocity); Shallow point (Vesterhav Syd) [56.142N, 8.042E].

Appendix D Baseline

D.1 Data collection

Met-ocean data including water levels, tidal currents and waves has been collated from a variety of stations located in the vicinity of Vesterhav Nord and Syd OWF. Position and type of data is shown in Figure D.1 and Table D.1.

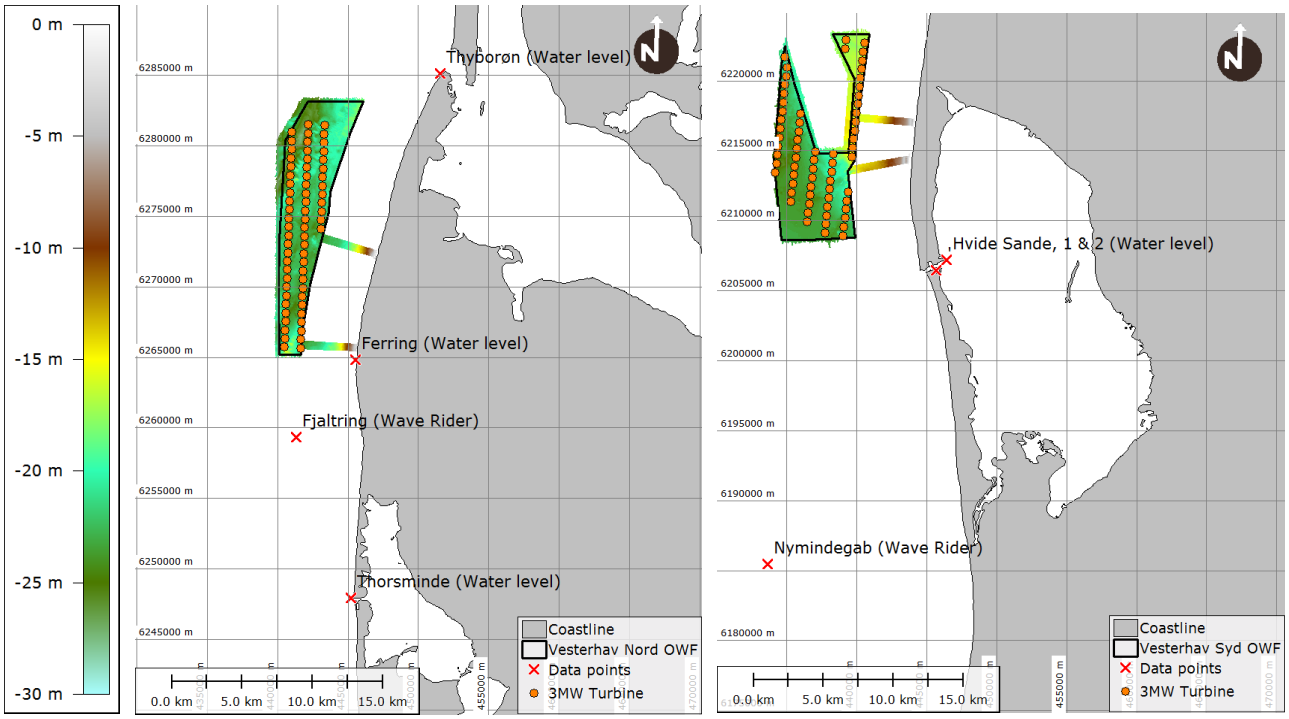

Figure D.1 Data points in the vicinity of the Vesterhav Nord and Vesterhav Syd OWF areas.

Table D.1 Details of each data point.

Observation location name	Type of data	Time series		Data owner	Position (lat, lon)
		Start	End		
Ferring	Water level	01-01-2003	29-10-2013	DMI	56.524593; 8.115164
Thyborøn	Water level	01-01-2003	01-02-2014	DMI	56.707733; 8.208776
Thorsminde	Water level	01-01-2003	01-02-2014	DMI	56.372643; 8.113573
Hvide Sande, 1	Water level	01-01-2003	31-01-2014	DMI	56.000458; 8.128977
Hvide Sande, 2	Water level	01-01-2003	01-02-2014	DMI	56.0072; 8.1412;
Fjaltring (Wave Rider)	Waves	01-01-2011	31-12-2012	KDI	56.475; 8.048
Nymindegab (Wave Rider)	Waves	01-01-2011	31-12-2012	KDI	55.810; 7.941

D.2 Water levels

Table D.2 Distribution of water levels vs. months at Ferring. Frequency of occurrence [%].

Month/water level (m.dvr90)	Jan	Feb	Mar	Apr	May	Jun	Jul	Aug	Sep	Oct	Nov	Dec	Year
<-1.0	<0.1	0.1	0.1	<0.1	-	-	-	-	<0.1	<0.1	<0.1	0.1	0.3
-1.0-(-)0.8	<0.1	0.1	0.1	<0.1	<0.1	-	<0.1	-	<0.1	<0.1	<0.1	0.1	0.5
-0.8-(-)0.6	0.2	0.3	0.5	0.2	0.1	<0.1	<0.1	<0.1	<0.1	0.1	0.1	0.2	1.7
-0.6-(-)0.4	0.4	0.7	0.9	1.0	0.7	0.5	0.3	0.2	0.2	0.3	0.2	0.5	5.9
-0.4-(-)0.2	0.8	1.2	1.7	1.9	1.9	1.8	1.4	1.2	0.9	0.8	0.7	0.8	15.1
-0.2-0.0	1.2	1.4	1.9	2.0	2.3	2.3	2.2	2.1	1.6	1.2	1.1	1.3	20.7
0.0-0.2	1.3	1.4	1.8	1.8	2.2	2.2	2.2	2.2	1.9	1.5	1.4	1.5	21.6
0.2-0.4	1.2	1.2	1.1	1.0	1.4	1.5	1.7	1.8	1.6	1.4	1.5	1.4	16.8
0.4-0.6	0.9	0.7	0.6	0.4	0.5	0.5	0.6	0.8	1.0	1.0	1.2	1.0	9.2
0.6-0.8	0.7	0.3	0.2	0.1	0.1	0.1	0.1	0.2	0.5	0.5	0.8	0.6	4.3
0.8-1.0	0.5	0.1	0.1	<0.1	<0.1	<0.1	<0.1	0.1	0.2	0.2	0.4	0.4	2.0
1.0-1.2	0.3	<0.1	<0.1	-	<0.1	<0.1	<0.1	<0.1	0.1	0.1	0.2	0.2	0.9
1.2-1.4	0.2	<0.1	<0.1	-	-	-	-	-	<0.1	<0.1	0.1	0.1	0.5
1.4-1.6	0.1	<0.1	<0.1	-	-	-	-	-	<0.1	<0.1	0.1	0.1	0.3
1.6-1.8	0.1	<0.1	<0.1	-	-	-	-	-	-	-	<0.1	<0.1	0.1
1.8-2.0	<0.1	<0.1	<0.1	-	-	-	-	-	-	-	<0.1	<0.1	<0.1
>2.0	<0.1	-	-	-	-	-	-	-	-	-	<0.1	<0.1	<0.1
Sum	8.0	7.6	9.0	8.5	9.3	9.0	8.6	8.5	8.1	7.2	7.9	8.2	100

D.3 Currents

Currents are described based on two years of model results from DMI-HBM inside the project area. The two locations are shown in Figure D.2 and represent the deepest and shallowest location in the DMI-HBM model bathymetry inside the pre-investigation area for the Vesterhav Nord OWF:

› Deep point : 56.575°N, 8.042°E, depth: 22.5 m

› Shallow point : 56.658°N, 8.097°E, depth: 17.3 m

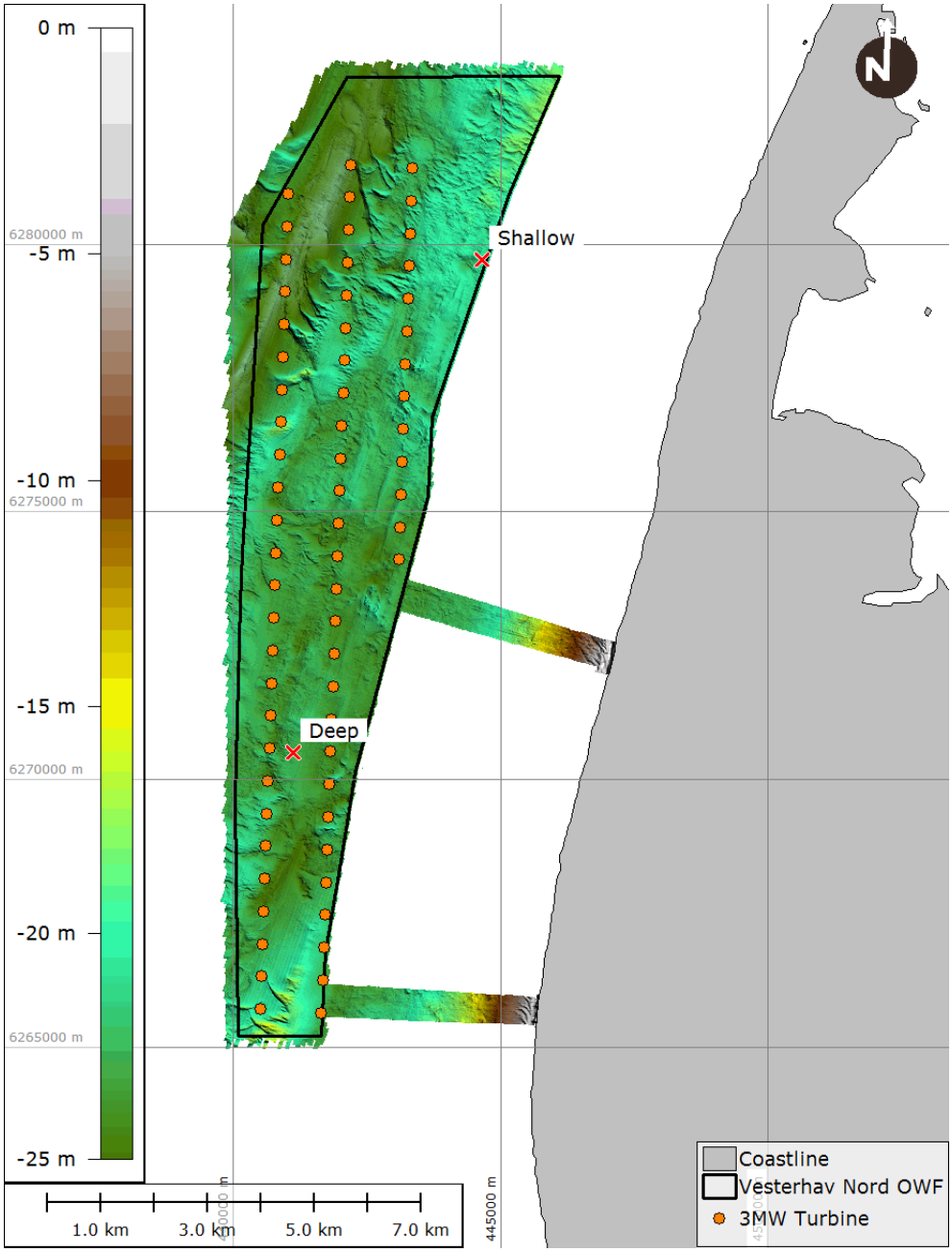

Figure D.2 Location of deep and shallow extraction points.

Table D.3 Distribution of month vs. current velocities (deep point – DMI HMB model) [56.575°N, 8.042°E] . Frequency of occurrence pr. month [%].

Month / current speed (m/s)	Jan	Feb	Mar	Apr	Maj	Jun	Jul	Aug	Sep	Okt	Nov	Dec	Year
0.0-0.1	19.2	21.1	19.3	21.3	19.8	19.9	21.6	19.4	19.2	15.5	17.7	17.0	19.2
0.1-0.2	22.5	21.5	22.7	18.1	22.5	21.1	23.0	21.6	18.8	18.9	21.0	17.1	20.7
0.2-0.3	18.6	20.0	22.3	21.5	21.4	19.8	20.2	20.9	16.8	16.0	17.8	14.7	19.1
0.3-0.4	16.6	16.8	17.1	16.7	16.3	15.3	15.9	16.7	15.5	13.1	13.8	14.0	15.7
0.4-0.5	12.7	12.0	12.0	13.5	12.7	13.7	10.1	8.9	10.6	13.5	9.7	11.0	11.7
0.5-0.6	6.0	5.6	4.6	6.5	4.8	5.6	5.2	6.3	9.3	9.0	7.6	8.0	6.5
0.6-0.7	2.9	1.6	1.6	2.1	1.6	2.8	2.4	3.6	5.0	4.5	3.8	5.8	3.1
0.7-0.8	0.9	1.0	0.3	0.2	0.6	1.5	1.1	2.3	2.4	2.8	2.7	3.9	1.6
0.8-0.9	0.5	0.5	-	-	0.2	0.2	0.4	0.3	0.5	2.4	2.5	2.7	0.9
0.9-1.0	0.2	-	-	-	0.1	-	0.1	0.1	0.6	1.1	0.8	1.7	0.4
1.0-1.1	-	-	-	-	-	-	-	-	0.5	0.7	0.9	1.9	0.3
>1.1	-	-	-	-	-	-	-	-	0.8	2.6	1.7	2.0	0.6
Total	100	100	100	100	100	100	100	100	100	100	100	100	100

Table D.4 Distribution of direction vs. current velocities (deep point – DMI HMB model) [56.575°N, 8.042°E] . Frequency of occurrence [%].

Direction / current speed (m/s)	0	30	60	90	120	150	180	210	240	270	300	330	Omni
0.0-0.1	2.9	3.3	1.0	0.4	0.4	0.5	1.5	3.9	2.1	1.1	0.8	1.3	19.2
0.1-0.2	3.0	8.0	0.1	-	-	<0.1	0.8	8.3	0.5	<0.1	-	<0.1	20.7
0.2-0.3	1.4	9.2	-	-	-	-	0.1	8.4	<0.1	-	-	-	19.1
0.3-0.4	0.5	8.9	-	-	-	-	<0.1	6.2	-	-	-	-	15.7
0.4-0.5	0.2	7.6	-	-	-	-	<0.1	3.8	-	-	-	-	11.7
0.5-0.6	0.1	4.9	-	-	-	-	-	1.5	-	-	-	-	6.5
0.6-0.7	0.1	2.7	-	-	-	-	-	0.4	-	-	-	-	3.1
0.7-0.8	0.1	1.4	-	-	-	-	-	0.2	-	-	-	-	1.6
0.8-0.9	<0.1	0.8	-	-	-	-	-	0.1	-	-	-	-	0.9
0.9-1.0	<0.1	0.4	-	-	-	-	-	<0.1	-	-	-	-	0.4
1.0-1.1	<0.1	0.3	-	-	-	-	-	<0.1	-	-	-	-	0.3
>1.1	<0.1	0.5	-	-	-	-	-	<0.1	-	-	-	-	0.6
Total	8.4	48.1	1.1	0.4	0.4	0.5	2.5	32.8	2.7	1.1	0.8	1.3	100

Table D.5 Distribution of month vs. current velocities (shallow point – DMI HMB model) [56.658°N, 8.097°E]. Frequency of occurrence pr. month [%].

Month / current speed (m/s)	Jan	Feb	Mar	Apr	Maj	Jun	Jul	Aug	Sep	Okt	Nov	Dec	Year
0.0-0.1	30.6	31.8	30.4	30.4	30.0	30.6	33.6	30.0	29.0	25.4	29.0	25.0	29.6
0.1-0.2	28.0	30.3	32.1	28.9	31.0	29.9	32.8	31.9	26.3	25.5	27.2	24.4	29.0
0.2-0.3	23.5	22.4	24.7	26.3	25.7	24.0	21.2	21.6	21.3	21.1	21.7	20.2	22.8
0.3-0.4	13.5	11.8	11.2	11.8	10.8	11.8	9.3	10.0	14.7	15.4	12.5	14.1	12.2
0.4-0.5	3.6	2.8	1.5	2.6	1.7	3.1	2.9	5.5	5.9	6.4	5.4	8.1	4.1
0.5-0.6	0.5	0.9	0.1	-	0.6	0.6	0.3	1.0	1.4	3.0	2.0	3.8	1.2
0.6-0.7	0.3	-	-	-	0.1	-	-	-	0.8	1.1	1.3	3.1	0.6
0.7-0.8	-	-	-	-	-	-	-	-	0.8	0.7	0.1	1.1	0.2
0.8-0.9	-	-	-	-	-	-	-	-	-	0.8	0.3	0.2	0.1
0.9-1.0	-	-	-	-	-	-	-	-	-	0.3	0.2	-	<0.1
1.0-1.1	-	-	-	-	-	-	-	-	-	0.1	0.3	-	<0.1
>1.1	-	-	-	-	-	-	-	-	-	0.1	-	-	<0.1
Total	100	100	100	100	100	100	100	100	100	100	100	100	100

Table D.6 Distribution of direction vs. current velocities (shallow point – DMI HMB model) [56.658°N, 8.097°E]. Frequency of occurrence [%].

Direction / current speed (m/s)	0	30	60	90	120	150	180	210	240	270	300	330	Omni
0.0-0.1	15.4	<0.1	<0.1	<0.1	<0.1	13.9	<0.1	<0.1	<0.1	0.1	29.6	15.4	<0.1
0.1-0.2	16.0	-	-	-	-	13.0	-	-	-	-	29.0	16.0	-
0.2-0.3	13.6	-	-	-	-	9.2	-	-	-	-	22.8	13.6	-
0.3-0.4	8.8	-	-	-	-	3.4	-	-	-	-	12.2	8.8	-
0.4-0.5	3.5	-	-	-	-	0.6	-	-	-	-	4.1	3.5	-
0.5-0.6	1.0	-	-	-	-	0.2	-	-	-	-	1.2	1.0	-
0.6-0.7	0.5	-	-	-	-	0.1	-	-	-	-	0.6	0.5	-
0.7-0.8	0.2	-	-	-	-	<0.1	-	-	-	-	0.2	0.2	-
0.8-0.9	0.1	-	-	-	-	<0.1	-	-	-	-	0.1	0.1	-
0.9-1.0	<0.1	-	-	-	-	<0.1	-	-	-	-	<0.1	<0.1	-
1.0-1.1	<0.1	-	-	-	-	-	-	-	-	-	<0.1	<0.1	-
>1.1	<0.1	-	-	-	-	-	-	-	-	-	<0.1	<0.1	-
Total	59.3	<0.1	<0.1	<0.1	<0.1	40.5	<0.1	<0.1	<0.1	0.1	100	59.3	<0.1

D.4 Wave climate

The wave climate is described based on two years of measurements (wave rider). The wave rider is located approx. 4.5 km from the coast at Fjaltring, shown in Figure D.1.

Table D.7 Distribution of mean wave direction vs. significant wave height (Fjaltring). Frequency of occurrence [%].

MWD (°) / H_{m0} (m)	0	30	60	90	120	150	180	210	240	270	300	330	Omni
0-0.5	0.8	<0.1	<0.1	0.2	0.2	0.1	0.2	0.6	1.0	0.6	3.7	1.6	8.9
0.5-1	2.1	<0.1	0.1	0.2	0.2	0.1	0.6	4.4	4.3	2.2	9.9	4.4	28.5
1-1.5	0.4	-	-	<0.1	0.1	<0.1	0.1	2.5	6.5	3.6	7.0	3.0	23.2
1.5-2	<0.1	-	-	-	-	-	<0.1	0.6	5.1	3.6	5.6	2.0	16.9
2-2.5	-	-	-	-	-	-	-	0.1	2.7	2.6	3.4	1.1	9.9
2.5-3	-	-	-	-	-	-	-	<0.1	1.4	2.1	2.5	0.5	6.5
3-3.5	-	-	-	-	-	-	-	-	0.7	1.0	1.1	0.3	3.0
3.5-4	-	-	-	-	-	-	-	-	0.3	0.5	0.9	0.1	1.7
4-4.5	-	-	-	-	-	-	-	-	0.1	0.2	0.3	0.1	0.8
4.5-5	-	-	-	-	-	-	-	-	0.1	0.1	0.2	<0.1	0.4
5-5.5	-	-	-	-	-	-	-	-	<0.1	0.1	<0.1	-	0.1
5.5-6	-	-	-	-	-	-	-	-	<0.1	<0.1	<0.1	-	0.1
>6	-	-	-	-	-	-	-	-	<0.1	0.1	<0.1	-	0.1
Sum	3.3	<0.1	0.1	0.4	0.4	0.1	0.9	8.2	22.1	16.7	34.6	13.1	100

Table D.8 Distribution of mean wave direction vs. peak wave period (Fjaltring). Frequency of occurrence [%].

MWD (°) / T_p (s)	0	30	60	90	120	150	180	210	240	270	300	330	Omni
<3	0.1	<0.1	0.1	0.3	0.3	0.1	0.1	<0.1	0.1	<0.1	<0.1	0.1	1.2
3-4	0.2	-	<0.1	<0.1	0.1	<0.1	0.4	0.9	0.3	0.3	0.2	0.1	2.5
4-5	0.6	-	-	-	<0.1	-	0.4	2.8	1.5	1.0	0.6	0.7	7.7
5-6	1.7	<0.1	<0.1	<0.1	<0.1	<0.1	0.1	3.6	5.4	3.0	3.1	2.1	19.0
6-7	0.6	-	-	-	-	-	<0.1	0.8	4.9	2.6	4.0	2.1	15.0
7-8	0.1	-	-	-	-	-	-	0.1	5.5	4.2	6.1	2.2	18.2
8-9	<0.1	-	-	-	-	<0.1	-	<0.1	2.4	1.9	3.5	0.7	8.6
9-10	<0.1	-	-	-	-	-	-	-	1.1	1.6	2.6	0.5	5.8
10-11	-	-	-	-	-	-	<0.1	-	0.7	1.5	4.6	1.2	8.0
11-12	-	-	-	-	-	-	-	-	0.1	0.3	4.1	1.4	5.9
12-13	-	-	-	-	-	-	-	-	<0.1	0.1	2.0	0.6	2.6
13-14	-	-	-	-	-	-	-	-	-	<0.1	1.4	0.5	1.9
14-15	-	-	-	-	-	-	-	-	-	<0.1	1.3	0.3	1.6
>15	<0.1	-	-	-	-	-	<0.1	-	-	<0.1	1.3	0.6	1.9
Sum	3.3	<0.1	0.1	0.4	0.4	0.1	0.9	8.2	22.1	16.7	34.6	13.1	100

Table D.9 Distribution of significant wave height vs. peak wave period (Fjaltring). Frequency of occurrence [%].

H_{m0} (m) / T_p (s)	0.0-0.5	0.5-1.0	1.0-1.5	1.5-2.0	2.0-2.5	2.5-3.0	3.0-3.5	3.5-4.0	4.0-4.5	4.5-5.0	5.0-5.5	5.5-6.0	>6	Sum
<3	0.6	0.6	<0.1	-	-	-	-	-	-	-	-	-	-	1.2
3-4	0.6	1.8	0.2	-	-	-	-	-	-	-	-	-	-	2.5
4-5	1.6	4.4	1.6	0.1	-	-	-	-	-	-	-	-	-	7.7
5-6	1.5	7.6	7.4	2.3	0.3	<0.1	-	-	-	-	-	-	-	19.0
6-7	0.3	2.7	5.2	4.7	1.7	0.4	<0.1	-	-	-	-	-	-	15.0
7-8	0.3	1.2	4.2	5.8	4.0	2.3	0.5	0.1	<0.1	-	-	-	-	18.2
8-9	0.3	0.6	1.0	2.0	1.9	1.5	0.9	0.3	0.1	<0.1	-	-	-	8.6
9-10	0.3	0.8	0.5	0.8	1.1	1.0	0.7	0.4	0.1	<0.1	-	-	-	5.8
10-11	0.9	2.1	0.9	0.5	0.6	0.9	0.7	0.8	0.4	0.1	<0.1	<0.1	<0.1	8.0
11-12	1.3	2.2	0.9	0.4	0.2	0.2	0.2	0.2	0.2	0.1	<0.1	<0.1	<0.1	5.9
12-13	0.5	1.3	0.4	0.1	0.1	<0.1	<0.1	<0.1	<0.1	<0.1	<0.1	<0.1	<0.1	2.6
13-14	0.3	1.1	0.3	<0.1	<0.1	<0.1	<0.1	<0.1	<0.1	<0.1	<0.1	<0.1	<0.1	1.9
14-15	0.2	1.0	0.3	0.1	<0.1	<0.1	-	<0.1	<0.1	<0.1	<0.1	<0.1	<0.1	1.6
>15	0.3	1.0	0.3	0.2	<0.1	<0.1	-	<0.1	-	<0.1	-	<0.1	<0.1	1.9
Sum	8.9	28.5	23.2	16.9	9.9	6.5	3.0	1.7	0.8	0.4	0.1	0.1	0.1	100

Table D.10 Distribution of month vs. significant wave height (Fjaltring). Frequency of occurrence pr. month [%].

Months / H_{m0} (m)	Jan	Feb	Mar	Apr	Maj	Jun	Jul	Aug	Sep	Okt	Nov	Dec	Sum
0-0.5	-	10.3	0.3	13.9	23.1	9.6	10.1	18.0	3.0	8.3	9.5	3.3	8.9
0.5-1	22.4	26.1	39.1	44.6	22.8	40.4	32.1	36.2	20.1	18.5	28.4	19.4	28.5
1-1.5	25.7	22.1	24.6	16.0	24.0	25.5	30.8	17.6	25.6	26.2	22.2	18.9	23.2
1.5-2	20.5	18.0	19.4	12.5	14.8	13.0	19.0	12.7	22.1	14.6	18.1	17.0	16.9
2-2.5	15.1	9.0	9.2	8.1	7.1	7.7	4.7	8.0	13.7	10.5	8.9	14.0	9.9
2.5-3	7.0	6.5	4.5	1.5	5.7	3.0	2.8	3.5	9.6	13.0	6.2	10.9	6.5
3-3.5	2.6	3.7	1.0	2.2	1.7	0.8	0.5	3.0	3.7	5.3	3.1	6.9	3.0
3.5-4	2.4	2.9	1.2	1.0	0.9	-	-	0.7	0.9	2.8	2.1	4.6	1.7
4-4.5	2.6	1.2	0.5	0.2	-	-	-	0.2	0.8	0.8	0.5	1.6	0.8
4.5-5	1.0	0.3	0.1	-	-	-	-	-	0.4	0.1	0.2	1.7	0.4
5-5.5	0.1	0.1	0.1	-	-	-	-	-	0.1	-	0.3	0.7	0.1
5.5-6	0.1	-	-	-	-	-	-	-	-	-	0.1	0.4	0.1
>6	0.4	-	-	-	-	-	-	-	-	-	0.3	0.5	0.1
Sum	100	100	100	100	100	100	100	100	100	100	100	100	100

Appendix E Sediment spill – Scenario definition

E.1 Purpose

The EIA assessment will be compiled upon a comprehensive description of the technical project encompassing wind turbines specifications, foundation strategy and installation methods for inter-array and export cables, respectively. However, the description will not be constrained to one exact definition of the project, but instead describe the boundaries and span of a project that incorporates the “most likely” with a “worst-case” in mind. The reason for this approach is that the Danish Energy Agency has not yet assigned concession of construction and operation of the offshore wind farms and therefore preserves degrees of freedom in the technical aspects of the project.

This project note defines the assumed scenarios for sediment spill during installation of turbine foundations as well as inter-array and export cables at the Vesterhav Nord Offshore Windfarm.

The sediment spill scenarios will be used as input for numerical modelling in MIKE 21 MT.

E.2 Methodology

The spill during dredging/excavation and jetting operations are closely related to the characteristics of the sediments found within the upper 1-2 meters of the seabed substrata.

A geophysical survey was conducted by EGS International in December 2013 [ref. /9/] and COWI conducted soil classification tests and laboratory testing on sediment samples. The results of the tests are presented in [ref. /25/]. Additional laboratory testing by GEO is available for two cable corridors towards shore [ref. /10/].

E.2.1 Seabed characteristics

An overview of the bathymetry and sample locations is shown in Figure E.1.

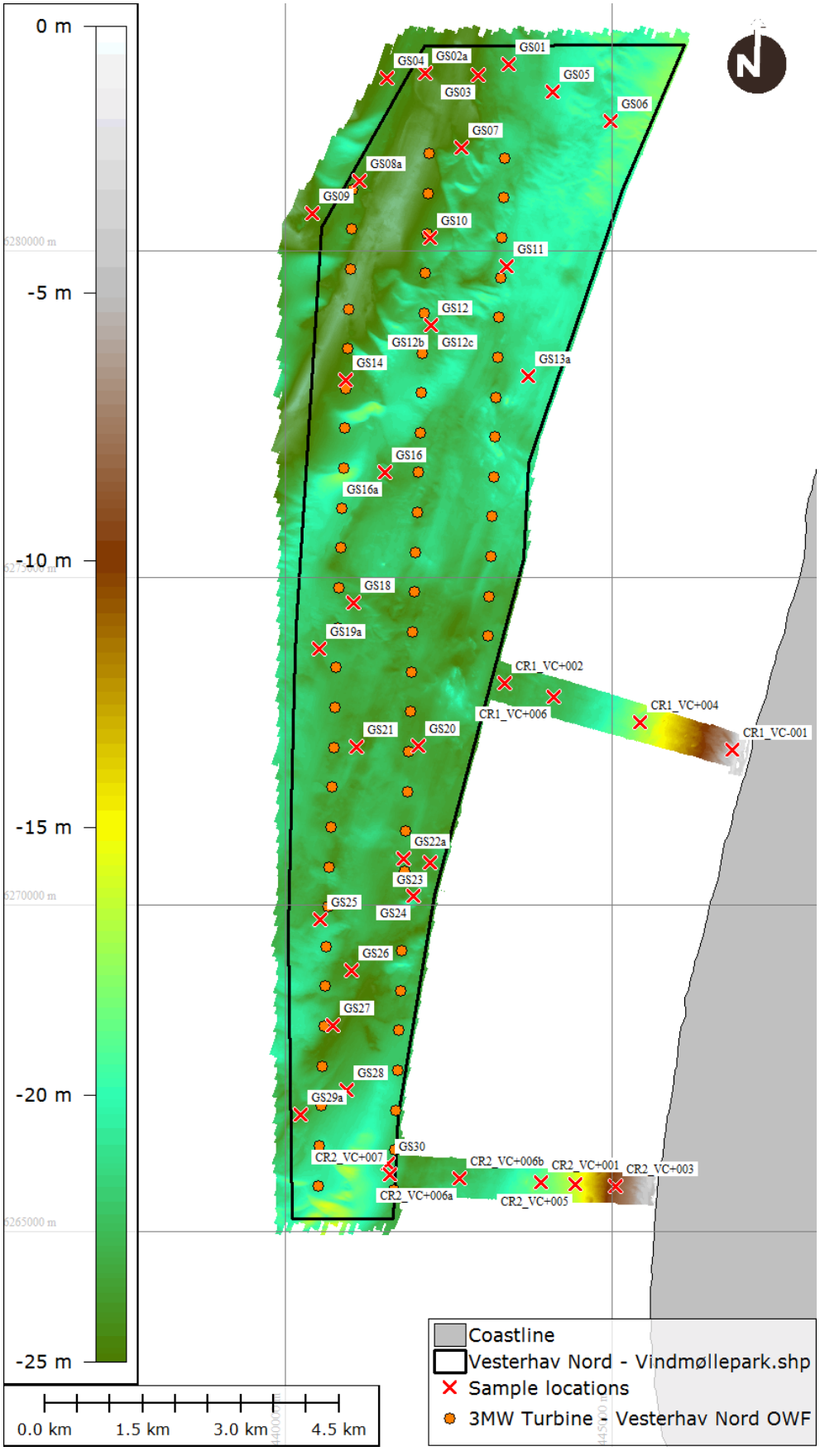

Figure E.1 Vesterhav Nord, OWF layout (3 MW) and location of geotechnical samples.

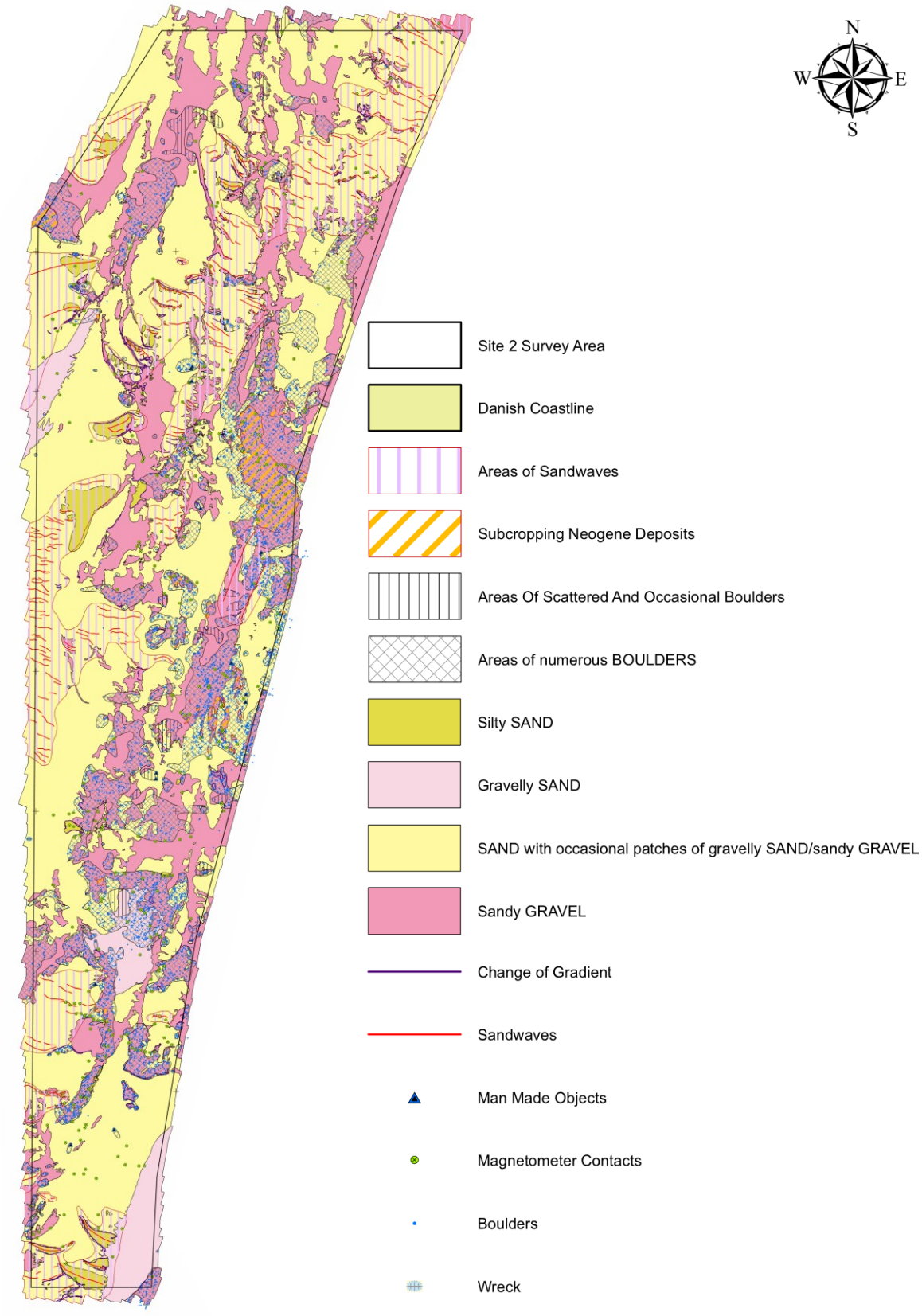

Figure E.2 Surface and subsurface sediment types in wind farm area [ref /9/]

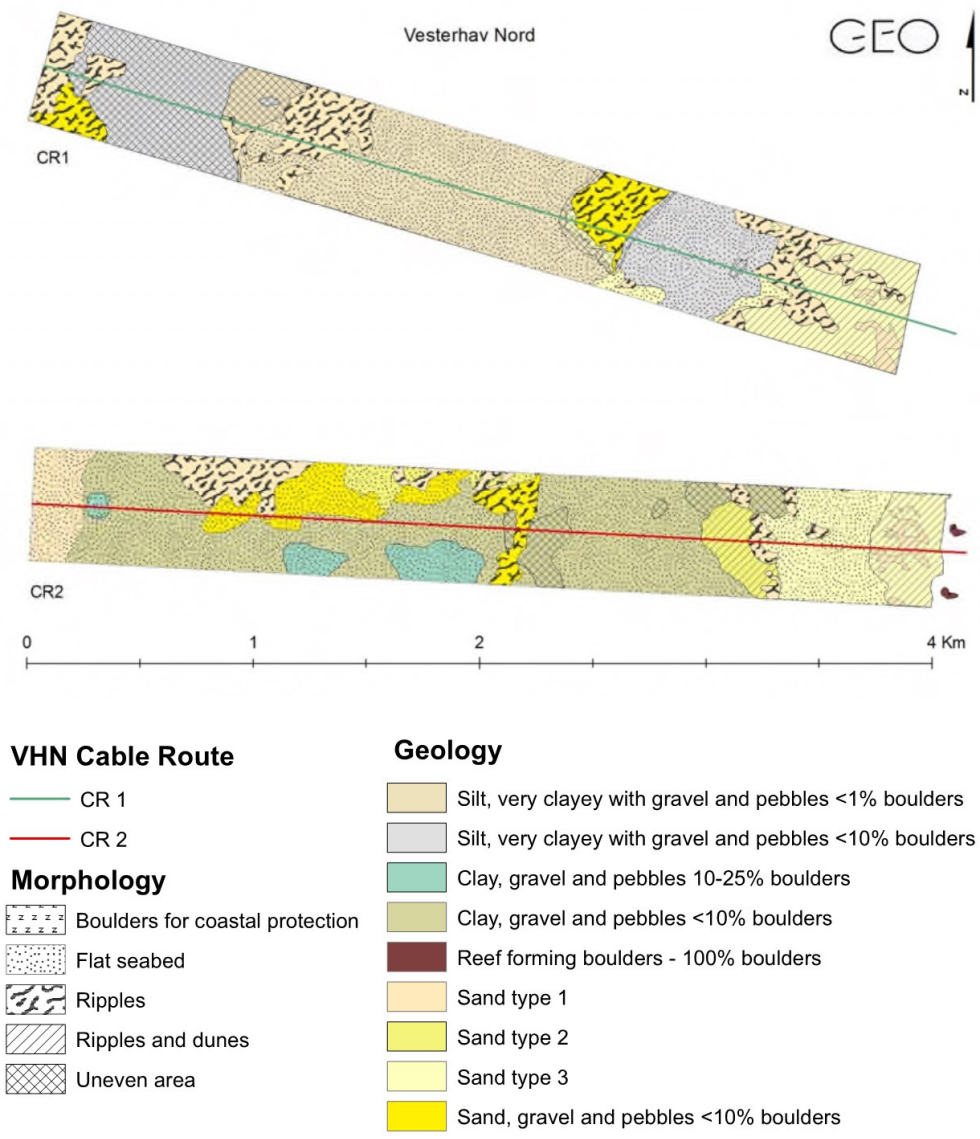

Figure E.3 Geology and morphology at cable corridors [ref. /10/].

As shown in Figure E.2 and Figure E.3 the seabed and subsurface sediment consists mainly of sand and gravel. In the cable corridors, the grain size shifts to silt and clay, with some gravel content.

As shown in Table E.1, 77 % of the surficial sediment samples are characterized as ”SAND” or “GRAVEL”, while 8 %, 12 % and 4 % are characterized as “CLAY”, “CLAY TILL” and “SILT”. The Wentworth grain-size classification scheme shown in Table E.3 is used for the description of the grain-size distribution [ref. /26/].

Table E.1 Surficial sediment characteristics and average distribution of fines/organic contend of each sediment type (classification).

Classification	Coarse silt 31-63 µm	Medium silt 15.6-31 µm	Fine silt 7.8-15.6 µm	Very fine silt 3.9-7.8 µm	Clay i 2-3.9 µm	Clay ii <2 µm	Loss on ignition	% of samples
GRAVEL	2.9%	0.0%	0.0%	0.0%	0.0%	0.0%	1.1%	23%
SAND	2.1%	0.0%	0.0%	0.0%	0.0%	0.2%	0.6%	54%
SILT	9.0%	17.0%	10.0%	15.0%	13.0%	33.0%	9.3%	4%
CLAY TILL	3.0%	7.0%	5.0%	6.3%	6.7%	22.3%	3.8%	12%
CLAY	6.7%	13.7%	10.7%	13.0%	8.0%	24.7%	5.1%	8%
Total	2.9%	2.0%	1.4%	1.9%	1.4%	4.5%	1.6%	100%

Grain size distributions are summarised in Table E.3.

Sediment spill scenarios are based on the average sediment characteristics as described in Table E.1 and Table E.3. The scenarios will thus not consider the spatial variation of the seabed substrate. This simplification is justifiable because sediment samples and wind turbines are evenly distributed in the project area.

Table E.2 The Wentworth grain-size classification scheme, [ref. /26/].

Millimeters (mm)	Micrometers (µm)	Phi (ϕ)	Wentworth size class		Rock type
4096		-12.0	Boulder		
256		-8.0	Cobble	Gravel	Conglomerate/ Breccia
64		-6.0	Pebble		
4		-2.0	Granule		
2.00		-1.0			
1.00		0.0	Very coarse sand		
1/2 0.50	500	1.0	Coarse sand		
1/4 0.25	250	2.0	Medium sand	Sand	Sandstone
1/8 0.125	125	3.0	Fine sand		
1/16 0.0625	63	4.0	Very fine sand		
1/32 0.031	31	5.0	Coarse silt		
1/64 0.0156	15.6	6.0	Medium silt		
1/128 0.0078	7.8	7.0	Fine silt	Silt	Siltstone
1/256 0.0039	3.9	8.0	Very fine silt		
0.00006	0.06	14.0	Clay	Mud	Claystone

Table E.3 Grain size distribution at Vesterhav Nord OWF.

Classification	Sample	Coarse silt 31-63 µm	Medium silt 15.6-31 µm	Fine silt 7.8-15.6 µm	Very fine silt 3.9-7.8 µm	Clay i 2-3.9 µm	Clay ii <2 µm	Loss on ignition
SAND	GS01	1%	0%	0%	0%	0%	0%	0.5%
SAND	GS02a	2%	0%	0%	0%	0%	0%	0.7%
GRAVEL	GS03	9%	0%	0%	0%	0%	0%	1.5%
SAND	GS04	2%	0%	0%	0%	0%	0%	0.7%
SAND	GS05	1%	0%	0%	0%	0%	0%	0.3%
SAND	GS06	1%	0%	0%	0%	0%	0%	0.3%
SAND	GS07	5%	0%	0%	0%	0%	0%	0.3%
CLAY	GS08	5%	9%	9%	15%	10%	29%	4.6%
CLAY	GS08a	10%	4%	6%	12%	8%	28%	4.2%
SAND	GS10	2%	0%	0%	0%	0%	0%	0.7%
GRAVEL	GS11	1%	0%	0%	0%	0%	0%	0.9%
GRAVEL	GS12b	0%	0%	0%	0%	0%	0%	0.8%
GRAVEL	GS12c	0%	0%	0%	0%	0%	0%	0.5%
SAND	GS13a	0%	0%	0%	0%	0%	0%	0.3%
SAND	GS14	3%	0%	0%	0%	0%	0%	0.8%
SAND	GS16	4%	0%	0%	0%	0%	0%	0.6%
SAND	GS16a	1%	0%	0%	0%	0%	0%	0.3%
SAND	GS18	0%	0%	0%	0%	0%	0%	0.3%
SAND	GS19a	1%	0%	0%	0%	0%	0%	0.3%
SAND	GS20	3%	1%	0%	1%	0%	5%	1.7%
GRAVEL	GS21	1%	0%	0%	0%	0%	0%	1.0%
SAND	GS22a	3%	0%	0%	0%	0%	0%	0.9%
GRAVEL	GS23	1%	0%	0%	0%	0%	0%	0.9%
SAND	GS24	4%	0%	0%	0%	0%	0%	1.0%
SAND	GS25	2%	0%	0%	0%	0%	0%	0.9%
SAND	GS27	3%	0%	0%	0%	0%	0%	0.7%
SAND	GS28	3%	0%	0%	0%	0%	0%	1.0%
GRAVEL	GS29a	10%	0%	0%	0%	0%	0%	2.9%
SAND	GS30	1%	0%	0%	0%	0%	0%	0.3%
CLAY	CR1+002	5%	28%	17%	12%	6%	17%	6.5%
CLAY TILL	CR1+004	3%	9%	4%	7%	7%	21%	5.9%
SILT	CR1+006	9%	17%	10%	15%	13%	33%	9.3%
SAND	CR1-001	0%	0%	0%	0%	0%	0%	0.3%
CLAY TILL	CR2+001	3%	6%	5%	6%	6%	24%	3.4%
SAND	CR2+003	3%	0%	0%	0%	0%	0%	0.5%
CLAY TILL	CR2+005	3%	6%	6%	6%	7%	22%	2.1%
GRAVEL	CR2+006b_1.2D	1%	0%	0%	0%	0%	0%	0.8%
SAND	CR2+006b_1.3D	4%	0%	0%	0%	0%	0%	0.8%

SAND	CR2+007	2%	0%	0%	0%	0%	0%	0.4%
Average		**2.9%**	**2.0%**	**1.4%**	**1.9%**	**1.4%**	**4.5%**	**1.6%**
Standard deviation		2.7%	5.5%	3.6%	4.3%	3.3%	9.8%	2.0%

Fractions	**Fraction 1 "Coarse Silt" 31-63 µm**	**Fraction 2 "Medium – fine silt" 3.9-31 µm**	**Fraction 3 "Clay" <3.9µm**	**"Fines" <63 µm**
Average	2.9%	5.3%	5.9%	14.0%

E.2.2 Sediment spill properties

During dredging/excavation operations total spill is related to the amount of fines in the dredged material. If the fines content below 63 µm (silt and clay) is high, then the spill volume will be equally high and the sediment plume can be expected to affect a larger area due to low settling velocities. The average amount of fines below 63 µm in 49 samples is 14.0% (see Table E.3).

Coarse sand and gravel fractions will typically settle quickly with velocities of 10 cm/s and 2 m/s. Hence, even under strong currents sand will settle within 50-100 m and gravel will settle within 5-10 m from the dredger. Therefore, only silt and clay fractions are considered in the spill scenarios.

Clay minerals, together with organic material and fractions of silt aggregate to form flocs. The process of aggregation and break-up is called *flocculation*.

The flocculation process generates a more cause sediment fraction with particles of lower density than the "solitary" clay and silt particles that they enchain. The aggregates formed will have higher settling velocities than individual quartz particles, but this is somewhat balanced by the reduction of the particle density.

The relation between the settling velocity of aggregates (w_f) and "solitary" sediments (w_{sd}) is defined with a flocculation factor (f) (see Figure E.4).

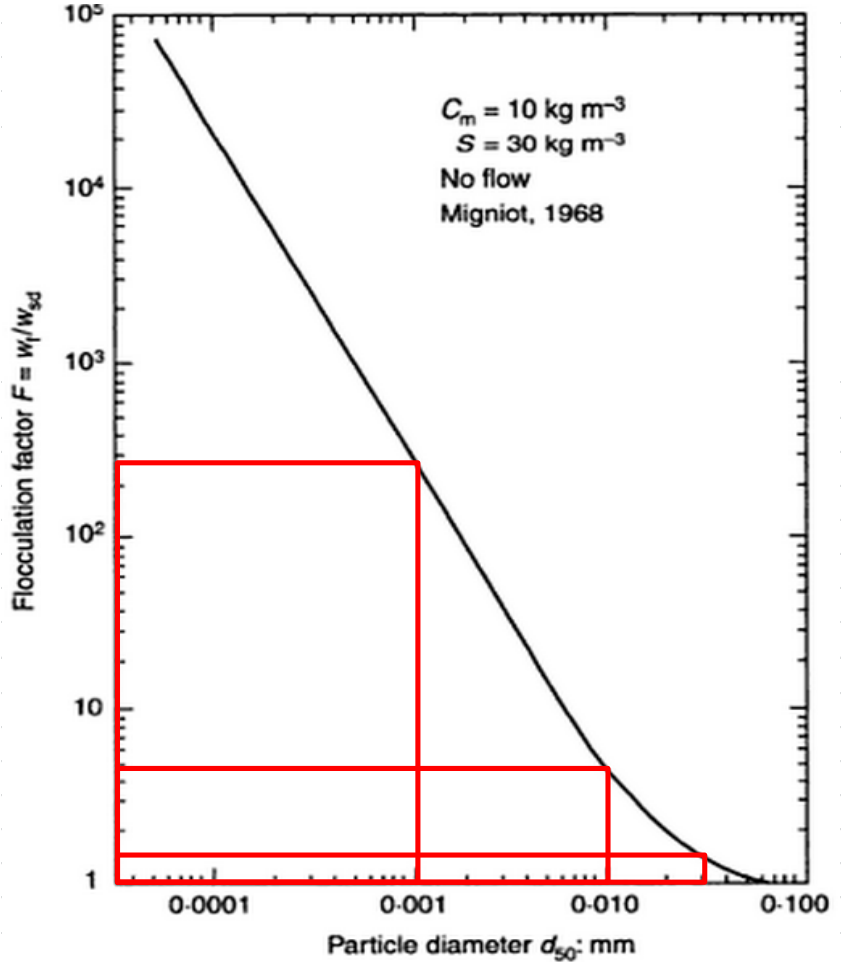

Figure E.4 *Relation between flocculation factor (f) and "solitary" particle diameter (d_{50}) [ref. /27/].*

Settling velocities w_{sd} of "solitary" particles are calculated using Stokes law:

$$w_{sd} = \frac{1}{18} \cdot \frac{g\, d^2(\rho_s - \rho_w)}{\mu}$$

Where d is the average particle diameter of a given fraction, ρ_s is the particle density, ρ_w is the water density and μ is the kinematic viscosity of water (0.0013 kg/m/s at 10°C).

The settling velocity of flocs is $w_f = f \cdot w_{sd}$.

Settling velocities and erosion parameters etc. are given in Table E.4.

Table E.4 Sediment and bed properties.

Properties			Fraction 1 "coarse silt"	Fraction 2 "medium – fine silt"	Fraction 3 "clay"
Fraction	d	[µm]	**31-63**	**3.9-31**	**<3.9**
Mean particle size	d50	[mm]	0.04	0.01	0.001
"Solitary" Settling velocity	W_{sd}	[mm/s]	1.1	0.07	0.0007
Flocculation factor	f	-	1	5	280
Settling velocity of flocs	W_f	[mm/s]	1.10	0.34	0.19
Water density	ρ_w	[kg/m^3]	1013	1013	1013
Particle density	ρ_s	[kg/m^3]	2650	2650	2650
Dry density	ρ_d	[kg/m^3]	1600	1600	1600
Wet density	ρ_b	[kg/m^3]	2000	2000	2000
Critical bed shear stress (Erosion)	$\tau_{e,c}$	[N/m^2]	0.4		
Critical bed shear stress (Deposition)	$\tau_{d,c}$	[N/m^2]	0.04		
Erosion Rate Coefficient	M_{se}	kg/(m²s)	4e-5		
Bed density "Weakly consolidated" (Dry)	$\rho_{bed,d}$	[kg/m^3]	200		
Bed density "Weakly consolidated" (Wet)	$\rho_{bed,b}$	[kg/m^3]	1140		

E.2.3 Sea bed properties

Sedimentation of spilled particles is studied in MIKE 21 MT based on a number of deposition and erosion parameters. When the particles reach the seabed they will deposit permanently or temporarily depending on wave and current climate (bed shear stress) at the time.

The fine material will form a layer of mobile fluid mud which will consolidate over time. During this stage, the self-weight of the particles expels the pore water and

forces the particles closer together. This in time causes the dry density of the seabed to increase and the layer thickness to decrease (see Table E.5).

Table E.5 Typical dry density and consolidation of muds [ref. /28/].

Sediment stage	General description	Rheological behavior	Dry density (kg/m^3)
Freshly deposited (1 day)	Fluff	Mobile fluid mud	50-100
Weakly consolidated (1 week)	Mud	Fluid stationary mud	100-250
Medium consolidated (1 month)		Deforming cohesive bed	250-400
Highly consolidated (1 year)		Stationary cohesive bed	400-550
Stiff mud (10 years)	Stiff clay	Stationary cohesive bed	550-650

The erosive properties of deposited spill material also depend on the consolidation and dry density of the bed layer. Mobile fluid mud will thus be much more likely to get re-suspended than a consolidated cohesive seabed. Table E.6 shows the critical bed shear stress for erosion of different soil types and bulk dry densities.

In MIKE 21 MT the bed parameters are assessed for a dry density of $\rho_{bed,d}$ =200 kg/m^3, which corresponds to "fluid stationary mud" after 1 week of consolidation. The critical shear stress for erosion is assessed from Table E.6 as $\tau_{e,c}$ = 0.4 N/m^2.

The surface erosion rate constant, M_{se}, is also calculated based on the dry density of "fluid stationary mud" based on [ref. /29/]:

$$log_{10}(M_{se}) = 0.23 \exp\left[\frac{0.198}{\rho_{bed,b} - \rho_w}\right] \rightarrow M_{se} = 4 * 10^{-5}\, {kg}/{m^2 s}$$

Where,

Bulk wet density: $\rho_{bed,b} = \rho_w \epsilon + \rho_s(1-\epsilon) = 1.140 g/cm^3$

Porosity: $\epsilon = \frac{\rho_s - \rho_{bed,d}}{\rho_s} = 0.925$

Table E.6 Critical bed shear stress for surface erosion for different bulk dry densities [ref. /30/].

Soil Type	Sand	Organic	τ_{se}^{c} = critical shear stress for surface erosion [Pa]				
	[%]	[%]	ρ_b =100 [kg/m3]	ρ_b =150 [kg/m3]	ρ_b =200 [kg/m3]	ρ_b =250 [kg/m3]	ρ_b =300 [kg/m3]
Kaolinite (saline water)	0	0	-	0.05 – 0.10	0.30 – 0.40	-	-
Kaolinite (distilled water)	0	0	-	0.05 – 0.10	0.15 – 0.20	0.20 – 0.25	0.25 – 0.30
Hollands Diep 1 (lake)	9	10	0.15 – 0.25	0.30 – 0.40	0.40 – 0.50	0.60 – 0.80	-
Hollands Diep 2 (lake)	23	9	0.15 – 0.25	0.30 – 0.40	0.40 – 0.50	0.80 – 1.00	-
Ketelmeer (lake)	7	12	0.10 – 0.20	0.20 – 0.25	0.25 – 0.35	0.50 – 0.70	-
Biesbosch (lake)	8	8	0.20 – 0.25	0.25 – 0.30	0.30 – 0.35	0.50 – 0.70	-
Maas (river)	36	8	0.15 – 0.30	0.30 – 0.40	0.40 – 0.50	0.80 – 1.00	-
Breskens Harbour (estuary)	27	5	0.15 – 0.25	0.25 – 0.35	0.35 – 0.45	0.60 – 0.80	-
Delfzijl Harbour (estuary)	60	2	0.05 – 0.15	0.15 – 0.20	0.20 – 0.25	0.40 – 0.60	-
Loswal Noord (sea)	69	2	0.20 – 0.30	0.30 – 0.35	0.35 – 0.45	0.60 – 0.80	-
Brisbane, Grangemouth and Belawan	0	-	0.20 – 0.30	0.40 – 0.60	0.80 – 1.00	-	-
Loire	-	-	0.10 – 0.15	0.15 – 0.20	0.20 – 0.30	0.30 – 0.40	0.80 – 1.20
Cardiff Bay	-	-	0.20 – 0.30	0.40 – 0.50	0.60 – 0.70	0.70 – 0.90	-

E.3 Operations

E.3.1 Seabed preparation for installation of concrete gravity base foundation

Gravity based foundations generally require more dredging/excavation works to be performed than other types of foundations. Therefore the gravity based foundation type is considered worst case in terms of sediment spill.

Preparation of the seabed by removal of the topsoil and replacement by a stone bed is normally required prior to installation of the gravity base structures. Depending on the seabed/ground conditions, water depth and available equipment, the seabed preparation can be performed in the following sequence:

- Removal of the top surface of the seabed to a level where undisturbed soil is encountered.
- Gravel is placed into the excavated hole to form a firm level base.

The quantities for seabed preparation depend on the seabed/ground conditions including variations within the area of the wind farm. Quantities are presented in

Table E.7 for two different sizes of turbines considering the expected average water depth at each of the six offshore wind farms.

Table E.7 General estimate of Dredgin/excavation for gravity base foundation.

Gravity base	Smålandsfarvandet and Sæby		Bornholm and Sejerø Bugt		Vesterhav Nord and Vesterhav Syd	
Average water depth (and range) [m]	12.5 (5-20)		17.5 (10-25)		20 (15-25)	
Wind turbine size (number of turbines)	3.0 MW (66)	10.0 MW* (20)	3.0 MW (66)	10.0 MW* (20)	3.0 MW (66)	10.0 MW* (20)
Size of excavation (diameter) [m]	23-26	26-29	24-27	27-30	25-28	40-50
Volume of excavation [m³] (per foundation)	1,000-1,300	1,600-2,200	1,100-1,500	1,800-2,400	1,200-1,600	2,000-3,200

* rough estimate

The excavated material may be used as ballast within the gravity base structures or loaded onto split-hopper barges and transported to use elsewhere or to a registered disposal site at sea.

The Dredgin/excavation may be carried out by dredger or using a back-hoe excavator from a barge. The approximate duration of dredging/excavation (average 2 m depth) is expected to be 2 days for each gravity base.

The spill scenarios will be based the installation of 66 x 3 MW turbines, because this will result in a larger total volume of dredging/excavation and thus larger spill volumes than installation of 20 x10 MW turbines. dredging/excavation works for 66 x 3 MW gravity based foundations and 1,600 m^3 of dredging/excavation per foundation is considered “worst-case”.

Furthermore, the scenarios will assume that Dredgind/excavation is performed at two foundations in parallel (by two dredgers). This assumption is considered “worst -case” because intense Dredgind/excavation activities result in larger turbidity.

The experience of “Sund og Bælt” from the Øresund bridge project was, that backhoe dredgers cause 2.7-3.9 % of spill when dredging/excavation in clay till (see Table E.8). The “worst case” assumption is that 5 % of the material is spilled, and that all spill will be particles smaller than 63 µm. The gradation and volume of the spill is defined in Table E.9. It is assumed that the spill will occur at the water surface (z=0).

Table E.8 Measured sediment spill for all dredging activities during the Øresund bridge project [ref. /11/].

Dredging Area	Dredged amount	Spill						Equipment	Dominating material	Typical layer thickness	Dredging period
		Dredging	Reclama-tion	Total	Dredging	Reclama-tion	Total				
	(m3)	(ton)	(ton)	(ton)	(%)	(%)	(%)	(-)	(-)	(m)	(ww/yy)
Peninsula Harbour	86.000	7.288	71	7.359	4,5%	0,0%	4,5%	Dipper	Limestone	1 - 2	45/95-49/95
Island harbour no. 1	179.000	8.469	1.027	9.496	2,4%	0,3%	2,7%	Dipper	Clay till	1 - 3	02/96-18/96
Island harbour no. 3	41.000	1.258	138	1.396	1,6%	0,2%	1,7%	Dipper	Clay till	2 - 3	14/96-15/96
South west access channel	263.000	14.666	787	15.452	2,8%	0,2%	3,0%	Dipper	Clay till	1 - 2	49/95-19/96
CD#3-1	632.000	23.411	2.082	25.493	1,9%	0,2%	2,1%	Dipper	Clay till	1 - 2	19/96-35/96
East access channel	201.000	15.128	1.211	16.340	4,0%	0,3%	4,3%	Dipper	Clay till	0.5 - 2	10/96-15/96
Flinte Channel, central area	217.000	11.142	623	11.764	2,7%	0,2%	2,9%	Dipper	Clay till	0.5 - 1	42/95-18/96
Tunnel Trench (Castor)	2.189.000	167.789	2.506	170.295	4,0%	0,1%	4,1%	Cutter	Limestone	10 - 13	29/96-35/97
CD#1	207.000	33.292	162	33.454	8,6%	0,0%	8,6%	Cutter	Limestone	1 - 3	48/96-51/96
CD#3-2	680.000	59.578	2.613	62.191	4,5%	0,2%	4,7%	Cutter	Clay till	2 - 3	24/97-34/97
Flinte Channel, other areas	2.050.000	113.931	9.352	123.284	2,9%	0,2%				0.1 - 1	16/97-52/98
Tunnel Trench (back-hoe)	68.000	2.323	92	2.416	1,8%	0,1%	1,9%	Back-hoe	Limestone	10 - 12	20/98-34/98
Drogden Construction channel	133.000	12.582	892	13.475	5,0%	0,4%	5,4%	Back-hoe	Limestone	0.1 - 1	14/97-20/97
East Construction channel	164.000	11.016	2.770	13.786	3,4%	0,9%				0.5 - 2	30/96-34/96
Drogden Navigation channel	243.000	12.548	326	12.874	2,7%	0,1%				0.1 - 1	33/97-48/98
Access channel Lernacken	309.000	23.578	1.046	24.624	3,9%	0,2%				2 - 4	41/96-24/97
Foundation pits for Bridge piers	295.000	30.847	3.717	34.563	5,3%	0,6%	5,9%	Back-hoe	Limestone	10	46/96-10/99
Total	7.957.000	548.846	29.414	578.261	3,6%	0,2%	3,8%				

Table E.9 Spill gradation and volume per foundation.

	Fraction 1 "coarse silt"	Fraction 2 "medium – fine silt"	Fraction 3 "clay"	Total
% of all	1.0%	1.9%	2.1%	5.0%
% of spill	20%	38%	42%	100%
Dry density [kg/m3]	1,600	1,600	1,600	-
Spill [m3]	16	30	34	80
Spill [kg]	26,000	48,000	54,000	128,000

E.3.2 Jetting of cables

The installation of the export cables is assumed to be carried out by a specialist cable laying vessel, with the cables stored on a turn-table, designed to carry the necessary lengths and maintain the minimum bend radius.

All the submarine cables, both array and export cables will be buried to provide protection from fishing activity, dragging of anchors etc.

Depending on the seabed condition the cable will be jetted, ploughed, installed in a pre-excavated trench or rock covered for protection. However, as a "worst case" assumption jetting will be assumed for the sediment spill study.

Water jetting is a cable protection method in which an underwater machine (usually a ROV) that is equipped with water jets fed by high power water pumps liquefy the

sediment below the cable, allowing it to sink to a specified depth (dependent on the penetrating length of the swords), after which coarse sediments are deposited.

The width of the seabed affected by the jetting operation itself will be in approx. 0.7-1.2 meters depending on the size of cable and the jetting equipment used. A sketch of the jetted trench with indicative dimensions is shown in Figure E.5. The jetting trench has an area of approximately 1.6 m^3/m.

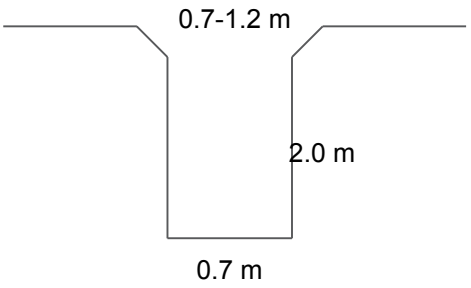

Figure E.5 Sketch of the jetted trench with indicative dimensions.

The rate of progress, of the jetting operation, is depending on the seabed encountered. Generally, a progress of 500-2000 m/day can be expected.

The spill scenarios will be based on the assumption that 2000 m is jetted per day, corresponding to 3200 m^3 per day. It is conservatively assumed that all fines (<0.063 mm) will be spilled, corresponding to 14.0 % of spill ~ 449 m^3/day 720 tons/day (see Table E.10). Particles are released very close to the seabed, but in the modelling scenarios, it is assumed that sediment is released 2 m above seabed.

Table E.10 Spill gradation and volume per 2000 m (1 day) of jetting.

	Fraction 1 "coarse silt"	Fraction 2 "medium – fine silt"	Fraction 3 "clay"	Total
Average	2.9%	5.3%	5.9%	14.0%
% of spill (total)	20%	38%	42%	100%
Dry density [kg/m3]	1,600	1,600	1,600	-
Spill [m3]	91	169	189	449
Spill [kg]	145,000	270,000	300,000	720,000

E.4 Scenarios

The two spill scenarios are described below.

› Scenario 1 - Seabed preparation

› Scenario 2 – Jetting of cables

Both scenarios are based on works being performed during typical current conditions at the project location. The reference period is a three month period which is selected based on two years for currents inside the boundaries of the wind farm. The two year dataset is derived from DMI's operational flow model DMI-HBM in 22.5 m water depth [56.58°N, 8.04°E].

Based on the evaluation the reference period is selected as 01.06.2012 to 30.08.2012. Current roses for the two years dataset and the reference period are presented in Figure 3.9 and Table 3.5.

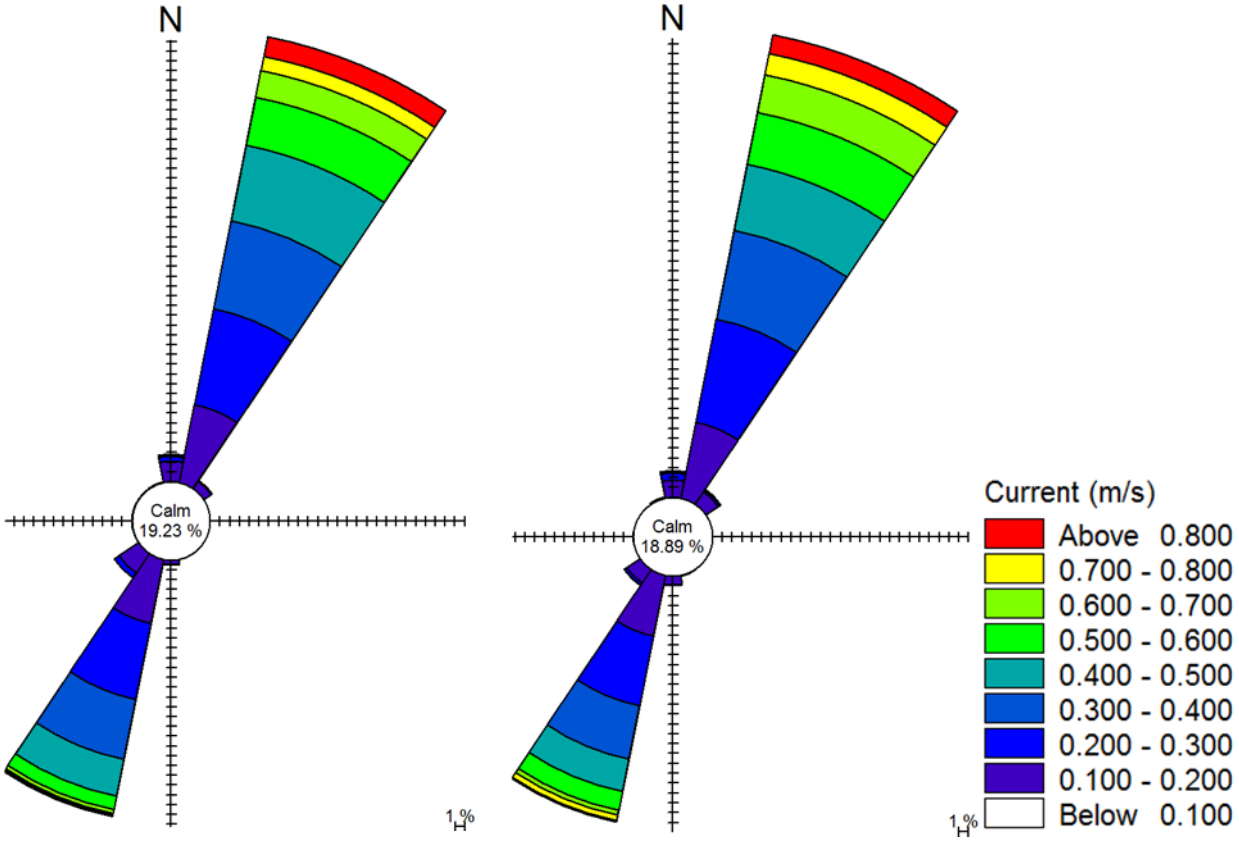

2011-2012 *01.06.2012 – 30.08.2012*

Figure E.6 *Current rose during 3 month reference period and two year dataset at [56.58°N, 8.04°E], 22.5 m water depth. Dataset: DMI-HMB hindcast.*

Table E.11 Current statistics during reference period and two year dataset at [56.58°N, 8.04°E], 22.5 m water depth. Dataset: DMI-HMB hindcast.

		Current vector component [m/s]		
	Current direction	**Minimum**	**Maximum**	**Average**
2011 - 2012	East/West, U	-0.51	0.64	0.028
	North/South, V	-1.25	2.19	0.098
June. 2012 - Augp. 2012	East/West, U	-0.39	0.45	0.031
	North/South, V	-0.90	1.33	0.092

E.4.1 Scenario 1 – Seabed preparation

The 3 MW - layout of the Vesterhav Nord OWF is presented in Figure E.7. It is noted that the turbines are placed in a rectangular mesh, containing the rows 1-27 and columns B-D.

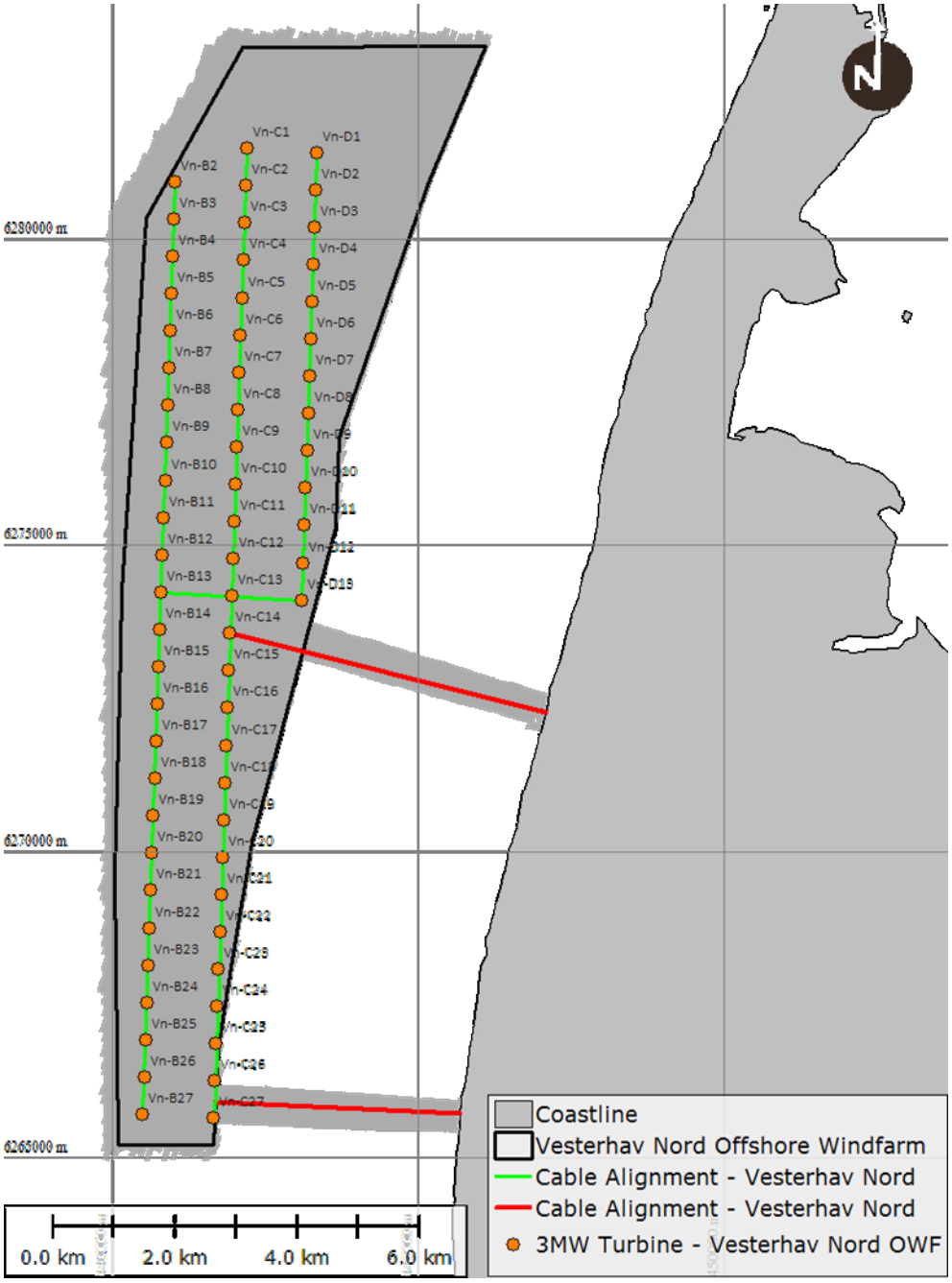

Figure E.7 Tentative 3MW layout of Vesterhav Nord OWF.

As described in section E.3.1, seabed preparation will be performed at two foundations in parallel with two dredgers. It is assumes that dredging/excavation will be performed one column at the time starting in the row closest to shore. Dredger no 1 will start at D1 and dredger no 2 will start at C12, see Table E.12 and Figure E.7.

Dredging/excavation will last for 66 consecutive days starting 01-06-2012 and ending 06-08-2012. The simulation will be extended another 14 days (20.08.2012) in order to allow the spill material to settle.

In total 105,600 m^3 is dredged as part of the seabed preparation and 8,450 tons of fines are spilled during the works.

Table E.12 Definition of scenario 1 – Seabed preparation.

			Fraction 1			Fraction 2			Fraction 3			Dredging/excavation schedule		
Turbine id	Duration [days]	Volume [m3]	Spill [%]	Spil [kg]	Spill-rate [kg/s]	Spill [%]	Spil [kg]	Spill-rate [kg/s]	Spill [%]	Spil [kg]	Spill-rate [kg/s]	Dredger id	Start date	End date
Vn-D1	2	1600	1.0%	26011	0.15	1.9%	48143	0.28	2.1%	53847	0.31	1	01-06-2012 00:00	03-06-2012 00:00
…	…	…	…	…	…	…	…	…	…	…	…	…	…	…
Vn-B10	2	1600	1.0%	26011	0.15	1.9%	48143	0.28	2.1%	53847	0.31	1	04-08-2012 00:00	06-08-2012 00:00
Vn-C12	2	1600	1.0%	26011	0.15	1.9%	48143	0.28	2.1%	53847	0.31	2	01-06-2012 00:00	03-06-2012 00:00
…	…	…	…	…	…	…	…	…	…	…	…	…	…	…
Vn-B27	2	1600	1.0%	26011	0.15	1.9%	48143	0.28	2.1%	53847	0.31	2	04-08-2012 00:00	06-08-2012 00:00
Total	66 d			1717 t			3177 t			3554 t			66 days	

E.4.2 Scenario 2 – Jetting of cables

The turbines are connected with 33 kV cables allowing 36 MW of wind turbines to be connected to each cable. The layout of the inter-array and export cables has not been defined at this stage, but in the spill scenario it is assumed that turbines are connected as shown in Figure E.8.

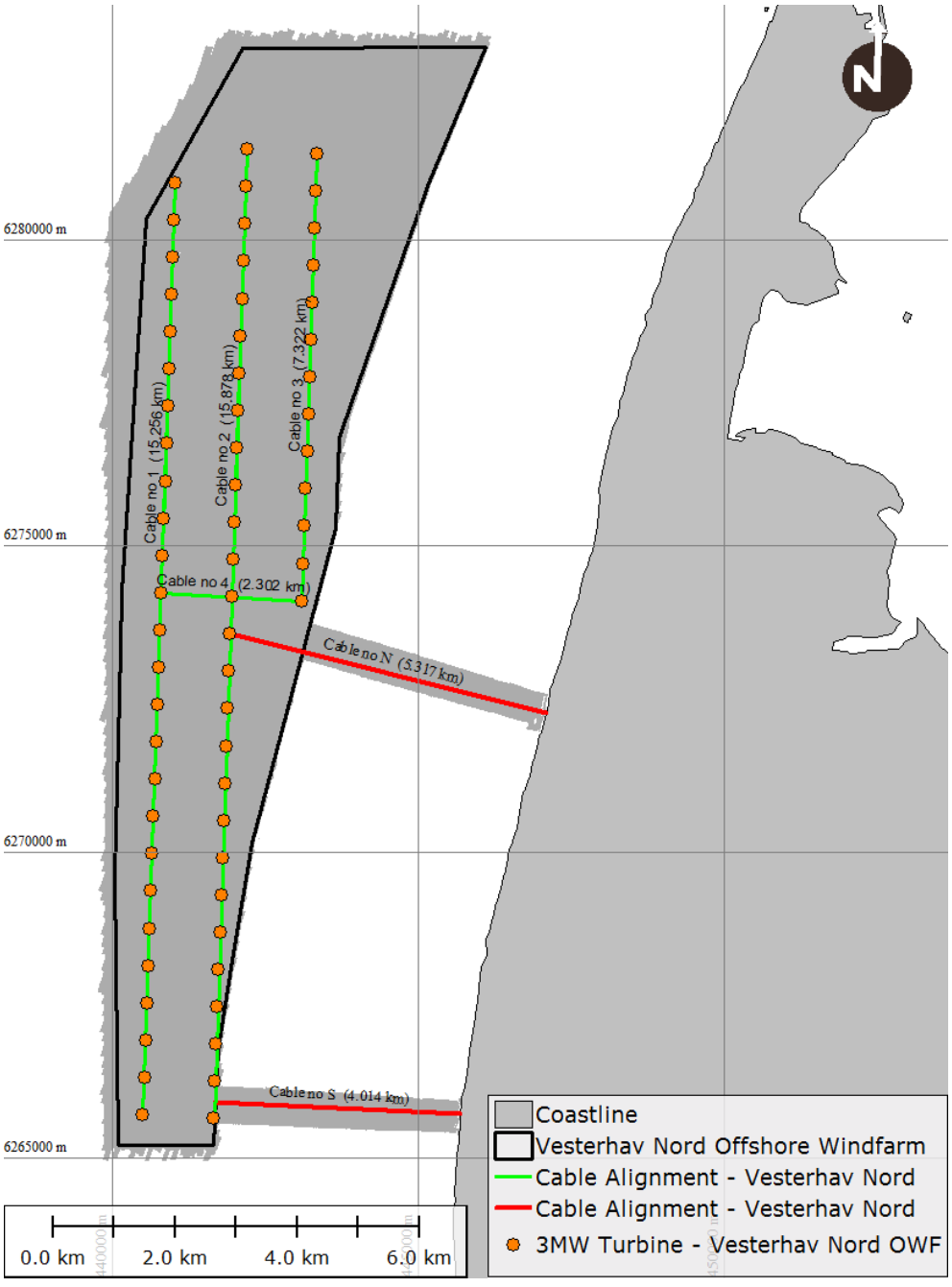

Figure E.8 Layout of inter-array cables (green) and export cables (red) for the 3MW Layout of Vesterhav Nord OWF.

In total 41 km will be jetted inside the park area and the operation will last for 21 days.

At the present stage, two export cable corridors are considered as shown in Figure E.8. The northern and southern corridors are 5.3 km and 4.0 km long. The spill

scenarios will assume that 200 MW are transmitted in both corridors, corresponding to 6 x 33 kV cables. The six cables are jetted individually in parallel trenches with 50-100 m spacing.

In spill scenarios it is assumes that jetting of exports cables will be undertaken by two jetting ROVs. Jetting ROV no 1 will install the 6 cables the northern corridor while Jetting ROV no 2 will install the 6 cables in the southern corridor. The two operations will be performed in parallel, but ROV no 1 will finish after 16 days whereas ROV no 2 will finish after 12 days.

It is assumed that export cables are jetted after inter-array cables. Consequently, the total jetting operation will last for 21+16 days = 37 days. Starting on 01-06-2012 and ending on 07-07-2012. And simulation will be extended another 14 days (21-07-2012) in order to allow the spill material to settle.

In total 154,800 m^3 of material will be jetted and 34,700 tons of fines will be spilled.

Table E.13 Definition of scenario 2 – Jetting of cables.

				Fraction 1			Fraction 2			Fraction 3			Dredging/excavation schedule		
Cable no	Length [m]	Duration [days]	Volume [m3]	Spill [%]	Spill [kg]	Spill-rate [kg/s]	Spill [%]	Spill [kg]	Spill-rate [kg/s]	Spill [%]	Spill [kg]	Spill-rate [kg/s]	Jetting rov id	Start date	End date
1	15,256	7.6	24,410	2.9	1,113,078	1.69	5.3	2,060,170	3.13	5.9%	2,304,266	3.50	1	01-06-2012 00:00	08-06-2012 15:00
…	…	…	…	…	…	…	…	…	…	…	…	…	…	…	…
4	2,302	1.2	3,683	2.9	167,954	1.69	5.3%	310,862	3.13	5.9%	347,694	3.50	1	20-06-2012 06:00	21-06-2012 10:00
N 1	5,317	2.7	8,507	2.9	387,928	1.69	5.3%	718,008	3.13	5.9%	803,080	3.50	1	21-06-2012 10:00	24-06-2012 02:00
…	…	…	…	…	…	…	…	…	…	…	…	…	…	…	…
N 6	5,317	2.7	8,507	2.9	387,928	1.69	5.3%	718,008	3.13	5.9%	803,080	3.50	1	04-07-2012 18:00	07-07-2012 10:00
S 1	4,014	2.0	6,422	2.9	292,861	1.69	5.3%	542,051	3.13	5.9%	606,275	3.50	2	21-06-2012 10:00	23-06-2012 10:00
…	…	…	…	…	…	…	…	…	…	…	…	…	…	…	…
S 6	4,014	2.0	6,422	2.9	292,861	1.69	5.3%	542,051	3.13	5.9%	606,275	3.50	2	01-07-2012 10:00	03-07-2012 10:00
Total	97 km				3,530 t			6,530 t			7,310 t			37 days	